ANALYTICA CHIMICA ACTA

International monthly devoted to all branches of analytical chemistry
Revue mensuelle internationale consacrée à tous les domaines de la chimie analytique
Internationale Monatsschrift für alle Gebiete der analytischen Chemie

ELSEVIER SCIENTIFIC PUBLISHING COMPANY

AMSTERDAM

Anal. Chim. Acta, Vol. 89, No. 1, 1–230, March 1977

Published monthly

ANALYTICA CHIMICA ACTA

Publication Schedule for 1977

Vol. 88, No. 1	January 1977	
Vol. 88, No. 2	February 1977	(completing Vol. 88)
Vol. 89, No. 1	March 1977	
Vol. 89, No. 2	April 1977	(completing Vol. 89)
Vol. 90	May 1977	(complete in one issue)
Vol. 91, No. 1	June 1977	
Vol. 91, No. 2	July 1977	(completing Vol. 91)
Vol. 92, No. 1	August 1977	
Vol. 92, No. 2	September 1977	(completing Vol. 92)
Vol. 93	October 1977	(complete in one issue)
Vol. 94, No. 1	November 1977	
Vol. 94, No. 2	December 1977	(completing Vol. 94)

Subscription price for 1977 (Vols. 88–95): Dfl. 920.00 plus Dfl. 112.00 postage (approx. U.S.$412.80 inclusive of postage). Claims for issues not received should be made within three months of publication of the issues; if not, they cannot be honoured free of charge. Subscribers in the U.S.A. and Canada receive their copies by airmail. Additional charges for airmail to other countries are available on request. For advertising rates apply to the publishers.

Subscriptions should be sent to:
Elsevier Scientific Publishing Company, P.O. Box 211, Amsterdam, The Netherlands.

GENERAL INFORMATION

Languages

Papers will be published in English, French or German.

Detailed information

Authors should consult Vol. 73, p. 435 for detailed instructions. Reprints of this information are obtainable from Dr. Macdonald or from: Elsevier Editorial Services Ltd., Mayfield House, 256 Banbury Road, Oxford (Great Britain)

Submission of papers

Papers should be sent to:

Prof. Philip W. West,
Coates Chemical Laboratories,
College of Chemistry and Physics,
Louisiana State University,
Baton Rouge 3,
La. 70803 (U.S.A.)

or to:

Dr. A.M.G. Macdonald,
Department of Chemistry,
The University,
P.O. Box 363
Birmingham B15 2TT (Great Britain)

Reprints

Fifty reprints will be supplied free of charge. Additional reprints (minimum 100) can be ordered at quoted prices. They must be ordered on order forms which are sent together with the proofs.

CHROMATOGRAPHY '77

INTERNATIONAL SYMPOSIUM ON ADVANCES IN CHROMATOGRAPHY

The 12th International Symposium on Advances in Chromatography will be held in November 7-10, 1977 at the International Congress Centre RAI Amsterdam, The Netherlands.

The scope of the meeting will cover papers and informal discussion groups by outstanding researchers from throughout the world in all fields of chromatography. In particular, new developments in gas, liquid and high performance thin-layer chromatography will be included. There will also be a commercial exhibition of the latest instrumentation and books.

Participation in the symposium will be on the basis of invited papers as well as unsolicited contributions. Authors desiring to present papers must submit 500-word abstracts by April 1, 1977. The deadline for receipt of manuscripts of accepted papers is June 1, 1977. A group flight for U.S. delegates is being arranged departing New York in November 4 and returning November 12.

All correspondence concerning the symposium should be directed to:

Professor A. Zlatkis,
Chemistry Department,
University of Houston,
Houston, Texas 77004, U.S.A.

Potential exhibitors should contact:

Organisatie Bureau Amsterdam
International Congress Centre RAI
P.O. Box 7205,
Amsterdam, The Netherlands

41 VG

HPTLC High Performance Thin-Layer Chromatography

edited by **A. ZLATKIS,** University of Houston, Houston, Texas, and **R.E. KAISER,** Institute of Chromatography, Bad Dürkheim

JOURNAL OF CHROMATOGRAPHY LIBRARY, Vol. 9

1976. 240 pages. US $43.95/Dfl. 110.00.
ISBN 0-444-41525-4

HPTLC is the advanced technology of TLC and is defined as the combined action of several variables which include: an optimized coating material with a separation power superior to the best high performance liquid chromatographic separation material - a new method of feeding the mobile phase - a novel procedure for layer conditioning - a considerably improved dosage method and a competent data acquisition and processing system. The potential and scope of this new technique is discussed and specific examples of biological samples are given. Speed, precision, quantitation, sensitivity and automation are described in detail.
The contributors to this book have demonstrated that HPTLC, as a new competitive analytical method, is able to provide solutions for complex separation problems.

CONTENTS: Simplified theory of TLC. The separation number in linear and circular TLC. Advantages, limits and disadvantages of the ring development technique. The U-chamber. Dosage techniques in HPTLC. HPTLC: development, data and results. Consideration on the reproducibility of TLC. Potential and experience in quantitative HPTLC. Application of a new high performance layer in quantitative TLC. Appendix. Subject Index.

ELSEVIER SCIENTIFIC PUBLISHING COMPANY
P.O. Box 211, Amsterdam,
The Netherlands

Distributor in the U.S.A. and Canada:
ELSEVIER NORTH-HOLLAND, INC.,
52 Vanderbilt Ave., New York, N.Y. 10017

The Dutch guilder price is definitive.
US $ prices are subject to exchange rate fluctuations.

2087 E

ANALYTICA CHIMICA ACTA
Vol. 89 (1977)

ANALYTICA CHIMICA ACTA

International monthly devoted to all branches of analytical chemistry
Revue mensuelle internationale consacrée à tous les domaines de la chimie analytique
Internationale Monatsschrift für alle Gebiete der analytischen Chemie

ELSEVIER SCIENTIFIC PUBLISHING COMPANY

AMSTERDAM

Anal. Chim. Acta, Vol. 89 (1977)

PRINTED IN THE NETHERLANDS

Analytica Chimica Acta, 89 (1977) 1—8

A TECHNIQUE FOR CURIE-POINT PYROLYSIS MASS SPECTROMETRY WITH A KNUDSEN REACTOR

P. P. SCHMID and W. SIMON

Department of Organic Chemistry, Swiss Federal Institute of Technology, CH-8092 Zurich (Switzerland)

(Received 8th September 1976)

SUMMARY

A pyrolysis mass spectrometer based on a magnetic scanning double-focusing instrument is described. Samples (1 μg or less) are thermally fragmented at low pressure in a ferromagnetic tube by the Curie-point technique. Under these conditions, the probability of the formation of undesirable recombination products is negligible. This behaviour is in agreement with simple model calculations.

Pyrolysis mass spectrometry is an attractive technique for the study of organic matter of low volatility such as natural and synthetic polymers [1—3]. Because of instrumental limitations and the advance of pyrolysis gas chromatography [4] for preparing characteristic fingerprints of organic material, the full potential of this technique was not realised until recently [5, 6]. The Curie-point pyrolysis technique [7] simplifies the geometry of the pyrolysis zone, ensures high reproducibility of the thermal fragmentation [5, 6, 8] and has therefore been proposed for coupling with mass spectrometry [9]. The potential of Curie-point pyrolysis in combination with electron impact mass spectrometry for fingerprint characterization of complex organic material such as bacteria [5], peptides [6], and glucose polymers [10] has been clearly demonstrated in pioneering contributions by Meuzelaar, Kistemaker and their colleagues [5, 6, 8, 10, 11]. Although the pyrolysis set-up of these authors [5, 6] involves thermal fragmentation into a gold-coated expansion chamber at an initial pressure of about $2 \cdot 10^{-7}$ torr, undesired recombination products have been observed [11]. This is due to the rather high final pressure and relatively long residence time of the fragments within this chamber.

The present paper describes a Curie-point system that yields pyrolysis mass spectra void of practically any undesired recombination products. The sample is introduced into the pyrolysis zone through a simple vacuum lock that permits the recording of pyrolysis mass spectra without interfering background signals for sample sizes around 100 ng.

EXPERIMENTAL

Mass spectrometer

A double focusing instrument (reversed Nier-Johnson ion optics) with an electron impact ion source and electron impact ion detection (Varian MAT 112) was used. Vacuum generation was based on a differential pumping system; the air pumping speeds were 600 l s^{-1} for the ion source, and 150 l s^{-1} for the analyzer. Mass spectra were recorded with a scan speed of 500 amu s^{-1} on an optical recording oscillograph (Oscillofil L, Siemens).

Pyrolysis system

A schematic diagram of the pyrolyzer which is flanged on to the access port on the right hand side of the ion source housing of the mass spectrometer is shown in Fig. 1. Details of the pyrolysis zone are given in Fig. 2.

Sample preparation and pyrolysis

The ferromagnetic tubes [12] of different Curie points (760°C: steel 35/29, 1.6 mm o.d., 1.4 mm i.d., supplied by La Nationale SA, CH-1211 Genève; 700°, 600°, 500°, 400°, 300°C; supplied by Fischer Labor- und Verfahrenstechnik, D-53 Bonn-Bad Godesberg) were pretreated by chemical polishing [12], washed with acetone and annealed by inductive heating for 15 s in a flow of hydrogen within a quartz tube.

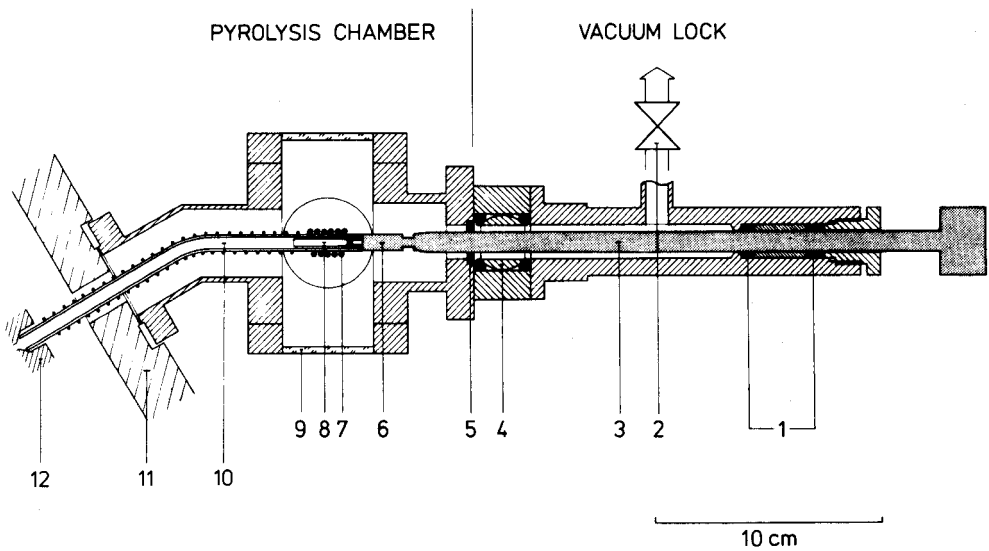

Fig. 1. Schematic diagram of pyrolyzer 1. Gasket ring (8 mm i.d., PTFE/silicone rubber). 2. High vacuum valve. 3. Inserting rod (9 mm o.d., stainless steel). 4. Ball valve (3/4-in i.d.). 5. Bearing (copper). 6. Carrier for quartz tube (stainless steel). 7. H.f. induction coil (3 mm o.d. stainless steel tube). 8. Quartz tube (holder for ferromagnetic tube). 9. Viewing port. 10. Connecting tube (5 mm i.d., quartz) with filament winding. 11. Housing of ion source. 12. Ion source. 13. Coil spring. 14. Clamp ring (steel). 15. Ferromagnetic tube.

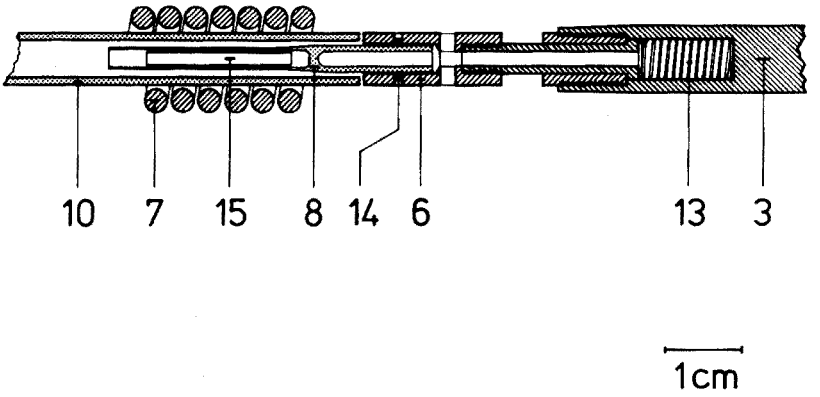

Fig. 2. Detailed view of pyrolysis zone (see text in Fig. 1).

Approximately 2 μl of a solution or suspension containing the sample in methanol or carbon disulfide was spread over the inner surface of the ferromagnetic tube. The solvent was evaporated by heating a quartz tube enclosing the ferromagnetic sample support with a hairdryer. The ferromagnetic tube was then transferred to the calcined quartz tube (Fig. 2) and the latter was fixed to the tip of the inserting rod. This assembly was introduced through the vacuum lock (ca. 10^{-2} torr, rotary pump with foreline trap) into the pyrolysis chamber. A visual check through the viewing port (Fig. 1) helps to make sure that the carrier for the quartz tube fits tightly to the heated quartz connecting tube (Figs. 1 and 2) which leads the thermal fragments into the electron impact ion source. The high-frequency (480 KHz) power is generated as described earlier [13] and fed to the air-cooled induction coil through flexible leads (600 mm length, 25 mm^2 cross-section). After the high-frequency generator has been adjusted (see Results and Discussion), the pyrolysis as well as the mass scan are initiated either manually (by observing the signal of the electron impact detector) or with a timer with a typical time lag of 0.5 s. In Fig. 3 the relative intensity of the signal at *m/e* 146 during the pyrolysis of 4-phenylbutyric acid, which corresponds to the partial pressure of this thermal fragment in the ion source, is given as a function of time. This justifies the time lag chosen.

RESULTS AND DISCUSSION

Temperature—time profiles of commercially available ferromagnetic tubes (see Experimental) obtained under vacuum for the pyrolysis conditions are shown in Fig. 4. The temperature of all the tubular conductors can be stabilized satisfactorily to the Curie point. Under more ideal conditions (thin walled tubes, careful impedance matching of oscillator and induction coil), temperature rise times (20—760°C) of less than 60 ms may be obtained with iron tubes of comparable dimensions [13].

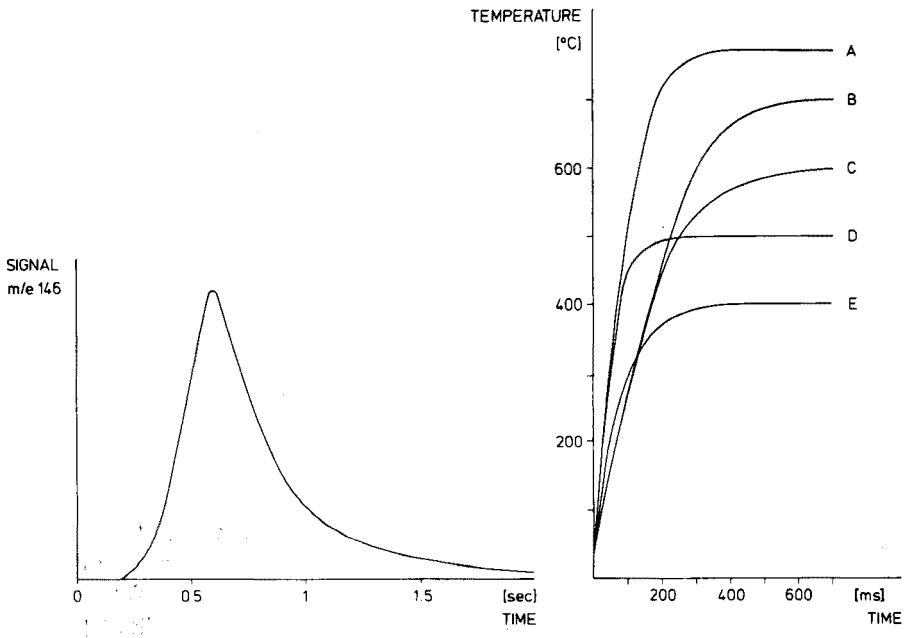

Fig. 3. Pyrolysis of 4-phenylbutyric acid at 760°C. Relative intensity of the fragment corresponding to *m/e* 146 as a function of time (iron tube; sample size, 0.5 μg).

Fig. 4. Temperature—time profiles of ferromagnetic tubes. These were determined in the pyrolysis position under high vacuum as described earlier [13]. The anode capacitor C_8 (Fig. 7 in [13]) was loaded to 4100 V and held there during pyrolysis. Curve A, Iron. Curves B—E, alloys with nominal Curie points of 700°, 600°, 500° and 400°C, respectively.

The pyrolysis should be conducted so as to obtain products which reflect the composition and structure of the starting material examined. Therefore unimolecular decomposition processes should be favoured and recombination reactions should be suppressed as far as possible. These conditions are met if the pyrolysis is performed in a Knudsen cell [14] and if the time between the formation of the fragments and their analysis is kept small. Assuming a closed reactor at negligible initial pressure and with a volume of 26.5 mm^3 (corresponding to a tubular reactor of 1.5 mm i.d., and 15 mm length), the mean free path of fragments was estimated for different sample sizes (Fig. 5). If it is further assumed that the pyrolysis leads to a single volatile fragment of the molar mass indicated, a mean free path larger than the diameter of the reactor used is obtained for sample sizes below 10 ng. Collisions of molecules therefore occur predominantly with the reactor wall [14], as required for Knudsen reactor conditions [14]. In a fragmentation experiment as described above, the products may leave the reactor to one side during pyrolysis. The number of fragments within the reactor is therefore decreased compared to the situation described in Fig. 5 (see Fig. 6). These estimates were based on kinetic data which have been presented for

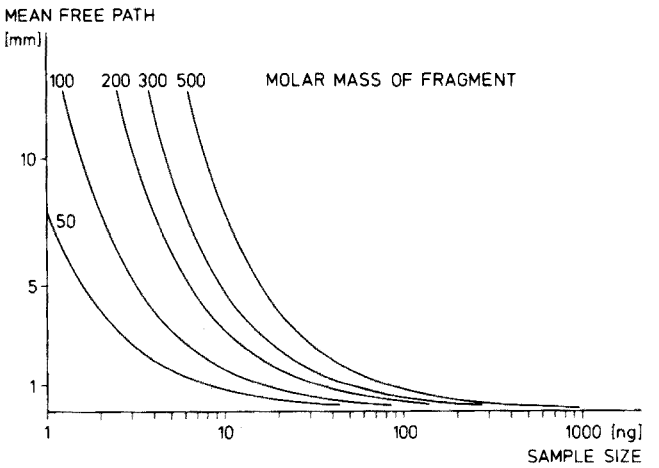

Fig. 5. Mean free path of fragments after pyrolysis in a closed reactor (26.5 mm^3 volume, negligible initial pressure). Only one volatile fragment of molar mass indicated is formed; for the calculation procedure, see [16].

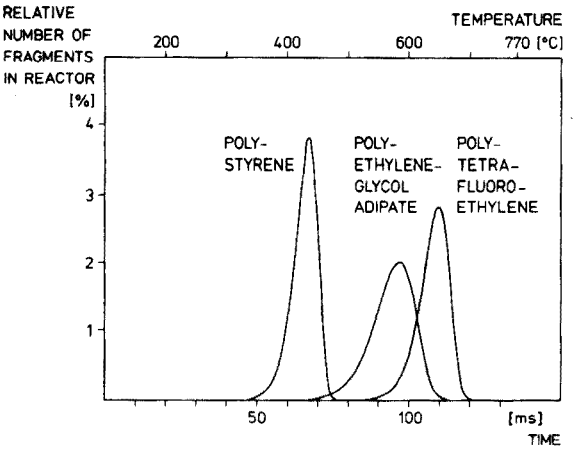

Fig. 6. Relative number of fragments in reactor as a function of pyrolysis temperature and time. Warm-up rate, 5° ms^{-1} (e.g. iron); molar mass of fragment 100; molecular effusion [14]; for kinetic parameters see [15].

the thermal decomposition of polymers [15]. A comparison of Figs. 5 and 6 demonstrates that a sample with kinetic data similar to those of polystyrene can be pyrolyzed under Knudsen reactor conditions [14] if the sample size is kept below about 200 ng. An inspection of Fig. 7 shows that pyrolysis mass spectra of around 100 ng of polystyrene may be obtained without interfering background signals.

The pyrolysis mass spectrum of 4-phenylbutyric acid shown in Fig. 8(A) indicates only a small signal at *m/e* 182, which is due to a recombination reaction leading to dibenzyl. For the experimental conditions described by

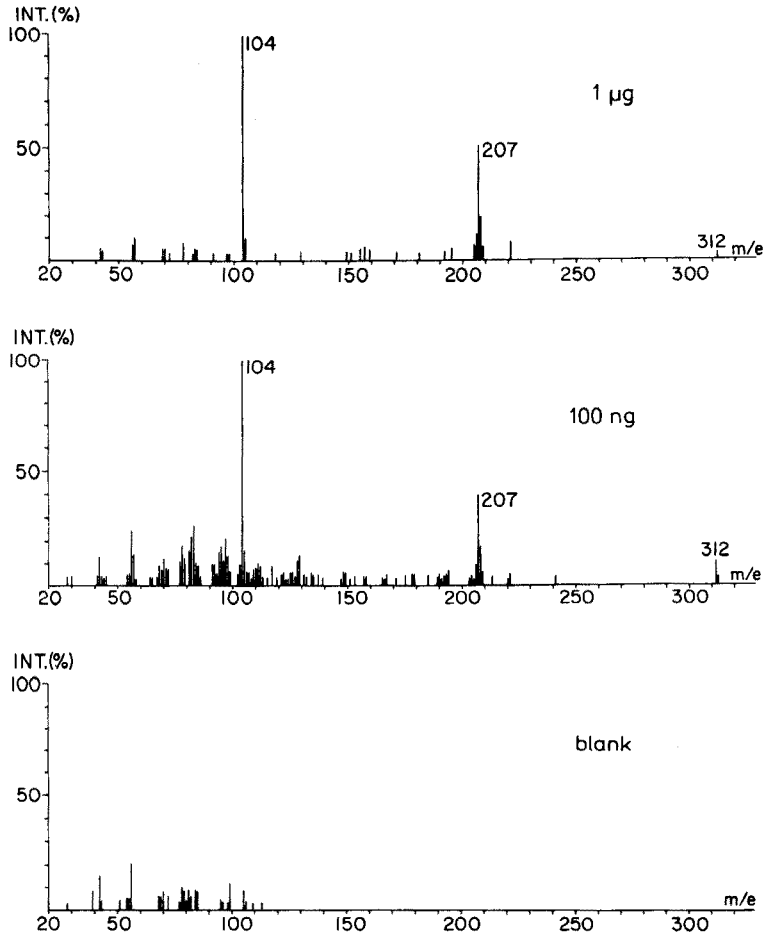

Fig. 7. Pyrolysis mass spectra of polystyrene of different sample sizes.

other authors [5], the probability for such undesired recombination reactions is much larger [11]. Correspondingly, the relative intensity of the signal at *m/e* 182 increases dramatically [11] (Fig. 8, B).

The pyrolysis mass spectrometer presented here has the capability of detecting even polar fragments of relatively high mass (see also [17—22]). An example is given in Fig. 9. Similar results were obtained for a series of pigment dyes[23]. The example given (Fig. 9) as well as the data for the other dyes studied demonstrates the correlation of the structure of the fragments with the structure of the starting material.

The pyrolysis mass spectrometry system described here has promising capabilities both for fingerprint characterization as well as for structural elucidation of complex and/or slightly volatile organic material [23].

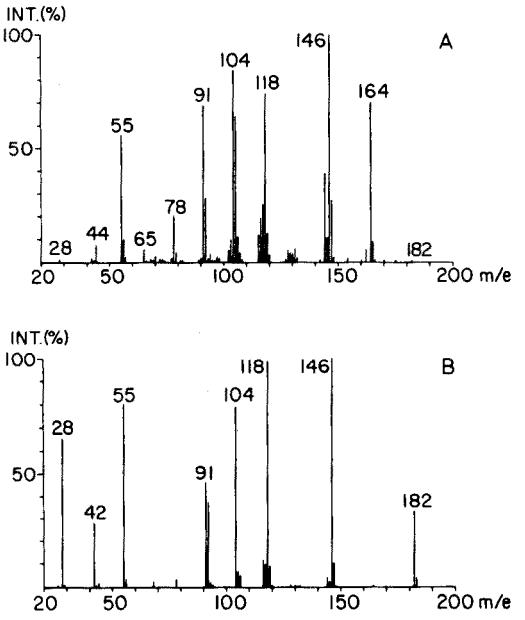

Fig. 8. Pyrolysis mass spectra of 4-phenylbutyric acid. A, Present work; sample size 2 μg; electron energy, 15 eV. B. See [11]; sample size, 2.5 μg; electron energy, 13 eV.

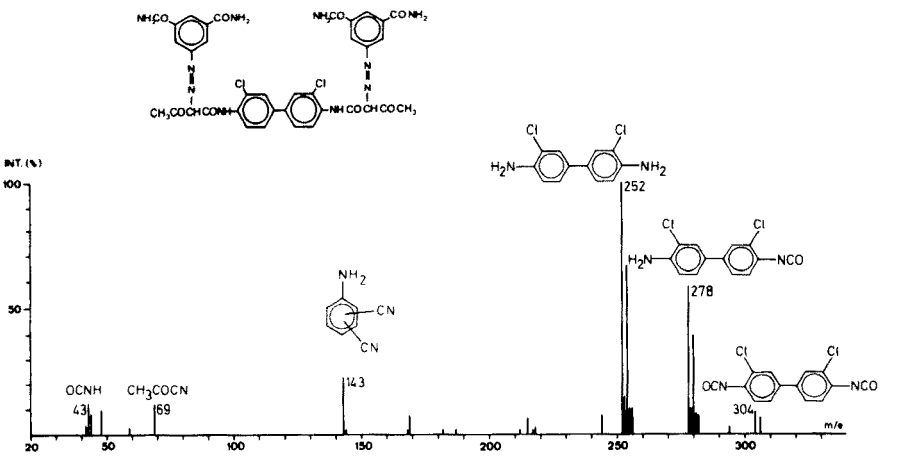

Fig. 9. Pyrolysis mass spectrum of a pigment dye. Electron energy, 15 eV.

REFERENCES

1 S. L. Madorsky and S. Straus, Ind. Eng. Chem., 40 (1948) 848.
2 L. A. Wall, J. Res. Nat. Bur. Stand., 41 (1948) 315.
3 P. D. Zemany, Anal. Chem., 24 (1952) 1709.
4 R. J. Kokes, H. Tobin Jr., and P. H. Emmett, J. Am. Chem. Soc., 77 (1955) 5860.

5 H. L. C. Meuzelaar and P. G. Kistemaker, Anal. Chem., 45 (1973) 587.
6 H. L. C. Meuzelaar, M. A. Posthumus, P. G. Kistemaker and J. Kistemaker, Anal. Chem., 45 (1973) 1546.
7 W. Simon and H. Giacobbo, Chem. Ing. Tech., 37 (1965) 709.
8 H. L. C. Meuzelaar and R. A. in't Veld, J. Chromatogr. Sci., 10 (1972) 213.
9 W. Simon and J. T. Clerc, Pure Appl. Chem., 26 (1971) 35.
10 M. A. Posthumus, A. J. H. Boerboom and H. L. C. Meuzelaar, Adv. Mass Spectrom., 6 (1974) 397.
11 M. A. Posthumus, N. M. M. Nibbering and A. J. H. Boerboom, Org. Mass Spectrom., 11 (1976) 907.
12 H. W. Dettner and J. Elze (Eds.), Handbuch der Galvanotechnik, Vol. 1, Carl Hanser, München, 1964, p. 833.
13 Ch. Oertli, Ch. Bühler and W. Simon, Chromatographia, 6 (1973) 499.
14 D. M. Golden, G. N. Spokes and S. W. Benson, Angew. Chem., 85 (1973) 602.
15 F. Farré-Rius and G. Guiochon, Anal. Chem., 40 (1968) 998.
16 S. W. Benson, The Foundations of Chemical Kinetics, McGraw-Hill, New York, 1960, p. 150.
17 I. Lüderwald, M. Przybylski and H. Ringsdorf, Mass Spectrometry in Biochemistry and Medicine, 1974, 245.
18 M. Przybylski, H. Ringsdorf and H. Ritter, Makromol. Chem., Suppl. 1 (1975) 297.
19 S. Caccamese, P. Maravigna and M. Przybylski, J. Polym. Sci., Polym. Chem. Ed., 13 (1975) 2061.
20 D. O. Hummel, H. J. Düssel, H. Rosen and K. Rübenacker, Makromol. Chem., Suppl. 1 (1975) 471.
21 J. P. Anhalt and C. Fenselau, Anal. Chem., 47 (1975) 219.
22 E. Blasius, H. Häusler and H. Lander, Talanta, 23 (1976) 301.
23 Ch. Oertli, Dissertation ETHZ, No. 5289, Zürich, 1974.

Analytica Chimica Acta, 89 (1977) 9—19

THE SIT IMAGE VIDICON AS A GAS-PHASE FLUORESCENCE DETECTOR FOR GAS CHROMATOGRAPHY

R. P. COONEY, T. VO-DINH, and J. D. WINEFORDNER*

Department of Chemistry, University of Florida, Gainesville, FL 32611 (U.S.A.)

(Received 10th August 1976)

SUMMARY

The feasibility of using an SIT Vidicon as a gas-phase fluorescence detector for gas chromatography is demonstrated. Operation of the SIT in both the "real time" and integration modes is discussed. The SIT system can subtract stored signals (spectra) from one another, so that background correction is possible and the spectral selectivity of vapor-phase fluorescence detection is enhanced. Gas-phase spectra and limits of detection for several polyaromatic hydrocarbons are given; the SIT gives limits of detection about a factor of five larger than those obtained with a photomultiplier (PM) tube (operated in a non-scanning mode). The relative merits of using the SIT system or a fast scanning (PM) system for measuring transient signals are discussed.

In recent years, fluorescence detectors have seen increasing use in liquid and thin-layer chromatography. Several workers have investigated the possibility of using fluorescence detectors in gas chromatography. Bowman and Beroza [1] trapped gas chromatographic eluents in a flowing liquid solvent stream and then monitored the fluorescence as the solvent stream was fed through a spectrophotofluorimeter. Burchfield et al. [2] used a heated transfer line from the gas chromatograph to a heated quartz cell in a spectrophotofluorimeter and observed fluorescence directly in the gas phase. They later modified their system with a gas-phase isolation and injection system in order to analyze polynuclear arenes in air particulates [3]. Freed and Faulkner [4] used a fast scanning fluorescence spectrometer to obtain gas-phase excitation and emission spectra of gas chromatographic eluents. Robinson and Goodbread [5] fabricated a simpler, less expensive, filter fluorimetric detector, useful primarily for quantitative analysis.

The present work involves the use of an SIT (silicon intensifier target) image device as a gas-phase fluorescence detector for gas chromatography. TV-type multichannel detector devices for optical spectroscopy have been reviewed [7, 8] and so, no thorough review will be made of previous uses of such detectors. In more recent work, Warner et al. [9] described a video fluorimeter with electronic processing to obtain three-dimensional graphical spectra involving 241 fluorescence spectra at 241 different exciting wavelengths at

*Author to whom all correspondence should be addressed.

16.7 ms per spectrum. In a paper by Vo-Dinh et al. [11], analytical figures of merit, including detection limits, were measured for a commercial spectrophotofluorimeter which had the photomultiplier-slit arrangement replaced by an SIT. Dessy et al. [10] have reported the use of a solid-state array detector with computer control as a molecular absorption spectrophotometric detector for liquid chromatography. In the present work, the performance of the SIT image detector was investigated and compared to that of the fast scanning fluorescence spectrometer, especially with regard to the detection of transient signals of gaseous species being eluted from a gas chromatograph; also analytical figures of merit and the limitations of the system were established.

Anthracene, benzo-[a]-pyrene, chrysene, phenanthrene, and pyrene were studied because they belong to the important class of polynuclear aromatic hydrocarbons (PAH), which are frequently encountered in air pollutants, urban water, tar, and cigarette smoke [12]. Many PAHs, such as pyrene and benzo-[a]-pyrene, have been shown to be highly carcinogenic.

EXPERIMENTAL

Apparatus

A Model 1400, gas chromatograph (Varian Instrument Division) was employed. Because evaluation of the detector was the sole object of this study, no actual chromatographic separations were carried out; a 3-ft length of 1/8-in. o.d. stainless steel tubing was used to simulate a chromatographic column. The chromatograph was connected to the spectrophotofluorimeter with a 1.5-ft. length of 1/16-in. o.d. stainless steel transfer line. The transfer line was heated with a 1-in. × 4-ft. heating tape (Briscoe Manufacturing Company, Columbus, OH); the temperature was controlled by a variable autotransformer (Staco Inc., Dayton, OH) and monitored with a calibrated iron—constantan thermocouple. The heating tape was covered with several layers of asbestos and aluminum foil. Samples were injected with a 10-μl syringe (Hamilton Company, Reno, NV).

The gas-phase fluorescence analysis system consisted of an Aminco spectrophotofluorimeter (American Instrument Company, Silver Springs, MD) which was adapted to the analysis of gas chromatographic eluents. The excitation light source was a 150-W Eimac xenon arc lamp regulated by a Varian d.c. power supply (Model 250S-2, Varian, Eimac Div., San Carlos CA). This source has been shown to improve limits of detection of condensed phase molecular luminescence by almost an order of magnitude [6]. A lens and a spherical mirror were used to divert the exciting light beam into the entrance slit of the f/4 Czerny-Turner-type excitation monochromator. A schematic diagram of the experimental arrangement is given in Fig. 1.

The gas flow cell was a 50-mm long rectangular quartz cell (Aminco, type B16-63019; 3-mm i.d., 5-mm o.d.). The cell was inserted inside the fluorimeter cell compartment which had been modified to contain a heated brass

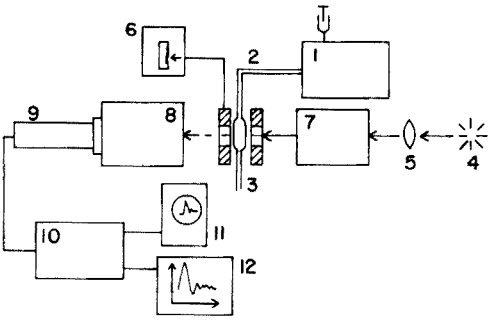

Fig. 1. Block diagram of the gas chromatograph and the fluorimeter—SIT image detector. 1. Gas chromatograph. 2. Transfer line. 3. Flow cell. 4. Light source. 5. Optics. 6. Heating device. 7. Excitation monochromator. 8. Emission monochromator. 9. SIT image converter. 10. Optical multichannel analyzer. 11. Oscilloscope. 12. Strip-chart recorder.

block which was bored to hold the gas cell and two cartridge heaters (Model 60213, General Electric). The heater output was controlled by an autotransformer (Superior Electric Company, Bristol, Connecticut). The cell temperature was varied between 200 and 280° C and was measured with another calibrated iron—constantan thermocouple. The sample compartment base plate and cover were made from asbestos to insulate the adjacent monochromators from heat generated by the cell holder. Appropriate fans were used to keep the two monochromators at 30—40° C under operating conditions. Because scattered light was a critical factor, it was desirable to use monochromator slit widths smaller than the cell dimensions. On the other hand, a decrease in the slit widths leads to smaller signal strengths. Although larger slits would lower the limits of detection (discussed in a later section), slit widths of 2 mm in the excitation path and 1 mm in the emission path were chosen to provide a 5-nm spectral resolution.

The detection device was a silicon-intensifier-target (SIT) camera tube (Model 12Q5, Princeton Applied Research, Princeton, NJ), mounted directly on the exit of the analyzing (emission) monochromator of the spectrophotofluorimeter; the standard slit assembly and the photomultiplier were removed. The 12.5-mm wide SIT target, with 500 elements or channels, allowed multichannel detection over a selectable spectral interval of 62.5 nm. An optical multichannel analyzer (OMA, Model 1205 D, Princeton Applied Research) recorded the data which could be stored in either of two 500-word 21-bit memories (memory "A" or "B"). The SIT/OMA system can perform the following operations:

(i) in the "real-time mode", detection and recording in memory A, of a temporally changing signal, and display on an oscilloscope after each machine cycle (32.8 ms);

(ii) integration of data on all 500 channels for a specified time period, determined by a selectable number of presets (0—9999) and delays (0—9) — in all cases, a delay of 0 was used;

(iii) storage of the integrated data, either in memory A or B;

(iv) subtraction of the stored data from one another (A − B);

(v) provision of a digital display of the signal magnitudes and their corresponding spectral positions (channel number);

(vi) summation of the magnitudes of the signals between specified spectral ranges (peak areas);

(vii) provision of an analog output which could be used to record the spectra on a chart recorder.

In most of our experiments, the luminescence signal plus background (scattered light; dark signal) were stored in memory A and the background alone in memory B. The background corrected signal A − B, which was of interest, was displayed on an oscilloscope (Model 1220A Hewlett Packard) and read-out by a strip-chart recorder (Model SRG, Sargent Welch Scientific, Skokie, IL).

Reagents

The polynuclear arenes employed were anthracene and pyrene (Chem Service, West Chester, PA), phenanthrene (Eastman Organic Chemicals, Rochester, NY), chrysene and benzo-[a]-pyrene (Research Organic/Inorganic Chemical Corp., Sun Valley, CA). The solvent used was cyclohexane (Reagent ACS, Matheson Coleman and Bell, Norwood, OH).

Procedures

The Eimac xenon arc lamp, the spectrophotofluorimeter, the gas chromatograph and the SIT/OMA system were operated according to the manufacturer's instructions and as discussed previously [11].

RESULTS AND DISCUSSION

Real-time mode (Fig. 2A, B)

One of the main features of the SIT is the capability to detect and display instantaneously a temporally changing signal (over a wide spectral region), which makes this device quite suitable for chromatographic techniques. The experimenter can observe the whole spectra of the compounds under study as they pass through the flow-cell, making possible a rapid, semi-qualitative identification. The real-time signal from any of the 500 channels is also fed into a strip-chart recorder to give a conventional fluorescence chromatogram which is similar to that obtained with a single-channel detector (e.g., photomultiplier). However, in this mode, the SIT has a 50—100 times poorer sensitivity than the photomultiplier. Therefore, for quantitative analysis, the integration mode of the SIT, which will be discussed in the next section, is preferred.

Integration mode (Fig. 2A, C)

In the integration mode, the SIT—OMA system accumulates data over a designated time period. The final recorded spectrum consists of the total

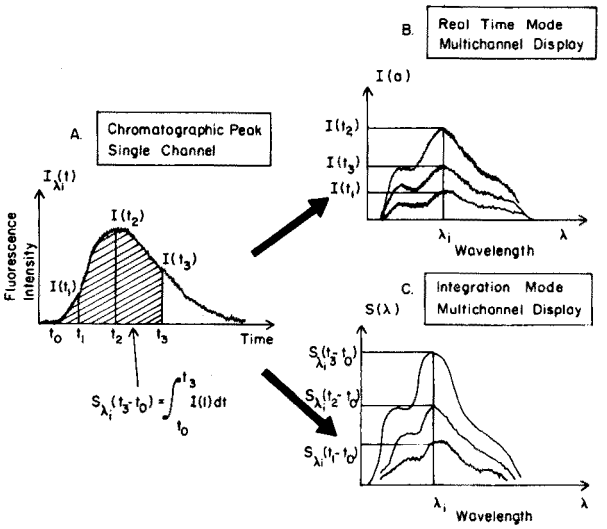

Fig. 2. Various operating modes of the SIT—OMA device. A. The change in sample concentration (or fluorescence intensity) observed at one wavelength λ_i. B. Real-time mode display by the OMA of the whole spectrum, observed at times t_1, t_2, and t_3. C. Multichannel display of the fluorescence spectra after data accumulation over a time period between t_1 and t_0, t_2 and t_0, t_3 and t_0, (A—B mode).

integrated signals of each of the 500 channels accumulated over the entire observation time. These principles are illustrated in Fig. 2A, C. Data accumulation leads to a significant improvement in the signal-to-noise ratio as discussed below. The linearity of the SIT response versus measurement time has been previously investigated [11] and is known to be quite suitable for chromatographic detection. There are two practical factors which limit the integration time of a SIT; the dynamic range is limited by overflow of the memory (ca. 10^5 counts), and the chromatographic peak width is limited. Data accumulation times longer than the chromatographic width will not lead to any signal-to-noise enhancement. Figure 3 shows the integration results in two typical cases. Figure 3A shows that for a chromatographic peak halfwidth of 18 s, integration times up to 12.8 s provide significant signal-to-noise improvements; where the chromatographic halfwidth is only 2 s, an accumulation time of 6.4 s does not provide any increase in signal-to-noise ratio over an accumulation time of 2 s (Fig. 3B).

Background correction

Background correction was accomplished by use of the A − B mode, as described in the Experimental section. Luminescence background from the solvent or carrier gas impurities could be corrected by recording into memory B the signal, if any, generated by injecting a solvent blank. Because scattered light contributed significantly to the observed signal, this correction procedure

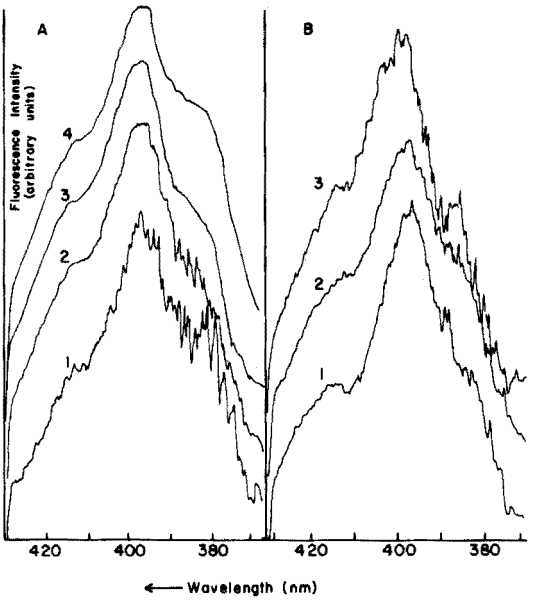

Fig. 3. Dependence of signal-to-noise ratio on chromatographic peak width and on integration time. A. For a peak halfwidth of 18 s, data taken over 12 (curve 1), 50 (curve 2), 200 (curve 3) and 800 (curve 4) accumulation cycles. B. For a peak halfwidth of 2 s, data taken over 12 (curve 1), 50 (curve 2) and 200 (curve 3) accumulation cycles. The peak heights of each spectrum were normalized to have the same value.

was most important. At the same time, all other undesired interferences, such as quartz cell emission and dark signal from the detector, were also corrected for.

Spectral selectivity and mixture analysis

As has been pointed out by previous authors [1—5], the combination of fluorescence and chromatography provides a powerful tool for the analysis of mixtures containing fluorescent compounds. Because of its inherent sensitivity, the fluorescence system can detect many compounds at the nanogram or sub-nanogram level; and, of course, non-fluorescing compounds do not interfere with an analysis as they might with a more universal detector. Fluorescent compounds themselves can be resolved chromatographically and/or spectroscopically. For example, two or more fluorescent compounds which fluorescence spectrometry alone might not be able to differentiate in a mixture can often be separated chromatographically, so that the detector can examine each compound separately. Alternatively, compounds which are not separated chromatographically may be discriminated from one another and identified by means of their characteristic fluorescence excitation and/or emission spectra.

The use of the SIT—OMA system enhances the spectral selectivity of vapor-phase fluorescence detection. Even though simultaneously eluting compounds

with overlapping emission spectra can perhaps be partially resolved by the selective excitation of one of the compounds, complete resolution may not always be possible. In this case, the ability of the OMA to subtract stored signals from one another can be used to obtain the desired information. An illustration of this capability is shown in Fig. 4. Curve 1 represents the combined emission signals from a mixture of anthracene and benzo-[a]-pyrene. When the signal obtained from an injection of pure anthracene (same amount in both cases) is subtracted from curve 1, the spectrum of benzo-[a]-pyrene (curve 2) is obtained. Similarly, the spectrum of anthracene (curve 3) is obtained when the signal from an injection of pure benzo-[a]-pyrene (same amount in both cases) is subtracted from curve 1.

Gas-phase luminescence spectra

The gas-phase luminescence spectra observed at gas chromatographic temperatures illustrate a few typical features which deserve comment. In Fig. 5, two gas-phase (curves 1 and 2) and one condensed-phase (curve 3) spectra of anthracene obtained with the SIT system are shown (5 nm spectral band pass). The dependence of the shape of the gas-phase spectrum on

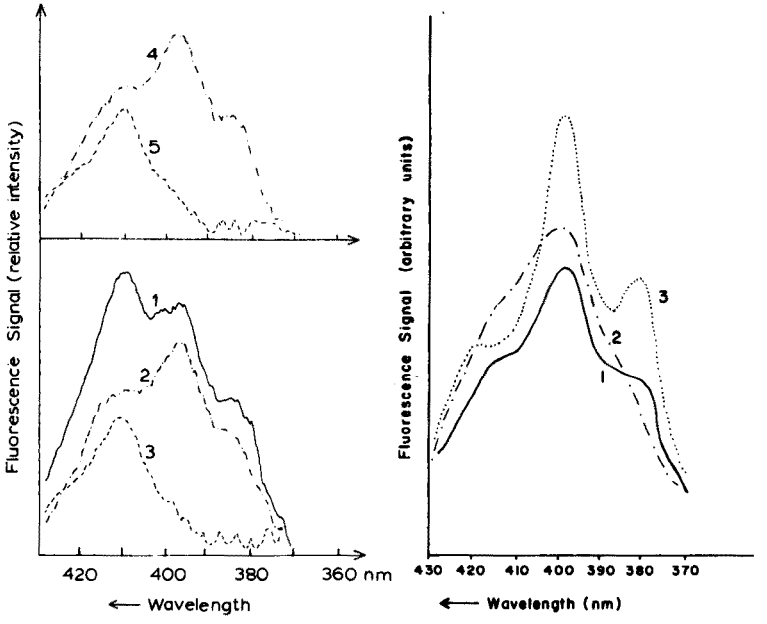

Fig. 4. (left) Gas-phase fluorescence spectrum of a mixture of anthracene and benzo-[a]-pyrene. 1. Original spectrum of the mixture. 2. After subtraction of the benzo-[a]-pyrene spectrum. 3. After subtraction of the anthracene spectrum. 4. Spectrum of pure anthracene. 5. Spectrum of pure benzo-[a]-pyrene.

Fig. 5. (right) Fluorescence spectra of anthracene. 1. Gas phase, λ_{ex} = 367 nm. 2. Gas phase, λ_{ex} = 266 nm. 3. Condensed phase, λ_{ex} = 266 nm.

excitation wavelength is evident, with the spectrum resulting from the O—O band excitation (366 nm) bearing a closer resemblance to the condensed-phase spectrum. The typical blue shift (about 5 nm) which occurs when going from the condensed to gas phase fluorescence is also shown, along with a general blurring of the spectrum. At the elevated temperatures needed to separate high-boiling polyaromatic hydrocarbons by gas chromatography, the free rotational molecular motions and Doppler and collisional broadening processes are believed to contribute to the diffuseness of the vapor-phase luminescence spectra. As shown in curve 2 (Fig. 5), increase in the energy of excitation (266 nm) gives rise to a red shift along with a change of the intensity distribution in the vapor-phase fluorescence spectrum. These results are in agreement with data reported by previous workers [11—13]. From these considerations, great care must clearly be taken to perform quantitative analyses at constant temperature and specified excitation energy.

Limits of detection and analytical curves

The analytical curve for anthracene was found to be linear for the range 50—900 ng of anthracene. The detection limits for anthracene and several polyaromatic hydrocarbon molecules are shown in Table 1. Peak heights at the peak fluorescence wavelengths in the accumulated spectrum were used as a measure of luminescence intensity. The experimental gas chromatographic temperature is 265° C for benzo-[a]-pyrene and 200° C for all other compounds. The data accumulation time was 6.4 s for most compounds, except for pyrene (9.6 s). Typical limits of detection reported together with the corresponding values obtained with a photomultiplier tube. Detection limits

TABLE 1

Limits of detection of several polyaromatic hydrocarbons by an SIT image Vidicon fluorescence detector gas chromatographic system

Compound	λ_{ex} [nm]	λ_{em} [nm]	Temp. [° C]	Integration Time [s]	L.O.D.[a]	
					SIT[b] [ng]	PM[c] [ng]
Anthracene	(266)	400	200	6.4	1.0	0.20
Pyrene	(316)	360	200	9.6	1.5	0.23
Phenanthrene	(256)	375	200	6.4	2.5	0.51
Chrysene	(265)	400	200	6.4	15.0	2.0
Benzo-[a]-pyrene	(281)	430	265	6.4	6.5	—

[a] Limit of detection is that amount of analyte, in ng, resulting in a $S/N = 3$ (N = r.m.s. noise).

[b] SIT = Silicon intensified target detector, spectral bandwidth of 5 nm, observation time of 6.4 s for all compounds except pyrene (9.6 s).

[c] PM = Photomultiplier detector, spectral bandwidth of 25 nm, observation time of 1 s, operated in non-scanning mode.

with the SIT, although 3—5 times larger than those obtained with the photomultiplier, are particularly low and are all at the nanogram level.

At or near the limit of detection, the limiting noise is equivalent to the noise on the baseline observed on the A − B display, where both memories have accumulated background for the same period of time. When measuring either dark counts or background scatter from the xenon lamp, the signal-to-noise ratio improves by a factor of about 1.75 when the accumulation time is increased by a factor of 4. This nearly square-root dependence indicates that the noise is predominantly shot-noise, and that a further improvement in the limit of detection could be obtained by increasing the light throughput of the system.

Another characteristic of the SIT is a coherent sinusoidal noise pattern (possibly 120 Hz) which is observable on the real-time display and is carried through to the A (or B) memory display(s) in the accumulation mode. This pattern may or may not show up in the A − B mode, depending on whether or not the pattern in memory B is in or out of phase with that in memory A. The relative magnitude of this effect is inversely proportional to the number of accumulation cycles. The coherent noise can therefore diminish the signal-to-noise ratio by a significant factor, e.g., 2 or 3, if the light flux to the detector is small. It should be stressed here that grounding of the measurement system is very important to minimize the coherent noise.

When used as detectors for liquid [14] or gas chromatography, both fast scanning (single channel) and SIT (multichannel) systems are measuring transient signals, the intensities of which vary as the compound of interest passes through the detector. The actual period of time (t_0) that either system spends observing the analyte signal is limited to an optimal value of t_w, the peak width of the eluting substance.

A fast scanning system looks sequentially at a total number, N, of spectral intervals, $\Delta\lambda$ (where $\Delta\lambda$ is determined by the spectral bandpass of the spectrometer). The total wavelength region covered by a scan is $N\Delta\lambda$. The actual time spent observing each individual spectral interval ($\Delta\lambda_i$) would be $(1/N)t_0$, while the rest of the time, $(N - 1/N)t_0$, would be spent examining the remaining $N - 1$ spectral intervals.

As mentioned earlier, the SIT partitions a spectral region of interest into 500 spectral components, or channels, Each channel is "on", accumulating data, over 99.9% of the time, being "off" only momentarily once every 32.8 ms while its data are being stored in memory. Thus, if equivalent resolution, observation time, and total spectral region covered are assumed, the SIT will collect $(0.999)/(1/N)$ or about N times as much information as the fast scanning system. It should be noted that, because of the limitations of both systems (discussed below), the assumed conditions will rarely, if ever, be met in practice.

Because of the sequential nature of the fast scanning system, there is an unavoidable lag between the time the ith spectral interval is observed and the time the jth spectral interval is observed. During this time lag $[(j\text{-}i)/N]\,t_0$, there

will be a change of analyte concentration in the detector cell causing a change in overall signal intensity, which may result in a distortion of the observed spectrum. The distortion becomes worse for lower scan rates and/or a larger spectral region to be covered and/or a greater mass flow rate through the detector. The problem of distortion can be counteracted somewhat by increasing scan rate, so that the relative intensities of the individual spectral intervals vary little throughout the duration of the scan. Increasing the scan rate however decreases the observation time, t_0, thus wasting useful information. In addition, after the scan rate is increased past a certain point, resolution deteriorates (even if special readout equipment is used, resolution still may degrade).

As discussed earlier, each of the SIT spectral channels obtains information simultaneously, in parallel. As a result, not only is analyte signal observed for the entire peak width, t_w, but also there is little or no spectral distortion from the transient nature of the signal.

There is no provision for background correction in a fast scanning system. If the background is not constant over the wavelength region scanned, then the observed spectrum will be distorted. As pointed out in the Experimental section, background variation is accounted for with the SIT detector. However, both the SIT and the photomultiplier have the disadvantage of variation of sensitivity (spectral) with wavelength; the SIT in addition has a response which varies with channel number (spatial). The fast scanning system has the distinct advantage of being able to recover both excitation and emission spectra, while the SIT is limited to emission spectra only.

The SIT system in this work can at any one time examine a total spectral region of only about 60 nm. Because no one 60-nm region encompasses the emission spectra of all possible fluorescent compounds of interest, this is a drawback of the present SIT system. Indeed, the emission spectra of some compounds are themselves more than 60 nm wide. This problem could be overcome by decreasing the spectral dispersion of the spectrometer (with concomitant loss of resolution) or alternatively by progress in vidicon technology to provide a larger active surface on the face of the TV tube. A fast scanning system possesses the ability to scan the entire wavelength region from 200 to 800 nm. However, as discussed earlier, scanning larger wavelength regions results in problems of spectrum distortion and decreased observation time for each spectral interval scanned.

Conclusions

This investigation has shown that the use of a TV-type image device as a fluorimetric detector for gas chromatography offers a sensitive and selective method of analysis. The multichannel detection capability considerably enhances the ability of the analyst to characterize components in a complex mixture. The sensitivity is comparable to that of a fast-scanning spectrometer with a photomultiplier detector. One of the most promising features of the SIT—OMA system is its capability of being interfaced easily with a computer

or some other remote control device which could significantly increase its power and utility. Another extension of this system is in the area of liquid chromatography where more detailed spectral information would be gathered.

This work was supported solely by Grant NIH GM11373-13

REFERENCES

1 M. C. Bowman and M. Beroza, Anal. Chem., 40 (1968) 535.
2 H. P. Burchfield, R. J. Wheeler, and J. B. Bernos, Anal. Chem., 43 (1971) 1976.
3 H. P. Burchfield, E. E. Green, R. J. Wheeler, and S. M. Billedeau, J. Chromatogr., 99 (1974) 697.
4 D. J. Freed and L. R. Faulkner, Anal. Chem., 44 (1972) 1194.
5 J. W. Robinson and J. P. Goodbread, Anal. Chim. Acta, 66 (1973) 239.
6 R. J. Perchulski, J. D. Winefordner, and B. J. Wileler, Anal. Chem., 47 (1975) 1993.
7 Y. Talmi, Anal. Chem., 47 (1975) 658A; 47 (1975) 697A.
8 J. D. Winefordner, J. J. Fitzgerald and N. Omenetto, Appl. Spectrosc., 27 (1975) 369.
9 I. M. Warner, J. B. Callis, E. R. Davidson, M. Gouterman, and G. D. Christian, Anal. Lett., 8 (1975) 665.
10 R. E. Dessy, W. G. Hann, C. A. Titus, and W. R. Reynolds, J. Chromatogr. Sci., 14 (1976) 195.
11 T. Vo-Dinh, D. J. Johnson, and J. D. Winefordner, Spectrochim. Acta A, in press.
12 S. Udenfriend, Fluorescence Assay in Biology and Medicine, Academic Press, N.Y., (1969), pp. 568—572.
13 H. V. P. Klochkov and A. M. Makusheuko, Opt. Spectrosc., 15 (1963) 25.
14 E. D. Pellizzari and C. M. Sparacino, Anal. Chem., 45 (1973) 378.

Analytica Chimica Acta, 89 (1977) 21—28

AN AUTOMATED FLUORESCENCE METHOD FOR THE DETERMINATION OF TOTAL AMINO ACIDS IN NATURAL WATERS

BJÖRN JOSEFSSON, PETER LINDROTH and GÖRAN ÖSTLING

Department of Analytical Chemistry, University of Gothenburg, Fack, S-402 20 Göteborg 5 (Sweden)

(Received 26th August 1976)

SUMMARY

An automated procedure, with *o*-phthaldialdehyde as a fluorogenic reagent for the determination of total α-amino acids in natural waters is given. The response of different amino acids, dipeptides and amino sugars has been tested as well as the interference of other nitrogen-containing substances. The method is well suited to determinations of the amino acid content in the range 0.05—15 μM with an analysis rate of 20 samples per hour.

There has recently been great interest in studying the dissolved free amino acids in oceanic and estuarine waters. It is believed that chemical studies of marine productivity will be enhanced by the development of suitable methods for the determination of extremely low concentrations of such nitrogen-containing substances as amino acids. The need for accuracy is high in sea-water analysis because the variations in the distribution of the components can be rather small in the open sea. Estuarine waters, in particular, require analysis of large numbers of samples because of the complexity of mixing of different waters as well as seasonal effects. It is desirable to have a rapid, simple and robust sea-going technique with a minimum of manual operations.

Several methods of determining specific amino acids in sea water have been developed [1—3]. These involve a desalting step and subsequent chromatographic separation. However, the time consumption and the considerable operative complexities of these techniques make them rather unattractive for on-board routine analysis. Thus the samples have to be stored and the determinations carried out after the cruise. The delay will often lead to changed composition of the original amino acids.

Methods used in the field to study the nitrogen nutrient budget are often based on colorimetric measurements of ammonia and nitrite. The organic part of the total nitrogen is usually calculated from measurements before and after a Kjeldahl digestion procedure and a reduction of nitrate to nitrite.

An automated field method for total dissolved free amino acids in sea water was reported by Coughenower and Curl [4]. Ninhydrin was used as colorimetric reagent with a detection limit of 0.5 μM. In a wide salinity range a salt correction was necessary.

Recently, reagents for primary amines have been reported by Roth [5] and Udenfriend et al. [6]. The reagents fluorescamine and *o*-phthaldialdehyde give rise to strongly fluorescent compounds on reaction with primary amines without heating, and the reactions are well suited to automatization. The sensitivity is much better than that of the colorimetric ninhydrin procedure [5].

Fluorescamine was used by North [7] in a manual study of primary amines in Californian coastal waters. The *o*-phthaldialdehyde reagent gives about the same response with most primary amino acids, whereas the response of the fluorescamine reaction product differs more, according to Fourche et al. [8]. *o*-Phthaldialdehyde was also reported to be more sensitive [9]. Accordingly, *o*-phthaldialdehyde was applied for automated analyses of primary amines in sea water in the work described here.

EXPERIMENTAL

Apparatus

The analyzing system consisted of the following three parts. A flow scheme for the setup is shown in Fig. 1.

Proportioning pump. Three different pumps were used on different occasions, a Technicon AutoAnalyzer I, an Ismatec Micro Pump and a Desaga; all were found to function well. The connections were standard T-junctions, modified with inserted tubings, as indicated in the flow scheme, to minimize carry-over effects. Tygon tubing was used in the pump. Tubes to the fluoromonitor and from sample and reagent bottles were of teflon, with an inside diameter of 0.3 mm.

Fluoromonitor. A LDC double-beam fluoromonitor model 1309 equipped with flow-cells of about 10-μl volume was used. One of the flow-cells was connected to the flow system, and the fluorescence was recorded against

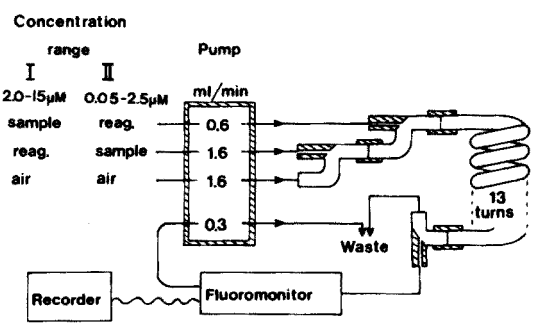

Fig. 1. Flow scheme for the apparatus for analysis of amino acids.

the air-filled reference cell. Filter characteristics were 320—400 nm for excitation and 400—700 nm for emission.

Recorder. The recorder used was a Houston Instrument Omniscribe, operated on the 10-mV scale.

The flow system could be changed easily to operate at two different concentration ranges simply by changing the sample and reagent connections at the pump inlet. The throughput time from sample inlet to recorder response was about 1.5 min, and a correct base-line after analyzing a 10 μM glycine solution was obtained after 2 min.

A different flow scheme taking advantage of the possibility of making a simultaneous background correction was also tested. In this procedure, a second flow stream with sample diluted with borate buffer was connected to the reference cell of the fluoromonitor. However, this method was later abandoned because of the loss of information on the sea-water background fluorescence.

Reagents

o-Phthaldialdehyde solution. 100 mg of compound (Durrum) was dissolved in 10 ml of ethanol (99.5%).

Borate buffer. Boric acid solution (0.4 M) was adjusted to pH 9.5 with 1 M NaOH.

Buffered reagent solution. 2-Mercaptoethanol (2 drops; Serra, Feinbiochemica, Heidelberg) was added to 100 ml of the borate buffer and mixed. Then 2.5 ml of *o*-phthaldialdehyde solution was added and mixed. The reagent could be used after 30 minutes, and was stable for about two days at room temperature. When the response diminishes, an addition of two more drops of mercaptoethanol will restore the reagent to working condition.

Sample solutions

Stock solutions. The amino acids, dipeptides and amino sugars were dissolved to give 2.0-mM aqueous solutions and kept at room temperature. Calibration solutions were freshly prepared from the stock solutions.

Sea-water samples. The method described is intended for use as a field technique for immediate analysis. If direct analysis is not possible, the samples should be preserved by adding two drops of toluene per 100 ml of sample as soon as possible. Samples will then be stable in total amino acid concentration for at least one week.

Procedure

A calibration curve with glycine solutions was prepared before every sample series. Response graphs recorded when glycine solutions were introduced at 2-min intervals for two concentration intervals are shown in Fig. 2. The calibration curve was corrected for the background originating from reacting substances in the re-distilled water used to prepare the glycine

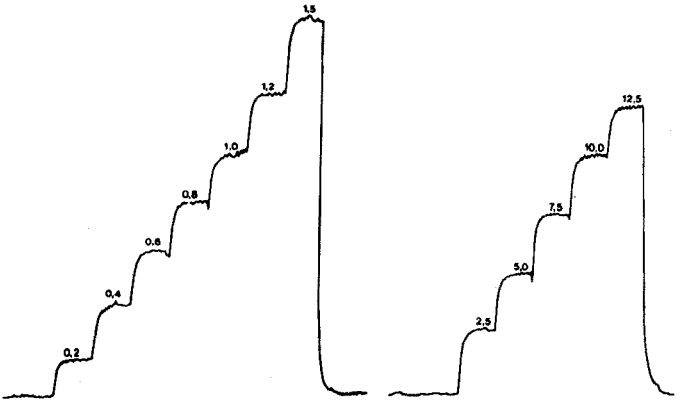

Fig. 2. The fluorescence intensity recorded (arbitrary units) on introducing calibration solutions at 2-min interval. The numbers inserted above each response correspond to the glycine concentration in μM.

solutions, as follows. First, the buffered *o*-phthaldialdehyde reagent was pumped both as sample and reagent. When a stable line was obtained, the distilled water was pumped as sample (Fig. 3); in Fig. 3, the buffered reagent gave a background intensity of 41 mm, and 16 mm when diluted with distilled water. If the water were absolutely free from amino acids or other reacting substances, the expected intensity would be (41 × 0.6/2.2) = 11 mm. The contribution to the intensity from amino acids in the distilled water is therefore (16 — 11) = 5 mm, which should be subtracted from the intensities of the glycine standards.

Samples were then analyzed successively with distilled water used as rinse between the samples, and finally the background fluorescences of the samples were recorded, diluted with distilled water instead of reagent solution.

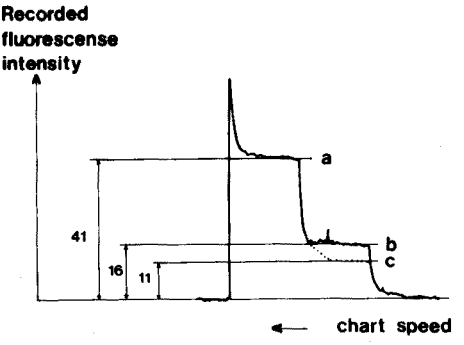

Fig. 3. The fluorescence intensity (arbitrary units) recorded for the amino acid content in the distilled water used to make up calibration solutions. (a) Buffered reagent solution is pumped both as sample and reagent. (b) The distilled water is pumped as sample. (c) The expected response for distilled water free from amino acids.

RESULTS

Response and precision

Amino acids. The fluorescence intensities recorded are closely related to the molecular structure of the amino acid. According to Roth [5] and Fourche et al. [8], only those amino acids with the amino group in the α-position will give fluorescent products with the reagent. Analyses for amino acids with the automatic equipment confirm their results (Table 1).

Dipeptides and amino sugars. Various compounds were analyzed and related to a glycine calibration curve. The relative responses in glycine units are shown in Table 2.

The precision of the automated method was evaluated by 15 determinations of a 10-μM glycine solution. The standard deviation was calculated to $s = \pm 0.63$. With a signal-to-noise ratio of 3:1, the detection limit is 0.05-μM glycine units.

TABLE 1

Relative fluorescence intensities (in glycine units) for 10-μM amino acid solutions

Amino acid	F.I.	Amino acid	F.I.	Amino acid	F.I.
Glycine	10.0	Leucine	12.4	Histidine	8.6
Alanine	9.0	Norleucine	12.5	Phenylalanine	10.3
Serine	5.2	Aspartic acid	9.0	Ornithine	1.5
Proline	0.6	Glutamine	9.5	Arginine	10.6
Threonine	0.9	Lysine	0.7	Tyrosine	11.1
Valine	10.2	Glutamic acid	6.9	Tryptophan	11.8
Cysteine	0.3	Methionine	12.3	Cystine	0.9
Hydroxyproline	0.0	Asparagine	11.0	Tranexamic acid	9.3
Isoleucine	12.8				

TABLE 2

Relative fluorescence intensities (in glycine units) for 1.0-μM dipeptides, 1.0-μM amino sugars and 10-μM nitrogen-containing compound solutions

Dipeptide	F.I.	Amino sugar	F.I.	N-compound	F.I.
Glycyl glycine	<0.05	*N*-Acetyl-D-mannosamine	<0.05	Ammonia	1.8
Glycyl serine	0.27	D-Mannosamine	0.50	Urea	0.0
Glycyl alanine	0.32	*N*-Acetyl-D-galactosamine	0.06	Hydroxylamine	0.0
Alanyl glycine	0.09	D-Galactosamine HCl	0.65		
Alanyl alanine	0.08	Glucosamine	0.37		
Leucyl glycine	0.14				
Glycyl leucine	0.23				
Alanyl phenylalanine	0.28				

Interferences

As has been shown earlier, *o*-phthaldialdehyde is basically a primary amine reagent. In analyses for the total concentration of amino acids in natural waters, it is of interest to know the influence of other nitrogen substances as well as the influence of bulk electrolytes. No salt effect was observed in the analysis of glycine solutions prepared in dilutions of Standard Sea Water from 35 to 0 S °/₀₀. The response for some common nitrogen compounds in natural waters is listed in Table 2 (columns 5 and 6).

It should be pointed out that, for work in the sea-water concentration range, it is important not to deposit fingerprints on stoppers or other surfaces that might come in contact with the sample solution. Even airborne particles in the laboratory contain enough amino acids to cause severe contamination.

Amino acid determinations in the Gothenburg archipelago

In June 1976 water from nine different places in the Gothenburg archipelago (Fig. 4) were collected and analyzed for their amino acid content. The samples were treated as follows: (a) no treatment; (b) filtered through 0.45-μm Millipore HA filters with a syringe; (c) preserved with toluene; (d) filtered as above and preserved with toluene.

The samples were analyzed immediately after sampling and then after one and six days. The results of these analyses are shown in Table 3. The data show clearly the fast depletion of the amino acid content in untreated samples, and that no severe reduction in concentration occurs after the samples have been preserved with toluene. There is a marked difference in

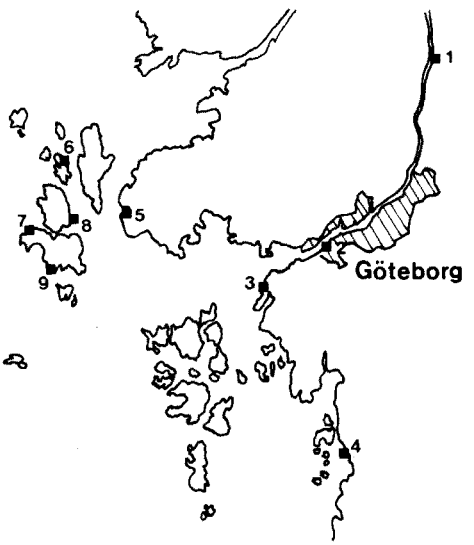

Fig. 4. The location of stations 1—9.

TABLE 3

Total free amino acid concentrations in samples from the Göta River and the archipelago of Göteborg in glycine units (μM) (for further information, see text.)

Station	After 3—5 h	After 1 d	After 6 d	Station	After 3—5 h	After 1 d	After 6 d
1 a	0.68	0.09	0.12	6 a	1.60	0.70	0.39
b	0.73	0.38	0.14	b	1.70	0.87	0.34
c	0.96	0.93	0.91	c	1.71	1.75	1.63
d	0.70	0.66	0.62	d	1.74	1.77	1.63
2 a	0.43	0.15	0.18	7 a	0.64	0.12	0.19
b	0.38	0.32	0.09	b	0.65	0.35	0.19
c	0.63	0.58	0.61	c	0.67	0.62	0.71
d	0.44	0.37	0.36	d	0.65	0.62	0.70
3 a	0.09	0.02	0	8 a	0.86	0.18	0.35
b	0.14	0.07	0	b	0.90	0.26	0.21
c	0.23	0.20	0.17	c	0.96	1.01	1.05
d	0.14	0.10	0.07	d	0.92	0.96	0.97
4 a	0.24	0.05	0.07	9 a	1.12	0.48	0.69
b	0.28	0.13	0	b	1.16	0.32	0.57
c	1.47	1.50	1.60	c	1.21	1.36	0.74
d	0.34	0.27	0.23	d	1.21	1.23	1.23
5 a	0.77	0.39	0.48				
b	0.75	0.24	0.26				
c	0.91	0.93	0.95				
d	0.82	0.86	0.80				

the "particle-bound" and "free" amino acid concentration for stations 1—4, which are all of low salinity, but not for stations 5—9, which are of higher salinity.

The data also indicate that interesting information may be found when more complete analyses of the samples containing nitrate, nitrite and total nitrogen are performed.

DISCUSSION

There is no doubt that a total amino acid measurement will not give a full understanding of the prevailing amino acid status of a sample. Further analyses, including a separation step, are necessary for the acquisition of detailed data. The method given in this paper should be regarded as a procedure that gives quickly a picture of which samples should be studied further. It is, of course, possible to connect the apparatus to a chromatographic column and make a measurement of the different amino acids of a selected sample. Such a procedure is now being developed in this laboratory.

It is somewhat unsatisfactory that the reaction product of *o*-phthaldialdehyde and primary amino acids is not known. Thus the lack of reactivity or

weak response of some primary amines (see Table 1) cannot be explained. Primary amino acids with an OH end group (serine, threonine), an SH end group (cysteine), and an NH_2 end group (lysine, ornithine), give weak responses.

Ninhydrin reagent also gives different responses with different amino acids, especially cystine, arginine and histidine (which are overestimated) [4]. Proteins and peptides will also give colored products on reaction with ninhydrin. The reaction products of *o*-phthaldialdehyde with these compounds are weakly fluorescent, so that combined amino acids are not measured.

The simplicity of the technique outlined indicates that the analytical method presented should be found to work well not only in analytical chemistry laboratories but also in field work.

The authors express their thanks to Professor David Dyrssen for valuable discussions, and to Miss Christel Carlsson for technical assistance. This work was supported by the Swedish Natural Science Research Council.

REFERENCES

1 A. Siegel and E. T. Degens, Science, 151 (1966) 1098.
2 J. P. Riley and D. A. Segar, J. Mar. Biol. Ass., U.K., 50 (1970) 713.
3 R. Pocklington, Anal. Biochem., 45 (1972) 403.
4 D. D. Coughenower and H. C. Curl, Jr., Limnol. Oceanogr., 20 (1975) 128.
5 M. Roth, Anal. Chem., 43 (1971) 880.
6 S. Udenfriend, S. Stein, P. Bohlen, W. Dairman, W. Leimgruber and M. Weigele, Science, 178 (1972) 871.
7 B. B. North, Limnol. Oceanogr., 20 (1975) 20.
8 J. Fourche, H. Jensen and E. Neuzil, Anal. Chem., 48 (1976) 155.
9 J. R. Benson and P. E. Hare, Proc. Nat. Acad. Sci., U.S.A., 72 (1975) 619.

Analytica Chimica Acta, 89 (1977) 29—35

AN AUTOMATED FLUORIMETRIC METHOD FOR THE DETERMINATION OF NANOGRAM QUANTITIES OF SELENIUM

M. W. BROWN and J. H. WATKINSON

Ministry of Agriculture and Fisheries, Soil and Field Research Organisation, Ruakura Agricultural Research Centre, Hamilton (New Zealand)

(Received 6th September 1976)

SUMMARY

An automated solvent extraction method, based on the fluorescence of 4,5-benzopiazselenol has been developed for the determination of nanogram quantities of selenium. Sample extracts, analysed at a rate of 40 per hour, gave standard deviations of 0.022, 0.054, 0.096 ng g^{-1} at levels of 1, 5 and 10 ng g^{-1} respectively. The detection limit was therefore approximately 0.044 ng g^{-1}. Of the more common ions at 1 mM concentration, only palladium(II) and tin(IV) caused appreciable interference in the presence of oxalate or ethylenediaminetetraacetic acid.

In conducting research into selenium deficiencies in animals, and studies of selenium in the environment, relatively large numbers of analyses are required for parts per billion (p.p.b., ng g^{-1}) levels of selenium. The manual method based on the fluorescence of 4,5-benzopiazselenol (DAN-Se) [1], is time-consuming and requires the services of a skilled analyst. With Technicon Auto-Analyzer equipment and a Turner fluorimeter, an automated system, developed from the manual method, permits the analysis of 40 sample solutions per hour with a precision, accuracy, and sensitivity similar to that of the manual method [1].

EXPERIMENTAL

Apparatus

The major items of equipment were a Technicon Sampler IV, Technicon pump III (Technicon Instruments Corporation, Tarrytown, New York), Turner fluorimeter model 111 (G. K. Turner Associates, Palo Alto, California), and a Rikadenki "Kasset" strip-chart recorder coupled in that order.

The Sampler IV and pump III were standard Technicon modules, except that a pyrex glass probe replaced the standard stainless steel probe of the sampler. (This avoided the possibility of contamination from iron(III) by the action of the hydrochloric acid and the adsorption of trace amounts of selenite on the oxide surface.) The Turner fluorimeter was fitted with the Automated

Chemistry Adapter supplied by the manufacturer. The adapter flow-cell had a relatively large internal volume (1 ml), which gave poor wash characteristics and a sluggish response. Therefore an improved flow-cell with an internal volume of ca. 0.3 ml and an optical area of 75% of the original was fitted. The dimensions of the flow-cell are detailed in Fig. 1. The optical system of the fluorimeter consisted of (a) a general purpose mercury lamp and narrow pass filter, number 7-60, providing irradiating ultraviolet light peaked at 360 nm, and (b) a secondary filter (Schott interference type DAL) having maximum transmission at 550 nm.

The strip-chart recorder was fitted with a multi-range input unit set at 0.1 V full scale deflection.

The Auto-Analyzer manifold, designed for extracts containing 0—10 p.p.b. of selenium, is detailed in Fig. 2. Standard Technicon Auto-Analyzer II parts were used throughout.

Manifold procedures

The crucial stage of the system is the phase separation. A trace of aqueous phase passing into the flow-cell produces an enhanced fluorescence. Any aqueous solution adhering to the flow-cell walls must be cleared before analysis can continue. The phase separation is optimized by: (a) adjusting the flow rates to waste from the phase separator, so that slightly less cyclohexane than air is pumped from the upper outlet of the separator; (b) injecting the cyclohexane at two points so spaced that the solvent is evenly distributed within the aqueous phase; (c) using a phase separator cleaned in concentrated nitric acid; (d) by-passing the pump air-bar for the air-line to the separator. (The more positive injection of air when using the air-bar sometimes causes pressure changes within the separator that result in some aqueous phase passing into the flow-cell.)

It is essential to use glass tubing for all transmission lines between the injection of aqueous 2,3-diaminonaphthalene (DAN) and the phase separator, since DAN-Se is absorbed by plastic tubing. Also, ultraviolet light must be excluded to prevent photochemical reactions with the aqueous DAN.

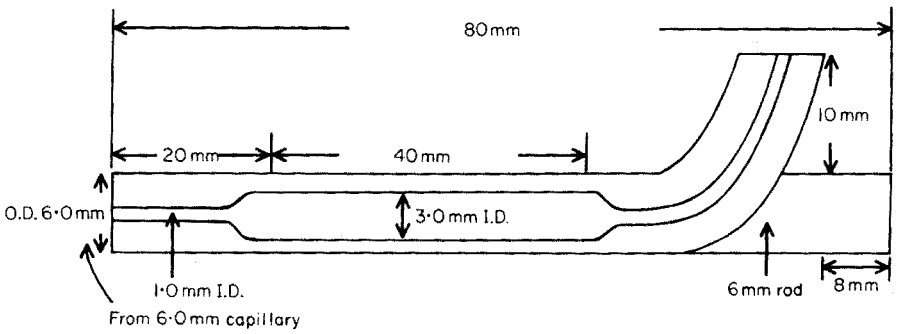

Fig. 1. Cylindrical flow-cell constructed from pyrex glass.

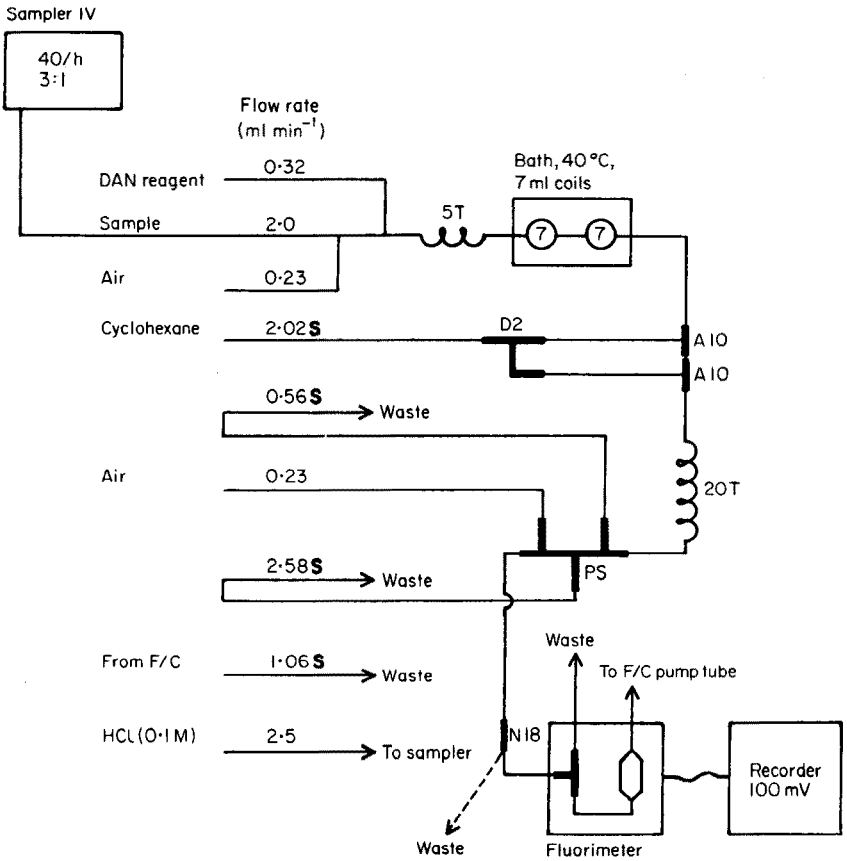

Fig. 2. Auto-Analyzer Manifold. S after flow rate indicates solvaflex tubing. F/C denotes flow-cell. PS denotes a 5-point phase separator with teflon insert. Transmission line from separator to fluorimeter is polythene (i.d. 0.03 in.). All other transmission lines are glass.

In practice, this is effected by covering the water bath to keep the reaction coils in darkness. For the remainder of the manifold, it is sufficient to screen out ultraviolet radiation from daylight.

While the system is reaching a steady state, the nipple joint in the polythene line connecting the phase separator with the flow-cell is disconnected to allow any aqueous phase passing through the separator to flow directly to waste. Residual water is then removed by allowing a small amount of ethanol to pass to waste through the air inlet of the separator and the polythene line, before reconnecting to the flow-cell.

When a batch of analyses has been completed, the DAN reagent is replaced by 0.1 M hydrochloric acid so that the DAN is flushed out of the system and later deposition of DAN polymer is prevented. The flow-cell is cleaned and filled with 10% (v/v) petroleum ether in ethanol (the mixture having a similar density to cyclohexane) to prevent a slow increase in cell

fluorescence. If, during an analysis, some of the aqueous phase inadvertently enters and remains in the flow-cell, the cell is similarly cleaned after the flow-cell has been disconnected from the phase separator.

Reagents

2,3-Diaminonaphthalene dihydrochloride in 0.1 M HCl (0.5% w/v). Keep the reagent in a brown bottle under cyclohexane after having shaken the two phases to purify the reagent. The dihydrochloride was prepared from technical grade DAN by recrystallization from (1 + 1) HCl. Redistilled cyclohexane was used.

Analysis of samples

The system was designed primarily to allow easier and more rapid handling of blood analyses, but by suitable preparation of sample solutions the system can be applied to other materials. Specific applications of the method to biological systems will be the subject of later papers.

The essential requirements for any solution intended for analysis by the above method are that: (a) the selenium should be present as selenium(IV); (b) the sample solution should be in the pH range 1—2; (c) complexing agents should be added when interfering ions are present. The reasons for these requirements are detailed below.

RESULTS AND DISCUSSION

Experimental conditions

DAN reacts specifically with selenous acid; the three factors controlling the reaction are pH, temperature, and the concentration of DAN.

The pH for maximum fluorescence of the resultant DAN—Se in cyclohexane by the manual method was established as pH 1—2. This is the same range as for maximum absorbance of DAN—Se in aqueous solution [2]. In the present instance the sample solution is mixed with the acidic DAN reagent in the ratio 1:7, so that even neutral weakly buffered solutions would be in the required pH range after mixing. Also, solutions with pH 0.1—1.0 could be analysed, at slightly lower sensitivity, provided that they all had the same pH value

The effects of temperature and concentration of DAN dihydrochloride on the reaction of DAN with selenous acid are shown in Fig. 3. A concentration of 0.5% (w/v) of DAN dihydrochloride and a reaction temperature of 40°C were selected as standard operating conditions. At greater reagent concentrations there was a tendency for the DAN to crystallize out on cooling between the heating bath exit and the point of injection of cyclohexane. This caused breakdown of the bubble pattern and eventual blockage of the line. Higher temperatures resulted in slightly poorer precision at low concentrations of selenium. This was caused by an increase in both the absolute value of the baseline (reagent blank) from the DAN (Fig. 4), and its variation with time.

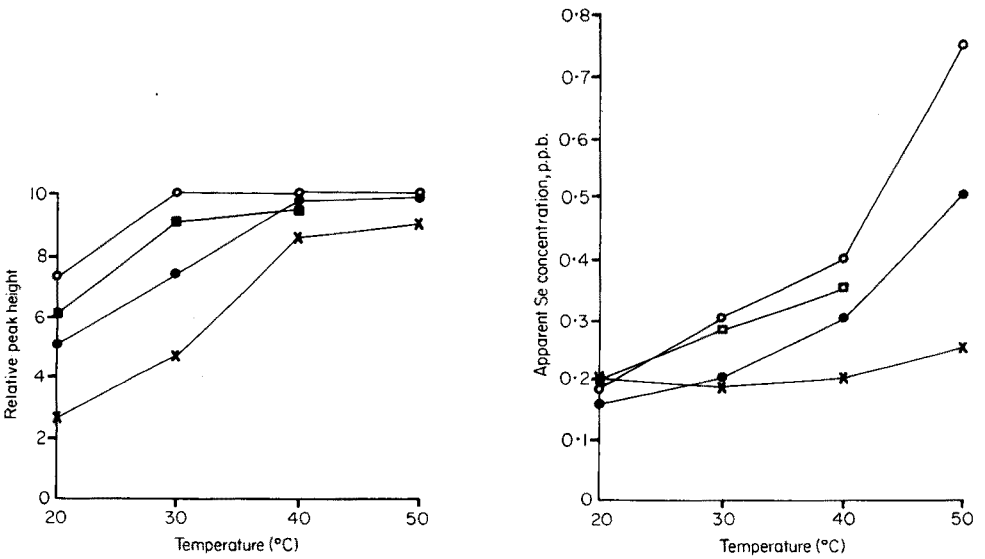

Fig. 3. The variation of sensitivity (at 10 p.p.b. Se) with temperature and concentration of DAN. (x) 0.25%, (•) 0.50%, (▪) 0.75%, (○) 1.0% DAN dihydrochloride.

Fig. 4. The variation of reagent blank with temperature and concentration of DAN. Symbols as for Fig. 3.

Precision, sensitivity and linearity

Fluorescence values were measured for quadruplicates of 1, 5 and 10 p.p.b. selenium standard solutions on thirty occasions over a period of four months. The mean values found for the 1 and 5 p.p.b. standards were 10.09% and 50.09% respectively of that found for the 10 p.p.b. standard solution.

The standard deviations at the three concentrations 1, 5 and 10 p.p.b. were 0.022, 0.054 and 0.096 p.p.b., respectively. The error variances clearly differ for the three levels of concentration ($P < 0.001$). Taking the detection limit to be twice the standard deviation at 1 p.p.b. gives a value of 0.044 p.p.b. In absolute quantities this corresponds to a detection limit of 0.088 ng, since the system utilizes 2 ml of sample solution.

For each of the 30 sets, an unweighted linear regression contrast of means was tested against a standard error based on the three pooled-within-levels variances. All were statistically significant ($P < 0.001$), giving 30 estimates of the linear coefficient with mean 0.9987 (s.d. 0.004).

The orthogonal contrast of deviation from linearity was statistically, but not analytically, significant for several sets, but equally often for positive and negative curvature. The differences between the observed value and 5 p.p.b., and that predicted from interpolation between 1 and 10 p.p.b. levels, gave a mean of −0.004 (s.d. 0.09). Clearly, any bias in using a linear calibration would be negligible.

Interferences

Most of the ions commonly encountered have been investigated for possible interferences in earlier work [1, 2—5]. Those that apparently interfered were retested, and some ions not previously tested were also investigated e.g. silver(I) (in perchlorate media), platinum(IV), zirconium(IV), vanadium(V), molybdenum(VI) and tungsten(VI). In addition, to validate procedures for avoiding interference from nitrite and vanadium(V), the previously reported non-interference from nitrate [2] and vanadium(IV) [1] was also checked. Possible interference from the above ions was examined by analyzing a 5 p.p.b. ($6 \cdot 10^{-8}$ M) selenium standard solution containing 1 mM of the ion under test, 4 mM ethylenediaminetetraacetic acid (EDTA), and 0.1 M hydrochloric acid; Table 1 presents results that gave a mean recovery of 5 p.p.b. selenium within experimental error. Of these ions, silver(I) and titanium(IV) were studied in the absence of EDTA, and gave values of 5.03 and 4.83 p.p.b., respectively. The result for titanium(IV) is significantly low.

The ions that caused a significant error in the presence of EDTA are listed in Table 2. There is a low recovery in the presence of iron(II),

TABLE 1

Ions at 1 mM giving no interference in 4 mM EDTA solution. The values shown are the mean of 10 replicate analyses of a 5 p.p.b. Se solution

Ag(I)	5.02				
Co(II)	5.01; Cu(II)	5.03; Mn(II)	4.99; Ni(II)	5.00; Pb(II)	5.02
Al(III)	5.04; Cr(III)	4.99; Fe(III)	4.99; Sb(III)	5.03	
Ti(IV)	5.01; V(IV)	5.04			
Mo(VI)	4.99				
Nitrate	4.99; Sulphate 5.02; Citrate 5.02; Oxalate 4.99				

TABLE 2

Ions at 1 mM causing interference in a 5 p.p.b. Se solution containing 4 mM EDTA or oxalate

Ion (1 mM)	No complexing agent			EDTA (4 mM)			Oxalate (4 mM)		
	Mean	s[a]	Sig.[b]	Mean	s[a]	Sig.[b]	Mean	s[a]	Sig.[b]
Fe(II)	4.98	0.018	N.S.	3.96	0.053	***	5.03	0.084	N.S.
Pd(II)				4.00	0.060	***	4.26	0.064	***
Pt(IV)	6.74	0.284	***	5.38	0.050	***	5.18	0.047	***
Sn(IV)	0.67	0.028	***	0.57	0.036	***	4.54	0.044	***
Zr(IV)	1.75	0.057	***	4.78	0.028	***	5.07	0.067	*
V(V)				10.38	0.092	***			
W(VI)				4.73	0.169	***	5.04	0.044	*
NO_2^-				5.54	0.040	***			

[a]Standard deviation. [b]Significance of difference of mean from 5 p.p.b. Se. N.S. Not significant. *$0.05 \geq P > 0.01$. *** $0.001 > P$.

palladium(II), tin(IV), zirconium(IV), and tungsten(VI). With iron(II) there may be partial reduction of selenium(IV) by the iron—EDTA complex, but there is no interference from iron(II) itself. The interference caused by palladium(II) is probably due to the formation of a stable addition compound between DAN—Se and palladium(II) [6]. The anomalous results caused by tin(IV), zirconium(IV) and tungsten(VI) probably arise from the reaction of selenium(IV) with trace quantities of the hydrous oxides of these elements (cf. titanium(IV) in the absence of EDTA).

The enhanced values in the presence of platinum(IV) and vanadium(V) are probably a result of the oxidation of DAN. Nitrous acid would give an increased fluorescence through the formation of 2,3-naphthotriazole with DAN [5].

Some of these interfering ions form stable complexes with oxalate, and results of tests carried out in the presence of 4 mM oxalate are also reported in Table 2. Further tests on nitrite and vanadium(V) were not carried out because they are readily oxidized or reduced by citric acid [7] to the non-interfering nitrate and vanadium(IV). Oxalate improves the recovery of selenium in the presence of each ion, although for palladium(II) and possibly tin(IV), other means of avoiding errors would be needed. For platinum(IV) there is a small carry-over effect, giving increased values for consecutive samples, which is greater with EDTA than with oxalate.

Both strong oxidizing or reducing agents react with either DAN or selenium(IV). The reduced or oxidized forms of many substances are stable to selenium(IV), so that such interferences can be avoided by reduction or oxidation during the preliminary preparation of the sample solution.

Conclusions

The automated method is considerably more rapid and less laborious than the manual method and possesses at least equal sensitivity and precision. By control of oxidation conditions and the addition of EDTA or oxalate, significant interference is not encountered from common ions at 1 mM concentrations, with the exceptions of palladium(II) and tin(IV). Consequently, the method can be used for the analysis of a wide variety of materials containing trace levels of selenium.

The authors are grateful to C. B. Wright for making the flow-cell; Elysia K. Patterson and Gael V. Montgomery-Griffith for analytical assistance; and D. M. Duganzich for statistical analyses.

REFERENCES

1 J. H. Watkinson, Anal. Chem., 38 (1966) 92.
2 P. F. Lott, P. Cukor, G. Moriber and J. Solga, Anal. Chem., 35 (1963) 1159.
3 P. Cukor, J. Walzcyk and P. F. Lott, Anal. Chim. Acta, 30 (1964) 473.
4 J. A. Raihle, Environ. Sci. Technol., 6 (1972) 621.
5 E. L. Wheeler and P. F. Lott, Microchem. J., 19 (1974) 390.
6 H. K. Y. Lau and P. F. Lott, Talanta, 17 (1970) 717.
7 J. H. Watkinson, N.Z. J. Sci., 1 (1958) 201.

Analytica Chimica Acta, 89 (1977) 37—46

A CATALYTIC-KINETIC METHOD FOR THE DETERMINATION OF TRACES OF FLUORIDE IN BIOLOGICAL MATERIAL

DIETER KLOCKOW and JÜRGEN AUFFARTH

Chemisches Laboratorium der Universität Freiburg, Lehrstuhl für Analytische Chemie, D-78 Freiburg (B.R.D.)

CHLODWIG KOPP

Tierhygienisches Institut, D-78 Freiburg (B.R.D.)

(Received 2nd September 1976)

SUMMARY

A catalytic-kinetic method for the determination of nanogram amounts of fluoride, based on its inhibiting action on the catalyst in the zirconium-catalyzed reaction between perborate and iodide, is described. The rate measurements are accomplished very simply by using a Landolt reaction system with a biamperometric detection of the induction period. The standard deviation in the working range 19—190 ng of fluoride (1—10 nmol) is ± 2 ng. The method can be made specific by combining it with a separation of the fluoride by microdiffusion. This has been demonstrated by analyzing biological material and comparing the results with the fluoride contents obtained with other methods.

The effects of fluoride-containing emissions on vegetation and livestock have been thoroughly investigated during the past two decades [1—3]. Over long periods of exposure even low concentrations of such materials can lead to substantial poisoning. Therefore, sensitive and reliable methods for the determination of small amounts of fluoride in various materials are still of practical interest.

Many problems in applied trace analysis become complicated by the difficulty of recognizing and avoiding systematic errors. This is also the case in the determination of fluoride in biological material. Reliable analytical statements can be made only if two or three independent parallel methods yield comparable results for the same sample. For this reason we present a technique alternative to the existing analytical procedures.

During recent years, trace amounts of fluoride have been determined most commonly by the photometric alizarin complexan method [4] or by using a fluoride-selective electrode [5]. A kinetic method has been proposed [6]; this is based on the inhibiting effect of fluoride on the reaction between perborate and iodide with zirconium as a catalyst. The fluoride inhibition of the catalyst was measured by a 'stat'-technique (potentiostat).

The latter technique has been applied to the analysis of clean air aerosols and satisfactory results have been obtained in the range 0.05—1 $\mu g\ F^-\ m^{-3}$ [7]. However, the procedure was considered to be too complicated for practical

routine work, and a simpler version of the method was therefore developed. The perborate—iodide reaction was modified to a Landolt-system by adding a small amount of ascorbic acid. This same system has been used by Thompson and Svehla [8] for the determination of iron and molybdenum. By this means, the highly sensitive inhibition of zirconium by fluoride can be combined with the very simple 'chronometric' or 'variable time' technique, which is well known in kinetic methods of analysis.

The slow reaction between perborate and iodide,

$$BO_3^- + 2\,I^- \rightarrow BO_3^{3-} + I_2,$$

catalyzed by zirconium at pH 1—2, is coupled to the fast consecutive reaction between iodine and ascorbic acid:

$$I_2 + \text{ascorbic acid} \rightarrow 2\,HI + \text{dehydroascorbic acid.}$$

Free iodine cannot appear in the reaction mixture until all the ascorbic acid has been oxidized. The time between the start of the reaction, $BO_3^- + 2\,I^-$ + ascorbic acid $\xrightarrow{Zr/F^-}$, and the complete consumption of the ascorbic acid is measured by detecting the free iodine biamperometrically. At constant pH and temperature, this time — the 'induction period' — depends only on the amount of ascorbic acid present and on the rate of the catalyzed reaction. If the same concentrations of ascorbic acid, perborate (in large excess with respect to ascorbic acid), iodide, and zirconium catalyst are always used, then the induction period is determined by the amount of fluoride added to the mixture.

The Landolt reaction system described can be used to determine fluoride in the range 1—10 nmol (19—190 ng F^-). Gaál et al. [9] have recently described similar chronometric techniques for the determination of fluoride at the μg—mg level. It has been shown [6] that several cations and anions interfere with the catalytic-kinetic method for fluoride. The inhibition of the zirconium catalyst is selective for fluoride but not specific. Therefore a separation of the fluoride from the bulk material will be necessary for most practical analytical problems. In order to determine traces of fluoride in biological materials, the Landolt reaction technique can be combined with a separation by microdiffusion with hexamethyldisiloxane [10, 11].

EXPERIMENTAL

Apparatus

A thermostat (temperature stability ± 0.1 °C) with a water bath and a recirculating pump was used with a double-walled reaction vessel, made of borosilicate glass (capacity ca. 8 ml), black coated to avoid light influence on the reaction (Fig. 1).

A biamperonetric detector with a timer (Electronica, Spezial-Messgeräte Gmbh, P.O. Box 17, D-7051 Hegnach) was used. This device (Fig. 2) can supply a variable polarization voltage of 15—30 mV to two platinum

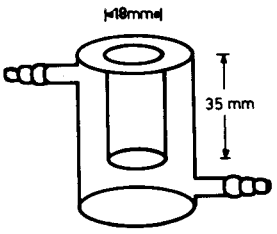

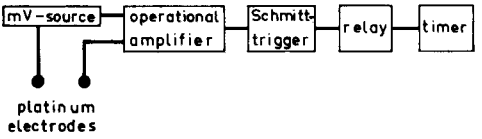

Fig. 1. Reaction vessel.

Fig. 2. Biamperometric detector with timer, block diagram.

electrodes inserted into the medium under study, and at the same time initiate a timer. A change in the chemical composition of the mixture, causing depolarization of the electrodes, produces an increasing depolarization current, which coupled with an operational amplifier fires the Schmitt-trigger. If the depolarization current exceeds a preset limit, the Schmitt-trigger switches off the timer through a relay. A built-in time delay relay prevents the counter from being prematurely switched off by the brief initial polarization current, produced by the initial energizing of the electrodes.

A double platinum indicator electrode was used, e.g. model Pt-880-M5 (Dr. W. Ingold KG, D-6000 Frankfurt/Main 1).

Eppendorf microliter pipettes (10, 20, 50, 100, 200, 500, 1000 μl; Eppendorf Gerätebau Netheler + Hinz, D-2000 Hamburg 63), Eppendorf micro test tubes (polypropylene, 1.5 ml), and high-density polyethylene vials (capacity ca. 20 ml) with polyethylene caps, as used in liquid scintillation counting were required. The tubes and vials were rinsed with twice-distilled water before use. An electric rotator with a disc held the polyethylene vials in nearly horizontal positions (Fig. 3).

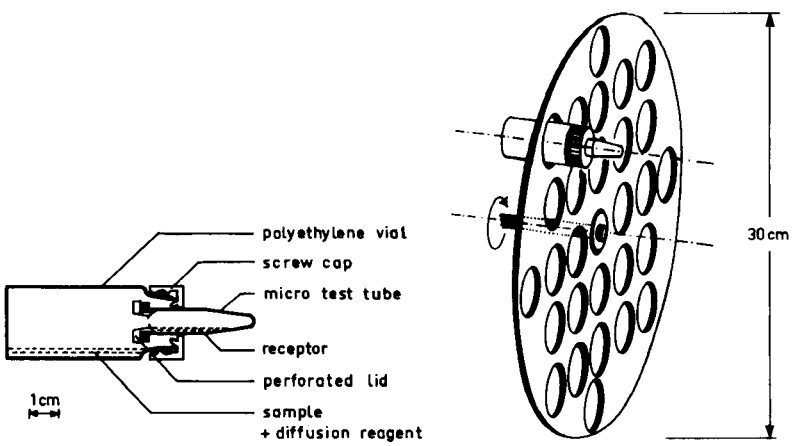

Fig. 3. Diffusion device and rotator disc.

Solutions and reagents

I. Zirconium stock solution, 10^{-2} M. Dissolve 322.25 mg of $ZrOCl_2 \cdot 8 H_2O$ (Merck, p.a.) and dilute to 100 ml with 0.1 M HCl. Store in a refrigerator at about 4 °C for at least one month and then use for the preparation of the 10^{-4} M working solution [6].

II. Zirconium working solution, 10^{-4} M. Dilute 1 ml of (I) to 100 ml with 0.1 M HCl. Store in a refrigerator for at least 24 h before first using it [6].

III. Perborate solution, 0.02 M. Dissolve 308 mg of $NaBO_2 \cdot H_2O_2 \cdot 3 H_2O$ (Riedel de Haen) and dilute to 100 ml with twice-distilled water. Store in a polyethylene bottle in a refrigerator at about 4 °C. It should be discarded after two weeks.

IV. Ascorbic acid stock solution, 0.1 M. Dissolve 1.761 g of L(+)-ascorbic acid (Merck, cryst., extra pure) in twice-distilled water and dilute to 100 ml. Store in a black-coated polyethylene bottle in a refrigerator, and discard after one month.

V. Ascorbic acid working solution, 10^{-3} M. Dilute 100 µl of solution (IV) with 10 ml of cold (4 °C) twice-distilled water, which has been purged with nitrogen gas for 15 min. The solution is very sensitive to oxidation and must be kept in an ice bath with light excluded. Prepare daily.

VI. Sodium fluoride standard solution, 10^{-4} M. Store in a polyethylene bottle.

Solutions (I), (II), (III), and (IV) should always be kept in a refrigerator at about 4 °C and should always be prepared in the same flasks. The solutions must be discarded if they get too warm, especially the zirconium catalyst solutions (I) and (II) [6].

VII. Reagent for microdiffusion. Dissolve ca. 100 mg of Ag_2SO_4 (Merck, p.a.) in 50 ml of 23 % perchloric acid, made from 70 % perchloric acid (Merck, p.a.). Saturate this solution with hexamethyldisiloxane (Fluka, puriss.) by shaking in a separatory funnel. The silver ions will precipitate some anions which might diffuse as volatile acids, especially chloride.

Determination of fluoride

At least one hour before starting the measurements prepare the ascorbic acid working solution (V). Put it along with some quantities of solutions (II) and (III) in glass-stoppered vessels in an ice bath. Store the sample solutions as well as the 0.1 M potassium iodide and 1 M hydrochloric acid solutions in the thermostat at 22 °C.

For the measurements, transfer 4 ml of the sample solution, containing 1—10 nmol of fluoride to the thermostated (22 °C) reaction vessel. Insert the double platinum indicator electrode into the vessel. Acidify, with magnetic stirring (PTFE-coated bar), with 500 µl of 1 M HCl to pH 1—2 and add 100 µl of the zirconium working solution (II, 0 °C). To guarantee reproducible temperature conditions in each successive measurement, the subsequent additions of 50 µl of the perborate solution (III, 0 °C) and of 50 µl of the ascorbic acid working solution (V, 0 °C) should be accomplished within

a fixed time of 1 min. Wait two further minutes for thermal equilibration and then start the Landolt reaction by adding 100 μl of 0.1 M potassium iodide solution (22 °C). Simultaneously switch on the biamperometric detector and timer.

In the Landolt reaction the ascorbic acid is exhausted after some minutes of reaction time. The iodine concentration then increases and subsequently the electrodes become more and more depolarized. When the depolarization current exceeds a fixed preset value, the timer stops, and the induction period is read directly from the timer.

Drain off the reaction mixture with a water jet pump and rinse the reaction vessel and the electrode thoroughly with twice-distilled water. After the last liquid droplets have been carefully removed by suction, the apparatus is ready for the next measurement.

The first two runs of each series are used only for conditioning the system, and the results are rejected. Identical amounts of fluoride will result in equal induction periods only if the conditions of the reaction are kept constant. Therefore, the measurement of the reagents and the order of their addition according to a fixed time schedule must be kept reproducible.

Three calibration standards, 1, 5 and 10 nmol of fluoride, are processed in duplicate together with each series of unknown samples (see below).

Microdiffusion for the separation of traces of fluoride from a matrix

Weigh several milligrams of the sample material, e.g. plant ashes, directly into the polyethylene vials and dissolve as completely as possible in 1 ml of twice-distilled water by ultrasonic agitation. Press a micro test tube with a perforated lid into the punched screw cap of the vial (see Fig. 3). Then pipet the receptor solution, consisting of 200 μl of 0.1 M NaOH and 20 μl of 2-propanol (Merck, p.a.) as a wetting agent, into the micro test tube. Fix the polyethylene vial in a nearly horizontal position in the rotator disc (see Fig. 3). Finally transfer 200 μl of the diffusion reagent (VII) into the vial and seal the vial as quickly as possible with the screw cap, containing the loaded receptor compartment (Fig. 3).

In the same way a series of diffusion devices can be prepared and fixed in the rotation disc. The latter is allowed to rotate slowly (ca. 20 r.p.m.) at room temperature for several hours. By this means the diffusion mixture and the receptor solution are agitated constantly. The time necessary for the complete diffusion of the fluoride depends on the type of sample to be analyzed. In general, a diffusion time of about 15 h (overnight) is sufficient.

Then mix the receptor solution with 1000 μl of twice-distilled water. The total volume is then approximately 1200 μl. Dilute an aliquot, equivalent to 1—10 nmol of fluoride, to 4 ml with twice-distilled water and analyze by the above method. Discard the polyethylene vial and the micro test tube after use.

When fluoride is separated by microdiffusion, the calibration procedure must also include the diffusion step. For this purpose, appropriate amounts of the 10^{-4} M NaF standard solution (VI) are treated in the same manner as the samples.

RESULTS AND DISCUSSION

Calibration graph and evaluation method

The quantity obtained in each measurement is the induction period, t_i [s], of the inhibited reaction system. By means of a calibration relationship this time must be assigned to a corresponding amount of the inhibitor (fluoride). Evaluation is based on the empirical calibration function

$$t_i \sim \exp\left(-\frac{\text{mole fluoride}}{\text{mole zirconium}}\right) \text{ or } t_i \sim \exp(-MR)$$

The molar ratio (MR) should be between 0.1 and 1.0. This function yields a straight line with a negative slope in the range 1—10 nmol of fluoride, when 10 nmol of zirconium are applied (cf. Fig. 4).

The calibration graph is prepared with standard amounts of 1.0, 5.0 and 10.0 nmol of fluoride. The calibration measurements are done before and after each series of samples. The mean values of the induction periods obtained are plotted against the corresponding values of exp (−MR). When fluoride is to be determined, the unknown amount (nmol of fluoride) must be calculated from the value of exp (−MR) which has been found from the induction period measured.

Relationship between the induction period and the concentration of the inhibitor

The chemical basis of the proposed method is the slow reaction between perborate and iodide, catalyzed by zirconium at pH 1—2. The activity of the zirconium catalyst, present in aqueous solution in the form of hydrolysed polynuclear complexes [12—14], is greatly reduced by low amounts of fluoride [6]. With the addition of a well defined amount of ascorbic acid, a Landolt reaction system results. For the determination of fluoride, the experimental parameters were established as follows. To achieve a calibration

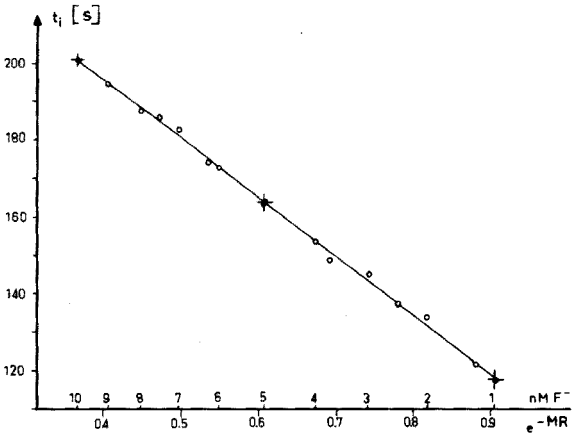

Fig. 4. Calibration graph.

line as shown in Fig. 4, the molar ratio F^-: Zr (MR) should have a value between 0.1 and 1.0; outside these thresholds, the plot becomes curved. The molar ratio BO_3^- : Zr should not exceed a value of 100. Above this limit, an increasing inhibition of the catalyst by the substrate occurs [6]. Finally, the amount of ascorbic acid added should not consume more than about 10 % of the perborate. This guarantees a measurement in the initial state of the perborate—iodide reaction.

The time between the start of the Landolt reaction and the appearance of free iodine, indicated by an increase of the depolarization current, is the induction period t. This period, which is measured with the timer, depends on the concentration C of the catalyst [15]:

$$1/t = Ch + e \tag{1}$$

where h and e are constants. This relation has often been applied to the determination of catalysts in the μg-range by other Landolt systems.

On addition of the inhibitor fluoride, the activity of the zirconium catalyst is reduced measurably. A formal mass balance, $C = C_0 - C_i$, yields

$$1/t_i = (C_0 - C_i)\, h + e \tag{2}$$

where C_0 denotes the analytical concentration of the catalyst, C_i the concentration of the inhibited catalyst, and t_i the induction period of the partly inhibited catalyzed Landolt reaction system. For the uninhibited reaction, eqn. (1) can be written as

$$1/t_0 = C_0\, h + e \tag{3}$$

and subtraction of eqn. (2) from eqn. (3) yields

$$1/t_0 - 1/t_i = C_i\, h \tag{4}$$

By this means, the additive term e, which contains only parameters of the uncatalyzed part of the perborate—iodide reaction [15], is eliminated.

In order to obtain more information on the inhibition of the zirconium catalyst, the differences $(1/t_0 - 1/t_i)$ were measured as a function of MR at two different amounts of the catalyst. The results are shown in Fig. 5. The curves indicate that the inhibition of the reaction is not correlated linearly to the amount of fluoride applied. If the difference $(1/t_0 - 1/t_i)$ is considered to be a measure of the inhibited part, C_i, of the catalyst (see eqn. 4), the shapes of the curves in Fig. 5 suggest a formal comparison with a Langmuir isotherm. From this consideration the following equations can be derived:

$$1/t_0 - 1/t_i = a\ \mathrm{MR}/(b + \mathrm{MR})\ (\mathrm{a,b} = \text{constant}) \tag{5}$$

$$\mathrm{MR}/(1/t_0 - 1/t_i) = 1/a\ (b + \mathrm{MR}) \tag{6}$$

The validity of eqn. (6) is demonstrated by Fig. 6. From eqn. (5) a calibration function can be obtained for the determination of fluoride

$$1/(1/t_0 - 1/t_i) = b/a \cdot 1/\mathrm{MR} + 1/a \tag{7}$$

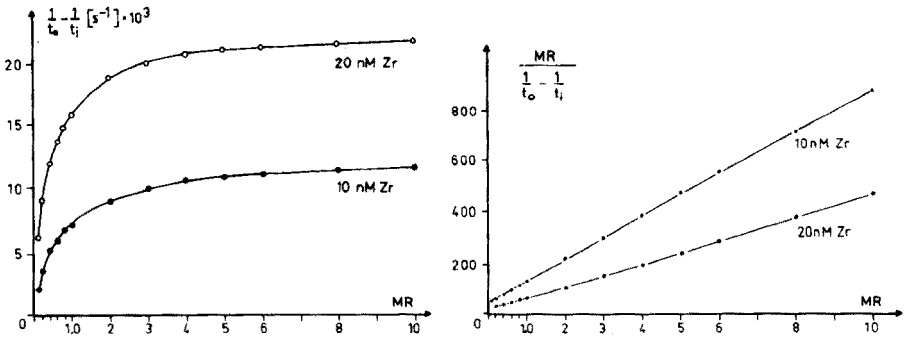

Fig. 5. Inhibition of the catalyst as a function of the molar ratio F^- : Zr, MR.

Fig. 6. Experimental confirmation of eqn. (6).

The calibration graph resulting from eqn. (7), however, is not convenient for practical use, because the measured induction period t_i has to be converted to $1/(1/t_0 - 1/t_i)$, and not MR but 1/MR has to be plotted. This makes a graphic evaluation uncertain, especially in the upper part of the working range. For this reason a different calibration function, more suitable for analytical purposes, was sought. A semilogarithmic plot, $1/t_i \sim -\log MR$, can be obtained from eqn. (5), but it is also not convenient for the reasons just mentioned. Finally, a calibration curve of the type shown in Fig. 4 was selected. The relationship $t_i \sim \exp(-MR)$ was not derived mathematically from eqns. (5)—(7), but results from an empirical treatment of the data.

Results of the analysis of pure fluoride solutions

Numerous fluoride determinations in the range 1—10 nmol (19—190 ng F^-) were carried out with the described method. From 30 values, obtained with pure sodium fluoride solutions, a standard deviation of $s = \pm 2$ ng was calculated for the entire working range [16]. Thirty determinations can be accomplished within one day, including all necessary operations except microdiffusion.

Interferences

The ions listed in Table 1 of the previous paper [6] were investigated for their influence on the Landolt reaction system. The corresponding salts were added to pure sodium fluoride solutions in varying concentrations, and these solutions then analyzed by the technique described (without microdiffusion). With two exceptions, the interferences found compared well with the results reported earlier [6]. The tolerable amount of sulfate, 500 nmol in the working range, was higher, whereas the maximum permissible amount of aluminium, only 3 nmol in the working range, was considerably lower compared to the potentiostat technique [6]. The difference in the influence of aluminium

can be explained by dilution effects [17]: the final volumes of the reaction mixtures are about 5 ml in the Landolt technique, and about 50 ml in the potentiostat technique.

All the interferences studied are unimportant, if the fluoride is separated from the matrix by microdiffusion.

Comparison of the proposed technique with other methods in an interlaboratory study

Three samples of biological materials, dried leaves and grass, were analyzed for their fluoride contents by four laboratories. The methods used for mineralization and determination were:

Lab. A. Dry ashing; alkali fusion of the ash; separation of the fluoride by a modified Willard-Winter distillation; photometric determination, alizarin complexan method [18].

Lab. B. Oxygen flask combustion; direct potentiometric determination of fluoride in the buffered absorber solution with a fluoride-selective electrode [19].

Lab. C. Dry ashing; alkali fusion of the ash; separation of interfering cations by a cation-exchange resin; determination of fluoride in the buffered eluate with a fluoride-selective electrode.

Lab. D. (present method). Dry ashing; alkali fusion of the ash; microdiffusion of fluoride with hexamethyldisiloxane; kinetic determination of fluoride with a Landolt reaction system.

The results (Table 1) show reasonably good agreement of the fluoride contents found by using very different methods. It should be mentioned that for the kinetic fluoride determination (Lab. D) only a few milligrams of sample were necessary.

At present, the combination of microdiffusion, accelerated by hexamethyldisiloxane, and chronometry is being studied for the determination of fluoride in air and rain water.

TABLE 1

Results of interlaboratory study

Sample	Material	Fluoride content, p.p.m., found by			
		Lab. A	Lab. B	Lab. C.	Lab. D
3	Apple leaves	29.5	31	27.8	30.5
6	Apple leaves	12.2	12	11.4	13.5
10	Couch grass	4.1	7	5.1	3.6

We wish to express our thanks to W. Oelschläger, University of Hohenheim, for supplying reference material for the interlaboratory study, and to the "Fonds der chemischen Industrie" for financial support.

REFERENCES

1 Deutsche Forschungsgemeinschaft, Forschungsberichte 14, "Fluor-Wirkungen", Franz Steiner Verlag, Wiesbaden, 1968.
2 C. S. Brandt and W. W. Heck, Effects of Air Pollutants on Vegetation, in A. C. Stern (Ed.), Air Pollution, Academic Press (New York-London), 2nd edn., 1968, Vol. I, p. 401 ff.
3 H. E. Stokinger and D. L. Coffin, Biologic Effects of Air Pollutants, ref. (2), p. 445 ff.
4 R. Belcher and T. S. West, Talanta, 8 (1963) 853, 863.
5 A. K. Covington, CRC Crit. Rev. Anal. Chem., 3 (1974) 355.
6 D. Klockow, H. Ludwig and M. A. Giraudo, Anal. Chem., 42 (1970) 1682.
7 G. Rönicke and D. Klockow, unpublished studies.
8 H. I. Thompson and G. Svehla, Z. Anal. Chem., 247 (1969) 244.
9 F. F. Gaál, V. I. Sörös and V. D. Canić, Mikrochim. Acta, (1975) 689.
10 D. R. Taves, Talanta, 15 (1968) 969.
11 R. J. Hall, Talanta, 16 (1969) 129.
12 Gmelins Handbuch der Anorganischen Chemie, Zirkonium (System-Nr. 42), Verlag Chemie, Weinheim, 8. Aufl., 1958, p. 306.
13 J. S. Johnson and K. A. Kraus, J. Am. Chem. Soc., 78 (1956) 3937.
14 E. S. Pilkington and W. Wilson, Anal. Chim. Acta, 33 (1965) 577.
15 G. Svehla, Analyst (London), 94 (1969) 513.
16 G. Gottschalk, Statistik in der quantitativen chemischen Analyse, F. Enke-Verlag, Stuttgart, 1962.
17 N. Shiraishi, Y. Murata, G. Nakagawa and K. Kodama, Anal. Lett., 6 (1973) 893.
18 W. Oelschläger and W. Wöhlbier, Deutsche Forschungsgemeinschaft, Forschungsberichte 14, "Fluor-Wirkungen", Franz Steiner Verlag, Wiesbaden, 1968, p. 6 ff.
19 D. A. Levaggi, W. Oyung and M. Feldstein, J. Air Pollut. Contr. Assoc., 21 (1971) 277.

Analytica Chimica Acta, 89 (1977) 47—54

SOME NEW APPLICATIONS OF THE BIAMPEROSTAT CATALYTIC-KINETIC DETERMINATION OF COPPER, PEROXIDASE, GLUCOSE OXIDASE, THYROXINE AND 5-CHLORO-7-IODO-8-HYDROXYQUINOLINE

SIEGBERT PANTEL and HERBERT WEISZ

Lehrstuhl für Analytische Chemie, Chemisches Laboratorium der Universität, Freiburg i.Br. (Federal Republic of Germany)

(Received 15th September 1976)

SUMMARY

Biamperometrically observable reactions can be evaluated by the "potentiostat" method with a current-to-voltage transducer. Some further examples of the application of this "biamperostat" are described: the copper(II)-catalyzed autodecomposition of hydrogen peroxide, the horseradish peroxidase-catalyzed oxidation of iodide with hydrogen peroxide, the glucose oxidase-catalyzed oxidation of glucose with molecular oxygen and the iodine (in organic compounds)-catalyzed oxidation of arsenic(III) with cerium(IV). 1,10-Phenanthroline is determined indirectly by its inhibitory action on copper(II).

An important group of catalytic-kinetic analytical methods uses "open systems" in which, during the course of the reaction, a reactant is added or a product is removed or even both. The so-called "stat" methods belong to this group [1]. In these "stat" methods, a preset stationary state within the catalyzed system is kept constant by adding a suitable reagent so that any change of a concentration is just compensated; pH-stat [2, 3], potentiostat [4, 5], absorptiostat [1, 6] and luminostat [7] methods have been described. Some time ago, a biamperostat [8] was developed similarly; here a preset biamperometric current — corresponding to a definite concentration of a biamperometrically active substance — is kept just constant. The rate of addition of the appropriate reagent provides a measure for the concentration of the catalyst to be determined.

In the present paper some more examples of the application of the biamperometric technique are described.

EXPERIMENTAL

The apparatus used consists of the Combi-Titrator 3D (Metrohm Herisau, Switzerland) with a current-to-voltage transducer (Fig. 1) connected. This apparatus has already been described in detail [8].

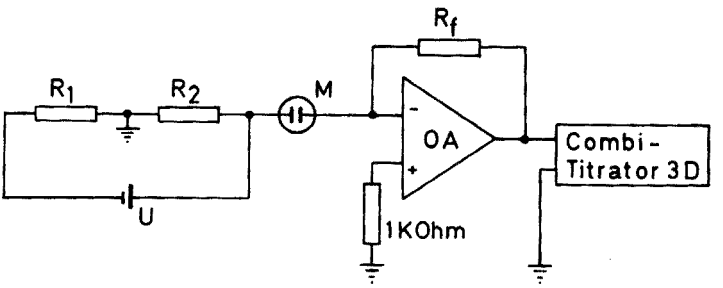

Fig. 1. Schematic representation of the "Biamperostat". M, measuring vessel with double platinum electrode Pt-880-M 5. OA, operational amplifier Philbrick-Nexus Q 200. U, Mallory battery RM 42 R (1.35 V). R_1, R_2, R_f, resistors as mentioned in the text.

A 15-ml test tube with a flat bottom (20 mm o.d.), mounted in a hollow thermostated aluminium block, is used as reaction vessel. A micro-scale double platinum electrode (Ingold, Type Pt-880-M 5) and the capillary end of the burette (Mikrodosimat, 1-ml burette) are fitted through the teflon cover of this vessel. A 5-mm bore hole in the cover is used to insert the tip of a 500-μl Eppendorf pipette, if necessary (see below). The reaction mixture is stirred using a magnetic stirrer.

In all cases the recorder speed was 10 mm min^{-1}, and the working temperature was 25.0 ± 0.2°C.

DETERMINATION OF COPPER(II) BASED ON THE CATALYZED AUTODECOMPOSITION OF HYDROGEN PEROXIDE

The autodecomposition of hydrogen peroxide is catalyzed by catalase [9] as well as by a number of metal ions [10]; the concentration of hydrogen peroxide may be monitored polarographically [11] or biamperometrically [8]. This has been used in both cases for stat methods. Among the metal ions, copper(II) in ammoniacal solution [12] has the highest activity [13]. But it has been found [14] that the calibration graph for the determination of copper is linear only when a high concentration of hydrogen peroxide (0.6 mg/8 ml) is kept constant. In this case most inhibitors for the copper catalyst are partially oxidized during the measuring time and therefore cannot be determined in this way. This disadvantage can be avoided by working in sodium hydroxide—tartaric acid solution; in this case the calibration graph is linear already for a much lower stationary hydrogen peroxide concentration (about 0.03 mg/8 ml).

Procedure

To the measuring vessel are added 1 ml of 0.3 M sodium hydroxide containing 0.6 mg of tartaric acid, 0.5 ml of a copper standard solution (0.6—6 μg Cu as copper(II) sulphate) for preparing the calibration graph or 0.5 ml of the neutralized sample solution, and twice-distilled water to 8 ml.

After thermostating for 10 min, the addition of hydrogen peroxide (0.3 mg ml^{-1}) with the automatic burette is started, the stationary concentration of hydrogen peroxide being kept constant at about 30 μg/8 ml. In this case (see Fig. 1), R_f was made 2.6 Mohm; R_1 and R_2 were 100 Kohm and 3.3 Kohm, respectively, corresponding to a polarization potential of about 40 mV. The preset working potential was 300 mV.

A recorder graph for one particular measurement is shown in Fig. 2. A calibration graph is drawn by plotting $(\tan \alpha)^{\frac{1}{2}}$ versus a number of copper standard concentrations; it is linear within the range 0.6—6 μg Cu(II)/8 ml and passes, as is to be expected, through the origin of the coordinates.

Some results for the determination of copper are given in Table 1.

INDIRECT DETERMINATION OF 1,10-PHENANTHROLINE

The catalytic activity of copper(II) on the autodecomposition of hydrogen peroxide can be reduced by strongly complexing agents such as EDTA, ChelCD or 1,10-phenanthroline. Therefore, these substances can be determined by measuring the residual catalytic activity of a definite amount of excess copper. This is shown by the example of 1,10-phenanthroline.

Procedure

To the measuring vessel are added 1 ml of 0.3 M sodium hydroxide containing 0.6 mg of tartaric acid, 1.5 ml of copper standard solution (4 μg Cu ml^{-1}), 1 ml of 1,10-phenanthroline standard solution (1,10-phenanthroline monohydrate, 2—20 μg ml^{-1}, dissolved in a minimum amount of 2 M HCl and adjusted to pH 5) or 1 ml of neutralized sample solution. The solution is then diluted with twice-distilled water to 8 ml and thermostated; the automatic addition of hydrogen peroxide follows as described for copper.

Evaluation of the calibration graph mathematically shows that the composition of the 1,10-phenanthroline—copper(II) complex is under these

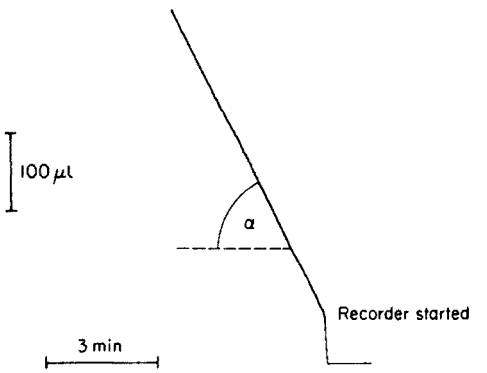

Fig. 2. Recorder graph for 4.25 μg of copper(II) in 8 ml.

TABLE 1

Results of the catalytic-kinetic determinations

Sample	Unit	Amount taken	Found
Copper(II)	μg Cu/8 ml	1.20	1.25
		2.40	2.40
		3.20	3.35
		4.80	4.75
		5.60	5.50
1,10-Phenanthroline	μg phen/8 ml	2.0	2.40
		6.0	6.0
		12.0	12.2
		16.0	16.6
		20.0	19.0
Horseradish peroxidase	mU HRP/8.5 ml	14	15
		42	41
		84	85
		112	111
		140	140
Glucose oxidase	mU GOD/8.5 ml	10	8
		40	40
		60	62
		80	78
		100	102
L-Thyroxine	μg thy/8 ml	0.17	0.16
		0.34	0.35
		0.52	0.58
		0.92	0.97
		1.15	1.20
5-Chloro-7-iodo-8-hydroxyquinoline	μg ClO/8 ml	0.10	0.12
		0.30	0.27
		0.50	0.47
		0.80	0.90
		1.00	1.03

conditions Cu:L = 1:1. The calibration graph is linear within the range 2—20 μg of 1,10-phenanthroline monohydrate/8 ml. Some results are given in Table 1.

DETERMINATION OF HORSERADISH PEROXIDASE (HRP; *E.C.* 1.11.1.7) BASED ON THE PEROXIDASE-CATALYZED OXIDATION OF IODIDE WITH HYDROGEN PEROXIDE

Peroxidases catalyze not only the oxidation of organic compounds (such as phenols, aromatic amines, hydroquinone), but also of inorganic substances (such as iodide or nitrite) with the aid of peroxides [9, 15]. The rather complicated mechanism of the oxidation reaction has been discussed in detail [16].

For the determination of HRP, the oxidation of iodide with hydrogen peroxide [17] can be used and the concentration of iodine can be indicated biamperometrically. This is possible because the depolarization potential of the redox pair I^-/I_2 is much smaller than that of hydrogen peroxide, as has already been mentioned in the determination of molybdenum [8]. Moreover, the sensitivity of the biamperometric indication of hydrogen peroxide is much lower in acidic solution (as used in this example) than in alkaline medium.

The reaction rate of peroxidases is, in general, strongly dependent on the nature and the concentration of the donor molecule and only slightly dependent on the concentration of hydrogen peroxide [9].

Procedure

To the measuring vessel are added 2 ml of acetate buffer pH 4.3 (0.2 M), 0.5 ml of hydrogen peroxide (1 mg ml^{-1}) and twice-distilled water to 7.5 ml. After thermostating for 10 min, the reaction is started by adding 0.5 ml of peroxidase standard solution (10—150 mU) for preparing a calibration graph or 0.5 ml of sample solution, and 0.5 ml of 0.03 M potassium iodide, both from Eppendorf pipettes. The iodine formed during the enzymatic oxidation reaction is removed by automatic addition of standard 0.02 N sodium thiosulphate solution to maintain a preset iodine concentration (about 50 μg in 8.5 ml). This iodine concentration is too low to cause measurable iodination of proteins. The depolarization potential applied was about 20 mV (R_1 = 100 Kohm and R_2 = 1.5 Kohm; see Fig. 1) and the feed-back resistor R_f was set to 700 Kohm, thus maintaining the above-mentioned fixed iodine concentration. The preset working potential was about 300 mV.

The HRP standard solution was prepared from HRP (Boehringer, Mannheim) purity I by dissolving and diluting with 0.9% sodium chloride solution.

The calibration graph is linear within the range 10—150 mU HRP/8.5 ml when tan α is plotted against peroxidase concentration, but does not go through the origin of the coordinates.

The results shown in Table 1 are given in International Units (1 mU = 0.001 U), standardized with guaiacol and hydrogen peroxide as substrates [9].

DETERMINATION OF GLUCOSE OXIDASE (GOD; *E.C.* 1.1.3.4) BASED ON THE MOLYBDENUM(VI)-CATALYZED OXIDATION OF IODIDE WITH HYDROGEN PEROXIDE FORMED BY THE ENZYMATIC OXIDATION OF GLUCOSE

Glucose oxidase catalyzes the oxidation of glucose at carbon-1 by molecular oxygen with formation of hydrogen peroxide [15]. This reaction may be combined with the peroxidase-catalyzed oxidation of a suitable substrate with hydrogen peroxide [18], but long ago this enzymatic step was replaced by metal ion catalysis. Molybdenum(VI) has proved best [18]

$$\text{Glucose} + O_2 + H_2O \xrightarrow{\text{GOD}} \text{glucono-1,5-lactone} + H_2O_2$$

$$\text{Glucono-1,5-lactone} + H_2O \longrightarrow \text{gluconic acid}$$

$$H_2O_2 + 2\,I^- + 2\,H^+ \xrightarrow{\text{Mo(VI)}} I_2 + 2\,H_2O$$

In this way, glucose and glucose oxidase can be determined kinetically; the course of the reaction can be followed either photometrically or electrometrically.

Procedure

To the measuring vessel are added 2 ml of acetate buffer pH 4.3 (0.2 M), 0.5 ml of 0.1 M potassium iodide, 1 ml of sodium molybdate standard solution (50 μg Mo ml^{-1}), 1 ml of glucose solution (10 mg ml^{-1}), and twice-distilled water to 8 ml. After thermostating for 10 min, the reaction is started by adding 0.5 ml of glucose oxidase standard solution (10—100 mU) for preparing a calibration graph, or 0.5 ml of sample solution with the aid of an Eppendorf pipette.

During the reaction the hydrogen peroxide formed in the first step liberates iodine in the third step (excess of Mo catalyst). The speed of the iodine formation is a measure of the GOD concentration to be determined. This speed is here measured by automatic addition of standard 0.001 N sodium thiosulphate solution to maintain the preset iodine concentration (about 15 μg in 8.5 ml).

The depolarization potential applied was again 20 mV (R_1 = 100 Kohm and R_2 = 1.5 Kohm; see Fig. 1) and the feed-back resistor R_f was set to 1.6 Mohm; the preset working potential was 300 mV.

The GOD standard solution was prepared from mould fungus glucose oxidase (Boehringer, Mannheim) purity II by dissolving and diluting with 0.9% sodium chloride solution.

Plotting tan α versus GOD concentration gives a linear calibration graph within the range 10—100 mU/8.5 ml, but the plot does not go through the origin of the coordinates.

The results shown in Table 1 for the determination of GOD are given in U, standardized with glucose and *o*-dianisidine as substrates [9].

DETERMINATION OF IODINE IN ORGANIC COMPOUNDS BASED ON THE IODINE-CATALYZED OXIDATION OF ARSENIC(III) WITH CERIUM(IV)

The oxidation of arsenic(III) with cerium(IV) is catalyzed not only by inorganic iodide [19] but also by iodine in organic compounds such as thyroxine [20—22] or iodine-containing proteins [20, 23, 24]. The kinetics of the Sandell—Kolthoff reaction have been studied in detail. It has been shown that the sensitivity of this reaction is better in perchloric than in sulphuric acid medium [25]. Quite a number of iodine-containing organic compounds are of interest in biochemical and medical problems, e.g. hormones and various substances used therapeutically [26].

The determinations of L-thyroxine and of the disinfectant 5-chloro-7-iodo-8-hydroxyquinoline illustrate the applicability of the biamperostat technique to such analyses.

Procedure

To the measuring vessel are added 0.5 ml of standard solution (0.1—1 μg of thyroxine or 0.1—1 μg of 5-chloro-7-iodo-8-hydroxyquinoline) for preparing a calibration graph or 0.5 ml of sample solution, followed by 4 ml of 4 M perchloric acid (containing some chloride), 0.7 ml of sodium arsenite solution (5 g of As_2O_3 dissolved in a minimum amount of 2 M NaOH, pH adjusted to 8 with perchloric acid and made up with twice-distilled water to 250 ml) and twice-distilled water to 8 ml. After thermostating for 10 min, the reaction is started by automatic addition of standard 0.002 M cerium(IV) sulphate solution to maintain a preset cerium(IV) concentration of about 30 μg in 8 ml.

The depolarization potential applied was 300 mV (R_1 = 100 Kohm and R_2 = 27 Kohm; see Fig. 1) and the feed-back resistor R_f was set to 400 Kohm; the preset working potential was 300 mV.

Plotting tan α versus iodine-compound concentration gave a linear calibration graph within the range 0.1—1 μg/8 ml, which passed through the origin of the coordinates.

Some results are given in Table 1. The catalytic activity of iodine in organic compounds is inferior to that of inorganic iodide; the activity of about 5 μmol of iodine in thyroxine or 4 μmol of iodine in 5-chloro-7-iodo-8-hydroxyquinoline corresponds to the activity of only 2 μmol of inorganic iodide.

REFERENCES

1 D. Klockow, H. Weisz and K. Rothmaier, Z. Anal. Chem., 264 (1973) 385.
2 K. M. Møller, Biochim. Biophys. Acta, 16 (1955) 162.
3 H. V. Malmstadt and E. H. Piepmeier, Anal. Chem., 37 (1965) 34.
4 H. Weisz, D. Klockow and H. Ludwig, Talanta, 16 (1969) 921.
5 D. Klockow, H. Ludwig and M. A. Giraudo, Anal. Chem., 42 (1970) 1682.
6 H. Weisz and K. Rothmaier, Anal. Chim. Acta, 75 (1975) 119.
7 S. Pantel and H. Weisz, Anal. Chim. Acta, 74 (1975) 275.
8 S. Pantel and H. Weisz, Anal. Chim. Acta, 70 (1974) 391.
9 H. U. Bergmeyer (Ed.), Methods of Enzymatic Analysis Vol. I, Verlag Chemie, Weinheim, 2nd edn., 1974.
10 J. H. Baxendale, Adv. Catal., 4 (1952) 31.
11 J. L. Haining and J. S. Legan, Anal. Biochem., 45 (1972) 469.
12 B. Kirson, Bull. Soc. Chim. France, (1952) 957.
13 W. Meiners, Diploma Thesis, Freiburg, i.Br., June 1974.
14 K. B. Siedle, Diploma Thesis, Freiburg i.Br., July 1975.
15 P. D. Boyer, H. Lardy and K. Myrbäck, (Eds.), The Enzymes, Vols. VII and VIII, Academic Press, New York, 2nd edn., 1963.
16 T. P. Singer (Ed.), Biological Oxidations, Interscience, New York, 1968.
17 F. Björkstén, Biochim. Biophys. Acta, 212 (1970) 396.

18 G. G. Guilbault, Enzymatic Methods of Analysis, Pergamon Press, Oxford, 1970.
19 E. B. Sandell and I. M. Kolthoff, J. Am. Chem. Soc., 56 (1934) 1426.
20 W. Heerspink and G. J. Op de Weegh, Clin. Chim. Acta, 39(2) (1972) 327; Anal. Abstr., 24 (1973) 970.
21 J. C. Arcq and A. Arcq, Clin. Chim. Acta, 48 (1973) 287; Z. Anal. Chem., 275 (1975) 414.
22 H. P. de Vries, Z. Klin. Chem. Klin. Biochem., 13 (1975) 97; Anal. Abstr., 29 (1975) 4 D 114.
23 H. V. Malmstadt and T. P. Hadjiioannou, Anal. Chem., 35 (1963) 2157.
24 P. J. Ke, R. J. Thibert, R. J. Walton and D. K. Soules, Mikrochim. Acta [Wien], (1973) 569.
25 T. Fukasawa, M. Iwatsuki and K. Uesugi, Japan Analyst, 21 (1972) 1169; Z. Anal. Chem., 267 (1973) 214.
26 E. Mutschler, Arzneimittelwirkungen, Wissenschaftl. Verlagsgesellschaft, Stuttgart, 1970.

Analytica Chimica Acta, 89 (1977) 55—63

KINETIC IDENTIFICATION AND DETERMINATION OF CERTAIN CARBOHYDRATES WITH A PERIODATE-SENSITIVE PERCHLORATE-SELECTIVE ELECTRODE

C. E. EFSTATHIOU and T. P. HADJIIOANNOU*

Laboratory of Analytical Chemistry, University of Athens, Athens (Greece)

(Received 29th July 1976)

SUMMARY

The reactions between periodate and carbohydrates are easily monitored with a perchlorate-selective electrode as a periodate sensor. The relative reaction rate constant of each carbohydrate compared to glucose is introduced as a new characteristic constant, the "periodate index", which could be related to the molecular configuration. Since appreciable differences are observed between the "periodate index" values of various carbohydrates, this constant can be used for the identification of 20-mg amounts of single pure compounds. An automatic potentiometric reaction rate method is described and shown to be simple, rapid and accurate for the determination of glucose. Amounts of glucose in the range 7—54 mg were determined in 20—140 s with precision and relative errors of about 0.4 and 0.8 %, respectively.

Oxidation with periodate, undoubtedly one of the most widely used reactions in carbohydrate chemistry [1], has been used to determine the number, type and arrangement of adjacent hydroxyl groups [2]. Most procedures are based on the reaction of the carbohydrate with a large excess of periodate, and the subsequent identification and determination of the reaction products. Although useful information such as adjacent hydroxyl groups *cis* or *trans* arrangement, steric hindrance, etc., may be obtained from reaction kinetics, only a limited amount of work has been done in this area, probably because of lack of a convenient periodate monitoring system. Hitherto, most kinetic studies of periodate reactions have been carried out by the tedious "sampling" technique in which aliquots from the reaction mixture are taken at various time intervals, quenched, and analyzed for the unreacted periodate.

Recently a perchlorate-selective electrode was reported to respond quantitatively to periodate and the application of the electrode to the potentiometric determination of vicinal glycols was described [3]. This paper shows that periodate oxidation of several carbohydrates can be easily monitored with the perchlorate electrode as a periodate sensor. Reaction rate constants determined in the range pH 3.5—7.5 show significant differences in the constants for various carbohydrates as well as a pH dependence. The relative reaction rate constant of each carbohydrate compared to glucose is introduced

*To whom correspondence should be addressed.

as a new characteristic constant, the "periodate index", which could be used for identification purposes.

Mutarotation phenomena, when present, affect the reaction rate, therefore, equilibria between various anomeric and ring forms of monasaccharides must be established before making any kind of kinetic measurement. However, kinetics of reactions between carbohydrates and periodate may be used as an alternative method for monitoring mutarotation phenomena, as demonstrated in this paper for glucose.

In addition to kinetic identification, the various carbohydrates can also be quantified by the same chemical system and experimental set-up. As an example, an automatic potentiometric kinetic method was developed for determining glucose by periodate oxidation. Thus, the time required for the potential of the perchlorate electrode to increase by a pre-selected amount (10 mV) during the reaction is measured automatically and related directly to the glucose concentration. Amounts of glucose in the range 7 to 54 mg were determined with relative errors of about 0.8 % and measurement times of about 20 to 140 s.

GENERAL CONSIDERATIONS

Carbohydrates—periodate reaction kinetics. The perchlorate-selective electrode (Orion Model 92-81) employed shows a linear response for the range 10^{-1}—10^{-5} M periodate, which is in accordance with the Nernst equation if the usual RT/F term is multiplied by a "slope normalization factor", a [4]; the a value depends on electrode age and pH, and in the pH range 4—7.5 is usually equal to 1 ± 0.05.

When dilute periodate solutions (ca. 10^{-4} M $NaIO_4$) react with an excess (at least ten-fold) of a carbohydrate, there is a good approach to an overall reaction according to the following reaction scheme

$$IO_4^- + C \xrightarrow{k} IO_3^- + \text{product} \qquad (1)$$

where C is the carbohydrate and k is the overall reaction rate constant. The product is an acyclic molecule, since periodate cleaves the ring of the carbohydrate molecule between two hydroxyls, preferably of *cis* configuration. Consecutive reactions between the primary product and periodate are unlikely because of the large excess of carbohydrate. After a carbohydrate is dissolved in water, equilibration between various forms of the carbohydrate occurs quickly in most cases. Although each form is expected to react with periodate at a different rate, the overall kinetics is well described by

$$\frac{d[IO_4^-]}{dt} = -k[IO_4^-][C] \qquad (2)$$

where the reaction rate constant, k, is equal to the weighted average of rate constants for each carbohydrate species.

Differentiation of the Nernst equation, modified by term a, followed by

rearrangement of eqn. (2), and combination of the resulting equations, yields

$$\frac{dE}{dt} = a\,k\,\frac{RT}{F}\,[C] \qquad (3)$$

Since all terms except [C] in eqn. (3) are constant and [C] remains practically constant during the reaction because the carbohydrate is in large excess (the ratio of carbohydrate to periodate is in the range 10—80), the rate of change of potential is essentially constant and linear reaction curves (E vs. time) are obtained, provided that the periodate concentration remains in the range where the modified Nernst equation is valid (the lowest periodate concentration should not be smaller than 10^{-5} M). Therefore, dE/dt may be replaced by $\Delta E/\Delta t$, which is the measurable parameter, and k values can be calculated from

$$k = \frac{F}{aRT} \cdot \frac{1}{[C]} \cdot \frac{\Delta E}{\Delta t} \qquad (4)$$

Figure 1 shows experimentally determined k values for nine carbohydrates at various pH levels. When necessary, carbohydrate solutions were equilibrated for 48 h at room temperature. In some cases small deviations from the simple kinetic scheme of reaction (1) became apparent from small curvatures of the recorded potentials toward the time axis. For these cases the initial slope values were used, and they are distinguished with dashed lines in Fig. 1.

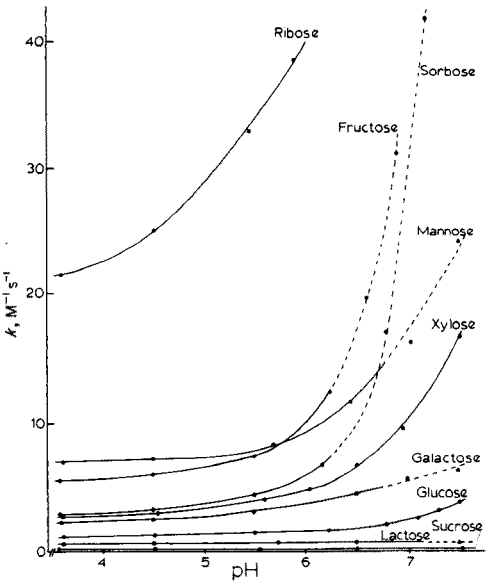

Fig. 1. Dependence of k values on pH for the reaction $IO_4^- + C \rightarrow IO_3^- +$ product. Carbohydrate concentration, $3.12 \cdot 10^{-3}$ M; initial periodate concentration, $2.8 \cdot 10^{-4}$ M. Composite acetate—phosphate buffer, total acetate = total phosphate = $9.4 \cdot 10^{-3}$ M. Temperature 25 °C.

Mutarotation effect on glucose—periodate kinetics

Erroneous results may be obtained if kinetic measurements are carried out during mutarotation of the carbohydrate solution. This is clearly demonstrated for the case of glucose. Since the α-form reacts with periodate much faster than the β-form, the rate of the periodate—glucose reaction will decrease with glucose solution age. This is illustrated by Figure 2(a), in which the rate of the reaction, measured and expressed as $\Delta E/\Delta t$, is plotted as a function of the glucose solution age. Aliquots of the glucose solution at pH 6.0 and 8.0 were taken at various time intervals and treated with periodate at pH 4.5. Values of $\Delta E/\Delta t$ were measured from the recorded reaction curves. In parallel experiments, optical rotation was measured with a Perkin-Elmer 141 Digital Photoelectric Polarimeter under the same pH, glucose concentration, and temperature conditions. Figure 2(b) shows that there is close similarity between the functions $\alpha^0 = f(\text{time})_{pH}$ and $\Delta E/\Delta t = f'(\text{time})_{pH}$.

Relative reactivity of carbohydrates toward periodate. ("Periodate index")

The reaction rate constant, k, has a characteristic value for each carbohydrate. However, exact values of k are difficult to calculate from eqn. (4) since the slope normalization factor a should be known exactly. It is more convenient to calculate the relative reaction rate constant, k_r, of each carbohydrate compared with a common carbohydrate, e.g. glucose. The constant, k_r, hereafter referred to as the molecular periodate index, is determined by conducting two measurements successively with equimolar solutions of the carbohydrate, C, and glucose, since eqn. (4) gives

$$k_r = k_c/k_{\text{glucose}} = (\Delta E/\Delta t)_c/(\Delta E/\Delta t)_{\text{glucose}} \qquad (5)$$

Alternatively, equal weight solutions of C and glucose can be used, especially if the molecular weight of the carbohydrate under test is unknown, and the relative reaction rate constant k_r^w, the periodate index by weight (or simply

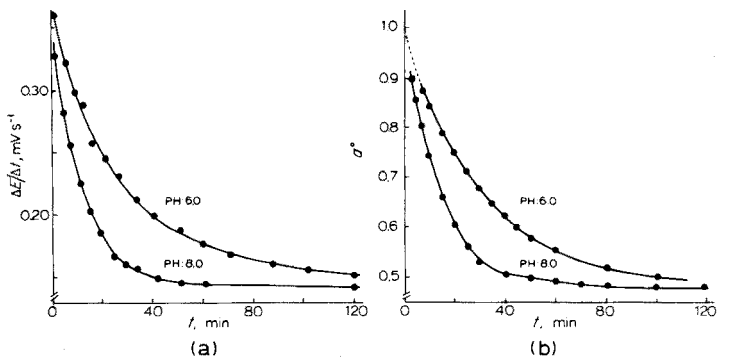

Fig. 2. Dependence of (a) $\Delta E/\Delta t$ and (b) α° (optical rotation) on glucose solution age at pH 6.0 and 8.0, 0.0500 M glucose in phosphate buffers (total phosphate, 0.02 M) kept at 22 °C. Kinetic measurements: 2.00 ml of glucose solution are pipetted into 18.0 ml of a composite solution, $[NaIO_4] = 2.5 \cdot 10^{-4}$ M—0.042 M total acetate; pH 4.5.

the periodate index) can be determined from an equation analogous to eqn. (5). The periodate index k_r^w is related to the molecular periodate index k_r by eqn. (6)

$$k_r^w = \frac{\text{Mol. weight of glucose}}{\text{Mol. weight of C}} \cdot k_r \qquad (6)$$

Since the reaction rate constant, k, for each carbohydrate depends on pH, all measurements for the determination of k_r or k_r^w should be done at the same pH. A pH of 4.5, very close to the maximum buffering capacity of the acetate buffer used, is preferred and Fig. 1 shows that a small variation of pH in this region has in most cases practically no effect on the rate constant k. Both constants, k_r and k_r^w, may be used for the identification of a carbohydrate.

Kinetic determination of glucose

The kinetic method for the determination of vicinal glycols [3] was modified as follows. First, a working temperature of 28.0 ± 0.1 °C was chosen; lower temperatures result in larger time measurements, whereas higher temperatures may result in faster electrode deterioration. The specific temperature chosen is not critical but temperature control is essential. A variation of ±1 °C results in an error of ±3—4 %. Secondly, a voltage interval of 10 mV was chosen so that measurement times are in the range 20—140 s. The measurement starts automatically after a premeasurement time equal to about 60 % of the measurement time. Thirdly, the concentration of glucose was selected in the range 0.002—0.015 M. The use of $1.9 \cdot 10^{-4}$ M periodate solution was chosen to ensure a 10—80-fold excess of glucose over periodate. Finally, a pH of 4.5 was chosen, but any pH in the range 4—7 is satisfactory.

EXPERIMENTAL

Apparatus

The electrodes and reaction cell used were the same as previously reported [3].

The recording and measurement system (Fig. 3) consists of the following units:

(a) A Heath/Schlumberger EU-205B Recording System which consists of the EU-205-11 multi-speed recorder mainframe, capable of recording at total span of −0.2 V to 1.0 V (with the SU-205-01 Centimeter Chart Transport), the EU-200-01 Potentiometric Amplifier Module, and the EU-200-02 Offset Module. The EU-200-30 pH/pIon electrometer is inserted between the electrodes and the recorder for impedance matching (Range/Volt out knob always at the position "1000 mV").

(b) An Analog-Digital Designer Heath/Malmstadt-Enke 801A with a specially designed circuit constructed on the EU-50-MD Blank PC Card. This circuit consists mainly of an operational amplifier (Burr-Brown 3308/12C)

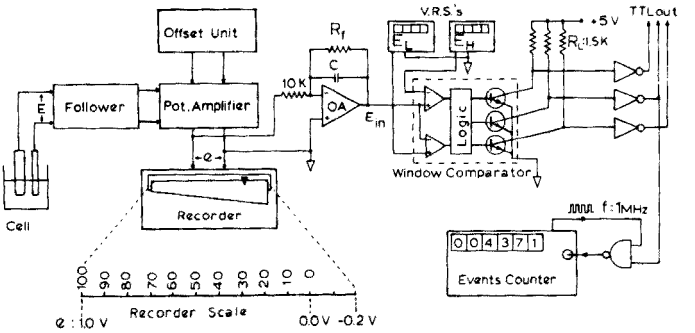

Fig. 3. Schematic diagram of the measurement system.

and a Window Comparator (Burr-Brown 4115/04) (5). A NAND gate card, EU-800 JC, is aslo used.

(c) A Universal Digital Instrument Heath/Malmstadt-Enke EU-805A (U.D.I.

(d) Two Voltage Reference Sources (VRS), Heath-EU-80A.

As shown in Fig. (3), various positions of the recorder mainframe pen on the chart paper correspond to various values for the recorder input potential e ranging from -0.2 V to 1.0 V (Potential E after amplification and voltage offset becomes potential e). A parallel connection to the output of the Poten tiometric Amplifier Module drives a small portion of the current to the input of the operational amplifier, OA, and in this way the electrode signal is further amplified. Resistor R_f and capacitor C are variable, so as to control amplification and noise reduction. The OA output, E_{in}, is driven to the input of the Window Comparator (Double Comparator), the upper and lower limits E_H and E_L of which are preset externally using the two VRS's. The Window Comparator output is inverted (TTL inverters) and subsequently is driven to the card TTL output pin connectors. The TTL output which corresponds to the "GO" state (in logic 1 when $E_L<E_{in}<E_H$) controls the dual input NAND gate which in the "GO" state permits the passing of a 1 MHz square signal. The 1 MHz signal is provided from the rear panel of the Universal Digital Instrument. The same instrument, in the "Events Counter" mode counts the 1 MHz signal, after proper scaling.

Reagents

All solutions were prepared with deionized, distilled water from reagent-grade materials, except where stated.

Sodium metaperiodate stock solution, 0.050 M. Dissolve 10.7 g of $NaIO_4$ (G. F. Smith Co., Columbus, Ohio) in water and dilute to 1 l. More dilute solutions are prepared daily by dilution. All periodate solutions are kept in amber bottles.

Acetate buffers, pH 4.5. Prepare solutions 0.1 and 0.25 M in total acetate.

Carbohydrate solutions. All carbohydrates were Fluka (puriss. grade), except ribose which was of purum grade, and were used without further

purification. Two solutions were prepared for each carbohydrate, 0.0500 M and 1.00 % (w/v). In addition, prepare 0.200 M glucose stock solution for the kinetic determination. Prepare working standards (0.02, 0.05, 0.10 and 0.15 M) from the stock solution by dilution. Keep all carbohydrate solutions, standards, and samples, for 2 d at room temperature to equilibrate and store in the refrigerator. Alternatively, equilibration can be achieved rapidly either by adding 2 drops of concentrated ammonia solution per 100 ml of the carbohydrate solution or by boiling.

All carbohydrate solutions, the dilute periodate solution, and the buffer solutions are thermostated at 25° ± 0.1 °C for the determination of the periodate index and at 28.0 ± 0.1 °C for the kinetic method.

Procedure

Determination of the periodate index. Pipet 20.00 ml of $3.0 \cdot 10^{-4}$ M $NaIO_4$ solution and 3.00 ml of 0.25 M buffer solution into the thermostated reaction cell at 25 ± 0.1 °C. Set the recorder span at 50 mV. Start the recorder, quickly add 2.00 ml of 1.00 % solution of the carbohydrate C to the cell by pipette, and record a large portion of the linear part of the reaction curve or until the recording becomes noisy. Repeat the measurement with 1.00 % glucose solution, and calculate the periodate index from the recorded curves by eqn. (7)

$$k_r^w = (\Delta E/\Delta t)_{1\ \%C}/(\Delta E/\Delta t)_{1\ \%\ \text{glucose}} \qquad (7)$$

For the determination of the molecular periodate index, use 0.0500 M carbohydrate C and glucose solutions and eqn. (5).

Kinetic determination of glucose. Set the recorder span at 50 mV (signal amplification × 20) and the OA amplification at -×10 (use a 100 K R_f resistor and a 0.47—1 μF capacitor in parallel). Adjust the VRS's at $E_H = 0.00$ V and $E_L = -2.00$ V. With these adjustments, the time measurement starts and stops when the pen recorder crosses the "0" and "20" chart indications respectively, and thus the time required for the electrode potential E to increase by 10 mV is measured automatically. Adjust the Scaling factor of the Universal Digital Instrument at 10^4. Adjust the pen of the recorder to the right edge of the chart paper, press the Start button of the Universal Digital Instrument (at the "events counter" mode) and by pipet quickly add 2.00 ml of standard or sample glucose solution to the reaction cell. The analysis is completed automatically and the number on the digital readout (time in hundredths of a second) is recorded. Press the Reset button, empty the cell by suction, rinse the electrodes and the cell with water, and dry with suction. Repeat the procedure for each analysis.

RESULTS AND DISCUSSION

Calculated periodate index values (pH = 4.5) for several carbohydrates are given in Table 1. Table 1 in conjunction with Fig. 1 shows the following points First, there is a large difference in the rate constant and periodate index values

TABLE 1

Periodate index values[a] for carbohydrates

Carbohydrate	$k_r \pm s_{k_r}$	$k_r^w \pm s_{k_r^w}$
Ribose	21.8 ± 0.5	26.7 ± 0.4 (26.2)[b]
Mannose	5.98 ± 0.08	6.15 ± 0.11
Fructose	4.84 ± 0.10	4.88 ± 0.06
Sorbose	2.58 ± 0.06	2.60 ± 0.05
Xylose	2.40 ± 0.03	2.84 ± 0.05 (2.88)[b]
Galactose	2.03 ± 0.03	2.05 ± 0.02
Glucose	1[c]	1[c]
Lactose[d]	0.66 ± 0.01	0.34 ± 0.01 (0.33)[b]
Sucrose	0.1	0.05 (~0.05)[b]

[a] Average of four values at pH 4.5.
[b] The values in parentheses are calculated from the values of k_r using eqn. (6). For the other carbohydrates, $k_r^w = k_r$, because their molecular weight equals that of glucose.
[c] By definition.
[d] k_r^w is calculated for the monohydrate form.

for ribose compared with other carbohydrates. This difference can probably be attributed to the large number of *cis* hydroxyl groups in ribose. Secondly, for all carbohydrates the reaction rate increases smoothly with pH, except for the two ketoses tested, fructose and sorbose, for which k increases sharply at pH values greater than about 6. Thirdly, disaccharides react very slowly with periodate. Lactose, which contains *cis* hydroxyl groups, reacts faster than sucrose.

Recorded curves used for the construction of the working curve for the glucose—periodate reaction are shown in Fig. 4. Four glucose standards are run in duplicate and the method of least squares is applied for the evaluation of calibration plot fittings [6, 7]. The regression equation of the calibration plot (1000/t, $s^{-1} \times 10^3$ vs. glucose concentration, M) is: $1000/\Delta t = 0.656 + 339.9$ [glucose]; the standard error of regression (s_r) is 0.294, s.d. of the slope 1.6, s.d. of the intercept 0.151, and correlation coefficient 0.99993.

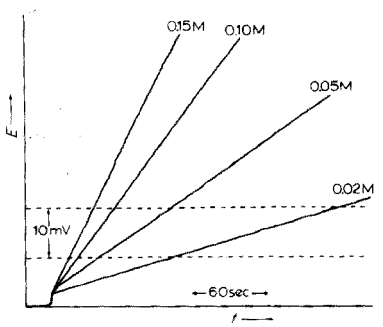

Fig. 4. Recorded curves of cell voltage vs. time for glucose—periodate reaction.

Analysis of aqueous glucose solutions gave the results shown in Table 2. Ten replicate determinations were made with 0.0750 M glucose solution. The average measurement time was 38.12 s (range = 0.46 s) and the relative standard deviation was 0.39 %.

Any substance which reacts with periodate interferes and should be eliminated prior to the measurements. The kinetic method can also be used for the determination of the other carbohydrates listed in Table 1, except for ribose which reacts with periodate very rapidly, and lactose and sucrose which react very slowly. The possibility of analyzing mixtures of carbohydrates by a differential kinetic method based on the difference in ratios of reaction rates at solutions of different pH is under investigation.

TABLE 2

Automatic results for aqueous glucose solutions

Sample No.	Δt (s)	Glucose, M		Error, %
		Taken	Found[a] ± C.L[b]	
1a	92.64	0.0300	0.0298 ± 0.0018	−0.7
1b	92.47	0.0300	0.0299 ± 0.0018	−0.3
2a	41,34	0.0700	0.0692 ± 0.0017	−1,1
2b	41.22	0.0700	0.0694 ± 0.0017	−0.9
3a	28.83	0.1000	0.1001 ± 0.0017	+0.1
3b	28.63	0.1000	0.1008 ± 0.0017	+0.8
4a	22.81	0.1300	0.1271 ± 0.0018	−2.2
4b	22.46	0.1300	0.1291 ± 0.0018	−0.6
				Av. 0.84

[a]Single measurements.
[b]C.L;95 % Confidence level [7].

The authors are grateful to H. Freiser, University of Arizona (U.S.A.), and J. D. R. Thomas, UWIST (U.K.), for helpful discussions made possible by NATO Research Grant No. 1000, and to I. Photaki for valuable suggestions.

REFERENCES

1 G. Dryhurst, Periodate Oxidation of Diol and Other Functional Groups, Pergamon Press, London, 1966, p. 1.
2 R. D. Guthrie and J. Honeyman, An Introduction to the Chemistry of Carbohydrates, 3d edn., Clarendon Press, Oxford, 1968, p. 68.
3 C. E. Efstathiou and T. P. Hadjiioannou, Anal. Chem., 47 (1975) 864.
4 C. E. Efstathiou, T. P. Hadjiioannou and E. J. McNelis, submitted.
5 Burr-Brown, Co., Tuscon, Arizona, Comparators Catalog, November, 1972, p. 8.
6 A. M. Neville and J. B. Kennedy, Basic Statistical Methods, Intertext Books, London, 1968, p. 203.
7 T. L. Larsen and J. J. Wagner, J. Chem. Educ., 52 (1975) 215.

Analytica Chimica Acta, 89 (1977) 65—70

CATALYTIC DETERMINATION OF ULTRATRACE AMOUNTS OF SELENIUM(IV)

TAKUJI KAWASHIMA, SHIZUKO KAI and SONOKO TAKASHIMA

Chemical Institute, College of Liberal Arts, Kagoshima University, Korimoto, Kagoshima 890 (Japan)

(Received 21st July 1976)

SUMMARY

A new sensitive catalytic method for determining selenium(IV) is proposed. Selenium catalyzes the oxidation of *p*-hydrazinobenzenesulfonic acid to *p*-diazobenzenediazonium ion, which then is converted to a yellow azo dye by coupling with *m*-phenylenediamine. As little as 10^{-7} M selenium(IV) can be determined easily; the effective molar absorptivity is $1.2 \cdot 10^6$ for selenium(IV). If the azo dye is extracted into an organic solvent, the effective molar absorptivity can be increased further to $2.4 \cdot 10^6$ for selenium(IV).

Catalytic methods are generally much more sensitive than spectrophotometric methods based on stoichiometric reactions [1, 2]. Most of these catalytic methods are based on oxidation—reduction reactions in which the catalyst, usually a multivalent ion, changes its oxidation state during the reaction [3].

Feigl and West [4] proposed a very sensitive qualitative test for selenium based on the catalytic reduction of methylene blue by sodium sulfide. The reaction was later developed to a determination of minute amounts of selenium [5, 6]. Kawashima and Tanaka [7] proposed a new sensitive catalytic determination of selenium(IV) based on its catalytic effect on the reduction of 1,4,6,11-tetraazanaphthacene by hypophosphorous acid, and attempts have been made [8] to apply this procedure for selenium(IV) in sea water.

When arylhydrazines are oxidized and then coupled with aromatic compounds, they produce intensely colored azo dyes [9]. Kawashima et al. [10] found that selenium(IV) in the presence of chlorate catalyzes the oxidative coupling reaction of *p*-hydrazinobenzenesulfonic acid with 1-naphthylamine to produce an intensely colored compound, and developed a new catalytic method for determining minute amounts of selenium(IV) based on this reaction [10]. In this paper, a new method of catalytic determination of selenium(IV) is proposed. 1-Naphthylamine is replaced by *m*-phenylenediamine, and the sensitivity and the reproducibility of results are greatly improved. The sensitivity of this proposed method can be increased further by extraction of the dyestuff into organic solvents.

EXPERIMENTAL

Reagents

All the chemicals used were of analytical grade. Deionized distilled water was used. Stock solutions of selenium(IV) (1 mg ml^{-1}) were prepared from anhydrous sodium selenite as described previously [10]. *p*-Hydrazinobenzenesulfonic acid solutions ($2.5 \cdot 10^{-2}$ M) were prepared by dissolving 475 mg of the compound (B.D.H., England) in 100 ml of 0.1 M hydrochloric acid with gentle warming. Aqueous $5.0 \cdot 10^{-2}$ M solutions of *m*-phenylenediamine dihydrochloride (Wako Pure Chemical Co., Japan), and aqueous $3.2 \cdot 10^{-1}$ M potassium chlorate solutions were also required. These solutions, except for the selenium solution, were prepared daily. Aqueous 3 % (w/v) solutions of zephiramine (tetradecyldimethylbenzylammonium chloride; Dojindo Co., Japan) were used. Organic solvents of analytical grade were used without further purification.

Apparatus

A Hitachi Perkin-Elmer Model 139 spectrophotometer with 10-mm glass cells was used for absorbance measurement; absorption spectra were obtained with a Shimadzu MPS-50L multipurpose recording spectrophotometer with 10-mm glass and quartz cells. A Hitachi-Horiba glass electrode pH meter, Model F-5, and a Taiyo Model C-550 circulating thermostated bath were also used.

Recommended procedure

To 15 ml of sample solution (about 0.15 M in hydrochloric acid) containing not more than 2.0 μg of selenium(IV) in a 25-ml volumetric flask, add a mixture of 2 ml of $2.5 \cdot 10^{-2}$ M *p*-hydrazinobenzenesulfonic acid and 3 ml of $5.0 \cdot 10^{-2}$ M *m*-phenylenediamine, and finally 3 ml of $3.2 \cdot 10^{-1}$ M potassium chlorate solution. Dilute to the mark with water, and heat to 50.0 ± 0.1 °C in a thermostat. Exactly 60 min after the initiation of the reaction, pipette about 5 ml of the reaction mixture into a dry test tube immersed in an ice-water bath. Then measure the absorbance at 454 nm in a 10-mm cell preferably within 30 min, against a distilled water reference. Obtain the net absorbance by subtracting a blank absorbance.

RESULTS AND DISCUSSION

p-Hydrazinobenzenesulfonic acid is oxidized by selenous acid to the *p*-sulfobenzenediazonium ion which is then coupled with *m*-phenylenediamine to form a yellow azo dyestuff, *p*-(2,4-diaminophenylazo) benzenesulfonic acid (λ_{max} = 454 nm). The elemental selenium formed is oxidized again by chlorate to selenous acid. Thus the oxidation of *p*-hydrazinobenzenesulfonic acid proceeds catalytically with a minute amount of selenium(IV). The above recommended procedure was developed on the basis of the following study.

Absorption spectra

The absorption spectra of the mixed reagents without selenium(IV) and the azo dyestuff formed during their catalytic reaction with selenium(IV) (Fig. 1) show that the absorption maximum occurs at 454 nm. At this wavelength, the reagent blank shows a small absorbance, so that a reagent blank was subtracted from the absorbances observed to compensate for any changes in color of the reagents on storage.

Effect of reaction variables

The effect of pH on the color development for the catalytic reaction was examined for a constant reaction time of 60 min at 50 °C. The color development was at a maximum and almost constant in the pH range 0.8—1.0, decreasing quite rapidly on both sides of this range.

The effect of temperature on the catalytic reaction was examined at 40°, 50° and 55 °C (Fig. 2). The reaction proceeds more quickly with increase in temperature. However, increase in temperature also increases the blank absorbance, particularly above 55 °C. Accordingly a reaction temperature between 50 and 55 °C was selected for the final procedure. An increase in the reaction time improves the sensitivity; for practical purposes, a reaction time of 60 min at 50 °C was found satisfactory. The absorbance of the reaction mixture remains unchanged for at least 50 min so long as the mixture is kept in ice-water, whereas it tends to increase slowly when the mixture is

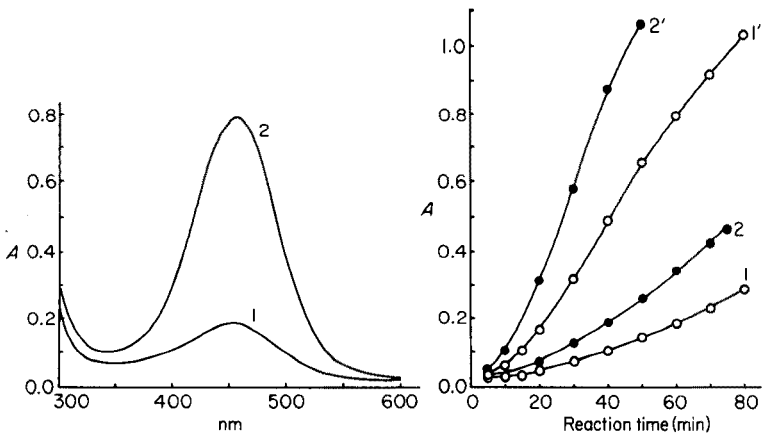

Fig. 1. Absorption spectra of the azo dyestuff. Curve 1, reagent blank. Curve 2, 1.00 μg of selenium(IV) added. Treated as in the procedure proposed.

Fig. 2. Effect of temperature on color development. Reaction temperature: ○, 50.0 ± 0.1 °C and ● 55.4 ± 0.2 °C. Curves 1 and 2, reagent blank. Curves 1′ and 2′, 1.00 μg of selenium(IV). *p*-Hydrazinobenzenesulfonic acid, $2.0 \cdot 10^{-3}$ M; *m*-phenylenediamine, $6.0 \cdot 10^{-3}$ M; potassium chlorate, $3.8 \cdot 10^{-2}$ M; pH, 0.9—0.96. The results at 40 °C are omitted because of the slow reaction rate.

left at room temperature after having been cooled in ice-water. Thus the reaction mixture must be kept in an ice-water bath until the absorbance is measured.

The color development was examined at three different concentrations of *p*-hydrazinobenzenesulfonic acid ($1.0 \cdot 10^{-3}$, $2.0 \cdot 10^{-3}$ and $3.0 \cdot 10^{-3}$ M) with different *m*-phenylenediamine concentrations (Fig. 3). The net absorbances shown were obtained by subtracting blank values from the observed values. For the $2.0 \cdot 10^{-3}$ M hydrazine concentration, the net absorbance remains constant over the range $4.8 \cdot 10^{-3}$—$8.0 \cdot 10^{-3}$ M diamine, while for the $1.0 \cdot 10^{-3}$ M hydrazine concentration, the absorbance is less; with hydrazine concentrations above $3.0 \cdot 10^{-3}$ M, the net absorbance tends to decrease with increase in the blank absorbance. Thus in the proposed procedure the concentrations of the hydrazine and the diamine were selected as $2.0 \cdot 10^{-3}$ M and $6.0 \cdot 10^{-3}$ M, respectively.

Figure 4 shows that the net absorbance increases as the concentration of chlorate increases, but a constant absorbance was obtained over the range $3.5 \cdot 10^{-2}$—$4.0 \cdot 10^{-2}$ M chlorate. Thus a chlorate concentration of $3.8 \cdot 10^{-2}$ M was selected.

Beer's Law and molar absorptivity

Typical working curves for the procedure show that Beer's law is obeyed over the range 0—2.0 μg of selenium(IV) per 25 ml of the working solution. The effective molar absorptivity is $1.2 \cdot 10^{6}$ for selenium(IV). The reproducibility is satisfactory with a standard deviation of ±0.03 μg for ten determinations of 1.00 μg of selenium(IV).

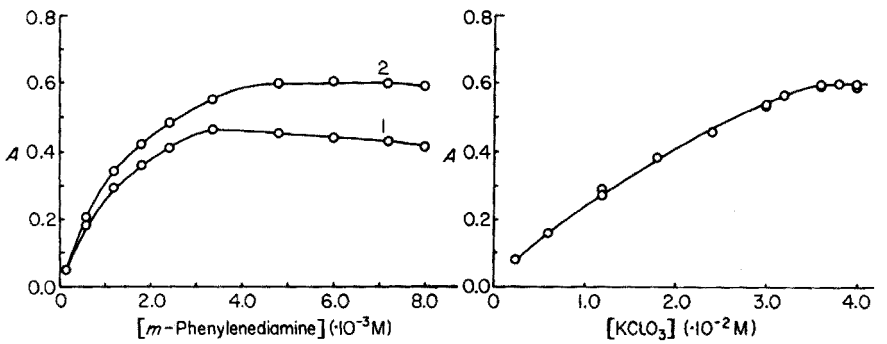

Fig. 3. Effect of *p*-hydrazinobenzenesulfonic acid and *m*-phenylenediamine concentrations. *p*-Hydrazinobenzenesulfonic acid: $1.0 \cdot 10^{-3}$ M for curve 1, and $2.0 \cdot 10^{-3}$ M for curve 2. With $3.0 \cdot 10^{-3}$ M of the hydrazine, the net absorbances decreased and the curve almost coincided with curve 1. Selenium(IV), 1.00 μg per 25 ml; potassium chlorate, $3.8 \cdot 10^{-3}$ M; pH, 0.9—0.96. All at 50 °C and 60 min. The absorbances given are net absorbances.

Fig. 4. Effect of chlorate concentration. *p*-Hydrazinobenzenesulfonic acid, $2.0 \cdot 10^{-3}$ M; *m*-phenylenediamine, $6.0 \cdot 10^{-3}$ M. Other conditions as for Fig. 3.

Effect of different ions

The effect of different ions on the determination of 1 μg of selenium(IV) was examined. The following ions caused no interference up to at least the concentrations indicated: 50 mg of NH_4(I), Na(I); 20 mg of K(I); 10 mg of Mg(II), Ca(II), Ba(II), Pb(II); 1 mg of Cd(II), Zn(II), Ni(II); 100 μg of Al(III), W(VI), Co(II); 50 μg of Sn(II), Sn(IV), As(V), Se(VI), Cr(III); 10 μg of Mo(VI), Ce(III), Ce(IV), Cu(II); 77 mg of Cl^-; 100 μg of Br^-; 10 μg of I^-; 30 mg of NO_3^-; 10 mg of SO_4^{2-}.

Copper(II), cerium(IV), molybdenum(VI) and iodide interfered in amounts of 100 μg (Table 1). Further, 10 μg of iron(III), vanadium(V) or chromium(VI) cause a positive interference; these ions seem to catalyze the color development. The interference of copper(II) can be suppressed by the addition of EDTA. The interferences of vanadium(V) and iron(III) can be eliminated by separation of these elements from selenium(IV) by solvent extraction with oxine. The co-existence of selenium(IV) and iodide in actual samples is rare, so that the iodide interference should not cause problems. Tellurium(IV) causes a negative interference which cannot as yet be avoided.

Increase in the sensitivity of the proposed method

The proposed method can be made more sensitive for selenium(IV) by extracting with organic solvents in the presence of zephiramine. In alkaline solution, the dissociated dyestuff should react with zephiramine cation to form an ion-association complex which can be extracted into organic solvents [11].

Several organic solvents were tested: methyl isobutyl ketone, isoamyl alcohol, n-amyl alcohol, n-butanol, carbon tetrachloride, chloroform, bromoform, 1,2-dichloroethane, benzene, chlorobenzene, toluene and hexane. The absorption maximum of the azo dye in the solvent, the effect of pH on

TABLE 1

Effect of interfering ions on the determination of 1.00 μg of selenium(IV)

Ion	Amount added (μg)	Se found (μg)	Ion	Amount added (μg)	Se found (μg)
Fe(III) ($FeCl_3 \cdot 6H_2O$)	1	1.29	Mo(VI) ($(NH_4)_6Mo_7O_{24} \cdot 4H_2O$)	10	1.14
	10	2		100	1.73
	10[a]	0.81	Cr(VI) ($K_2Cr_2O_7$)	10	1.22
Cu(II) ($Cu(NO_3)_2 \cdot 3H_2O$)	100	2	Ce(IV) ($Ce(SO_4)_2 2(NH_4)_2SO_4$)	10	0.99
	100[a]	1.01		100	1.22
V(V) (NH_4VO_3)	1	1.87	I^- (KI)	10	0.99
	1[a]	0.62		100	1.22
Te(IV) (Na_2TeO_3)	10	0.39	NO_2^- ($NaNO_2$)	100	1.21
	100	0.79			

[a]0.1 ml of EDTA (0.25 M) was added.

extraction, and the effect of the zephiramine concentration, were examined by the following procedure. In a 100-ml separatory funnel were placed 20—30 ml of a buffer solution, a definite aliquot of 3 % zephiramine solution and exactly 10 ml of the organic solvent. Then the whole product of the reaction obtained by the recommended procedure was added to the funnel, which was shaken for 5 min to ensure equilibration. After a few minutes, the organic phase was separated into a dry test tube for the absorbance measurement, while the pH of the remaining aqueous fraction was measured.

Table 2 shows the optimum pH ranges and zephiramine concentrations for different solvents. In all cases the λ_{max} was 440 nm. Methyl isobutyl ketone, isoamyl alcohol and n-amyl alcohol are recommended as the best extractants. The proposed procedure for the catalytic method coupled with the extraction process under the optimum conditions allows 0—0.5 μg selenium(IV) per 10 ml of extract to be determined. The effective molar absorptivity is $2.4 \cdot 10^6$ l mol^{-1} cm^{-1}.

TABLE 2

Optimum pH and zephiramine concentration for extraction of the azo dye

Solvent	pH range	Zephiramine concn. (g/25 ml)
Methyl isobutyl ketone	5.5—7.5	0.3—0.6
Isoamyl alcohol	6 —9	0.6—0.9
n-Amyl alcohol	6 —9	0.6—0.9

The authors thank Emeritus Prof. K. Sugawara (Nagoya University) for valuable suggestions and discussions.

REFERENCES

1 K. B. Yatsimirskii, Kinetic Methods of Analysis, Pergamon, Oxford (1966), p. xiv
2 V. Michaylova, B. Evtimowa and P. R. Bontchev, Mikrochim. Acta, (1968) 922.
3 P. R. Bontchev, Talanta, 17 (1970) 499.
4 F. Feigl and P. W. West, Anal. Chem., 19 (1947) 351.
5 H. Goto, T. Hirayama and S. Ikeda, Nippon Kagaku Zasshi (J. Chem. Soc. Jpn., Pure Chem. Sect.), 73 (1952) 652.
6 P. W. West and T. V. Ramakrishna, Anal. Chem., 40 (1968) 966.
7 T. Kawashima and M. Tanaka, Anal. Chim. Acta, 40 (1968) 137.
8 T. Kawashima and K. Yokoyama, Bunseki-Kiki (Anal. Instr.), 11 (1973) 784.
9 J. J. Postowsky, B. P. Lugowkin and G. T. Mandryk, Ber., 69 (1936) 1913.
10 T. Kawashima, S. Nakano and M. Tanaka, Anal. Chim. Acta, 49 (1970) 443.
11 G. H. Morrison and H. Freiser, Solvent Extraction in Analytical Chemistry, J. Wiley, New York, 1957, p. 30.

Analytica Chimica Acta, 89 (1977) 71—82

HIGH-PERFORMANCE PULSE AND DIFFERENTIAL PULSE POLAROGRAPHY
PART I. THEORETICAL CONSIDERATIONS

W. P. van BENNEKOM and (the late) J. B. SCHUTE

Gorlaeus Laboratoria, Department of Pharmaceutical Analysis and Analytical Chemistry, State University, Wassenaarseweg 76, Leiden (The Netherlands)

(Received 13th July 1976)

SUMMARY

A theoretical approach is given for complete elimination of the charging current caused by drop growth in modified normal and differential pulse polarography (n.p.p. and d.p.p.). Maximum sensitivity can be obtained in modified n.p.p., but the resolution of waves is better in modified d.p.p. or can be increased in differential modified n.p.p. The best overall performance can be achieved with modified d.p.p., considering sensitivity and wave resolution together. Preliminary results for the determination of chloramphenicol are described.

Differential pulse polarography (d.p.p.) has found wide application in both inorganic and organic systems, and has proved to be a versatile and reliable tool, even for trace analysis because of its sensitivity. The limit of detection for a reversible electrochemical reaction is about 10^{-8} M.

In inorganic analysis this limit of detection can be lowered by a combination of anodic stripping analysis and d.p.p., but generally this stripping technique cannot be used in analysis of organic compounds. In order to determine those compounds at levels below the detection limit of d.p.p., further improvements are required; the signal-to-noise ratio must therefore be considered in more detail.

In all polarographic modifications, the polarographic noise is largely some charging current rather than capillary or electronic noise. Recently, Christie et al. [1] described "alternate drop pulse polarography", by which it was possible to eliminate completely the charging current, so that they reached the level of capillary [2] and electronic noise. The Princeton Applied Research Corporation was able to eliminate the charging current in d.p.p. by subtracting a "memory" blank polarogram from the polarogram obtained with the electroactive substance(s) in their "microprocessed" PAR 374. Previously, Klein and Yarnitzky [3] had made some suggestions for eliminating completely the charging current in d.p.p. (their mode D) and some of their considerations are adopted and evaluated in more detail in the present paper.

THEORY

For an electrochemically reversible reaction when only the oxidized or reduced form is present in the solution, the (diffusion-controlled) faradaic current i_f and potential E are related by

$$E = E^r_{\frac{1}{2}} + \frac{RT}{nF} \ln \frac{i_{f,lim} - i_f}{i_f} \tag{1}$$

where $E^r_{\frac{1}{2}}$ is the reversible half-wave potential and $i_{f,lim}$ the limiting faradaic current. Relation (1) can be rearranged to

$$i_f = i_{f,lim} \left[\frac{1}{1 + \epsilon}\right] \tag{2}$$

where

$$\epsilon = \exp\left[\frac{nF}{RT}(E - E^r_{\frac{1}{2}})\right] \tag{3}$$

If the Heyrovský-Ilkovič equation can be introduced for $i_{f,lim}$ with a dropping mercury electrode (DME), then

$$i_{f,lim} = (7/3\pi)^{1/2}\, nFkm^{2/3}t^{1/6}D^{1/2}C \tag{4}$$

where t is the drop time of the DME, k a constant with a numerical value of 0.008515 $m^2\, kg^{-2/3}$, m the flow-rate of mercury through the capillary, and C the concentration of the oxidized or the reduced species in the bulk of the solution. Thus for the "classical" d.c. polarographic current $i_{f,dc}$, which is now a function of drop time and potential, we can write

$$i_{f,dc}(E,t) = (7/3\pi)^{1/2}\, nFkm^{2/3}t^{1/6}D^{1/2}C \left[\frac{1}{1 + \epsilon}\right] \tag{5}$$

In d.c. polarography this faradaic current is contaminated by a charging current $i_{c,dc}$, which also depends on both time and potential, so that

$$i_{c,dc}(E,t) = -\tfrac{2}{3}\, km^{2/3}Q(E)t^{-1/3} \tag{6}$$

where $Q(E)$ is the (potential-dependent) charge density on the electrode surface. Generally the measured d.c. polarographic current $i_{pol}(E,t)$ is given by

$$i_{pol}(E,t) = i_{f,dc}(E,t) + i_{c,dc}(E,t) \tag{7}$$

In modern electroanalytical chemistry, constant efforts have been made to eliminate completely the influence of the charging current i_c on the results.

Substitution of τ, which is the lifetime of the drop, for the drop time t ($0 < \tau < t$) in eqn. (7), gives

$$i_{pol}(E,\tau) = i_{f,dc}(E,\tau) + i_{c,dc}(E,\tau) \tag{8}$$

If the potential E is considered constant during the drop time t, which can be almost achieved by using a very slowly varying potential ramp (Fig. 1a), or

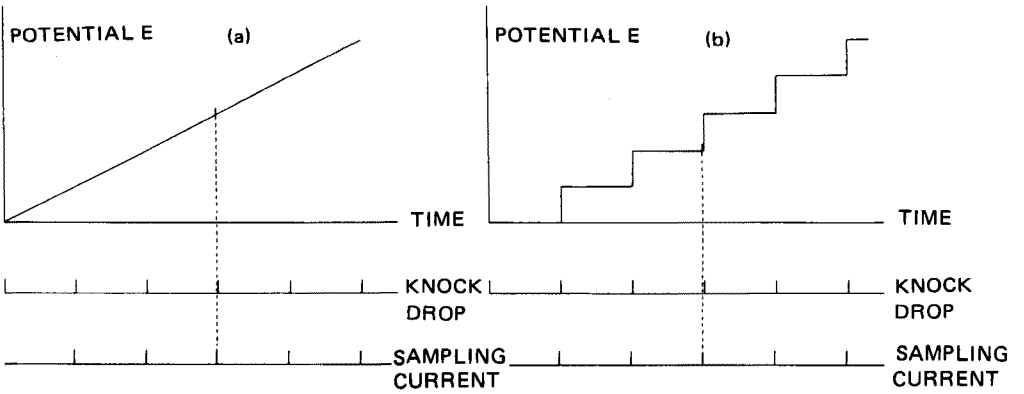

Fig. 1. Sampled d.c. polarography (a) with usual potential ramp, (b) with stepped potential.

essentially realised by using a stepped potential which is synchronized with the drop time (Fig. 1b), the capacitance current $i_{c,dc}$ can be reduced by taking a "current sample" at τ seconds nearly at the end of drop life (sampled d.c. polarography). Relation (6) can be rewritten as

$$i_{c,dc}(E,\tau) = -\tfrac{2}{3}\, km^{2/3}Q(E)\tau^{-1/3} \qquad (9)$$

This charging current $i_{c,dc}$ can be reduced more completely by sampling i_{pol} at τ and at $(\tau + \delta)$ seconds (Fig. 2) and subtracting both current samples (δ is some small delay time). The remaining difference in charging current ($\Delta i_{c,dc}$) will be

$$\Delta i_{c,dc} = i_{c,dc}(E,\tau) - i_{c,dc}(E,\tau + \delta) \qquad (10)$$

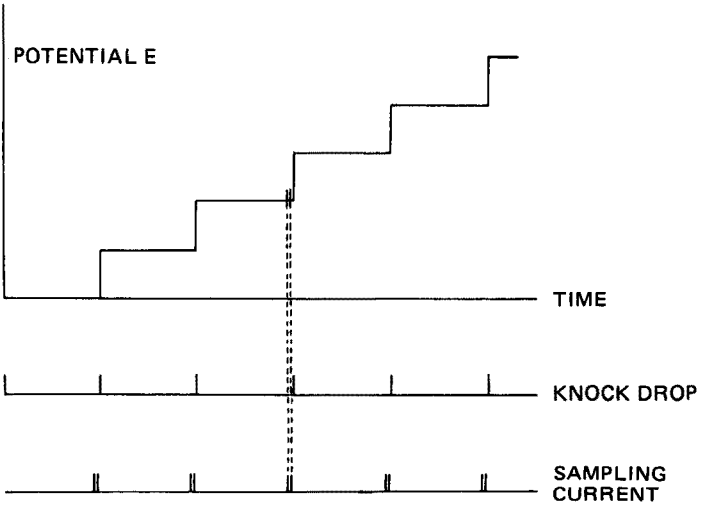

Fig. 2. Sampled d.c. polarography with stepped potential in the described modification.

or

$$\Delta i_{c,dc} = -\tfrac{2}{3}\, km^{2/3}Q(E)\tau^{-1/3}\left[1-\left(1+\frac{\delta}{\tau}\right)^{-1/3}\right] \tag{11}$$

Thus $\Delta i_{c,dc}$ will become smaller, the greater τ and the smaller δ. However in cases where $Q(E) \neq 0$, this difference can never be exactly zero. The difference in faradaic current ($\Delta i_{f,dc}$) in this "two sampling" method becomes

$$\Delta i_{f,dc} = i_{f,dc}(E,\tau) - i_{f,dc}(E,\tau+\delta) \tag{12}$$

or

$$\Delta i_{f,dc} = \left(\frac{7}{3\pi}\right)^{\frac{1}{2}} nFkm^{2/3}D^{1/2}C\left[\frac{1}{1+\epsilon}\right]\tau^{1/6}\left[1-\left(1+\frac{\delta}{\tau}\right)^{1/6}\right] \tag{13}$$

When δ is very small compared to τ, the last term between the brackets can be approximated by

$$\left(1+\frac{\delta}{\tau}\right)^{1/6} \approx 1+\frac{\delta}{6\tau} \tag{14}$$

Relation (13) can now be rewritten as

$$\Delta i_{f,dc} = \left(\frac{7}{3\pi}\right)^{\frac{1}{2}} nFkm^{2/3}D^{1/2}C\left[\frac{1}{1+\epsilon}\right]\tau^{1/6}\left[-\frac{\delta}{6\tau}\right] \tag{15}$$

The sensitivity of the method is reduced to $-\delta/6\tau$ (which is very small) of the original sampled d.c. polarographic faradaic current, and the method will not be analytically useful because of lack of sensitivity, although the signal-to-noise ratio is increased.

In eqn. (11), $\Delta i_{c,dc}$ can be made exactly zero — independent of the value of $Q(E)$ — by multiplying $i_{c,dc}(E,\tau+\delta)$, before subtracting, by a factor

$$\left(1+\frac{\delta}{\tau}\right)^{1/3} \tag{16}$$

which contains essentially instrumental parameters.

If relation (16) is generated instrumentally, the faradaic current is also multiplied by that factor; in that case, $\Delta i_{f,dc}$ will become

$$\Delta i_{f,dc} = \left(\frac{7}{3\pi}\right)^{\frac{1}{2}} nFkm^{2/3}D^{1/2}C\left[\frac{1}{1+\epsilon}\right]\tau^{1/6}\left[1-\left(1+\frac{\delta}{\tau}\right)^{1/2}\right] \tag{17}$$

If $\delta \ll \tau$, the current sensitivity is reduced to about $-\delta/2\tau$ of the original value of the sampled d.c. polarographic current, i.e., again there is a lack of sensitivity.

Normal pulse polarography

In normal pulse polarography (n.p.p.) nearly at the end of the drop life (at τ seconds), the potential is pulsed from E_1 (which is constant during the run and usually chosen so that no faradaic reaction occurs) to E_2, which is

different for each drop, but considered constant during the drop life (Fig. 3). At a delay time δ after pulse application, δ being much greater than the relaxation time for the cell-potentiostat system, the current $i_{npp}(E_2, \tau + \delta)$ is sampled. At potential E_1 there will be no faradaic current at all. Thus i_{npp} will contain a faradaic component only from the pulse application and is given by

$$i_{f,npp} = \frac{nFkm^{2/3}D^{1/2}C}{\pi^{1/2}} \left[\frac{1}{1+\epsilon_2}\right] \frac{\tau^{2/3}}{\delta^{1/2}} \left(1+\frac{\delta}{\tau}\right)^{2/3} \tag{18}$$

where

$$\epsilon_2 = \exp\left[\frac{nF}{RT}(E_2 - E_{\frac{1}{2}}^{r})\right] \tag{19}$$

The charging current caused by drop growth, which is the same in principle as in d.c. polarography, can be described by

$$i_{c,npp} = -\tfrac{2}{3}\, km^{2/3}Q(E_2)\tau^{-1/3}\left(1+\frac{\delta}{\tau}\right)^{-1/3} \tag{20}$$

The influence of this charging current on the results can be reduced by taking two current samples at delay times δ_1 and δ_2 (Fig. 4) and subtracting. The remaining charging current ($\Delta i_{c,npp}$) will become

$$\Delta i_{c,npp} = -\tfrac{2}{3}\, km^{2/3}Q(E_2)\tau^{-1/3}\left[\left(1+\frac{\delta_1}{\tau}\right)^{-1/3} - \left(1+\frac{\delta_2}{\tau}\right)^{-1/3}\right] \tag{21}$$

This current can be eliminated completely by multiplying the second sampling, before subtracting, by

$$\left[\frac{1+\frac{\delta_2}{\tau}}{1+\frac{\delta_1}{\tau}}\right]^{1/3} \tag{22}$$

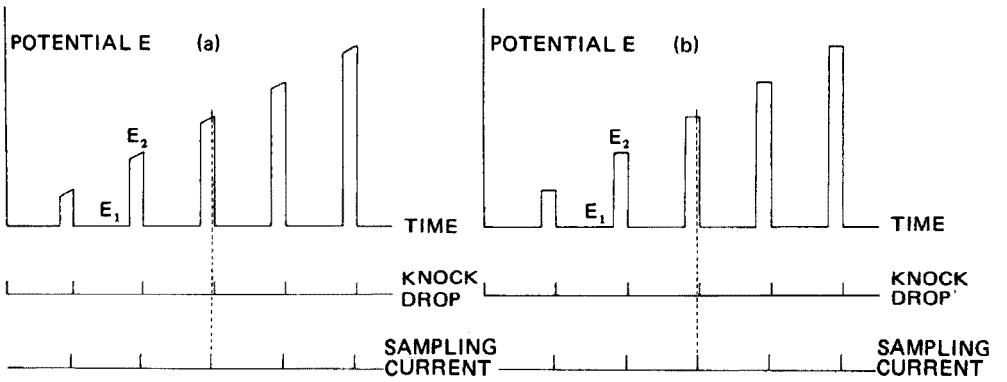

Fig. 3. Normal pulse polarography (a) with the usual wave-form, (b) with the optimal wave-form.

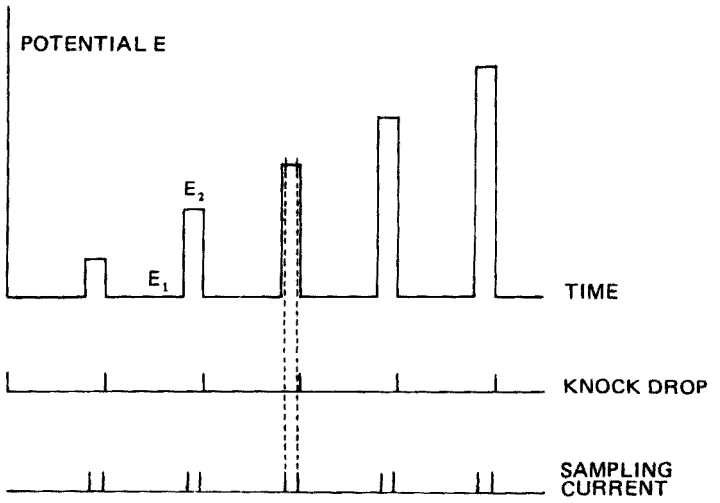

Fig. 4. Normal pulse polarography with the optimal wave-form in the modification described.

which contains essentially instrumentally determined parameters. In this modified n.p.p., the charging current caused by drop growth is eliminated, but the price paid is some reduction of the faradaic pulse response. The resulting $\Delta i_{f,npp}$ (before multiplication of the second sampling) becomes

$$\Delta i_{f,npp} = \frac{nFkm^{2/3}D^{1/2}C}{\pi^{1/2}} \left[\frac{1}{1+\epsilon_2}\right] \tau^{2/3} \left[\frac{\left(1+\frac{\delta_1}{\tau}\right)^{2/3}}{(\delta_1)^{1/2}} - \frac{\left(1+\frac{\delta_2}{\tau}\right)^{2/3}}{(\delta_2)^{1/2}}\right] \quad (23)$$

and after multiplication and then subtraction, the difference is

$$\Delta i_{f,npp} = \frac{nFkm^{2/3}D^{1/2}C}{\pi^{1/2}} \left[\frac{1}{1+\epsilon_2}\right] \left[\tau^{2/3} \left(1+\frac{\delta_1}{\tau}\right)^{-1/3}\right] \left[\frac{\left(1+\frac{\delta_1}{\tau}\right)}{(\delta_1)^{1/2}} - \frac{\left(1+\frac{\delta_2}{\tau}\right)}{(\delta_2)^{1/2}}\right] \quad (24)$$

Differential pulse polarography

In differential pulse polarography (d.p.p.) nearly at the end of drop life (at τ seconds), a pulse of constant value during the run (ΔE) is applied on a varying potential ramp or on a stepped potential E_1, which is synchronized with drop time (Fig. 5). The current is sampled at τ, just before the pulse application and at a delay time δ, at the end of the pulse. It was pointed out by Christie and Osteryoung [4] that the remaining capacitance current caused by drop growth can be described by (note that the second sampling is subtracted from the first here)

$$\Delta i_{c,dpp} = -\tfrac{2}{3}\, km^{2/3}\tau^{-1/3} \left[Q(E_1) - Q(E_2) \left(1+\frac{\delta}{\tau}\right)^{-1/3}\right] \quad (25)$$

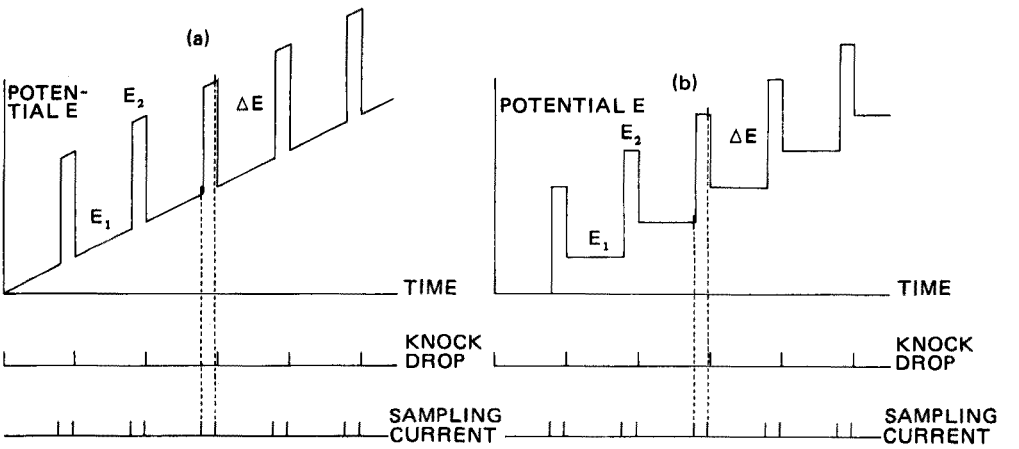

Fig. 5. Differential pulse polarography (a) with the usual wave-form, (b) with the optimal wave-form.

where $Q(E_1)$ is the charge density just before and $Q(E_2)$ the charge density during pulse application; potentials E_1 and $E_2 = E_1 + \Delta E$ are again considered constant during drop time t. Even when δ is very small compared to τ, there will remain a capacitance current which is proportional to $[Q(E_1) - Q(E_2)]$. This $\Delta i_{c,dpp}$ can never be made exactly zero for the whole run by multiplying the second sampling by some instrumentally determined factor, because this current still depends on $Q(E_1)$ and $Q(E_2)$, which are themselves non-linear potential-dependent quantities.

However, if current samples are taken at delay times δ_1 and δ_2 after pulse application (where δ_1 and δ_2 are again much greater than the relaxation time for the cell-potentiostat system), and if the sampling before pulse application at τ seconds is omitted (Fig. 6), then, since the potential E_2 is essentially the same for both samplings, relation (25) can be rewritten to give

$$\Delta i_{c,dpp} = -\tfrac{2}{3}\, km^{2/3} Q(E_2) \tau^{-1/3} \left[\left(1 + \frac{\delta_1}{\tau}\right)^{-1/3} - \left(1 + \frac{\delta_2}{\tau}\right)^{-1/3} \right] \qquad (26)$$

This capacitance current can be eliminated completely (as in modified n.p.p.) by multiplying the second sampling, before subtraction, by a factor, which is essentially the same factor as in modified n.p.p.:

$$\left[\frac{1 + \frac{\delta_2}{\tau}}{1 + \frac{\delta_1}{\tau}} \right]^{1/3} \qquad (27)$$

Again these are instrumentally determined parameters. Thus, with the modified d.p.p. complete elimination of charging current caused by drop growth is again achieved.

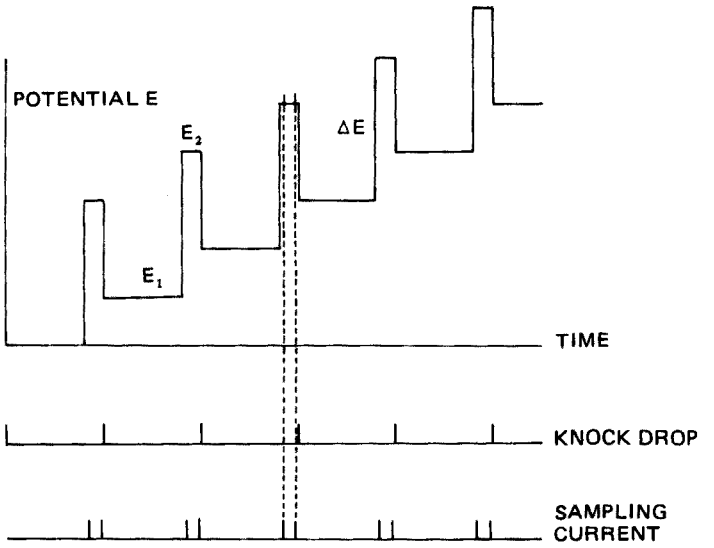

Fig. 6. Differential pulse polarography with the optimal wave-form in the modification described.

The faradaic currents in d.p.p. must be considered. Christie et al. [1] calculated the faradaic differential pulse current $i_{f,dpp}$, which is given by

$$i_{f,dpp} = \frac{nFkm^{2/3}D^{1/2}C}{\pi^{1/2}} \left[\frac{1}{1+\epsilon_2} - \frac{1}{1+\epsilon_1}\right] \frac{\tau^{2/3}}{\delta^{1/2}} \left(1+\frac{\delta}{\tau}\right)^{2/3} \tag{28}$$

where

$$\epsilon_1 = \exp\left[\frac{nF}{RT}(E_1 - E_{\frac{1}{2}}^r)\right] \quad \text{and} \quad \epsilon_2 = \exp\left[\frac{nF}{RT}(E_2 - E_{\frac{1}{2}}^r)\right] \tag{29}$$

A minor distortion of the faradaic pulse component arising from the term $i_{pol}(E_1,\tau) - i_{pol}(E_1,\tau+\delta)$ is ignored in relation (28), but can be calculated readily [4] from

$$\Delta i_{f,dc} = \left(\frac{7}{3\pi}\right)^{1/2} nFkm^{2/3}D^{1/2}C \left[\frac{1}{1+\epsilon_1}\right] \tau^{1/6} \left[1 - \left(1+\frac{\delta}{\tau}\right)^{1/6}\right] \tag{30}$$

which is essentially the same as relation (13).

For eqn. (28) taking current samples at δ_1 and δ_2 after pulse application and subtracting will result in

$$\Delta i_{f,dpp} = \frac{nFkm^{2/3}D^{1/2}C}{\pi^{1/2}} \left[\frac{1}{1+\epsilon_2} - \frac{1}{1+\epsilon_1}\right] \tau^{2/3} \left[\frac{\left(1+\frac{\delta_1}{\tau}\right)^{2/3}}{(\delta_1)^{1/2}} - \frac{\left(1+\frac{\delta_2}{\tau}\right)^{2/3}}{\delta^{1/2}}\right] \tag{31}$$

and for relation (30), the result will be

$$\Delta i_{f,dc} = \left(\frac{7}{3\pi}\right)^{1/2} nFkm^{2/3}D^{1/2}C \left[\frac{1}{1+\epsilon_1}\right] \tau^{1/6} \left[\left(1+\frac{\delta_1}{\tau}\right)^{1/6} - \left(1+\frac{\delta_2}{\tau}\right)^{1/6}\right] \quad (32)$$

For eqn. (31), multiplication of the second current sample by relation (27) before subtracting, in order to eliminate completely the influence of charging current, gives

$$\Delta i_{f,dpp} = \frac{nFkm^{2/3}D^{1/2}C}{\pi^{1/2}} \left[\frac{1}{1+\epsilon_2} - \frac{1}{1+\epsilon_1}\right] \left[\tau^{2/3} \left(1+\frac{\delta_1}{\tau}\right)^{-1/3}\right] \times \left[\frac{\left(1+\frac{\delta_1}{\tau}\right)}{(\delta_1)^{1/2}} - \frac{\left(1+\frac{\delta_2}{\tau}\right)}{(\delta_2)^{1/2}}\right] \quad (33)$$

and for eqn. (32)

$$\Delta i_{f,dc} = \left(\frac{7}{3\pi}\right)^{1/2} nFkm^{2/3}D^{1/2}C \left[\frac{1}{1+\epsilon_1}\right] \tau^{1/6} \left[\left(1+\frac{\delta_1}{\tau}\right)^{-1/3}\right] \times \left[\left(1+\frac{\delta_1}{\tau}\right)^{1/2} - \left(1+\frac{\delta_2}{\tau}\right)^{1/2}\right] \quad (34)$$

which can be approximated by

$$\Delta i_{f,dc} = \left(\frac{7}{3\pi}\right)^{1/2} nFkm^{2/3}D^{1/2}C \left[\frac{1}{1+\epsilon_1}\right] \tau^{1/6} \left[\left(1+\frac{\delta_1}{\tau}\right)^{-1/3}\right] \left[\frac{\delta_1-\delta_2}{2\tau}\right] \quad (35)$$

If the difference between the delay times δ_1 and δ_2 is made small compared to τ, this d.c. faradaic component can be ignored.

Comparison of the sensitivities of modified n.p.p. and modified d.p.p.

In relation (24), $\Delta i_{f,npp}$ will reach a maximum value when $\epsilon_2 = 0$, so that

$$(\Delta i_{f,npp})_{max} = \frac{nFkm^{2/3}D^{1/2}C}{\pi^{1/2}} \left[\tau^{2/3} \left(1+\frac{\delta_1}{\tau}\right)^{-1/3}\right] \left[\frac{\left(1+\frac{\delta_1}{\tau}\right)}{(\delta_1)^{1/2}} - \frac{\left(1+\frac{\delta_2}{\tau}\right)}{(\delta_2)^{1/2}}\right] \quad (36)$$

The sensitivity of modified d.p.p. will be smaller in all cases, except when $\epsilon_2 = 0$ and $\epsilon_1 = \infty$, thus using very large modulation amplitudes (ΔE).

Relation (28) has a maximum value when the term between the brackets is maximal; it was pointed out by Parry and Osteryoung [5] that $(i_{f,dpp})_{max}$ in the original d.p.p. mode can be written as

$$(i_{f,dpp})_{max} = \frac{nFkm^{2/3}D^{1/2}C}{\pi^{1/2}} \left[\frac{\tau^{2/3}}{\delta^{1/2}} \left(1+\frac{\delta}{\tau}\right)^{2/3}\right] \left[\frac{\sigma-1}{\sigma+1}\right] \quad (37)$$

where

$$\sigma = \exp\left[\frac{nF}{RT}\frac{(E_2-E_1)}{2}\right] = \exp\left[\frac{nF}{RT}\frac{\Delta E}{2}\right] \quad (38)$$

In the modified d.p.p. mode $(\Delta i_{f,dpp})_{max}$ will be

$$(\Delta i_{f,dpp})_{max} = \frac{nFkm^{2/3}D^{1/2}C}{\pi^{1/2}} \left[\tau^{2/3} \left(1 + \frac{\delta_1}{\tau}\right)^{-1/3}\right] \left[\frac{\left(1 + \frac{\delta_1}{\tau}\right)}{(\delta_1)^{1/2}} - \frac{\left(1 + \frac{\delta_2}{\tau}\right)}{(\delta_2)^{1/2}}\right] \left[\frac{\sigma - 1}{\sigma + 1}\right] \tag{39}$$

Thus the sensitivity of modified n.p.p. and modified d.p.p. can be related by

$$(\Delta i_{f,dpp})_{max} = (\Delta i_{f,npp})_{max} \left[\frac{\sigma - 1}{\sigma + 1}\right] \tag{40}$$

where $(\sigma - 1)/(\sigma + 1)$ is the diminution factor, which is in all cases less than 1. Since wave resolution is better in d.p.p. than in n.p.p., which is also true for the modified methods described, the resolution in modified n.p.p. can be increased by taking the difference between the faradaic response of two successive drops. Thus, for the differential modified n.p.p. method, $\Delta(\Delta i_{f,npp})$ can be written as

$$\Delta(\Delta i_{f,npp})_{max} = \frac{nFkm^{2/3}D^{1/2}C}{\pi^{1/2}} \left[\frac{1}{1 + \epsilon_2} - \frac{1}{1 + \epsilon_1}\right] \left[\tau^{2/3} \left(1 + \frac{\delta_1}{\tau}\right)^{-1/3}\right] \times \left[\frac{\left(1 + \frac{\delta_1}{\tau}\right)}{(\delta_1)^{1/2}} - \frac{\left(1 + \frac{\delta_2}{\tau}\right)}{(\delta_2)^{1/2}}\right] \tag{41}$$

which can be rewritten for the maximum value of the faradaic current $\Delta(\Delta i_{f,npp})_{max}$ by relation (39).

However, in this case $(E_2 - E_1)$ is the difference in potential between two successive drops, and since this difference is typically much smaller than the modulation amplitude ΔE in the d.p.p. mode, the sensitivity of differential modified n.p.p. is much smaller than that of modified d.p.p.

CONCLUSION

The charging current caused by drop growth, when the optimal wave-forms for n.p.p. (Fig. 4) and d.p.p. (Fig. 6) are used, can be reduced by sampling twice in the same pulse at essentially constant potential at delay times δ_1 and δ_2 after pulse application and subtracting the two samplings; this results in a better base-line. The sensitivity of both the described methods is then reduced to about 50% of the values obtained in the ordinary modes, but the signal-to-noise ratios are increased remarkably.

If the second sampling is multiplied by an essentially instrumentally determined factor before the subtraction, the charging current can be theoretically exactly zero. Maximum sensitivity is obtained in modified n.p.p., but when sensitivity is considered together with wave resolution, better performance can be achieved with modified d.p.p.

For ordinary and modified d.p.p. with the optimal wave-forms, the theoretical base-lines of a 0.1 M KCl solution were calculated (Fig. 7) from

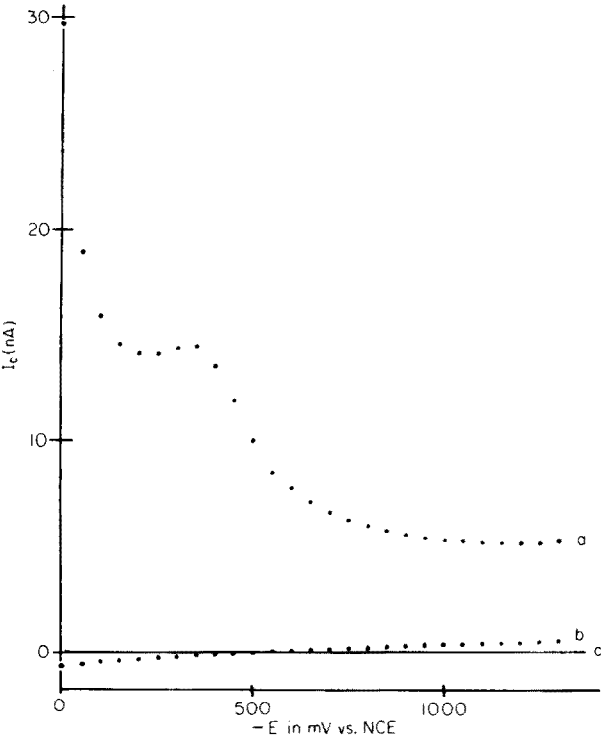

Fig. 7. Theoretical polarograms of 0.1 M KCl solution. Modulation amplitude d.p.p. 50 mV; $m = 2 \cdot 10^{-6}$ kg s^{-1}. a. Original d.p.p., $\tau = 2.000$ s and $\delta = 0.040$ s (relation 25). b. Modified d.p.p. $\tau = 2.000$ s and $\delta_1 = 0.010$ s and $\delta_2 = 0.040$ s (relation 26). c. Modified d.p.p. with multiplication of the second sampling by relation (27) before subtraction.

the charge density data of Grahame [6]; instantaneous values were taken for the charging current so that the "sampling width" is considered to be zero.

In Part II of this series, the proper choice of the delay times δ_1 and δ_2 will be evaluated with respect to the faradaic and charging currents involved in d.p.p. The influence of practical sampling width will be considered and incorporated in the requirements for optimal performance in d.p.p.

Some preliminary results are given here; the conventional d.p.p. wave-form was used (cf. Fig. 5a), the sampling currents being measured within the duration of the pulse with a modified Bruker E 310 modular research polarograph. The second sampling was not multiplied by the required factor before the subtraction. Figure 8 shows the polarographic curves for chloramphenicol. It can be seen that the signal-to-noise ratio in normal d.p.p. is about 3, but in modified d.p.p. about 21 for a 10^{-6} M chloramphenicol solution. Thus when the same polarographic noise levels are compared, modified d.p.p. is superior in sensitivity (note that drop time t is not exactly the same in all experiments). The detection limit obtained for this electrochemically incompletely reversible compound was 1 p.p.b. Under ideal

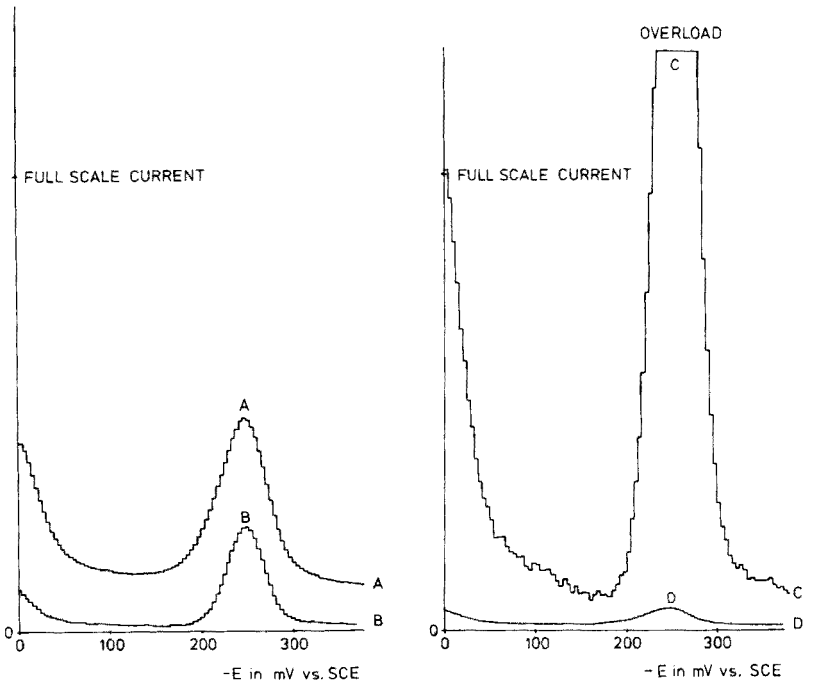

Fig. 8. Polarograms of 10^{-6} M chloramphenicol by the ordinary and modified d.p.p. modes. $\Delta E = -100$ mV; scan rate 2 mV s^{-1}; drop time 2 s; 0.1 M acetate buffer. A. Ordinary mode, full scale current 2 μA, $\delta = 0.045$ s; noise level at $E_p \approx 230$ nA. B. Modified mode, full scale current 2 μA, $\delta_1 = 0.045$ and $\delta_2 = 0.095$ s; noise level at $E_p \approx 20$ nA. C. Modified mode, full scale current 0.2 μA; about the same polarographic noise level as (A); noise level at $E_p \approx 18$ nA. D. Ordinary mode, full scale current 20 μA; about the same polarographic noise level as (B).

conditions (optimal wave-form, multiplication of the second sampling before subtraction and small sampling widths), a limit of detection even lower than 0.1 p.p.b. is expected.

The authors are indebted to Dr. P. Jung of the Electrochemical Division of Bruker Spectrospin, who modified the Bruker instrument, and Drs. J. J. van der Lee who did the chloramphenicol measurements.

REFERENCES

1 J. H. Christie, L. L. Jackson and R. A. Osteryoung, Anal. Chem., 48 (1976) 242.
2 G. C. Barker and A. W. Gardner, Z. Anal. Chem., 173 (1960) 79.
3 N. Klein and Ch. Yarnitzky, Electroanal. Chem. Interfacial Electrochem., 61 (1975) 1.
4 J. H. Christie and R. A. Osteryoung, Electroanal. Chem. Interfacial Electrochem., 49 (1974) 301.
5 E. P. Parry and R. A. Osteryoung, Anal. Chem., 37 (1965) 1634.
6 D. C. Grahame, J. Am. Chem. Soc., 71 (1949) 2975.

Analytica Chimica Acta, 89 (1977) 83—91

THE USE OF AMPEROMETRIC OXYGEN ELECTRODES FOR MEASUREMENTS OF ENZYME REACTIONS

LAWRENCE C. THOMAS* and GARY D. CHRISTIAN

Department of Chemistry, University of Washington, Seattle, Washington 98195 (U.S.A.)

(Received 21st May 1976)

SUMMARY

Amperometric oxygen electrodes are useful transducers for enzymatic analyses. One must, however, account for contributions from oxygen incorporation or depletion caused by sample introduction, stirring and diffusion, or non-enzymatic reactions, as well as for instrumental response time. Examples of various characteristics of these contributions are shown and discussed from a theoretical basis.

Amperometric oxygen probes, either of the bare-electrode variety or the Clark-like membrane electrode configuration, are useful in enzymatic determinations involving oxygen measurement [1—5]. The microelectrode current drawn, which is proportional to the oxygen concentration to which the electrode is exposed, is typically very small and the fraction of oxygen consumed in the electrode reaction is, in general, negligible. These electrodes are easy to use, generally respond rapidly, and can be used under a variety of in vivo or in vitro conditions, and for continuous measurements. For optimal use, the indicator electrode should be relatively noise-free and the residual current should be small. Ideally, the reaction system should be closed to the atmosphere to avoid transport of oxygen from outside the cell [6].

Bare-electrode systems are vulnerable to poisoning by various biological species and are less versatile than the Clark-like membrane electrodes. Clark electrodes exhibit only a small residual current, but they are subject to slight drifts, have slower response times than bare electrodes, and have substantial temperature coefficients. They should be maintained at steady state by providing sufficient agitation of the solution. An oxygen-permeable membrane protects these electrodes from interfering species and enhances the reproducibility of measurements.

Recent applications of Clark electrodes to enzymatic measurements have been described for the determination of glucose in serum with glucose oxidase [7—12], uric acid in serum with uricase [7, 13], tyrosine in serum with tyrosinase [14], alkaline phosphatase in serum with a phenol phosphate substrate and tyrosinase to catalyze air oxidation of the phenol product [15],

*Present address: Washington State Toxicology Laboratory, University of Washington, Seattle, Washington 98195 (U.S.A.)

and cholesterol in serum with cholesterol oxidase to catalyze the oxidation of cholesterol [16]. These methods are based on the work of Kadish et al. [17, 18], and utilize an oxygen probe and derivative circuitry to monitor continuously the rate of oxygen consumption.

In all these open oxidase systems, possible sources of error arise from the response time of the electrode system, generation or depletion of oxygen by other reactions, disproportionation of hydrogen peroxide produced in the enzyme reactions, the need for air presaturation of the system, and the transport of oxygen from outside the cell [17, 19]. Other systems, such as continuous flow systems, covered cells, and enzyme electrodes [20—24], must also consider some of these contributions.

This paper reports some of these contributions in enzymatic analyses. A theoretical basis of correcting for the various contributions is presented and practical applications are described for useful oxygen-dependent, enzyme-based methods.

EXPERIMENTAL

Reagents

Beckman Glucose Reagent (for glucose measurements) and Electrolytic Gel (for the oxygen electrode) were used. All other chemicals were reagent-grade quality, and deionized-distilled water was used to prepare all solutions.

Procedure

Procedures for glucose determinations, as recommended by Beckman Instruments, Inc. [7], were used unless otherwise stated.

Apparatus

A Beckman Glucose Analyzer, interfaced to a two-pen strip chart recorder, was used for all measurements. Monitoring the Analyzer output (direct current output or its derivative) on a recorder involves measuring output potentials from the amplifier-gain potentiometers. In either case, care must be taken to protect these circuits from drawing current. In these experiments, output potentials were picked from the third pin of the linear and derivative amplifier-gain potentiometers through $2.5 \cdot 10^5$ ohm resistors, and measured by a high-impedance input recorder.

The Beckman Glucose Analyzer incorporates five functional groups of apparatus; an oxygen electrode and potentiostat, a linear amplifier and a derivative amplifier with display electronics, a reagent storage and transfer system, a sample cell with a magnetic stirrer, and timing and logic circuitry.

The oxygen sensor is a conventional Clark electrode design containing an internal Ag/AgCl reference and a planar microelectrode covered with an electrolytic gel and a Teflon membrane. This working electrode operates at a potential on the first voltammetric plateau of oxygen [1] and gives an amperometric current proportional to the partial pressure of oxygen in the

solution to which the probe is exposed, if several seconds are allowed to achieve oxygen equilibrium across the Teflon membrane, and if the temperature and ionic strength remain constant.

The normal operation of the instrument involves delivery of 1 ml of glucose oxidase reagent (with iodide, molybdate, ethanol, and catalase added to consume hydrogen peroxide) to the sample cell, and the derivative "peak-picker" is inactivated for 30 s while the system stabilizes and the oxygen tension equilibrates across the Teflon membrane and with the surrounding atmosphere. Then a sample is introduced, and the glucose in the sample is oxidized by molecular oxygen in the presence of glucose oxidase to form gluconic acid and hydrogen peroxide. The rate of this oxygen consumption is proportional to the concentration of glucose in the sample [17].

RESULTS AND DISCUSSION

Response time

The response time for the Glucose Analyzer output, for sudden changes in oxygen concentration, shows a marked dependence on the magnitude of the change. The source of this variable instrumental time-constant is a combination of (1) the rate at which equilibrium across the Clark electrode membrane is achieved, (2) electronic time-constants inherent in the Glucose Analyzer circuitry, and (3) the recorder response time. The second of these is on the order of 1.5 s, as approximated by noise filtering. The third is very small, ca. 0.05 s/in. or 0.5 s for a current change of 30 nA. The first, the time constant for the membrane electrode, depends on the thickness of the membrane, the stirring rate of the solution, the thickness of the electrolyte gel layer, and diffusion parameters within the electrode.

The half-time of the total response was measured by adding various deaerated samples of water to the empty sample cup. The time required for the output from the linear amplifier to reach half the minimum value attained was plotted as a function of half the total current change (Fig. 1). The nature of this relationship indicates that, on sudden changes in oxygen tension, the maximum rate of change of the output signal is not quite directly proportional to the magnitude of the change. In addition, the time intercept indicates a 1.8 s half-time for very small and sudden increments of change. This approximates the noise filtering estimates of the time constant for the electronics.

If a linear relationship is assumed for Fig. 1, then the total instrument time-constant dependence on the change in current may be approximated by

$$t_{1/2(\Delta i)} = (1.8 + 0.16\ \Delta i) \qquad (1)$$

where Δi is given as nA and $t_{1/2}$ as s. This was determined for an electrode with an initial current at equilibrium in air of 30 nA. This response-time dependence varies from electrode to electrode, because of variations in membranes, stirring, electrolyte, etc.

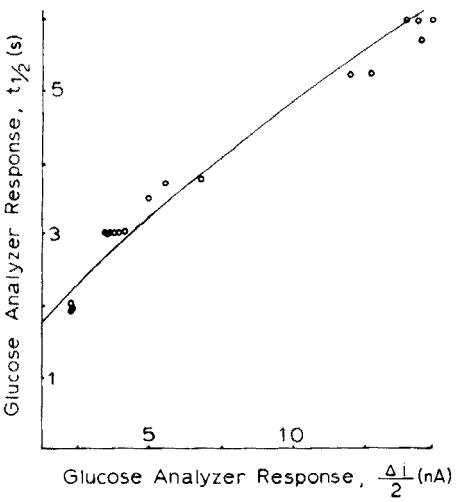

Fig. 1. Response half-time vs. half the total response change for Beckman Glucose Analyzer linear amplifier output.

Adaptation to enzymatic analyses

In the following discussion, the current caused by oxygen and the concentration of oxygen are used interchangeably, unless otherwise stated. The meanings of the symbols used are consistent with the list shown in Table 1 and with conventional chemical notation.

There are at least two practical problems involved in the adaptation of amperometric oxygen probes to the determination of oxygen-dependent substrates or enzymes. First, there is a sudden change in oxygen concentration in the sample cell on addition of a sample that has an oxygen tension different from that of the reagent solution already in the cell [18]. This sudden change will add to any chemically driven change in oxygen concentration in the cell. For the relatively small sample volumes used — ca. 1—50 μl added to 1 ml of reaction solution — this change is generally small and causes a small derivative signal with a half-time on the order of 10 s.

TABLE 1

List of subscripts

t	at time t (indicates time dependence)
0	initial
eq	at equilibrium (with air for $[O_2]$)
air	at equilibrium with air
S	caused by stirring
D	caused by diffusion
SD	caused by stirring and diffusion
T	total
N	non-enzymatic reactions
E	enzymatic reactions

The second practical problem involves the rate of change in oxygen concentration caused by stirring and diffusion of oxygen into or out of the solution when the reaction solution is not at equilibrium with the oxygen in the surrounding environment [6, 17, 25, 26]. This effect was evaluated by adding to the cell 1-ml samples of partially deaerated water which varied in their oxygen concentrations. The rate of oxygen incorporation into the sample cell was measured by the output of the derivative amplifier. This is plotted as a function of the "fraction saturation" in Fig. 2. In the Figure, $[O_2]/[O_2]_{air}$ is identical with $[O_2]/[O_2]_{eq}$ used in the following equations. The Figure indicates the relationship is nearly linear such that

$$\left(\frac{d[O_2]_t}{dt}\right)_{SD} \approx k\left(1 - \frac{[O_2]_t}{[O_2]_{eq}}\right) = k\left(\frac{[O_2]_{eq} - [O_2]_t}{[O_2]_{eq}}\right) \qquad (2)$$

Rate analyses. If the rate of change in oxygen concentration caused by enzymatic reactions has a half-time on the order of 30 s or greater, the sudden changes in oxygen concentration caused by the introduction of samples, as discussed above, may be neglected after ca. 30 s from initiation of the enzymatic reaction. The rate of change of oxygen concentration in the sample cell, if these sudden changes are negligible, may be written in the following form

$$\left(\frac{d[O_2]_t}{dt}\right)_T = \left(\frac{d[O_2]_t}{dt}\right)_E + \left(\frac{d[O_2]_t}{dt}\right)_N + \left(\frac{d[O_2]_t}{dt}\right)_{SD} \qquad (3)$$

That is, the total rate of change in oxygen concentration in the sample chamber (T) is a sum of the rates of change caused by the enzymatic reaction (E), the non-enzymatic (blank or interfering) reactions (N), and oxygen incorporation or depletion because of stirring and diffusion (SD). The signs preceding any of the forms may be positive or negative depending on the conditions. For the Beckman Glucose Reagent, the hydrogen peroxide generated by the enzymatic reaction is catalytically consumed by iodide and ethanol and therefore does not disproportionate to give oxygen, and the rate which arises from non-enzymatic reactions may be neglected.

For enzymatic reactions with no interfering non-enzymatic reactions, the total rate of change in oxygen tension can be estimated at any time as a summation of the second and fourth terms of eqn. (3). The fourth term is described in eqn. (2), and is negligible if the ratio $[O_2]_t/[O_2]_{eq}$ is very near unity. Therefore, rates of oxygen consumption measured before large amounts of oxygen are consumed have only small contributions arising from oxygen incorporation. However, rates measured when the ratio $[O_2]_t/[O_2]_{eq}$ is much different from unity, may require consideration of the contributions to the total rate caused by stirring and diffusion. The correction involves a simple subtraction of a derivative signal arising from the rate of oxygen incorporation. This may be accomplished by noting the oxygen tension at the time of the analytical derivative measurement, finding a correction factor from a graph similar to Fig. 2 at the appropriate oxygen tension, and subtrac-

ting it from the measured output (see Fig. 3). A correction graph like Fig. 2 must be constructed for the particular apparatus and solutions utilized.

Rate analyses of glucose [18, 27], uric acid [7, 11], tyrosine [14], cholesterol [16], and alkaline phosphatase [15] depend on measurement of the maximum rate of change in oxygen tension in a reaction solution. In all these cases, this measured rate includes a contribution from oxygen incorporation, and the apparent enzymatic rate of oxygen consumption does not exactly equal the rate of the enzymatic reactions (see Fig. 3). As long as standards and samples are run in the same manner, however, the error from the oxygen incorporation in this example may be neglected because the relationship in Fig. 2 is almost linear, i.e., the error is directly proportional to $[O_2]_{eq} - [O_2]_t$

Time Dependence. The oxygen concentration at any time t, starting with equilibrium oxygen tension at time $t = 0$, can be formulated for an oxygen-consuming enzymatic system. If non-enzymatic reactions consume oxygen also, the contribution from stirring and diffusion will be an influx of oxygen and we can write

$$[O_2]_t = [O_2]_{eq} - \int_0^t \left(\frac{d[O_2]_t}{dt}\right)_T dt \tag{4}$$

$$= [O_2]_{eq} - \int_0^t \left(\frac{d[O_2]_t}{dt}\right)_E dt - \int_0^t \left(\frac{d[O_2]_t}{dt}\right)_N dt + \int_0^t \left(\frac{t[O_2]_t}{dt}\right)_{SD} dt \tag{5}$$

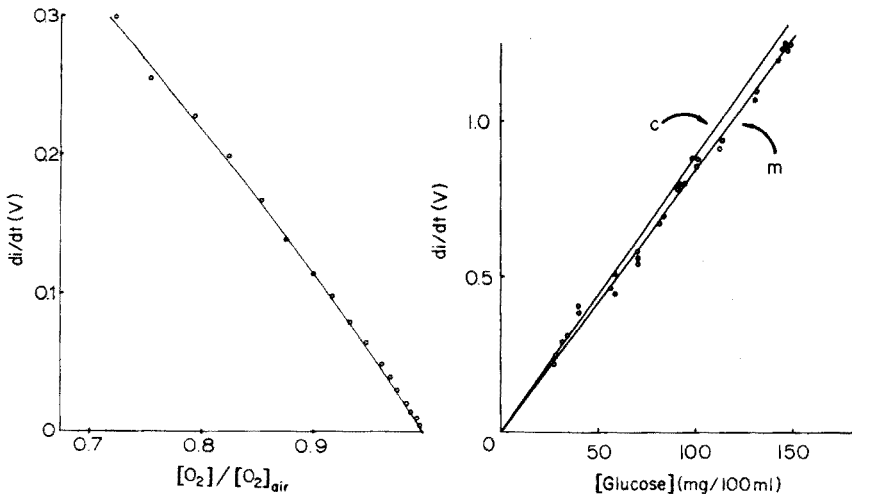

Fig. 2. Relative rate of oxygen incorporation into 1 ml of 0.01 M glucose solution, pH 5.5, 0.1 M Na_2HPO_4, as a function of degree of oxygen saturation in a Beckman Glucose Analyzer sample cell.

Fig. 3. Rate of oxygen consumption vs. concentration of glucose added to Beckman Glucose Reagent in Beckman Glucose Analyzer. (m) Rates as measured by derivative amplifier output; (c) rate as calculated ("corrected") by subtracting rate of oxygen incorporation at time of maximum rate, as determined by Fig. 2.

or,

$$[O_2]_t = [O_2]_{eq} - \int_0^t \left(\frac{d[O_2]_t}{dt}\right)_E dt - \int_0^t \left(\frac{d[O_2]_t}{dt}\right)_N dt + \int_0^t k \left(1 - \frac{[O_2]_t}{[O_2]_{eq}}\right) dt \quad (6)$$

Therefore,

$$[O_2]_{eq} - [O_2]_t = \int_0^t \left(\frac{d[O_2]_t}{dt}\right)_E dt + \int_0^t \left(\frac{d[O_2]_t}{dt}\right)_N dt - \int_0^t k \left(1 - \frac{[O_2]_t}{[O_2]_{eq}}\right) dt \quad (7)$$

and if non-enzymatic reactions are neglected

$$[O_2]_{eq} - [O_2]_t = \int_0^t \left(\frac{d[O_2]_t}{dt}\right)_E dt - \int_0^t k \left(1 - \frac{[O_2]_t}{[O_2]_{eq}}\right) dt \quad (8)$$

Equilibrium measurements. Analyses utilizing measurement of oxygen tension when the rate of oxygen consumption approaches the rate of oxygen incorporation at some time in the reaction when the measurement is made (i.e., a "pseudo-equilibrium" oxygen tension), may be more complicated than the measurements of rates described above. For the simplest case, in which the rate of the enzymatic reaction is constant with time and directly proportional to an initial enzyme concentration (and assuming no non-enzymatic interferences),

$$\left(\frac{d[O_2]_t}{dt}\right)_E = k'[E]_0 = \left(\frac{d[O_2]_t}{dt}\right)_{SD} = k \left(1 - \frac{[O_2]_t}{[O_2]_{eq}}\right) \quad (9)$$

Therefore,

$$[E]_0 = \frac{k}{k'[O_2]_{eq}} \left([O_2]_{eq} - [O_2]_t\right) \quad (10)$$

and the enzyme concentration is directly proportional to the difference between the equilibrium oxygen tension and the oxygen tension at "pseudo-equilibrium". Except for the trivial case, $[E]_0 = 0$, the apparent amount of oxygen consumed, $([O_2]_{eq} - [O_2]_t)$, is not a stoichiometric measure of the amount of substrate consumed, because oxygen is introduced into the system by stirring and diffusion.

Assays utilizing "pseudo-equilibrium" oxygen tensions therefore may show a direct proportionality between the enzyme concentration and the apparent amount of oxygen consumed, as indicated in eqn. (10). However, in enzymatic analyses of substrate concentrations, this relationship is not stoichiometric, and may approximate a stoichiometric change only if the enzymatic rate is very much faster than the rate of oxygen incorporation (see above). That is, if $(d[O_2]_t/dt)_E \gg (d[O_2]_t/dt)_{SD}$, and $(d[O_2]_t/dt)_N \approx 0$, setting the last two terms in eqn. (7) equal to zero implies that

$$[O_2]_{eq} - [O_2]_t = \int_0^t \left(\frac{d[O_2]}{dt}\right)_E dt \quad (11)$$

and the integral in eqn. (11), when all the substrate is consumed, will approximate a stoichiometric measure of the amount of substrate introduced. In an open system, the third term in eqn. (7) will not be zero if $[O_2]_t/[O_2]_{eq}$ differs from unity, which, of course, is the condition being measured. Therefore, minimizing the amount of oxygen introduced from stirring and diffusion by minimizing the time allowed for this process increases the accuracy of this "stoichiometric" method of analysis. High rates of enzymatic reaction make this minimization practical.

For other systems where the rate of the enzymatic reaction changes as the oxygen tension changes, or the enzymatic rate varies because of inhibition or activation by products of the reaction, or where interferences from non-enzymatic reactions are not negligible, the use of the "pseudo-equilibrium" oxygen measurements may be more complicated. For systems where non-enzymatic reactions may be neglected, the "pseudo-equilibrium" oxygen tension can be related to the integral of the enzymatic rate by rearrangement and iterative integration of eqn. (8), or by use of calibration plots [26].

Consideration of the interferences described above is necessary to assure the accuracy of amperometric oxygen measurements in enzymatic analyses. The discussion applies, in general, to reaction systems open to the atmosphere, but the same concepts apply to "closed systems" such as continuous flow devices.

REFERENCES

1 G. D. Christian, Adv. in Biomed. Eng. Med. Phys., 4 (1971) 95.
2 R. W. Estabrook, in Methods in Enzymology, Vol. 10, R. W. Estabrook and M. E. Pullman (Eds.), Academic Press, New York, 1967, p. 40.
3 M. A. Lessler and G. P. Brierley, Methods Biochem. Anal., 17 (1969) 1.
4 L. C. Thomas, Thesis, University of Washington, 1975.
5 R. L. Rawls, Chem. Eng. News, 54 (1) (1976) 19.
6 J. Robinson and J. M. Cooper, Anal. Biochem., 33 (1970) 390.
7 Beckman Instruments, Inc., Bulletin 6300, Fullerton, California.
8 M. H. McLean and D. Hearn, Clin. Chem., 20 (1974) 856.
9 J. Fischl, D. Federman and N. Talmor, Clin. Chem., 21 (1975) 760.
10 B. Morrison, Clin. Chim. Acta, 42 (1972) 192.
11 J. C. Sternberg and J. P. Frain, 24th Nat. Meet. Am. Ass. Clin. Chem., Cincinnati, Ohio, August 1972.
12 J. F. Stevens, Clin. Chim. Acta, 32 (1971) 199.
13 S. Meites and K. Saniel-Banrey, Clin. Chem., 19 (1973) 308.
14 A. Kumar and G. D. Christian. Clin. Chem., 21 (1975) 325.
15 A. Kumar and G. D. Christian, Anal. Chem., 48 (1976) 1283.
16 A. Kumar and G. D. Christian, Clin. Chim. Acta.
17 A. H. Kadish, R. L. Little and J. C. Sternberg, Clin. Chem., 14 (1968) 116.
18 A. H. Kadish and J. C. Sternberg, Diabetes, 18 (1969) 467.
19 R. A. Messing, Biotech. Bioeng., 16 (1974) 525.
20 L. C. Clark and C. Lyons, Ann. N. Y. Acad. Sci., 102 (1962) 29.

21 L. C. Clark, in Ezyme Engineering, L. Wingard (Ed.), Wiley-Interscience, New York, 1972.
22 S. J. Updike and G. P. Hicks, Nature, 214 (1967) 986.
23 M. Nanjo and G. G. Guilbault, Anal. Chem., 46 (1974) 1769; Anal. Chim. Acta, 73 (1974) 367; 75 (1975) 169.
24 G. G. Guilbault and M. Nanjo, Anal. Chim. Acta, 78 (1975) 69.
25 H. L. Pardue and R. K. Simon, Anal. Biochem., 9 (1964) 204.
26 L. C. Thomas and G. D. Christian, Anal. Chim. Acta, 77 (1975) 153.
27 N. H. Chin and W. Kroontje, Anal. Chem., 33 (1961) 1757.

Analytica Chimica Acta, 89 (1977) 93—99

DETECTION AND DETERMINATION OF XANTHINE IN XANTHOSINE BY ELECTROCHEMICAL METHODS

JAMES L. OWENS and GLENN DRYHURST*

Department of Chemistry, University of Oklahoma, Norman, Okla. 73019 (U.S.A.)

(Received 20th August 1976)

SUMMARY

Xanthine and xanthosine are oxidized voltammetrically at the pyrolytic graphite electrode (PGE) at different potentials. The difference between the peak potentials of xanthine and xanthosine becomes most pronounced at pH 7—8. The presence of small amounts of xanthine in xanthosine samples is readily detected by linear sweep voltammetry at the PGE by the appearance of the voltammetric peak of xanthine. Xanthine present in xanthosine can be determined by controlled potential coulometric oxidation of the xanthine. The reproducibility of the method is ± 5—10%.

An investigation of the electrochemical oxidation and interfacial behavior of xanthosine (I) was begun recently to gain a better understanding of the electron-transfer and adsorption of this biologically important molecule. During preliminary studies of the electrochemical oxidation of xanthosine at a pyrolytic graphite electrode (PGE) it was noted that it gave a number of voltammetric oxidation peaks. The first, least positive, peak occurred at the same potential as the single peak observed for xanthine (II). Controlled potential electrolysis and coulometry of xanthosine at potentials corresponding to the first voltammetric oxidation peak showed that this peak could be completely eliminated without affecting the more positive peaks. The experimental *n*-value was found to be 0.2—0.25. If the first voltammetric peak observed

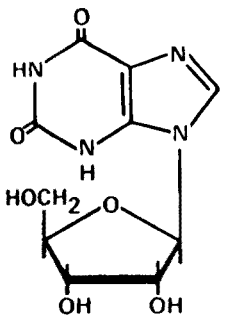

(I)

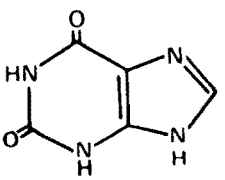

(II)

*To whom correspondence should be directed.

with commercial samples of xanthosine was an adsorption pre-peak, it could not have been eliminated without total electro-oxidation of xanthosine, with an *n*-value of 3—4 [1]. It was concluded, therefore, that commercial samples of xanthosine are contaminated with xanthine. Further studies of the electrochemical behavior of the first peak observed for commercial xanthosine samples showed that it exhibited behavior identical to the peak of pure xanthine [2].

Because the interfacial [3] and electro-oxidation [1] behavior of xanthine differs from that of xanthosine, it was necessary to devise an analytical method to screen xanthosine samples so that only those free of xanthine could be used. The ultraviolet absorption spectra of xanthine and xanthosine are virtually identical; the analysis of mixtures of these compounds by conventional spectrophotometry is impossible. Several qualitative methods, based on paper and thin-layer chromatography, for the detection of xanthine in the presence of xanthosine have been described [4—7] but they did not possess the speed and sensitivity required. A paper chromatographic method for the quantitative determination of many purine bases and their nucleosides [8] involves extracting the paper chromatogram after separation and determining the amount of each species by u.v. spectrophotometry. Apart from being time-consuming, this method applies only to samples containing relatively high concentrations of both the base and nucleoside. Tortolani and Colosi [9] employed a similar method, utilizing thin-layer chromatography on Sephadex G10-cellulose or Sephadex G10-silica gel. Brown et al. [10] employed high-pressure liquid chromatography to separate and determine xanthine and xanthosine in mixtures, although the peak resolution was rather poor.

Xanthine and xanthosine give well-separated voltammetric oxidation peak potentials at the PGE, and the use of electrochemical techniques to determine small quantities of xanthine in the presence of xanthosine has been investigated.

EXPERIMENTAL

Chemicals

Xanthosine (Calbiochem and Vega-Fox) and xanthine (Nutritional Biochemicals Corporation) were used.

Buffer solutions (ionic strength 0.5) were prepared from reagent grade chemicals.

Apparatus

For linear and cyclic sweep voltammetry, an instrument of conventional operational amplifier design [11] was used. Voltammograms were recorded on a Hewlett-Packard Model 7001A X-Y recorder. A conventional three-compartment electrochemical cell, thermostated at 25 ± 0.1°C, was utilized for voltammetry. Pyrolytic graphite was purchased from Super-Temp

Company, Santa Fe Springs, California. The fabrication of the micro PGE (4 mm diameter) and large electrodes for controlled potential coulometry has been described elsewhere [12].

Controlled potential coulometry was done with a Wenking Model LT73 potentiostat and a Koslow Scientific Model 541 coulometer. A two-compartment cell (each compartment ca. 130-ml capacity) was employed with a set of large pyrolytic graphite electrodes [12] (area ca. 42 cm^2) and a Fisher Fiber-Tip saturated calomel reference electrode (SCE) in one compartment and a platinum foil counter-electrode in the other. The usual volume of the electrolysis solution was 100—125 ml; this was stirrred magnetically. The counter-electrode compartment was filled with the appropriate buffer solution. All potentials are referred to the SCE at 25°C.

Procedure for detection of xanthine in xanthosine

The xanthosine (1—2 mg) is dissolved in 10.0 ml of the desired buffer. A buffer in the pH range 7—8 is most suitable. If there is a substantial amount of xanthine in the sample ($\geqslant 5\%$), it is often necessary to stir the solution for ca. 10—20 min. A voltammogram of the resulting solution is then run at a clean, resurfaced PGE starting at 0.0 V and sweeping towards positive potentials. The sweep rate for the voltammogram is not critical; in the interest of speed a sweep rate of 0.2 V s^{-1} is used. The appearance of a single peak at E_p = 0.86—0.88 V at pH 6—8 indicates that there is no significant xanthine present in the sample. In certain buffers (e.g., phosphate pH 7), some additional, small, ill-defined peaks at more positive potentials [1] from additional electrochemical oxidations of xanthosine are of no particular interest in the present context.

The appearance of a voltammetric peak before the first xanthosine peak (0.86—0.88 V, pH 6—8) at E_p = (1.11 — 0.063 pH) V indicates the presence of xanthine in the sample. Its very strong adsorption at the PGE [2] makes xanthine readily observable, even when it is present at 1% or lower concentrations.

Procedure for the determination of xanthine in the presence of xanthosine

Once the presence of xanthine in the xanthosine sample has been established, xanthine may be determined by controlled potential coulometry. Typically, a 10—20 mg sample is dissolved in 100—125 ml of the appropriate buffer solution and electrolysis is carried out at a potential ca. 50 mV positive of E_p for xanthine, as determined from the linear sweep voltammogram. The electrolysis is continued until the current decreases to a low, constant value; the number of coulombs of electricity is recorded and from this the coulombs recorded for a blank solution containing no xanthosine are subtracted. The weight of xanthine present in the sample may be calculated, since 1 coulomb ≡ 0.3938 mg xanthine. To check that the electrolysis of xanthine is complete, a single-sweep voltammogram of a small aliquot of the electrolyzed solution is run; only the xanthosine peak(s) should be observed. A typical electrolysis takes ca. 2—3 h.

RESULTS AND DISCUSSION

Linear sweep voltammetry

Over the range pH 3—8, xanthine exhibits a single well-formed voltammetric oxidation peak at the PGE; the peak potential, E_p, is given by the equation E_p = (1.11 — 0.063 pH) V at a sweep rate of 0.2 V s^{-1}. Under the same conditions, xanthosine exhibits a first and major peak at E_p = (1.24 — 0.063 pH) V between pH 3 and 6. At higher pH values, the peak potential for xanthosine is independent of pH, E_p = 0.86 ± 0.1 V. The difference between the peak potentials of xanthine and xanthosine is more clearly seen in Fig. 1; the optimum separation of these peak potentials occurs at pH 7—8 (Fig. 1). Figure 2 shows a typical linear sweep voltammogram of xanthosine containing about 3% by weight of xanthine.

The electrochemical oxidation of xanthine is a 4e process [2]; the oxidation of xanthosine involves between 3—4e [1]. The peak current for xanthine in Fig. 2 is large because xanthine is strongly adsorbed at the PGE [2, 13], giving a very pronounced enhancement of the xanthine peak current at low concentrations compared with that expected for a diffusion-controlled process.

Controlled potential coulometry

The voltammetric oxidation peak of xanthine exhibits a non-linear peak current versus concentration relationship [13] because of the strong adsorption of this compound. In addition, the xanthine peak current is

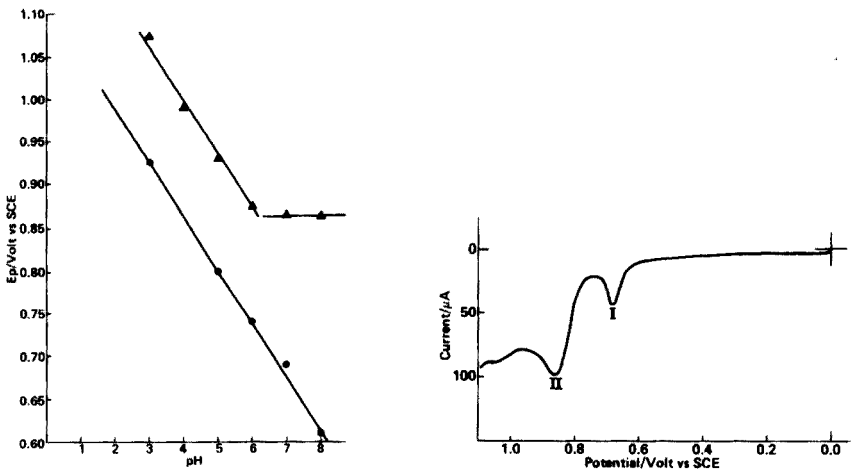

Fig. 1. E_p vs. pH relationships for (•) xanthine and (▲) xanthosine at the PGE (area 0.126 cm^2) at a sweep rate of 0.2 V s^{-1}.

Fig. 2. Linear sweep voltammogram of 0.5 mM xanthosine (peak II) containing ca. 0.03 mM xanthine (peak I) in pH 7 McIlvaine buffer at the PGE (area 0.126 cm^2). Sweep rate: 0.2 V s^{-1}.

probably dependent on the concentration of other adsorbable species such as xanthosine [14, 15] in solution. It was concluded, therefore, that a conventional voltammetric method for the determination of xanthine in the presence of xanthosine would not be satisfactory.

The voltammetric oxidation peak of xanthine in xanthosine—xanthine mixtures can be eliminated by controlled potential electrolysis at potentials at, or slightly more positive than, the xanthine peak potential, particularly at pH 7—8 where the peak separation is greatest. Under these conditions negligible electro-oxidation of xanthosine takes place. Accordingly, a controlled potential coulometric method was developed to determine xanthine in the presence of xanthosine (see Experimental); the optimum pH is between 7 and 8, where the xanthine and xanthosine peaks show their greatest peak separation (Fig. 1). However, lower pH values may be employed if necessary (vide infra).

Some typical analytical results for pure xanthosine to which known amounts of xanthine were added, are shown in Table 1. Good recoveries are obtained at pH 7 and 8 even when the xanthine occurs at 1% or less of the xanthosine concentration. At pH 5, the results are significantly poorer, because of partial electro-oxidation of small amounts of xanthosine at the potentials used to electrolyze xanthine.

Linear sweep voltammetry of solutions of several commercial samples of xanthosine at the PGE showed the presence of xanthine; quantitative analysis by controlled potential electrolysis indicated that appreciable quantities of xanthine were present (Table 2).

TABLE 1

Typical results for coulometric determination of xanthine in xanthosine[a]

McIlvaine buffer	Xanthine (mg)	
	Taken	Found
pH 7	0.65	0.70
	1.22	1.16
	1.76	1.79
	0.13	0.13
pH 8	0.63	0.61
	1.03	1.03
pH 5	0.22	0.31
	0.51	0.73
	0.73	1.12

[a]In each case 14—15 mg of pure anhydrous xanthosine in ca. 100 ml of the buffer was used.

TABLE 2

Coulometric determination of xanthine in commercial xanthosine samples

Sample	Wt. sample taken[a] (mg)	Wt. xanthine found (mg)	Xanthine % by weight
pH 7 McIlvaine buffer			
I[b]	18.66	0.56	3.0
	18.50	0.59	3.2
	17.13	0.56	3.2
	223.50	6.63	3.0
	17.54	0.59	3.3
II[c]	15.80	0.79	5.0
	16.80	1.05	6.0
	17.12	0.96	5.6
pH 8 McIlvaine buffer			
I[b]	16.12	0.45	2.8
	16.72	0.53	3.1
II[c]	17.16	0.85	5.0
	15.27	0.87	5.7
	15.89	0.91	5.7

[a]Dissolved in ca. 100 ml of buffer solution. [b]Vega-Fox, lot number H-1415. [c]Calbiochem.

Stability of xanthosine

To determine whether the xanthine present in commercial xanthosine samples arose from hydrolysis or other decomposition processes, xanthosine solutions at pH values between 5 and 8 were allowed to stand at room temperature for 2—4 d after all xanthine had been removed by controlled potential electrolysis. Under these conditions the voltammetric oxidation peak of xanthine did not reappear. Accordingly, it is unlikely that hydrolysis or other decomposition processes are responsible for the formation of xanthine from xanthosine.

Conclusion

Linear sweep voltammetry of solutions of xanthosine, particularly at pH 7—8, can be used to detect xanthine contamination simply and rapidly. Controlled potential coulometry gives a simple, direct determination of xanthine in xanthosine.

The authors thank Barbara M. Owens and Henry Marsh, for assistance with certain aspects of this work, and the National Institutes of Health for support through Grant No. GM-21034.

REFERENCES

1 J. L. Owens and G. Dryhurst, Unpublished work.
2 G. Dryhurst, J. Electrochem. Soc., 119 (1972) 1559.
3 H. Kinoshita and G. Dryhurst, Unpublished work.
4 K. Fink and W. S. Adams, J. Chromatogr., 22 (1966) 118.
5 K. Fink, R. E. Cline and R. M. Fink, Anal. Chem., 35 (1963) 389.
6 L. Rossi and C. Rossi, J. Chromatogr., 30 (1967) 278.
7 N. Kolassa, H. Roos and K. Pfleger, J. Chromatogr., 66 (1972) 175.
8 E. Gerlach, R. H. Dreisbach and B. Deuticke, J. Chromatogr., 18 (1965) 76.
9 G. Tortolani and M. E. Colosi, J. Chromatogr., 70 (1972) 182.
10 P. R. Brown, S. Bobick and F. L. Hanley, J. Chromatogr., 99 (1974) 587.
11 G. Dryhurst, M. Rosen and P. J. Elving, Anal. Chim. Acta, 42 (1968) 143.
12 D. L. McAllister and G. Dryhurst, J. Electroanal. Chem. Interfacial Electrochem., 47 (1973) 479.
13 G. Dryhurst, Bioelectrochem. Bioenergetics, 1 (1974) 49.
14 G. Dryhurst, Anal. Chim. Acta, 57 (1971) 137.
15 G. Dryhurst, Talanta, 19 (1972) 769.

Analytica Chimica Acta, 89 (1977) 101—109

OPTIMIZATION OF A SODIUM ION-SELECTIVE ELECTRODE FOR USE IN SERUM MEASUREMENTS

ULLA FIEDLER

Department of Analytical Chemistry, Chemical Center, University of Lund, S-220 07 Lund 7 (Sweden)

(Received 11th August 1976)

SUMMARY

A sodium ion-selective polymeric membrane electrode has been optimized, especially with reference to serum measurements. For a given combination of polymer and ligand, the choice of membrane solvent is critical. Potentiometric measurements and electrodialysis experiments have shown that the dielectric constant and solubility parameter of the solvent influence the electrode selectivities, stability, slope and limit of detection. For use in serum measurements, it is essential to use an appropriate analytical technique, such as Flow Injection Analysis, which permits exposures to serum for only short periods of time.

For monitoring sodium ion activities in biological systems, electrically neutral synthetic ligands have been proposed as the ion-selective components in liquid-membrane electrodes [1, 2]. When a polymeric ion-selective membrane, consisting of a polymer matrix, a plasticizer and a ligand, is constructed, the three components must be chosen so as to obtain mutual compatibility. PVC has repeatedly proved to be the most suitable polymer for membrane purposes [3, 4]. Thus, only the choice of membrane solvent remains so as to obtain optimum characteristics of the electrode.

The purpose of the present work was to investigate the influence of the membrane solvent on the performance of a sodium electrode for use in serum analysis. The effects of dielectric constant and solubility parameter were studied. Rigorous tests by long-term Na^+-monitoring in serum were performed. For analytical purposes, the recently introduced Flow Injection technique [5] was tested.

EXPERIMENTAL

Electrode system and measurement techniques

The sensor systems discussed here are based on polymeric membranes of the type described by Moody et al. [3]. The membrane composition is 0.6% (w/w) ligand, 66.3% solvent, 33.0% polymer, and 0.1% NaSCN.

The Na^+-selective ligand (I) was a synthetic, neutral carrier [1].

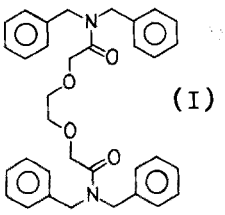

(I)

The solvents investigated, dibutylsebacate (DBS), di(2-ethylhexyl)sebacate (DEHS), di(2-ethylhexyl)adipate (DEHA), di(2-ethylhexyl)phthalate (DEHP) and *o*-nitro-phenyl-n-octyl-ether (*o*-NPOE), were all of analytical-grade quality. The polymer was PVC (SDP, hochmolekular, Lonza AG, Visp, Switzerland).

The membranes (ca. 0.2 mm thick) were incorporated into Philips IS-560 electrode bodies (N.V. Philips' Gloeilampenfabrieken, Eindhoven, Holland) [6]. Standard calomel electrodes, provided with a double junction (Radiometer type K 701) filled with 1.0 M LiAc, were used as reference electrodes.

The cell studied was:

Hg | Hg_2Cl_2 | KCl(sat) | | LiAc(1 M) | | sample solution | membrane | NaCl (0.01 M) | AgCl | Ag

All potential measurements were performed with a digital pH-meter 52 (Radiometer A/S, Copenhagen) accurate to within ± 0.1 mV, together with a Servogor recorder. The sample solutions were stirred and thermostated at 25.0 ± 0.1 °C.

All slopes were calculated by regression analysis on the linear part of the calibration curves.

Selectivity coefficients

These were determined by the separate solution technique on aqueous 0.01 M solutions of the chlorides, with the following relationship

$$pK_{NaM} = -\log K_{NaM} = \frac{(E_{Na^+} - E_{Mz^+})F}{2.303\,RT} - \log a_{Na^+} + \log a_{Mz^+}{}^{1/z}$$

where E_{Na^+} is the potential of the cell assembly, the sample being a 0.01 M NaCl solution; E_{Mz^+} is the potential of the cell assembly, the sample being a 0.01 M solution of the chloride of the interfering cation; z is the charge of the interfering ion M; and the other symbols have their usual meanings.

The selectivity coefficients were calculated from the potential data with a computer provided with a plotter. Results were recorded as pK vs. ion radius.

Ion activities

As activity standards the fundamental values described by Bates [7] were employed. For all alkali metal cations the activity coefficients γ_{Na} for Na^+

were used:

$$\log \gamma_{Na} = -\frac{0.51\sqrt{I}}{1 + 1.30\sqrt{I}} + 0.06I$$

where I denotes the ionic strength. The activity coefficients proposed for Ca^{2+} are described by

$$\log \gamma_{Ca} = -\frac{2.04\sqrt{I}}{1 + 1.55\sqrt{I}} + 0.2I$$

and were used for all other alkaline earth metal cations.

Reagents

Twice-distilled water (quartz apparatus) and chemicals of the highest purity available were used.

RESULTS AND DISCUSSION

Influence of the solvent dielectric constant

It has been pointed out [8, 9] that neutral carrier ligands of the type investigated preferentially form complexes with monovalent cations rather than divalent ones as the dielectric constant (ϵ) of the surrounding medium drops. The selectivity coefficients of the electrode system were therefore determined for two membrane solvents of different dielectric constant, DBS ($\epsilon \approx 4$) and *o*-NPOE ($\epsilon \approx 24$). Figure 1 clearly demonstrates the effect for *o*-NPOE and DBS.

Because the same complex equilibria would be expected to control the selectivity when ions are transported across the membrane by applying a potential difference, comparative electrodialysis experiments were performed. Thin membranes (ca. 0.04 mm thick) were mounted so as to separate the cell anode and cathode compartments, each equipped with Ag/AgCl electrodes [10]. Application of a potential difference of ca. 5 V, measuring the current-time integral, and sampling the cations transported into the cathode compartment by flameless atomic absorption spectrometry, gave the results shown in Table 1. The transference number, i.e. the fraction of

TABLE 1

Electrodialysis experiments

Salt solution		Membrane solvent	
Anode	Cathode	DBS	*o*-NPOE
NaCl 10^{-3} M	KCl 10^{-3} M	$t_{Na^+} = 0.92 \pm 0.08$[a]	$t_{Na^+} = 0.90 \pm 0.08$
NaCl $5 \cdot 10^{-4}$ M $CaCl_2$ $5 \cdot 10^{-4}$ M	KCl 10^{-3} M	$t_{Na^+} = 0.41 \pm 0.04$	$t_{Na^+} = 0.06 \pm 0.01$ $t_{Ca^{2+}} = 0.88 \pm 0.06$

[a]Limits indicated are standard deviations.

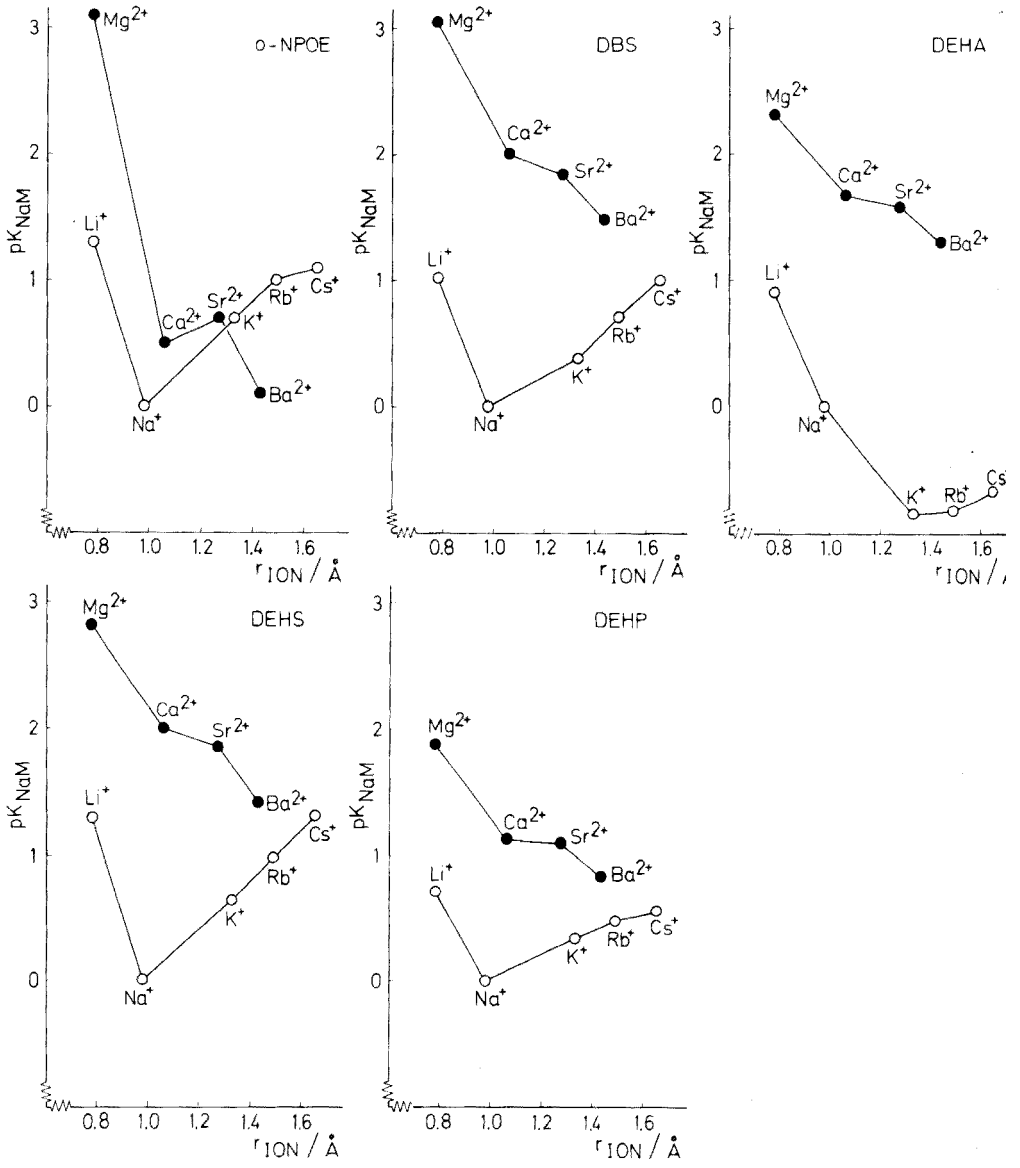

Fig. 1. Selectivities vs. ion radii for membrane solvents with different dielectric constants (*o*-NPOE and DBS), and with different solubility parameters (DBS, DEHA, DEHS, DEHP).

the electrical current transported by one species, may be approximated as

$$t_i = \frac{|z_i| J_i}{\Sigma |z_i| J_i} \; ; \sum t_i = 1$$

where J_i is the flux of ionic species i. t_{Na^+} was close to unity for both solvents

when no Ca^{2+} was present, thus proving pure cationic transport, excluding current transport by anions. In the presence of interfering calcium(II), t_{Na^+} decreased, and the decrease was far more drastic for the solvents with the higher ϵ value. Here the ligand behaves as a calcium carrier, confirmed by a high $t_{Ca^{2+}}$ value. As the flux J_i is proportional to the charge of the species i, the transport of divalent cations will always be favoured; for equal ligand selectivities for Na^+ and Ca^{2+}, the transference numbers would differ by a factor of 4, i.e. $t_{Na^+} = 0.2$ and $t_{Ca^{2+}} = 0.8$. When these transference numbers are considered, it should be noted that they are activity-dependent [11]. The results in Table 1 may thus be considered relevant only for a comparison of transference numbers in different membrane solvents.

Influence of the solubility parameters

Obviously, polymeric membranes require the mutual compatibility of the three membrane components [4]. Moreover, the stability of the electrodes depends on how readily the ligand is dissolved in the aqueous sample solution. In studies of the selection of ligand and plasticizer as well as membrane material in order to optimize the distribution ratio q of the ligand between membrane phase and aqueous phase, the concept of solubility parameters has proved to be helpful [12]. It has been shown that

$$\ln q = \frac{V_l V_m}{RT} \cdot [(d_l - d_{aq})^2 - (d_l - d_m)^2]$$

where V_l and V_m are volume fractions, and d_l and d_m are the solubility parameters of ligand and membrane material, respectively; d_{aq} is the solubility parameter of water.

Solubility parameters of the membranes were calculated from

$$d_m = w_{PVC} \cdot d_{PVC} + w_s \cdot d_s$$

where w refers to % by weight and d is the solubility parameter [13] ($d_{PVC} = 9.4$). Based on calculations by the method of Small [14], the solubility parameter for the ligand was found to be 9.1 ± 0.5 $(cal\ cm^{-3})^{1/2}$.

For a certain ligand and polymer the q-value can be optimized by choosing an appropriate solvent. The difference $d_l - d_m$ should be as small as possible, ideally zero. The solubility parameters together with experimentally determined values of slope and limit of detection are given in Table 2. From the limit of detection, DEHA should be the best solvent; this result also indicates that d_l is close to $d_{m(DEHA)}$, i.e. 8.9. For DEHP, $d_l > d_{m(DEHP)}$ and the ligand will dissolve more readily than the membrane material, yielding a higher limit of detection and a potential drift.

Selectivities

Selectivity coefficients for the electrodes based on four different membrane solvents of low dielectric constant (DBS, DEHA, DEHS, DEHP), are illustrated in Fig. 1. For use in serum measurements, the Na^+ electrode

TABLE 2

Solubility parameters

Solvent	d_s	d_m	Slope mV/pNa	Limit of detection (pNa)
	(cal cm^{-3})$^{1/2}$			
DBS	9.2	9.2	58.5	4.30
DEHA	8.7	8.9	60.1	4.46
DEHS	8.6	8.8	58.8	4.34
DEHP	7.9	8.3	49.5	4.03

should exhibit good selectivities, mainly against K^+ and Ca^{2+}. From this viewpoint, it can be concluded that DBS and DEHS seem to be the best solvents. For electrodes based on DEHP, ligand might have dissolved, thus yielding worse selectivities. The anomalous behaviour of the DEHA-containing membrane is due to the character of this solvent; it has been shown [4] that polymeric membranes with DEHA (without a ligand) exhibit a certain K^+-selectivity. DEHA is thus a suitable solvent in K^+-membranes, whereas it cannot be used in Na^+-electrodes irrespective of its suitable solubility parameter.

Serum measurements

The long-term stability of the electrodes when used in serum was investigated by recording the e.m.f. whilst the electrodes were immersed alternately for 20 min in serum electrolyte (141 mM Na^+, 5.0 mM K^+, 2.5 mM Ca^{2+} and 0.9 mM Mg^{2+}) and in serum (Technicon SMA Reference Serum 2). The procedure was repeated 4 times, followed by measurement in serum electrolyte for 20 min.

The results indicated that for such long periods of storage in serum, the electrode membranes are seriously affected by the entrance of lipophilic ions, and the potential drifts. The e.m.f. vs. time behaviour for the best electrode system (DBS) is shown in Fig. 2. From the first two runs (1a and 1b) an analytical estimation can be made; for ΔE = 5.7 (mV) and S (slope) = 58.5 (mV/pNa), the serum content was found to be 176 mM. The potential drift during the following runs gives rise to irreproducible results.

Flow Injection Analysis

This promising analytical technique [5] proved to be suitable for use in combination with ion-selective membrane electrodes. The actual flow diagram is shown in Fig. 3. The carrier stream was designed to have a constant ionic strength as well as pH, to obtain a stable base-line. The sodium sensor (electrode with solvent DBS) was first manually calibrated in solutions containing Tris (tris(hydroxymethyl)aminomethane) buffer (I = 0.04; pH = 7.5). A linear behaviour with a slope of 57.3 was observed down to pNa = 3.3 (Fig. 4). Then calibration was done in the Flow Injection

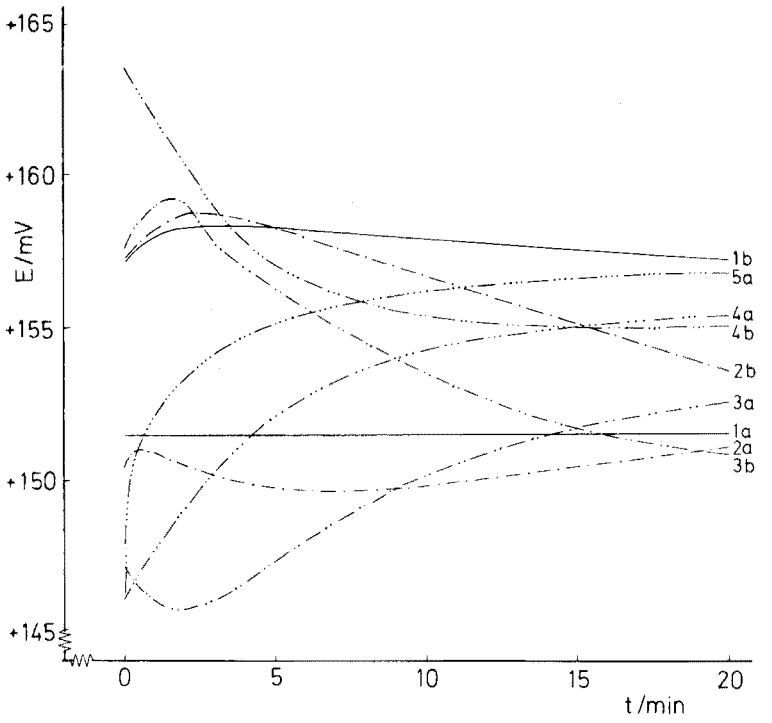

Fig. 2. Repeated recording of potential vs. time in (a) serum electrolyte, (b) serum, for electrodes with the membrane solvent DBS.

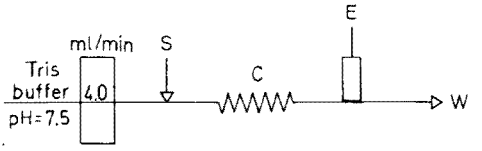

Fig. 3. Flow diagram for potentiometric determination of sodium in serum. S is the point of injection (0.2 ml), C is the mixing coil (0.645 m), E is the electrode, and W is waste.

system. When standard solutions (0.05 M, 0.10 M, 0.20 M, and 0.50 M NaCl solutions) were injected the standard deviation was 0.4 mV for 10 determinations on each solution. The electrode slope was 59.7 mV/pNa.

For the analysis of serum samples, standard solutions of different Na^+-content, containing 5.0 mM K^+, 2.5 mM Ca^{2+} and 0.9 mM Mg^{2+} (approximately as in serum), were prepared. During a 4-h period of analyzing serum samples, interrupted by standard samples, with a total capacity of 120 injections per hour, no drift whatsoever was observed in the results. For 50 analyses, the standard deviation was 0.7 mV, i.e. 3.0%, and the sodium content in the serum sample was determined to be 171 mM.

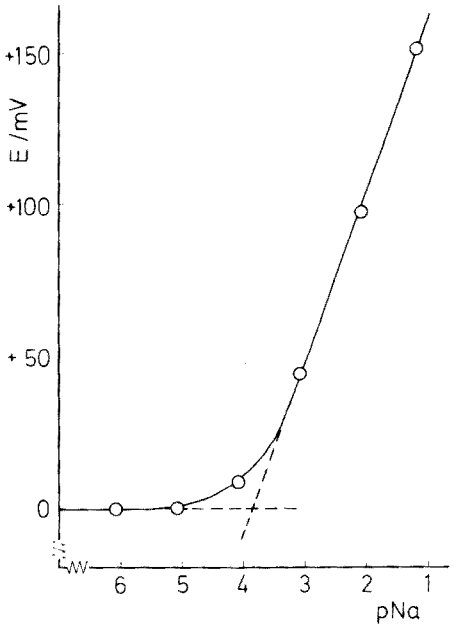

Fig. 4. Calibration curve for sodium electrode (with solvent DBS) in Tris buffer.

Conclusion

In attempts to improve the behaviour of a neutral carrier membrane electrode, it is necessary first to investigate the influence of the membrane solvent. Besides its function as a polymer plasticizer, this solvent has strong effects on the electrode performance. For special applications, such as serum measurements, where lipophilic ions might enter the membrane and change the equilibria, an additional demand has to be made on the analytical technique used. Flow Injection Analysis proved to fulfil the requirements; the method is rapid and precise, and the membrane remains unaffected.

The author expresses her sincere thanks to Professor W. Simon, ETH, Zürich, who suggested this problem. His helpful advice and critical discussions are gratefully acknowledged. Thanks are also due to Dr. J. Růžička, DTH, Lyngby, who made available the Flow Injection Analysis system, and to Mr. L. Gorton, Chemical Center, Lund, for technical assistance.

REFERENCES

1 D. Ammann, E. Pretsch and W. Simon, Anal. Lett., 7 (1974) 23.
2 D. Ammann, R. Bissig, Z. Cimerman, U. Fiedler, M. Güggi, W. E. Morf, M. Oehme, H. Osswald, E. Pretsch and W. Simon, Proc. Int. Workshop Ion Enzyme Electrodes Biol. Mec Urban and Schwarzenberg, Munich, 1976.

3 G. J. Moody, R. B. Oke and J. D. R. Thomas, Analyst (London), 95 (1970) 910.
4 U. Fiedler and J. Růžička, Anal. Chim. Acta, 67 (1973) 179.
5 J. Růžička and E. H. Hansen, Anal. Chim. Acta, 78 (1975) 145.
6 L. A. R. Pioda, V. Stankova and W. Simon, Anal. Lett., 2 (1969) 665.
7 R. G. Bates in Ion Selective Electrodes (R. A. Durst (Ed.)), N.B.S., Spec. Publ. 314, Washington, 1969.
8 W. Simon, W. E. Morf and P. Ch. Meier, in Structure and Bonding, Vol. 16, 114, Springer-Verlag, Heidelberg, 1973.
9 U. Fiedler, Anal. Chim. Acta, 89 (1977) 111.
10 P. Wuhrmann, A. P. Thoma and W. Simon, Chimia, 27 (1973) 637.
11 W. E. Morf, P. Wuhrmann and W. Simon, Anal. Chem., 48 (1976) 1031.
12 H. J. Nielsen and E. H. Hansen, Anal. Chim. Acta, 85 (1976) 1.
13 J. Brandrup and E. H. Immergut, Polymer Handbook, Interscience-Wiley, New York, 1966.
14 P. A. Small, J. Appl. Chem., 3 (1953) 71.

Analytica Chimica Acta, 89 (1977) 111—118

INFLUENCE OF THE DIELECTRIC CONSTANT OF THE MEDIUM ON THE SELECTIVITIES OF NEUTRAL CARRIER LIGANDS IN ELECTRODE MEMBRANES

ULLA FIEDLER

Department of Analytical Chemistry, Chemical Centre, University of Lund, S-220 07 Lund 7 (Sweden)

(Received 11th August 1976)

SUMMARY

The selectivities of potassium and calcium ion-selective liquid membrane electrodes, based on neutral carrier ligands, have been studied in relation to the dielectric constant of the membrane solvent. Potentiometric measurements have shown that the selectivity for monovalent cations is favoured by a low dielectric constant, and that for divalent cations by a high dielectric constant of the solvent. This is in good agreement with theoretical predictions. The size of the calcium-selective ligand has also been estimated.

Synthetic neutral carriers have been proposed for use as the ion-selective components in electrodes for alkali and alkaline earth metal cations [1, 2]. For the construction of polymeric membranes based on a PVC matrix, special demands are made on the membrane solvent: it must be compatible with ligand and polymer and must act as a plasticizer, and its polarity must be chosen appropriately. It has been shown [3] that neutral carrier ligands prefer to form complexes with monovalent cations rather than divalent ones as the dielectric constant (ϵ) of the surrounding medium drops, especially in the region $\epsilon < 10$. Thus, it becomes imperative to choose a solvent with a low dielectric constant for membranes designed for alkali metal cations based on neutral carriers.

The purpose of the present work was to investigate the stability of neutral carrier complexes, expressed as selectivity coefficients, as a function of the polarity of the embedding medium, expressed as the dielectric constant, and to correlate the experimental results with theoretical predictions.

THEORY

For a neutral carrier S to act as a ligand for the ion I^{z_i+} in membranes, the following equilibrium is relevant

$$I^{z_i+}(aq) \underset{\leftarrow}{\overset{K_i}{\rightleftarrows}} IS_{n_i}^{z_i+}\,(m)$$

The overall partition coefficient, K_i, can be described [4] by

$$K_i = K_{is}^{*} \cdot k_{is} \cdot (c_s/k_s)^{n_i} \qquad (1)$$

where K_{is}* is the complex stability constant in water; k_{is} is the partition coefficient of the complex between aqueous solution and membrane; k_s is the partition coefficient of free ligand between aqueous solution and membrane; c_s is the concentration of free ligand in the membrane; and 1: n_i is the stoichiometry of the cation-carrier complex.

Electrostatic models show that k_{is} depends on the square of the ionic charge and becomes smaller with decreasing dielectric constant of the membrane phase [4]

$$\log k_{is} \approx \frac{N(z_i e)^2}{2r \cdot R \cdot T \cdot \ln 10} \left(\frac{1}{78.5} - \frac{1}{\epsilon} \right) \tag{2}$$

where N is Avogadro's number; $z_i e$ the absolute charge of the complex; $2r$ the overall diameter of the complex; and ϵ the dielectric constant of the membrane solvent.

The selectivity behaviour of a membrane in contact with two cations of the same charge is determined by

$$I^{z+}\ (\text{compl., m}) + J^{z+}\ (\text{free, aq}) \overset{K_{ij}}{\rightleftarrows} J^{z+}\ (\text{compl., m}) + I^{z+}\ (\text{free, aq})$$

The equilibrium constant can be written as

$$K_{ij} = K_j / K_i \tag{3}$$

When the expressions for K_j and K_i according to eqns. (1) and (2) are introduced into eqn. (3), it becomes obvious that K_{ij} is independent of ϵ, assuming constant complex size and stoichiometry. The monovalent/divalent cation selectivity can be expressed as

$$I^{2+}\ (\text{compl., m}) + 2J^{+}\ (\text{free, aq}) \overset{K_{ij}}{\rightleftarrows} 2J^{+}\ (\text{compl., m}) + I^{2+}\ (\text{free, aq})$$

with

$$K_{ij} = K_j^2 / 2c \cdot K_i \tag{4}$$

where c is the concentration of the total cation sites at the membrane surface. Equations (1) and (2), together with eqn. (4), demonstrate that the selectivity is highly dependent on the dielectric constant of the medium

$$\log K_{ij} = \text{const.} + \frac{4\alpha}{2r} \cdot \frac{1}{\epsilon} \tag{5}$$

where α is a constant, including N, e, R and T. Thus, if the dielectric constant (ϵ) of the membrane solvent increases, $\log K_{ij}$ decreases, and selectivity for divalent cations will be favoured.

Conversely, if J^+ is the primary ion, the selectivity coefficient K_{ji} is described by

$K_{ji} = (1/K_{ij})^{\frac{1}{2}}$, i.e.

$$\log K_{ji} = \text{const.} - \frac{2\alpha}{2r} \cdot \frac{1}{\epsilon} \tag{6}$$

Thus, if ϵ of the membrane solvent decreases, log K_{ji} decreases and selectivity for monovalent cations will be favoured. For the derivation of eqns. (5) and (6), the complex size and stoichiometry are assumed to be constant.

EXPERIMENTAL

Electrode systems

The sensor systems discussed here are based on polymeric membranes of the type described by Moody et al. [5]. The membrane composition was (by weight) 1% ligand, 69.0% solvent, 30.0% polymer.

The K^+-selective ligand was valinomycin(I) [6]. The Ca^{2+}-selective ligand was N,N'-di[(11-ethoxycarbonyl)undecyl]-N,N',4,5-tetramethyl-3,6-dioxaoctane amide (II) [7].

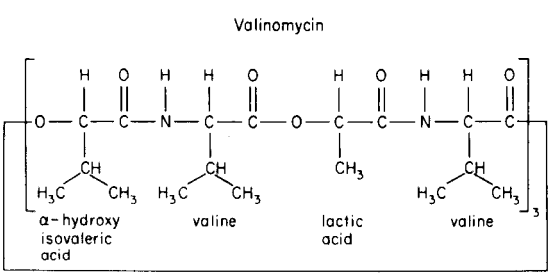

I

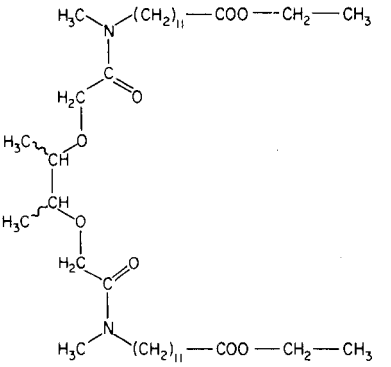

II

The solvent mixtures investigated contained di(2-ethylhexyl) adipate (DEHA) or dibutylsebacate (DBS) and *o*-nitrophenyl-n-octylether (*o*-NPOE), all of analytical-grade quality. The polymer was PVC (SDP, hochmolekular, Lonza AG, Visp, Switzerland). The membranes (ca. 0.2 mm thick) were incorporated into Philips IS-560 electrode bodies (N.V. Philips' Gloeilampenfabrieken, Eindhoven, Holland) [6].

Standard calomel electrodes, provided with a double junction (Radiometer type K701) filled with 0.10 M NH_4NO_3, were used as reference electrodes. The cells studied were:

A. Hg|Hg_2Cl_2|KCl(sat)||0.10 M NH_4NO_3||sample solution|membrane|. . .
. . . KCl(0.10 M)|AgCl|Ag

B. Hg|Hg_2Cl_2|KCl(sat)||0.10 M NH_4NO_3||sample solution|membrane|. . .
. . . $CaCl_2$(0.10 M)|AgCl|Ag

All potential measurements were done with a digital pH-meter (Radiometer A/S, Copenhagen) accurate to within ± 0.1 mV. The sample solutions were stirred and thermostated at 25.0 ± 0.1°C. The slopes of the graphs were calculated by regression analysis on the linear parts of the curves.

Reagents

Twice-distilled water (quartz still) and chemicals of the highest purity available were used.

Selectivity coefficients

These were determined by the separate solution technique on aqueous 0.10 M solutions of the chlorides based on the following relationships

$$pK_{KM} = -\log K_{KM} = \frac{(E_{K^+} - E_{M^{z+}})F}{2.303 \cdot R \cdot T} - \log a_{K^+} + \log a_{M^{z+}}^{1/z}$$

$$pK_{CaM} = -\log K_{CaM} = \frac{(E_{Ca^{2+}} - E_{M^{z+}})2F}{2.303 \cdot R \cdot T} - \log a_{Ca^{2+}} + \log a_{M^{z+}}^{2/z}$$

where E_{K^+} and $E_{Ca^{2+}}$ are the potentials of the cell assembly, the sample being 0.10 M KCl or 0.10 M $CaCl_2$; $E_{M^{z+}}$ is the potential of the cell assembly, the sample being a 0.10 M solution of the chloride of the interfering cation; z is the charge of the interfering ion, and the other symbols have their accepted meanings.

For comparison pK_{CaNa} and pK_{CaK} were also determined by the mixed solution technique, by taking a constant background of interfering ion, 0.10 M, and varying the calcium-ion activity. The selectivity coefficients were calculated from [8]

$$pK_{CaNa(K)} = 2 \cdot \log a_{Na^+(K^+)} - \log a_{Ca^{2+}}$$

where $a_{Ca^{2+}}$ is defined by the intercept of the horizontal interfering ion response line with the calcium calibration line.

The coefficients were calculated with a computer provided with a plotter, which recorded the results as pK vs. ion radius.

Ion activities were calculated for all alkali metal and all alkaline earth metal cations as described previously [9].

Solvent mixtures

For the preparation of K^+-selective membranes, solvent mixtures of DEHA and *o*-NPOE were used. For Ca^{2+}-selective membranes, solvent mixtures of DBS and *o*-NPOE were taken. Solvent data are given in Table 1 and the mole ratios of the mixtures in Table 2.

For a certain substance the molar polarization P can be expressed as

$$P = \frac{\epsilon - 1}{\epsilon + 2} \cdot \frac{M}{d}$$

where ϵ = dielectric constant, M = molecular weight and d = density. These values have been calculated for the separate solvents, and are given in Table 1. In a mixture of two substances 1 and 2

$$P_{12} = c_1P_1 + c_2P_2 = \frac{\epsilon_{12} - 1}{\epsilon_{12} + 2} \cdot \frac{c_1M_1 + c_2M_2}{d_{12}}$$

TABLE 1

Solvent data

Solvent	M g mol^{-1}	d g cm^{-3}	ϵ	P cm^3 mol^{-1}
DEHA	371	0.922	4.0	201
DBS	314	0.940	4.0	167
o-NPOE	251	1.014	23.6	219

where the index 12 refers to the mixture and c is the mole fraction [10]. Dielectric constants of the mixtures were calculated thus from experimental data on the separate solvents. Results are given in Table 2.

RESULTS AND DISCUSSION

The effect of the dielectric constant of the membrane solvent on the selectivities of neutral carrier ligands was demonstrated earlier for a calcium-selective ligand when several different solvents were tested [3]. However, the functional groups of the organic solvents might influence the selectivities quite considerably. To minimize this effect, only two solvents, with quite diverse dielectric constants, and mixtures thereof were tested in this study.

Potassium-selective electrodes

For the construction of K^+-selective electrodes, valinomycin (I) has proved to be the best ligand so far [6]. It has also been shown that the use of DEHA ($\epsilon \approx 4$) as a membrane solvent yields electrodes with favourable characteristics, such as slope [11], stability and selectivities (Fig. 1). To verify the theory proposed, membranes with higher polarity were prepared by using solvent mixtures of DEHA and *o*-NPOE ($\epsilon \approx 24$; see Table 2). Whereas selectivities for potassium against other monovalent cations were almost unaffected, there was less discrimination against the divalent cations. For example, when $-\log K_{KCa}$ was plotted against $1/\epsilon$ a straight line was obtained (Fig. 2).

TABLE 2

Dielectric constants and mole ratios of the solvent mixtures

DEHA/*o*-NPOE				DBS/*o*-NPOE			
c_{DEHA}	ϵ	c_{DEHA}	ϵ	c_{DBS}	ϵ	c_{DBS}	ϵ
1.0	4.0	0.4	7.5	1.0	4.0	0.4	8.1
0.9	4.3	0.3	9.0	0.9	4.4	0.3	9.7
0.8	4.7	0.2	11.1	0.8	4.8	0.2	12.2
0.7	5.1	0.1	15.2	0.7	5.4	0.1	16.3
0.6	5.7	0	23.6	0.6	6.1	0	23.6
0.5	6.5			0.5	6.9		

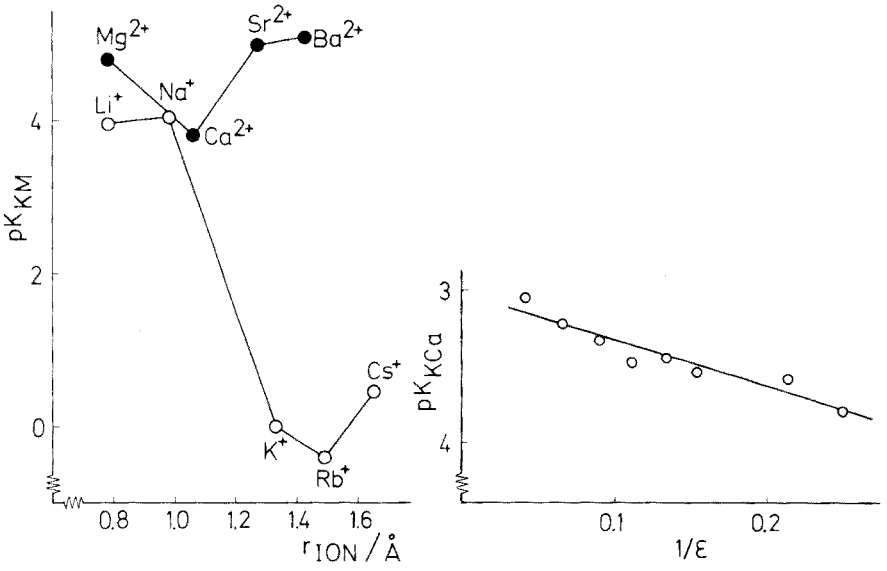

Fig. 1. Selectivities vs. ion radius for a membrane containing valinomycin in DEHA.

Fig. 2. pK_{KCa} for a valinomycin-based electrode as a function of the dielectric constant (ϵ) of the membrane solvent.

The same relation holds for the other divalent cations tested; Table 3 shows data from regression analysis on the lines obtained, when M is Mg, Ca, Sr and Ba. From the values of the intercepts it is obvious that Ca^{2+} is the most interfering divalent cation. The almost constant value of the slope (mean value = −3.4) indicates that the size of the complex is practically unaffected by the size of the cation complexed (cf. eqn. 6). Furthermore, as the valinomycin complex is quite large ($2r$ = 15 Å) the influence of the solvent dielectric constant on the selectivities is relatively small.

Calcium-selective electrodes

For the construction of Ca^{2+}-selective electrodes, a synthetic neutral carrier (II) with high selectivity for calcium has been used [7]. When the performance of this electrode was optimized, a membrane solvent with a high

TABLE 3

Data for the $-\log K_{KM}$ vs. $1/\epsilon$ plots for various divalent cations (M)

$\log K_{KM}$ vs. $1/\epsilon$	M = Mg	M = Ca	M = Sr	M = Ba
Correlation	0.935	0.951	0.943	0.950
Intercept	−3.90	−3.03	−4.06	−4.20
Slope	−3.49	−3.06	−3.61	−3.48

polarity, such as *o*-NPOE ($\epsilon \approx 24$), was found to be suitable. If the dielectric constant of the membrane medium is changed by adding an apolar solvent, such as DBS ($\epsilon \approx 4$), the effect on the selectivities against the monovalent cations is serious (Fig. 3). Plots of log K_{CaM} (M = Li, Na, K, Rb and Cs) vs. $1/\epsilon$ give straight lines, with regression analysis data as shown in Table 4. The values of the intercepts indicate that the selectivity coefficients for Na^+ and K^+ are practically the same, whereas Li^+ is the most interfering monovalent cation. It can also be seen that the size of the complex is almost constant (cf. eqn. 5), manifested by the value of the slope (mean value = 16.9).

This makes it possible to estimate the complex size: from $-2\alpha/2r$ (valinomycin) = -3.4 and $+4\alpha/2r$ (Ca-carrier) = 16.9, it follows that $2r$ (Ca-carrier) = 6.0 Å, if the value $2r$ (valinomycin) = 15.0 Å is used.

The influence of the membrane solvent should be of minor importance for the selectivities among cations within a given group of the periodic system (cf. eqn. 3). However, calculations have suggested a slight preference for larger cations as ϵ decreases [3]; this can be seen from the experimental results shown in Fig. 3, where Sr^{2+} and Ba^{2+} are far less discriminated against in nonpolar solvents.

Selectivity coefficients for the Ca^{2+}-selective ligand vs. Na^+ and K^+ were also determined by the mixed solution technique. In Fig. 4, values are shown from the determination of pK_{CaNa} for membranes with solvents of various dielectric constants. Data obtained by the mixed solution technique yield the same function as those obtained by the separate solution technique. Slightly better selectivities are obtained in mixed solutions, but the longer time consumed makes this approach less interesting.

Conclusion

It has been shown that the choice of membrane solvent for neutral carrier ligands is critical, as the selectivities change with the dielectric constant of the medium. Theoretical predictions for the size of the effect have also been verified.

TABLE 4

Data for the $-\log K_{CaM}$ vs. $1/\epsilon$ plots for alkali metal ions

log K_{CaM} vs. $1/\epsilon$	M = Li	M = Na	M = K	M = Rb	M = Cs
Correlation	0.998	0.995	0.997	0.997	0.996
Intercept	−3.50	−3.70	−3.70	−4.04	−3.89
Slope	17.2	16.0	16.0	17.7	17.4

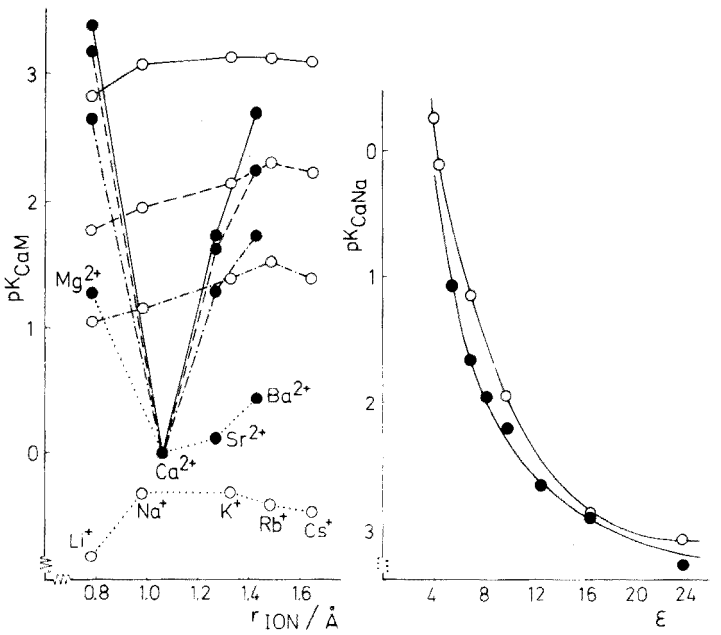

Fig. 3. Selectivities vs. ion radius for a Ca-membrane with solvents of different dielectric constants. (——) ϵ = 23.6; (— —) ϵ = 9.7; (— · —) ϵ = 6.9; (· · · ·) ϵ = 4.0.

Fig. 4. pK_{CaNa} for a calcium-carrier-based electrode as a function of the dielectric constant (ϵ) of the membrane solvent. Selectivities determined by the methods of separate solutions (○) and mixed solutions (●).

Sincere thanks are due to Professor W. Simon, ETH, Zürich, for helpful advice and critical discussions concerning this work.

REFERENCES

1 D. Ammann, R. Bissig, Z. Cimerman, U. Fiedler, M. Güggi, W. E. Morf, M. Oehme, H. Osswald, E. Pretsch and W. Simon, Proc. Int. Workshop Ion Enzyme Electrodes Biol. Med., Urban and Schwarzenberg, Munich, 1976.
2 D. Ammann, Diss. ETH Nr 5605, Zürich, 1975.
3 W. Simon, W. E. Morf and P. Ch. Meier in Structure and Bonding, Vol. 16, Springer-Verlag, Heidelberg, 1973.
4 W. Simon, W. E. Morf, E. Pretsch and P. Wuhrmann, Proc. Int. Symp. Calcium Transport in Contraction and Secretion, Bressanone, Italy, May, 1975.
5 G. J. Moody, R. B. Oke and J. D. R. Thomas, Analyst (London), 95 (1970) 910.
6 L. A. R. Pioda, V. Stankova and W. Simon, Anal. Lett., 2 (1969) 665.
7 D. Ammann, M. Güggi, E. Pretsch and W. Simon, Anal. Lett., 8 (1975) 709.
8 G. J. Moody and J. D. R. Thomas, Selective Ion-Sensitive Electrodes, Merrow, 1971.
9 U. Fiedler, Anal. Chim. Acta, 89 (1977) 101.
10 C. P. Smyth, Dielectric Behaviour and Structure, McGraw-Hill, New York, 1955.
11 U. Fiedler and J. Růžička, Anal. Chim. Acta, 67 (1973) 179.

Analytica Chimica Acta, 89 (1977) 119—126

DETERMINATION OF ALUMINIUM IN LOW-ALLOY AND STAINLESS STEELS BY FLAMELESS ATOMIC ABSORPTION SPECTROMETRY

JAN-ÅKE PERSSON, WOLFGANG FRECH and ANDERS CEDERGREN
Department of Analytical Chemistry, University of Umeå, S-901 87 Umeå (Sweden)
(Received 19th July 1976)

SUMMARY

A method for the determination of 1—500 p.p.m. of acid-soluble aluminium and 2—500 p.p.m. of acid-insoluble aluminium in low-alloy and stainless steels by flameless atomic absorption with a HGA 74 graphite furnace is described. A typical value of the relative standard deviation for acid-soluble aluminium at concentrations larger than 10 p.p.m. was 5 %. The steel sample was dissolved in hydrochloric and nitric acid and filtered. Ammonium sulphate was added to the filtered sample in order to overcome interferences caused by hydrochloric acid. No concentration steps were used. Acid-soluble aluminium was determined within 20 min. The influence of iron, chromium, nickel, molybdenum, hydrochloric acid, nitric acid and ammonium sulphate respectively was investigated.

Because of its high affinity for oxygen, aluminium is used frequently as an oxygen scavenger [1] during the manufacture of steels and cast iron. The major part of the added aluminium forms aluminium oxide compounds which are then removed with the slag. However, some compounds remain in the melt, as so-called acid-insoluble aluminium, in the form of aluminium oxides or aluminium combined with calcium or silica. For a certain amount of aluminium added to the melt, acid-soluble forms will also be present. Since even minute amounts of both acid-soluble and acid-insoluble aluminium in the steel will affect the properties of the final product, trace determination of aluminium during steel manufacture is important.

Byrne et al. [2] reviewed the methods for the determination of aluminium and other residual elements in rotor steel. Since then several atomic absorption procedures with the nitrous oxide—acetylene flame have been published [3—5]. However, in order to determine aluminium at low levels with these procedures concentrated sample solutions must be prepared. The iron matrix is removed by extraction in order to avoid clogging of the burner. Because of interferences from nickel, chromium and other alloying elements [3, 5, 6] the additional extraction step necessary for the determination of aluminium in high alloy steels [3] makes these procedures laborious and slow.

Rain and Menis [7] proposed flame emission spectrometry including repetitive optical scanning [8]. However, this technique requires special modifications of the spectrophotometer. Direct determinations of aluminium down to 2 p.p.m. were reported for low-alloy steels and ferrosilicates. No results on stainless steels were given.

Compared with flame atomic absorption techniques, the greater sensitivity of flameless atomic absorption makes it possible to omit the extraction steps. Shaw and Ottaway [9] used the graphite furnace technique for the determination of aluminium in cast irons and low-alloy steels down to 2 p.p.m. A typical value of the relative standard deviation for the flameless a.a.s. determination was 7%. Because of interferences caused by chloride, only nitric acid was used for dissolving the samples; this limits the applicability of the method to iron and low-alloy steels.

The aim of this work was to develop a flameless a.a.s. method for the determination of aluminium in low as well as high-alloy steels. In order to make use of a convenient dissolution procedure including nitric and hydrochloric acid, one fundamental requirement was to eliminate the interferences caused by chloride. Methods for the determination of antimony [10], bismuth [11], and lead [12, 13] by flameless a.a.s. with nitric and hydrochloric acid for dissolution of the samples have earlier been described.

EXPERIMENTAL

Instrumentation

A Perkin-Elmer HGA 2100 graphite furnace connected to a research spectrophotometer [14] was used. The instrument was equipped with a background corrector and a device for integration measurements. Peak absorbances were registered on a Houston Instrument recorder. Temperature settings were calibrated with a Ni—Cr/Ni thermocouple below 1100 °C and a pyrometer was used for higher temperatures. The instrumental parameters are given in Table 1.

TABLE 1

Instrumental parameters

	Time (s)	Temp (°C)		
Drying	40	90	Wavelength (nm)	309.3
Ashing	40	1230	Slit width (μm)	150
Delay	4	—	Metal lamp current (mA)	5
Atomization	8	2300	Hydrogen lamp current (mA)	20
Cleanout	6	max	Sample volume (μl)	5—20[a]
			Gas flow argon (l min^{-1})	
			internal	0.4[b]
			external	1.5
			Integration time (s)	7[c]

[a] Depending on the concentration of aluminium. The same volumes had to be used for standards and unknown samples.
[b] Gas stop during atomization.
[c] Integration started 0.4 s after the atomization sequence had started.

Reagents and materials

The following reagents and materials were used: 30 % hydrochloric acid (Suprapur, Merck), 18 M nitric acid (p.a. Merck), ammonium sulphate (p.a. Baker), sodium carbonate anhydrous (p.a. Merck), sodium tetraborate (p.a. Merck), aluminium, chromium, nickel, molybdenum metals (p.a. Merck), BCS Steel Standards (British Chemical Standards, Bureau of Analyzed Samples, Ltd.,), JK steel standards (Institutet för Metallforskning, Drottning Kristinas väg 48, Stockholm, Sweden). All materials were acid-washed with 4 M nitric acid. All solutions were stored in polyethene plastic bottles.

Procedure

Acid-soluble aluminium. Transfer 0.5 g of the sample to a 50-ml Erlenmeyer flask, add 3 ml of water, 5 ml of hydrochloric acid and 2.5 ml of nitric acid. Warm for at least 10 min or until the sample has dissolved. Cool, add about 10 ml of water and filter through a 0.22-μm Millipore filter. Wash the filter with hot water. Transfer to a 100-ml volumetric flask, add 25 ml of 2 M ammonium sulphate, and make up to the mark with water.

Acid-insoluble aluminium. Dissolve the filter in 2 ml of hot nitric acid and evaporate to dryness. Fuse the residue with 0.5 g of a mixture (2 : 1) of sodium carbonate and sodium tetraborate at 1000 °C for 30 min. Cool, moisten the melt with about 2 ml of water and add 5 ml of nitric acid (50 % (v/v)). Transfer the solution to a 100-ml volumetric flask, and make up to the mark with water.

Reference solutions

Acid-soluble aluminium. Add standards of aluminium to filtered steel standard solutions, e.g., JK 1C.

Acid-insoluble aluminium. Add standards of aluminium to steel sample solutions as prepared for acid-insoluble aluminium.

RESULTS AND DISCUSSION

In order to study the influence of hydrochloric and nitric acid on the sensitivity, samples containing 5000 p.p.m. of iron and 0.5 p.p.m. of aluminium were analyzed in the presence of various concentrations of acids under the conditions given in Table 1. Figure 1 shows that hydrochloric acid, compared with nitric, markedly decreased the sensitivity for aluminium. In addition, poorer reproducibility was obtained, as observed by Shaw and Ottaway [9].

Attempts were made to overcome the interference from hydrochloric acid by different procedures. The removal of chloride from an iron-chloride matrix is effective [15, 16] in a graphite tube if hydrogen is present during ashing at 550 °C. However, this procedure did not succeed in the present application. Attempts were therefore made to remove the chloride by the addition of chemicals likely to form volatile chloride compounds in an iron-chloride

matrix, e.g. sulphuric acid, ammonium hydroxide and ammonium sulphate. The most reproducible results were obtained with ammonium sulphate.

Figure 2 shows that the sensitivity for aluminium is increased in the presence of higher concentrations of ammonium sulphate in the dissolved steel sample. The experimental parameters used are given in Table 1. Except for the ammonium sulphate, the sample contained 0.3 p.p.m. of aluminium, 2000 p.p.m. of iron, 0.5 M of hydrochloric acid and 0.4 M of nitric acid. The results in Fig. 2 have been corrected for blank values, caused by ammonium sulphate, which corresponded to 3 % of the absorbance value for the most concentrated solution. A suitable choice of ammonium sulphate concentration was considered to be 0.5 M since the sensitivity is only slightly increased for higher concentrations. In addition, higher concentrations make the solution more viscous, resulting in poorer reproducibility of the sample delivery. Moreover, it is always desirable to limit the consumption of chemicals.

The effect of the ashing temperature on the sensitivity for aluminium is shown in Fig. 3. The lower curve represents a dissolved steel sample containing 0.3 p.p.m. of aluminium, 5000 p.p.m. of iron, 0.5 M hydrochloric acid and 0.4 M nitric acid. The upper curve shows the effect of 0.5 M ammonium sulphate present in the same steel sample solution. The sensitivity is lower at all temperatures for the sample to which no ammonium sulphate was added compared with the sample containing 0.5 M. Maximum sensitivity was obtained by ashing the ammonium sulphate-containing sample in the range 1200—1400 °C. The shape of the curves shown in Fig. 3 is now the subject of a fundamental study to increase the understanding of the chemical reactions involved.

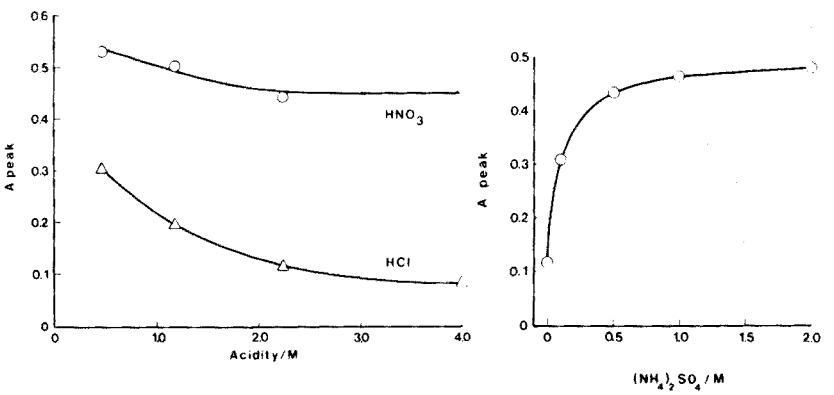

Fig. 1. Peak absorbance as a function of acidity for 20 µl of 0.5 p.p.m. of aluminium and 5000 p.p.m. of iron solutions.

Fig. 2. Peak absorbance as a function of ammonium sulphate concentrations. Samples (20 µl) containing 0.3 p.p.m. of aluminium, 2000 p.p.m. of iron. 0.5 M of hydrochloric acid and 0.4 M of nitric acid were used.

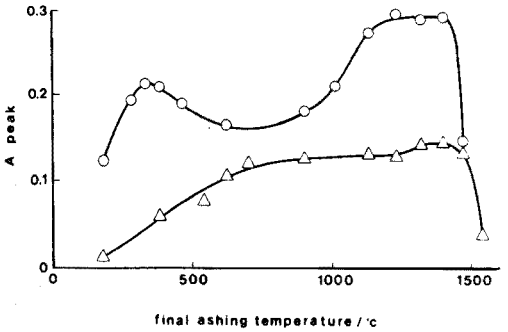

Fig. 3. Peak absorbance values as a function of ashing temperatures. Samples (20 μl) with 0.3 p.p.m. of aluminium added were used. (○) ultrapure steel JK 1C prepared by the procedure described for acid-soluble aluminium. (△) ultrapure steel JK 1C prepared by the procedure described for acid-soluble aluminium without ammonium sulphate added.

The effect of the major constituents in steel on the sensitivity for aluminium was also investigated. Figures 4(a—d) show the sensitivity for aluminium for various amounts of iron, chromium, molybdenum, and nickel. According to the described procedure, typical values of the amount of iron in the sample are in the range 20—100 μg. Figure 4(a) shows that the sensitivity is less, by about 20 % in this interval, than when no iron is present. Small variations in the amount of iron in the steel samples will cause only small variations in the sensitivity for aluminium. The single effect of the other metals, i.e. chromium, nickel, and molybdenum, in concentrations typical of these elements in normal steel grades is rather small. This indicates the possibility of analyzing both low-alloy and stainless steels by means of a single calibration curve.

In order to study the combined effects of the various elements constituting the steel samples calibration curves were constructed by making standard additions of aluminium to ultrapure steel JK 1C and austenitic stainless steel

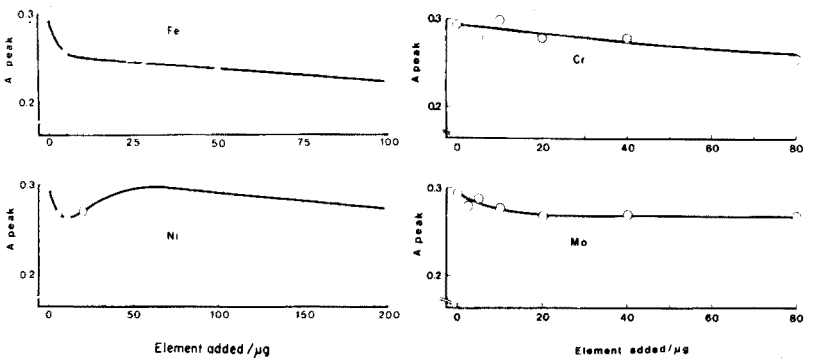

Fig. 4. Peak absorbance as a function of various amounts of elements added. Samples (20 μl) containing 0.3 p.p.m. of aluminium, 0.5 M hydrochloric acid and 0.4 M nitric acid were used.

JK 8C. No significant difference in the shape of the curves representing the two steels was found. These results indicate that variations in the composition of steel samples do not affect the sensitivity. Both integrated and peak height values were determined as shown in Fig. 5. The reproducibility (3.5 %) was only slightly improved (less than 0.5 %) by use of integration, although a more linear calibration curve was obtained for the high absorbance values.

Acid-insoluble aluminium

Millipore filters were used instead of paper pulp pads throughout this work; they have defined pore sizes and are dissolved easily in hot nitric acid. Samples could be filtered rapidly by water pump.

To investigate possible matrix effects caused by ultrapure steel, (JK 1C) or stainless steel (JK 8C), standard additions to the respective filters were made before the samples were fused, and the results compared with those obtained by standard addition to the respective final sample solutions. The sensitivity was unaffected by the fusion step. The calibration curves obtained for the respective steel samples showed identical slopes. Standard additions to blank solutions gave a slightly higher sensitivity compared with steel sample solutions.

Analytical results

Several steel samples were analyzed by the described procedures. The results are shown in Table 2; comparisons with other methods as well as certificated values are included, and the values represent mean values of 3—8 determinations. Unfortunately, samples with certificated values of acid-soluble aluminium in stainless steels were not available. For the stainless steels, series D and G, the values obtained with our method show good agreement with the values obtained by a flame method. Generally, it is difficult to compare methods adequately since intercalibration values show a large variation. Taking JK 8C as an example, the values reported cover the range 16—25 p.p.m. of aluminium.

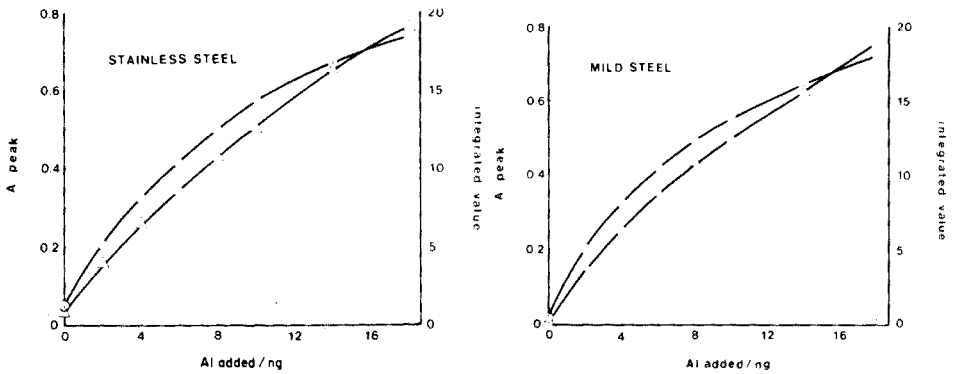

Fig. 5. Calibration curves for acid-soluble aluminium obtained by standard additions to stainless steel, JK 8C, and ultrapure steel, JK 1C. Sample volume, 20 μl (○) Peak values. (△) Integrated values.

TABLE 2

Comparison of results (p.p.m.) obtained for determination of aluminium with flameless atomic absorption with results obtained by other methods

Sample	Matrix	Described procedure	Al found	Values obtained by other methods
JK 1C	ultrapure mild steel	acid-soluble	2	2, 2, 2, 0
		acid-insoluble	2	0.4, 0.6, 7, 2
JK 8C	austenitic stainless steel type 316	acid-soluble	2	22 (total)[a]
		acid-insoluble	9	
JK 16A	ferromolybdenum	acid-soluble	9	47, 61, 77, 80 (total)
		acid-insoluble	45	
BCS 330	mild steel	acid-soluble	109	114
		acid-insoluble	74	190 (total)[a]
D 22058	0.5 % Si, 1.6 % Mn, 18 % Cr, 9 % Ni	acid-soluble	8	14[b]
D 21991	0.6 % Si, 1.7 % Mn, 19 % Cr, 0.3 % Mo	acid-soluble	13	13[b]
D 56633	0.6 % Si, 1.7 % Mn, 18 % Cr, 11 % Ni, 2.6 % Mo	acid-soluble	46	51[b]
G 1776-2	1.5 % Si, 1.6 % Mn, 19 % Cr, 9 % Ni	acid-soluble	278	240[b]
G 1760-2	0.5 % Si, 1.7 % Mn, 18 % Cr, 10 % Ni	acid-soluble	304	290[b]

[a] Certified values.
[b] Determination of aluminium by nitrous oxide—acetylene flame after separation of iron with methyl isobutyl ketone and addition of ethanol to the aqueous sample solutions (provided by Hagfors Steel Factory).

A typical value of the relative standard deviation with respect to acid-soluble aluminium at concentrations larger than 10 p.p.m. was about 5 % with the present method. The corresponding value for acid-insoluble aluminium is about 10 % which can be explained by the additional steps involved in that procedure. For acid-insoluble aluminium in BCS 330, the standard deviation obtained for eight analyses was 25 %; this may be caused by inhomogeneity in the steel samples.

The uncertainty in the atomic absorption measurements was tested by making repeated measurements of acid-soluble aluminium in JK 8C (1.8 p.p.m. aluminium) and JK 8C with 100 p.p.m. of aluminium added. The standard deviations were 0.3 and 4.0 p.p.m. respectively. Similar values were obtained for the determination of acid-insoluble aluminium. However, the detection limit of the present method cannot be evaluated from the value of the standard deviation given above since the blank results varied in the range 0.5—1.5 p.p.m. of aluminium. By means of the described method, acid-soluble aluminium can be determined in about 20 min; this is rapid compared with the conventional methods in use.

The authors wish to thank Professor Gillis Johansson and Dr. Walter Pälverinne, Hagfors Steel Factory, for valuable discussions.

REFERENCES

1 Gmelin-Durrer, Metallurgie des Eisens, Vol. 1a, Verlag Chemie, Weinheim, 1964.
2 F. P. Byrne, R. J. Nadalin, J. Penkrot, J. S. Rudolph and C. R. Wolfe, Am. Soc. Test. Mater., Spec. Tech. Publ., 407 (1968) 237.
3 J. B. Headridge and Alan Sowerbutts, Analyst (London), 98 (1973) 57.
4 W. D. Cobb, W. W. Foster and T. S. Harrison, Lab. Pract., March, 1975.
5 A. Condylis and B. Mejean, Analusis, 3 (1975) 2.
6 J. Musil, Z. Anal. Chem., 271 (1974) 352.
7 T. C. Rains and O. Menis, Anal. Lett., 7 (1974) 11.
8 W. Snellman, T. C. Rains, K. W. Yee, H. D. Cook and O. Menis, Anal. Chem., 42 (1970) 394.
9 F. Shaw and J. M. Ottaway, Analyst (London), 100 (1975) 1189.
10 W. Frech, Talanta, 21 (1974) 565.
11 W. Frech, Z. Anal. Chem., 275 (1975) 353.
12 W. Frech, Anal. Chim. Acta, 77 (1975) 43.
13 W. Frech, G. Lundgren and S-E Lunner, At. Absorpt. Newsl., 15 (1976) 3.
14 G. Lundgren and G. Johansson, Talanta, 21 (1974) 257.
15 W. Frech and A. Cedergren, Anal. Chim. Acta, 82 (1976) 83.
16 W. Frech and A. Cedergren, Anal. Chim. Acta, 82 (1976) 93.

Analytica Chimica Acta, 89 (1977) 127—140

DETERMINATION OF TEN TRACE ELEMENTS IN METEORITES AND LUNAR MATERIALS BY RADIOCHEMICAL NEUTRON ACTIVATION ANALYSIS

L. L. SUNDBERG* and W. V. BOYNTON

Department of Chemistry, and Institute of Geophysics and Planetary Physics, University of California, Los Angeles, CA 90024 (U.S.A.)

(Received 12th July 1976)

SUMMARY

A procedure is reported for the determination of Ni, Ge, Ru, Au, Ir, Zn, Ga, Cd, In and U in meteorites and lunar materials. The precision in multiple determinations at the 95% confidence level is less than 10% except for gold (15%). Ruthenium and uranium are determined by counting ^{97}Ru and ^{103}Ru x-rays; the chemical yield is determined from ^{106}Ru added before sample dissolution. The activity of ^{116m}In is determined with improved sensitivity from integral counts in the region 1.5—3.0 MeV on a NaI(Tl) detector.

A procedure for the analysis of meteorites and lunar materials for Au, Cd, Ga, Ge, In, Ir, Ni, Ru, U and Zn by radiochemical neutron activation analysis is reported. The procedure provides efficient recovery of all these elements, and for 100-mg samples, results in detection limits of less than 1 μg g^{-1} for Ni, 100 ng g^{-1} for Ga, U, Zn, 10 ng g^{-1} for Ru, 100 pg g^{-1} for Cd, Ge, In, Ir, and 1 pg g^{-1} for Au. The efforts of at least four persons are required during the first few hours following the irradiation.

EXPERIMENTAL

Preparation of samples

Weighed samples, typically 50—500 mg, were placed in 5-cm high-purity quartz vials (5 mm o.d., 3.6 mm i.d.) which had been cleaned in warm aqua regia, rinsed several times with distilled water, and dried with high-purity acetone. The vials were sealed and individually wrapped in aluminum foil.

Preparation of standards

Duplicate standards were prepared for each short-lived irradiation by evaporating weighed (ca. 25 mg) solutions onto 3 × 4 cm high-purity aluminum foil squares. A drop of dilute ammonia solution was added to the

*Present address: General Electric Co., San Jose, CA 95125, U.S.A.

acidic solutions to prevent attack on the aluminum. With the exception of Ir and U, monitor stock solutions were prepared by dilutions of carrier solutions with water (see Table 1). The Ir monitor was prepared gravimetrically by electrolytic dissolution of a high-purity Ir wire. The U monitor was prepared by dissolving U_3O_8 (NBS Standard Reference Material 950a) in nitric acid. All solutions were stored in polyethylene bottles.

The concentrations ($\mu g\ ml^{-1}$) of the monitor solutions were roughly: Au, 1.5; Ga, 75; In, 0.01; Ir, 20; Ge, 500; Ru, 15; Zn, 500; Cd, 80; Ni, $1 \cdot 10^4$; U, 400. The concentrations were chosen to minimize the effects of self-shielding, and to minimize contributions from the foil, which are incorporated into the monitor concentrations as necessary.

Experience has shown that with the exception of gold, these solutions are stable over a period of several years. The gold monitor is freshly prepared for each irradiation from a 200 μg Au ml^{-1} stock solution that is 10% in HCl and 5% in HNO_3.

Irradiations

After successive 1-min and 3-h irradiations for the purpose of analyzing for other elements by instrumental neutron activation, samples and standards were irradiated for 1—2 d at the University Research Reactor, Columbia, Missouri, at a thermal neutron flux of ca. $1 \cdot 10^{14}$ n $cm^{-2}\ s^{-1}$. Samples and standards were then re-irradiated for 3 h at the UCLA reactor with a flux of ca. $2 \cdot 10^{12}$ n $cm^{-2}\ s^{-1}$.

Table 2 shows the relevant nuclear data for the isotopes investigated. The UCLA irradiation served to build up the activity of the short-lived radionuclides, ^{65}Ni, ^{116m}In, ^{75}Ge, which have half-lives too short to survive transit from Missouri. Of the remaining nuclides, only ^{72}Ga was produced

TABLE 1

Preparation of carrier solutions

Element	Weighing form	Treatment	Final matrix	Concn. ($mg\ ml^{-1}$)
Au	Au metal	Aqua regia	10% HCl, 5% HNO_3	20
Cd	Cd metal	HCl	0.1 M HCl	20
Ga	Ga_2O_3	HCl	0.1 M HCl	10
Ge	Ge metal	—[a]	~H_2O	4
In	In_2O_3	HCl	0.1 M HCl	10
Ir	$(NH_4)_2IrCl_6$	Aqua regia	20% HCl, 10% HNO_3	4
Ni	Ni metal	HCl(HNO_3)	0.1 M HCl	10
Ru	$(NH_4)_2Ru(H_2O)Cl_5$	Aqua regia	10% HCl, 5% HNO_3	8
Zn	Zn metal	HCl	0.1 M HCl	10

[a]To 1 g of Ge metal, add 4.3 g of $H_2C_2O_4 \cdot 2H_2O$, 2.5 ml of NH_3 liquor, 15 ml of 30% H_2O_2, 3.5 ml of 40% HF, and 150 ml of H_2O. After dissolution and dilution with water, the Ge salt approximates to $(NH_4)_2Ge(C_2O_4)_3$.

TABLE 2

Relevant nuclear properties

Stable isotope	Abundance (%)	Cross-section (b)	Isotope formed and decay mode	Half-life	γ energies and abundances (keV, %)
^{114}Cd	28.86	1.1	^{115}Cd(β^-)	53.5 h	528(28); 336(^{115m}In^{30})
^{115}In	95.77	154	^{116m}In(β^-)	53.7 m	417(33); 1293(82); 1097(49)
^{191}Ir	37.30	750	^{192}Ir(β^-)	74.2 d	317(86); 468(50)
^{71}Ga	39.80	5	^{72}Ga(β^-)	14.1 h	834(96)
^{76}Ge	7.76	0.1	^{77}Ge(β^-)	11.3 h	265(64); 216(30) 211(32)
^{74}Ge	36.74	0.3	^{75}Ge(β^-)	82.8 h	265(11.9); 199(1.4)
^{70}Ge	20.55	3.2	^{71}Ge(EC)	11.4 d	Ga x-ray
^{64}Ni	1.16	1.5	^{65}Ni(β^-)	152 m	1482(25)
^{64}Zn	48.89	0.46	^{65}Zn(β^+)	243 d	1115(52)
^{197}Au	100	98.8	^{198}Au(β^-)	64.7 h	412(97)
^{96}Ru	5.46	0.2	^{97}Ru(EC)	69.1 h	215(90); Tc x-ray
^{102}Ru	31.60	1.4	^{103}Ru(β^-)	39.5 d	497(89); Rh(IC) x-ray
^{235}U	0.72	579(n,f)	^{103}Ru(β^-)	39.5 d	497(89); Rh(IC) x-ray

at UCLA in an amount comparable to that remaining from the Missouri irradiation.

Apparatus

Most γ-counting was performed on 7.5 × 7.5-cm well-type NaI(Tl) detectors with a resolution of 7.5—8% at 662 keV. Iridium samples were counted on a Ge(Li) coaxial detector with a resolution of 1.8 keV (FWHM) and a 40:1 peak-to-Compton ratio at 1332 keV, in conjunction with a 4096-channel analyzer. X-ray counting of Ru and Ge samples was done with a Si(Li) detector with a resolution of 247 eV (FWHM) at 5.89 keV. Solutions were counted in 17 × 100 mm disposable polypropylene tubes.

Most of the chemical yields were determined by atomic absorption spectrometry (a.a.s.) with a Perkin-Elmer Model 303 spectrometer. The lines yielding the highest precision, as recommended by the manufacturer, were used exclusively. Germanium chemical yields were determined colorimetrically (Cary-14 spectrophotometer).

Carrier preparation

The carriers shown in Table 1 (1 ml of each), and a solution containing 20 c.p.m. (on a Ge(Li) detector) of the 512-keV γ-peak of ^{106}Ru tracer were pipetted into zirconium crucibles. Ruthenium served as the carrier for uranium. Germanium carrier was added last, and the solution was rapidly neutralized with ammonia and taken to dryness. The neutralization prevents the volatilization of $GeCl_4$ and inhibits acid attack on the crucibles. The crucibles were stored in a desiccator until needed.

Carriers for the standards were pipetted into appropriate glassware containing the following solutions: Au, Ni, Zn, Cd, Ru, U into 10 ml of

concentrated HCl; Ga, In into 10 ml of concentrated HBr; Ge (100-ml round-bottom flask) into 20 ml of 4 M HCl; Ir into 10 ml of concentrated HCl and 5 ml of 4 M HNO_3. The ^{106}Ru tracer concentration for the U and Ru standards was roughly 4000 c.p.m.

Separation scheme

Figure 1 shows an abbreviated flow diagram of the separation scheme. Parenthetical designations such as (S1) in the discussion to follow refer to phases described in this Figure. Unless otherwise specified, all acids are concentrated. Holdback carriers were aqueous solutions of chloride salts whose concentrations were roughly 10 mg metal per ml.

Transfer the weighed sample to zirconium crucibles containing the carriers. Fuse the mixture with 8 g of Na_2O_2 for about 5 min with occasional swirling. After cooling, transfer the crucible to a 250-ml beaker, dislodge the fusion cake with 75 ml of water, and centrifuge in 50-ml plastic tubes. Decant the orange (RuO_4^{2-}) supernate (S1) into a 250-ml beaker containing 20 ml of 95% EtOH (the solution is 2—3 M in NaOH at this point). Dissolve the precipitate (P1) with 5 ml of 6 M HCl and retain for further processing. Boil the supernate (S1) until the volume is reduced to 50 ml and centrifuge the solution in 50-ml plastic centrifuge tubes. The precipitate (P2) contains Au metal and Ru hydrous oxide.

Combine the supernate (S2) with the acidified precipitate (P1). Adjust the solution to pH 1—2 with HCl. Add ammonia solution until the pH is 9—10, and centrifuge. The supernate (S3) contains the amine complexes of

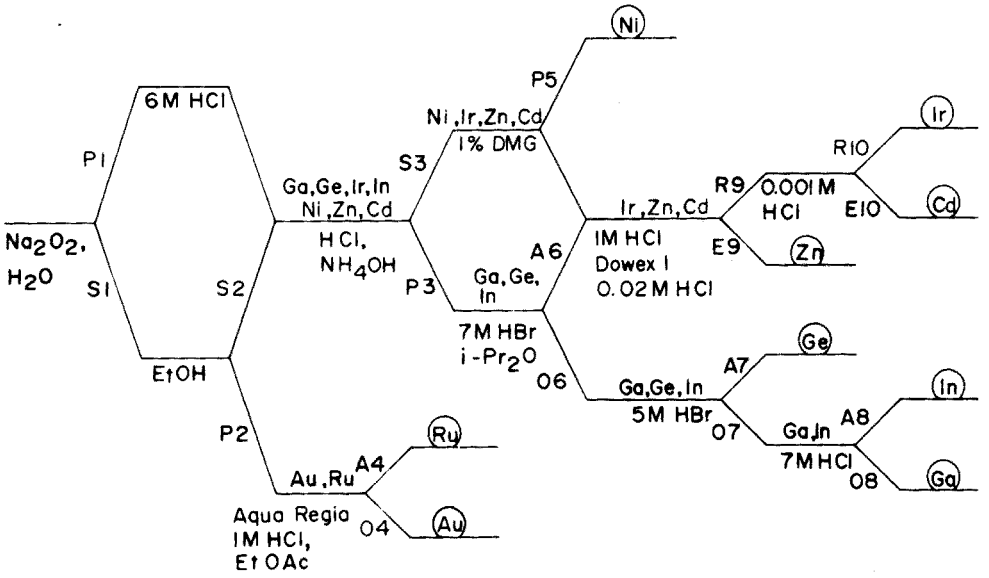

Fig. 1. Flow diagram of radiochemical separation procedure. Letters and numbers designate various phases to which the text refers: A, aqueous layer; E, eluate; O, organic layer; P, precipitate; R, resin; and S, supernate.

Ni, Zn, and Cd. The precipitate (P3) contains hydroxides of Ga, Ge, and In. Iridium partitions as the hydrous oxide into the precipitate (P3) and as the chloroiridate complex into the supernate (S3). Decant the ammoniacal supernate (S3) into a 250-ml beaker. Add 10 ml of 1% dimethylglyoxime (DMG) in ethanol to precipitate the nickel chelate (P5), and collect by filtration. Wash with 30 ml of water. The filtrate and wash (F5), containing Ir, Zn, and Cd, is collected in a 600-ml beaker and retained for further processing.

Dissolve the precipitate (P3) in 20 ml of HBr and measure the volume. Add HBr or water as required to yield a solution 7.0 M in HBr. Transfer the solution to a 250-ml separatory funnel containing 40 ml of isopropyl ether (i-Pr_2O) and shake. Drain the lower aqueous layer (A6) containing iridium into a 600-ml beaker. Wash the ether layer (O6) containing Ga, Ge, and In with 10 ml of 7 M HBr allowing the washings to run into the beaker and retain for processing of Ir, Zn and Cd.

Separation of Au and Ru. Transfer the mixed precipitate (P2) to a 250-ml beaker, and dissolve with aqua regia. Add Cr^{3+} holdback carrier, heat to incipient dryness and add HCl to expel nitrates. Heat again to incipient dryness and add 25 ml 1 M HCl. Cool, and transfer the solution to a 250-ml separatory funnel containing 40 ml of ethyl acetate and shake. Drain the lower aqueous phase (A4) containing Ru into a 250-ml beaker. The organic layer (O4) contains Au.

Separation of Ge, In, and Ga. Back-extract Ge from the ether layer (O6) with two 10-ml portions of 5 M HBr. Drain the lower aqueous phases (A7) into a 250-ml beaker; the organic layer (O7) still contains Ga and In. Back-extract indium from the ether layer (O7) with two 5-ml portions of 7 M HCl containing Co and Mn holdback carriers. Drain the lower aqueous phases (A8) into a 150-ml beaker; gallium remains in the ether layer (O8).

Separation of Zn, Cd, and Ir. Prepare an anion-exchange column, 1 × 10 cm, with Dowex 1-X8 resin, 100-200 mesh, chloride form. Precondition the column with 50 ml of freshly prepared 1 M HCl containing 0.05% cerium(IV).

Acidify the filtrate (F5) from the nickel precipitation with HCl and add holdback carriers for Hf, Co, Sc, Fe^{3+}, Cr^{3+}, and Cu. Boil the solution to incipient dryness and add 50 ml of 1 M HCl. To the aqueous phase (A6) from the Ga—Ge—In extraction, add 10 ml of HCl and the above holdback carriers. Bring this solution to the boil and reduce the volume by a factor of 3. Cautiously add 30% H_2O_2 until all bromides are expelled. If precipitation or frothing occurs during the peroxide addition add more HCl and continue adding H_2O_2. Boil this solution to incipient dryness, and add the processed (F5) nickel filtrate. Add about 1 g of $Ce(NH_4)_2(NO_3)_6$, cool, filter, and load onto the column.

The effluent may be discarded. Wash the column with the following sequence of solutions: two 5-ml portions of 1 M HCl (0.05% Ce), 20 ml of the same, and two 5-ml portions of 0.02 M HCl. Discard the washings.

Collect zinc (E9) in a 250-ml beaker with the following eluents: 75 ml of

0.02 M HCl, 5- and 10-ml portions of 0.001 M HCl. Collect cadmium (E10) in a 250-ml beaker with 100 ml of 0.001 M HCl. Iridium (R10) is retained on the resin.

Individual purifications

Gold. Prepare an anion-exchange column (1 × 10 cm) with Srafion NMRR resin, 0.3—1.2 mm, which has been equilibrated for several hours with 0.1 M HCl.

Gold purification is based on a modification of procedures reported by Sundberg [4]. Wash the ethyl acetate containing gold with two 25-ml portions of 1 M HCl, the first containing holdback carriers for Co, Cr^{3+}, Mn^{2+}, Ir^{3+}, and Ga; discard the washings. Transfer the gold containing ethyl acetate to the Srafion NMRR anion-exchange column. Pass the solution through the resin at a rate of 1—2 ml min^{-1}. Wash the column with four 15-ml portions of 0.1 M HCl, the first containing Fe^{3+} and Co holdback carriers. Discard the initial effluent and the washings. Elute gold into a 250-ml beaker with 100 ml of a 5% thiourea solution that is 0.05 M in HCl. Bring to a gentle boil, and precipitate Au_2S_3 by adding 10 ml of ammonia liquor. Reduce the volume to less than 50 ml, centrifuge in a 50-ml plastic centrifuge tube and discard the supernate. Add 25 ml of water to the precipitate, re-centrifuge, and discard the washings. Dissolve the sulfide in a few ml of aqua regia, transfer the solution to a counting tube, and dilute to 5 ml with water for counting. Count the 412-keV γ-peak of ^{198}Au on the NaI(Tl) detector. Dilute the sample by a factor of 500 with a solution 1.2 M in HCl and 0.8 M in HNO_3 for chemical yield determination by a.a.s.

Add a few ml of nitric acid to the dissolved standard and heat the solution to incipient dryness. Add 25 ml of 1 M HCl and extract gold into 40 ml of ethyl acetate. Treat the standards identically to the samples for the remainder of the procedure.

Cadmium. Prepare an anion-exchange column (1 × 10 cm) with Dowex 1-X8 resin, 100-200 mesh, chloride form, which has been pre-soaked in 3 M HCl.

Add a few ml of HCl and Fe^{3+} holdback carrier to the cadmium eluate (E10). Boil the solution to a volume of 10 ml, add ammonia solution to give pH 10, and centrifuge. Decant the cadmium-containing supernate into a 250-ml beaker containing Cu and Cr holdback carriers. Saturate the solution with H_2S and centrifuge. Discard the supernate and dissolve the CdS precipitate in 3 M HCl.

Place the solution on the column and add several 5-ml portions of 1 M HCl, followed by 50 ml of 0.01 M HCl. Discard the effluent and washings. Elute cadmium with 50 ml of 1 M ammonia solution. Heat the eluate to incipient dryness and dilute to 5 ml with water for counting. Allow 24 h to obtain secular equilibrium between the 4.5-h ^{115m}In daughter (336 keV) and 54-h ^{115}Cd (528 keV) before counting. Dilute the sample by a factor of 2500 with water for yield determination by a.a.s.

Heat the dissolved standards to incipient dryness. Add Fe holdback carriers as above, and treat identically to the samples for the remainder of the procedure.

Gallium. Back-extract gallium from the ether (O8) with two 10-ml portions of water into a 150-ml beaker. Add 1 ml of Fe^{3+} holdback carrier and 5 ml of 20% $TiCl_3$ solution. Heat to incipient boiling to insure reduction to Fe^{2+}. Cool, add about 25 ml of 11 M HCl, and extract Ga into 40 ml of isopropyl ether. Wash the ether twice with 7 M HCl and back-extract Ga with two 10-ml portions of water.

Reduce the volume of gallium solution to about 3 ml by boiling, being careful not to go to dryness since $GaCl_3$ is volatile. Transfer the liquid to a counting tube, dilute to 5 ml and shake to homogenize.

Count the samples on a NaI(Tl) detector and determine gallium from the 835-keV γ-peak of ^{72}Ga. Dilute the sample to 25 ml with water for yield determination by a.a.s.

Add 5 ml of water to the dissolved standards and extract gallium into 20 ml of isopropyl ether. Wash the ether with two 5-ml portions of 7 M HCl, back-extract with two 10-ml portions of water, reduce the volume to about 3 ml and transfer to counting tubes as for the samples.

Germanium. Make the solution (A7) 9 M in HCl, transfer to a 250-ml separatory funnel containing 40 ml of CCl_4 and shake. Drain the lower (CCl_4) layer to a second 250-ml separatory funnel and wash with 20 ml of 9 M HCl. Drain the CCl_4 layer into a third 250-ml separatory funnel and back-extract germanium into 10 ml of 4 M HCl. Drain the CCl_4 layer into a fourth 250-ml separatory funnel and back-extract germanium into an additional 10 ml of 4 M HCl. Drain off the CCl_4 and discard. Place the two 10-ml 4 M HCl fractions into a 100-ml round-bottom flask containing 16 ml of 8 M HCl, and As hold-back carrier. The HCl concentration of this solution must be just under 6 M HCl; $GeCl_4$ does not form at lower concentrations, but at higher concentrations forms too early and, in the absence of the $HCl:H_2O$ carrier gas, fails to condense. Distil $GeCl_4$ in presence of chlorine (to prevent codistillation of arsenic). Collect 5 ml of distillate in a glass counting tube and count the mixture of ^{72}Ge and ^{77}Ge on a NaI(Tl) detector (see Discussion).

Dissolve the germanium standards in 20 ml of 4 M HCl in a 100-ml round-bottom flask under reflux. Add 13 ml of 11 M HCl and 7 ml of water to bring the solution to just under 6 M HCl. Distil $GeCl_4$ in presence of chlorine as above.

Dilute the samples and standards to 100 ml with water. Determine the yield in duplicate colorimetrically with phenylfluorone [5, 6].

The following additional steps are usually added for runs including samples with low Ge contents. Pour the remaining solution from the colorimetric yield determination into a 250-ml beaker containing 50 ml of 11 M HCl. Saturate the solution with H_2S to precipitate GeS_2. Collect the precipitate on 2.4-cm GF/C Whatman filter paper and wash with 4 M HCl.

Dissolve the precipitate with 3 M ammonia solution, collecting the solution in a test tube. Wash any sulfur residue with a few ml of water and combine the wash with the other filtrate. Decant the filtrate into a 50-ml beaker, and add enough 9 M HCl to reprecipitate GeS_2 and give about 5 ml in excess. Resaturate the solution with H_2S, and collect the GeS_2 precipitate on a weighed 2.4-cm Whatman GF/C filter paper. Wash the precipitate with water, and then with methanol, and dry overnight at 110° C. Reweigh the precipitate, mount the filter on a card, cover with 0.25-mil Mylar film and count the Ge x-rays produced from the decay of 11-d ^{71}Ge on the Si(Li) detector. Recovery is calculated from the weight of the precipitate.

Indium. Add 2 drops each of Fe^{3+}, Sc, Cr^{3+}, Cr^{6+} carrier solutions and bromocresol purple indicator to the indium solution (A8). Cautiously add ammonia liquor until the solution just retains the purple color (pH 9); do not pass the end-point. Centrifuge In, Fe, and Sc hydroxides in a thin-walled, 50-ml pyrex centrifuge tube; discard the supernate. To the precipitate, add 2 drops of Cr^{3+} and Cr^{6+} holdback carriers. Cycle about 5 times through the following four steps: (1) add ca. 1 ml of 14 M HNO_3; (2) take to dryness over a burner flame; (3) add ca. 1 ml of 11 M HCl; (4) take to dryness over a burner flame. Add ca. 1 ml of 11 M HCl and take to near dryness. While the centrifuge tube is hot, add 5 ml of 20% $TiCl_3$ solution and allow to stand for 2—3 min. Add 10 ml of concentrated HBr and extract indium into 20 ml of isopropyl ether. Wash the ether twice with 5-ml portions of 6 M HBr, back-extract indium with two 5-ml portions of 7 M HCl containing Co and Mn^{2+} holdback carriers and collect in a 150-ml beaker. Add 2 drops of bromocresol purple indicator solution and cautiously add ammonia solution to the purple end-point. Centrifuge and discard the supernate. Dissolve the precipitate with 1 ml of concentrated HBr, transfer to a counting tube and dilute to 5 ml with water.

Count the samples on the NaI(Tl) detector, using the 417-keV γ-peak and/or the continuum between 1500—3000 keV of 54-min ^{116m}In for analysis. Count the samples twice within 1—2 h to check for isotopic purity and once the following day at the same analyzer calibration to determine the number of counts in the continuum from background and any long-lived contamination (see Discussion).

Dilute the sample to 50 ml with 1 M HCl for yield determinations by a.a.s.

Add 5 ml of water to the dissolved standard and extract indium into 20 ml of isopropyl ether. Wash with two 5-ml portions of 6 M HBr and back-extract with two 5-ml portions of 7 M HCl containing Co and Mn^{2+} holdback carriers. Precipitate $In(OH)_3$ as for the samples, dissolve in 1 ml of concentrated HBr and dilute for counting.

Iridium. Wash the resin (R10) containing Ir with 100 ml of 2 M acetic acid containing Cr^{3+} holdback carrier, followed by 15 ml of water, allowing the column to run dry. Transfer the resin containing the brown band of Ir to a 250-ml beaker with 50 ml of 10% (w/v) $NH_2OH \cdot HCl$, and add 50 ml of 8 M HCl. Soak the resin in this solution overnight to extract iridium.

Filter and retain the filtrate. Soak the resin again for another day in the same medium. Filter the resin and combine both filtrates. Boil the solution to a volume of 25 ml. Add sufficient 30% H_2O_2 to destroy the hydroxylamine. Add solid $NaHCO_3$ until the solution has a pH of 6, and digest for several minutes. Collect $IrO_2 \cdot xH_2O$ by centrifugation. Wash the precipitate several times with water, and discard all supernates. Dissolve the precipitate in HCl and dilute to 5 ml with water for counting. Count the 317- and 468-keV γ-peaks of ^{192}Ir on the Ge(Li) detector.

Determine the chemical yield by reactivating an aliquot of the Ir solutions in the presence of $Mg(NO_3)_2$ as an inert diluent. A complete description of the reactivation procedures is available elsewhere [7].

The standards require no chemical processing. After ten or more days when the major activated foil impurities (^{24}Na, ^{76}As) have decayed, the dissolved standards are diluted to 25 ml with water and an aliquot is removed for counting. The yield, which should be 100%, is determined by reactivation.

Nickel. Prepare an anion-exchange column (1 × 10 cm) with Dowex 1-X8 resin, 100-200 mesh, chloride form, which has been presoaked with 11 M HCl.

Dissolve the nickel precipitate (P5) with HCl, collect in a 250-ml beaker, add Fe^{3+} holdback carriers, and evaporate to about 5 ml. Cool, adjust the solution to pH 9.5 with ammonia, and add a few drops of H_2O_2 to oxidize Mn^{2+} to MnO_2. Transfer the slurry to 50-ml tubes and centrifuge. Decant the Ni-bearing supernate into a new centrifuge tube and discard the precipitate. Add 50 mg of Na holdback carrier, and add 10 ml of 1% dimethylglyoxime in ethanol to precipitate the nickel chelate. Centrifuge, discard the supernate, wash the precipitate with water, and centrifuge again. Dissolve the precipitate in a minimum volume of 11 M HCl.

To attain the maximum possible concentration of HCl, transfer the solutions to large glass centrifuge tubes and heat to dryness over a burner. After cooling, redissolve in less than 2 ml of 11 M HCl, and load onto the column. Elute nickel with 25 ml of 11 M HCl. Evaporate the eluate to near dryness and dilute to 5 ml with water for counting. Count the 1482-keV γ-peak of ^{65}Ni on the NaI(Tl) detector. After counting, dilute the sample to 100 ml with water for yield determinations by a.a.s.

Add ammonia solution to the dissolved standards until the solution is at pH 10. Add 10 ml of 1% DMG solution, and process identically to the samples as if this were the first precipitation of the nickel chelate.

Ruthenium—uranium. Boil the aqueous phase (A4) from the gold extraction to incipient dryness. Add 10 ml of water and 25 ml of 18 M H_2SO_4, and heat until the characteristic white fumes of SO_3 appear. Cool, and transfer the solution to a 100-ml round-bottom flask containing a few glass beads, 10 ml of water, and 2 g of CrO_3. Distil RuO_4 in a current of air at the rate of 2—3 bubbles per second. Immerse the stem of the delivery tube into a receiving solution of 6 M HCl. This reduces RuO_4 to nonvolatile lower valencies. When distillation is complete (usually after 10 min), the

residual solution may be discarded. Boil the distillate to incipient dryness. Add 10 ml of water, 15 ml of 3 M NaOH, and sufficient 5% NaOCl to oxidize ruthenium to perruthenate (yellow-green). After 5 min, add 10 ml of 95% ethanol and heat gently for about 15 min to coagulate the hydrous ruthenium oxide. Collect the precipitate on 2.4-cm Whatman GF/C filter paper and wash with several ml of 95% ethanol; the filtrate and washings may be discarded. Dry the precipitate for several hours at 110°C; the precipitate is both hygroscopic and nonstoichiometric. Cool, and mount the precipitate on cardboard. Cover the precipitate with 0.25-mil Mylar film, and count the Tc and Rh x-rays from the decay of ^{97}Ru and ^{103}Ru on the Si(Li) detector. Determine the chemical yield by counting the 512-keV γ-peak of the ^{106}Ru tracer and the 497-keV γ-peak of ^{103}Ru on the Ge(Li) detector (see Discussion).

Boil the standards to incipient dryness. Prepare for the distillation as above, and process them identically to the samples for the remainder of the procedure.

Zinc. Prepare an anion-exchange column (1 × 10 cm) with Dowex 1-X8 resin, 100-200 mesh, chloride form, which has been presoaked with 1 M HCl.

Add a few ml of 11 M HCl and Fe^{3+} holdback carrier to the zinc eluate (E9). Boil the solution to a volume of 10 ml, add ammonia solution to pH 10, and centrifuge. Decant the zinc supernate into a fresh centrifuge tube and saturate the solution with H_2S. Centrifuge, discard the supernate, and dissolve the ZnS precipitate with 3 M HCl.

Make the solution 1 M in HCl, load onto the column, and wash with several 10-ml portions of 1 M HCl. The original effluent and the washings may be discarded. Elute zinc from the column with 80 ml of 0.01 M HCl, evaporate to about 2 ml and dilute to 5 ml with water for counting. Count the 1115-keV γ-peak of ^{65}Zn on the NaI(Tl) detector. Dilute the sample by a factor of 2500 for the yield determination by a.a.s.

Heat the dissolved standards and reduce the volume to about 5 ml. Add Fe holdback carrier followed by ammonia liquor to pH 10, and treat identically to the samples for the remainder of the procedure.

DISCUSSION

Except for a few steps, the proposed elemental separation scheme (Fig. 1) is very straightforward. Most of the solvent extraction and ion-exchange separations are used in other published procedures. One innovation is the precipitation of Au and Ru (P2) simultaneously with ethanol from 2—3 M NaOH. This precipitation, which is reasonably quantitative, followed by isolation in 4—6 M NaOH, minimizes losses of the remaining elements.

The HBr concentration during the extraction of Ga, Ge, and In (O6) into isopropyl ether is critical. At 7 M HBr the bromide complexes of all these elements are quantitatively extracted, whereas little germanium is extracted from 5 M HBr.

The individual purification procedures are equally straightforward, and generally yield radiochemically pure counting solutions. For indium, the repeated evaporations with HCl and HNO_3 are necessary for the decomposition and equilibration of chromium complexes.

Counting

This research group generally uses the Wasson method for photopeak integration as opposed to methods which employ a total peak area; a detailed discussion has been given by Baedecker [8]. When necessary, the detector background is stripped from a spectrum before photopeak integration.

Purified germanium samples for γ-counting contained 82-min ^{75}Ge and 11-h ^{77}Ge. Activity was determined by summing the 199- and 265-keV γ-peaks of ^{75}Ge. However, the spectra are not pure because of the presence of ^{77}Ge which emits γ-rays at 210, 215 and 265 keV. Hence, an empirical correction curve must be employed to allow for deviations in the decay factor with an 82-min half-life [6].

The counting scheme and yield determination for ruthenium replace the procedures reported by Sundberg [9] in which the 497-keV γ-peak of ^{103}Ru was counted exclusively, and recovery was determined colorimetrically with thiourea. Ruthenium-103 is one of the more abundant products from the slow neutron fission of ^{235}U (2.9%). For samples containing an equal amount of Ru and natural U, a 13% correction must be applied to ruthenium if the analysis is based on the counting of ^{103}Ru. Since lunar samples contain uranium at levels well in excess of ruthenium, the correction becomes quite significant.

Ruthenium-97, which is not produced by fission, decays by electron capture with a 2.9-d half-life, emitting its principal (91% abundant) 215-keV γ-peak. The decision to count the Tc x-ray resulted from the low background and superior peak-to-total ratio of the Si(Li) x-ray detector, because the 215-keV γ-peak of ^{97}Ru is superimposed on the Compton plateau of the 497-keV γ-peak of ^{103}Ru.

The x-ray spectra of purified ruthenium samples contain Tc, Rh, and Ru x-rays: Tc from the electron capture decay of ^{97}Ru, Rh from internal conversion of the ^{103m}Rh daughter of ^{103}Ru, and Ru from the γ-ray-induced fluorescence of the precipitate. A sample spectrum is shown in Fig. 2. Though the Tc Kβ and Rh Kα x-rays are unresolvable, the contribution of the former is negligible.

The weak activity of ^{97}Ru requires that samples be placed directly on the beryllium window of the detector. Without a second count on a Ge(Li) detector to determine the yield, the inability to maintain a reproducible counting geometry would lead to serious errors in the determination. However, determining the decay-corrected activity of ^{103}Ru in each count (the Rh Kα x-ray on the Si(Li) detector and the 497-keV γ-peak on the Ge(Li) detector) makes a reproducible counting geometry unnecessary.

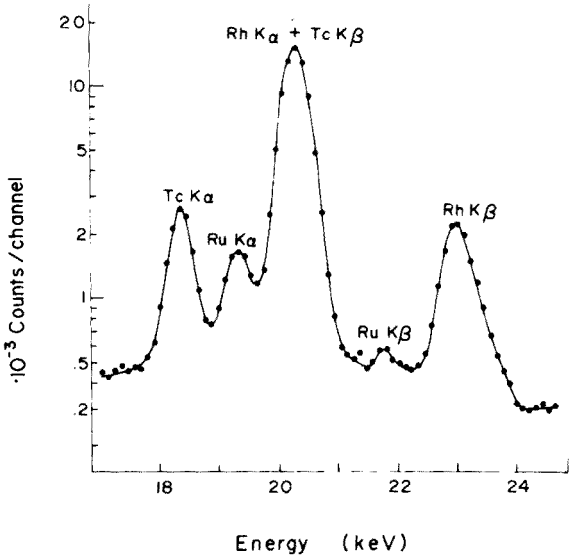

Fig. 2. X-ray spectrum of a typical lunar sample counted on a Si(Li) detector. The Tc Kα is used for Ru determination and the Rh Kα is used for U determination in samples with low Ru contents (see text). The Ru x-ray is from induced fluorescence of the precipitate.

Since the ratios of $^{97}Ru/^{103}Ru$ determined by x-rays and $^{103}Ru/^{106}Ru$ determined by γ-rays are unaffected by counting geometry, the ratio of $^{97}Ru/^{106}Ru$ is also unaffected. This ratio is the yield-corrected activity which is the measure of the total amount of ruthenium in the sample.

The emission cascade of the 512- and 622-keV γ-peaks of ^{106}Ru (^{106}Rh) leads to summing effects which depend on counting geometry. This could lead to errors in the yield determinations when γ-counting of the samples is performed at the lowest attainable geometry to minimize counting time. An approximation of the magnitude of the summing effects was established by counting a sample at several different geometries. The 497/512 counting rate ratio decreased by only 2.7% when the sample was moved from the detector face to a position 3 cm away. Thus, it seems reasonably certain that errors from coincident summing are negligible. Finally, the yield counts were corrected for the background 511-keV annihilation radiation. The amount of ^{106}Ru tracer added was considerably greater than 100 times the amount of ^{106}Ru produced by uranium fission in the sample.

Uranium is determined by correcting the total specific activity of the 497-keV γ-peak of ^{103}Ru for the ^{102}Ru (n,γ) ^{103}Ru reaction and relating to the uranium flux monitors. In a typical lunar sample, about 70—80% of the ^{103}Ru activity is due to uranium fission. However, in meteorites with high ruthenium contents, uranium cannot be determined by this technique. In those cases where ruthenium could not be detected from the Tc x-ray, an upper limit (based on $2\sqrt{N}$) is reported for ruthenium, and a range for

uranium is given. The upper uranium limit is determined by assuming no ruthenium in the sample, and the lower limit by correcting for the upper limit of ruthenium.

The detection limit for indium by neutron activation analysis based on 53.7-min ^{116m}In is clearly superior to that based on the 50-d ^{114}In. If the 1097- or 1293-keV γ-peaks of the short-lived isotope are to be used for analysis, the samples must be rigorously scavenged of ^{59}Fe because of the similar energies of its major γ-peaks (1099 and 1292 keV). Though use of the 417-keV ^{116m}In γ-peak avoids the ^{59}Fe contamination, better counting statistics are obtained in the continuum region between 1500 and 3000 keV. Indium-116m emits γ-rays at 1508, 1753, and 2112 keV, and several summation photopeaks also occur in this region. When the sample itself was used as a background count a day after the first two counts, the continuum was indeed found to decay with a 54-min half-life. In the experiments where this counting procedure was used (ca. 40 samples), the sample background was never found to exceed the normal detector background. Because no systematic differences were found between results obtained from the continuum and the 417-keV γ-peak, the former procedure is now used exclusively

Recovery

Typical recoveries (%) for the elements determined in the samples are as follows: Au, 60—80; U—Ru, 60—80; Ga, 40—60; In, 30—50; Cd, 40—60; Ni, 50—70; Zn, 50—70; Ge, 40—60; Ir, 20—40.

Atomic absorption is ideally suited for the determination of chemical yields, in that most interelement interferences are eliminated. This technique was used for all elements except Ge, Ir and Ru. The standards were prepared from the carrier solutions by dilution with the same matrix as the purified samples, in order to minimize matrix interferences. The detection limits of the yield determination methods were never approached. Yields were determined by fitting a six-point standard curve to a quadratic equation.

Precision and accuracy

As a measure of the precision and accuracy of the radiochemical procedures, replicate analyses of the USGS standard rock BCR-1 are shown in Table 3. Earlier data have been reported by Baedecker et al. [2]. Only the last few entries in Table 3 reflect the present modifications of the procedures. The recent changes have had little, if any, effect on the uncertainties associated with the data, so that these data should provide a fair test of precision. Confidence limits (95%) on the mean of two determinations were calculated by Student's t distribution. The siderophile elements, Au, Ru, Ir, and to a lesser degree nickel, tend to be heterogeneously distributed in BCR-1, hence their uncertainties (Table 3) are quite large. In lunar samples and standard rocks W-1 and PCC-1, the precision for Ni, Ir and Au is typically 6%, 10%, and 15%, respectively [10,11]. Too few data for U and Ru are available to evaluate the precision of these determinations satisfactorily.

TABLE 3

Concentration of volatile and siderophile elements in USGS standard rock BCR-1

Date	Mass	Ni[a]	Zn[a]	Ga[a]	Ge[a]	Ru[b]	Cd[b]	In[b]	Ir[b]	Au[b]
16.5.72	508	—	127	23.2	3.8[c]	—	125	90	0.076	—
8.8.72	516	10.1	129	24.5	1.54	—	143	82	20[c]	1.4[c]
30.8.72	522	10.0	138	24.2	1.49	—	138	90	100[c]	0.72
28.6.73	252	9.2	133	23.5	1.72	—	—	93	<0.10[c]	0.78
24.4.75	195	<11[c]	130	23.4	1.73	—	142	85	0.15	1.19
24.4.75	157	<9.2[c]	130	23.8	<3.6[c]	—	144	90	0.15	0.97
5.6.75	115	11.8	136	22.9	1.71	—	250[c]	86	0.50[c]	0.62
16.1.76	105	<14[c]	129	24.2	1.54	<5.4	160	92	0.016	0.50
Mean		10.3	132	23.7	1.62	<5.4	142	88	0.098	0.80
s		1.1	4	0.6	0.11	—	11	4	0.065	0.25
n		4	8	8	6	—	6	8	4	6
95% confidence limit (%)		20	2.6	2.1	7.7		9.1	3.8	120	36

[a] $\mu g\ g^{-1}$. [b] $ng\ g^{-1}$. [c] Not included in mean or in estimate of the standard deviation.

We are indebted to J. T. Wasson, J. Kimberlin, C.-L. Chou, P. H. Warren, R. W. Bild, P. A. Baedecker, R. Schaudy, and H. J. Chun for advice and technical assistance. This work was supported in part by NASA grant NGL-05-007-367.

REFERENCES

1 P. A. Baedecker, R. Shaudy, J. L. Elzie, J. Kimberlin, and J. T. Wasson, Proc. Second Lunar Sci. Conf., Geochim.Cosmochim. Acta Suppl. 2, M.I.T. Press, Cambridge, Mass., 1971, p. 1037.
2 P. A. Baedecker, C.-L. Chou, and J. T. Wasson, Proc. Third Lunar Sci. Conf., Geochim. Cosmochim. Acta Suppl. 3, M.I.T. Press, Cambridge, Mass., 1972, p. 1343.
3 P. A. Baedecker, C.-L. Chou, E. B. Grudewicz, and J. T. Wasson, Proc. Fourth Lunar Sc Conf., Geochim. Cosmochim. Acta Suppl. 4, Pergamon, Oxford, 1973, p. 1177.
4 L. L. Sundberg, Anal. Chem., 47 (1975) 2037.
5 H. J. Cluley, Analyst (London), 76 (1951) 523.
6 J. T. Wasson and J. Kimberlin, Radiochim. Acta, 5 (1966) 170.
7 J. Kimberlin, C. Charoonratana, and J. T. Wasson, Radiochim. Acta, 10 (1968) 69.
8 P. A. Baedecker, Anal. Chem., 43 (1971) 405.
9 L. L. Sundberg, Ph. D. Dissertation, University of California, Los Angeles, 1975.
10 P. A. Baedecker, C.-L. Chou, L. L. Sundberg and J. T. Wasson, Proc. Lunar Sci. Conf. 5th, (1974) p. 1625.
11 W. V. Boynton, P. A. Baedecker, C.-L. Chou, K. L. Robinson and J. T. Wasson, Proc. Lunar Sci. Conf. 6th (1975), p. 2241.

Analytica Chimica Acta, 89 (1977) 141—149

NON-DESTRUCTIVE DETERMINATION OF TRACE ELEMENTS IN TUNGSTEN BY HELIUM-3 ACTIVATION ANALYSIS

C. S. SASTRI, H. PETRI and G. ERDTMANN

Zentralabteilung für Chemische Analysen der Kernforschungsanlage Jülich, 5170 Jülich (Federal Republic of Germany)

(Received 21st June 1976)

SUMMARY

A non-destructive method is described for the determination of trace impurities at sub-p.p.m. levels in a tungsten matrix by 14-MeV ^{3}He activation analysis. A Ge(Li) spectrometer and a multichannel analyzer were used to determine V, Fe, Ni, Zn and Mo impurities. Interfering reactions are discussed in detail.

Tungsten metal is widely used in the electronics industry and solid state research. Its present applications are based mainly on its high melting point and chemical resistance. New techniques for the production and transport of energy and related industrial processes will require new constructional materials, and tungsten is expected to play an important role in these fields. As with many other metals, its properties are affected by the presence of impurities [1—3].

Analytical methods for the determination of these trace impurities are not well developed. Photometric methods are available, but they require chemical preparations which involve the risk of contamination by impurities in the reagents. The limit of determination for most of the elements is above 10 p.p.m. Multi-element analyses are not possible by these methods, though they are by mass spectrometry, emission spectrometry and x-ray fluorescence spectrometry. However, the tungsten matrix leads to problems with all these methods [4].

Neutron activation analysis is one of the most sensitive methods available for the determination of trace impurities in tungsten. Unfortunately, because of the high reaction cross-section of ^{186}W, the matrix becomes highly radioactive during thermal neutron irradiation, and it is essential to separate [5, 6] the interfering radionuclide ^{187}W from the radioactive impurities. Alternatively, ^{187}W ($t_{1/2}$ = 23.8 h) can be allowed to decay, but then only those impurities yielding very long-lived isotopes such as Sc, Cr, Fe, Co, Zn, Se, Ag, Eu, Hf and Ta can be determined [7, 8], and the procedure is time-consuming. There is no single "ideal" analytical method, and a combination of many methods is required to develop sensitive and reliable procedures. Activation analysis by charged particles should be very useful in this respect.

The application of charged particle activation for the determination of light and heavy elements has been described by several workers [9—13]. Protons, deuterons, ^{3}He and ^{4}He particles are commonly used for activation analysis of light elements; as first pointed out by Markowitz and Mahony [14] ^{3}He particles have analytically useful reaction cross-sections even at relatively low kinetic energies. ^{3}He-activation analysis has been used advantageously for light elements [15] and as a competing method for other elements [16—18]. The present paper reports ^{3}He activation for the non-destructive determination of trace elements in a tungsten matrix.

Principle of the method

According to Ricci and Hahn [19] a comparator method may be applied to charged particle activation analysis. The unknown amount of element U in the sample is calculated by

$$n_{U,x} = n_{U,s} \frac{I_s R_s}{I_x R_x} \frac{a_x}{a_s} \frac{[1 - \exp(-\lambda t_{B,s})]}{[1 - \exp(-\lambda t_{B,x})]} \quad (1)$$

where $n_{U,x}$ is the number of atoms U per g of sample; $n_{U,s}$ is the number of atoms U per g of standard; I_s/I_x is the ratio of the beam currents applied during irradiation of standard and sample; R_s and R_x are the ranges of the particles in standard and sample at the appropriate energy used for irradiation; a_s and a_x are the activities of standard and sample for a radionuclide formed from the element under study; λ is the decay constant of the radionuclide; and $t_{B,s}$ and $t_{B,x}$ are the irradiation times for the standard and the sample.

Equation (1) holds [19] with an accuracy of ± 8% from $Z = 4$ to $Z = 95$ provided that the energy of the particle beam is known. The comparator method requires "infinitely thick samples", which means that they must be thicker than the range of the irradiating particles. In the analyses described here, tungsten foils were used as samples, and foils of the elements to be determined were used as standards. The standards were irradiated for shorter periods and with lower beam currents to obtain decay rates comparable to those of the impurities in the samples.

EXPERIMENTAL

Sample and standard preparation

High-purity foils of tungsten and of the elements to be determined were cut to about 20 × 20 × 0.5 mm. The samples were cleaned before irradiation with a 1:1 mixture of 14 M nitric and 40% hydrofluoric acids. After cleaning and before being mounted on the target-holder, the samples and standards were stored in clean polythene bags.

Irradiation and counting

The irradiations were carried out in the internal beam (beam diameter, ca. 2 mm) of the isochronous cyclotron JULIC at the Kernforschungsanlage, Jülich. The beam energy at the irradiation position was 14 MeV. The samples were irradiated at a current of 5 μA for periods of 0.5—3 h; the standards were irradiated at a current of 50—200 nA for periods of 15—30 min. The short irradiation period of 0.5 h for the samples was used to measure the V and Ni impurities.

Standards and samples were irradiated separately by mounting them on the water-cooled target holder. The radius of the orbit at which the sample or standard has to be introduced and for which the ion beam has 14 MeV, was kept the same for all irradiations made on the same day. For irradiations made on different days, a new value for the radius which would give the same energy could be established because the energy available on the respective days in the outermost orbit, whose radius is known from the machine parameters, was known.

Experience showed that with the present machine currents in the range 50 nA—5 μA could be reproduced without difficulty. As a check, the thick target yields for some of the standards were measured periodically. Short irradiations of the order of 1—2 min for the standards were purposely avoided, to minimize the possible errors that might arise from occasional fluctuations of the order of a few seconds, in beam currents. A current integrator was not available.

After irradiation, the samples and standards were measured with a γ-ray spectrometer, consisting of a Canberra Ge(Li) detector (resolution, 3.1 KeV at 1332 KeV; detection efficiency, 3.8% relative to a 3 × 3-in NaI(Tl) detector for 662-KeV photons) and a 4096-channel pulse-height analyzer (Nuclear Data Inc.). The γ-spectra were evaluated with the programme ND 411077, which provided an output of γ-ray energies and peak areas.

Evaluation

The amount $m_{U,x}$ of the element U per g of sample was calculated from eqn. (1). Since $n_{U,x} : n_{U,s} = m_{U,x} : m_{U,s}$ where $m_{U,s} = 1$, the concentration of element U in $\mu g\ g^{-1}$ of sample may be obtained directly from

$$m_{U,x} = 10^6 \frac{I_s R_s}{I_x R_x} \frac{a_x}{a_s} \frac{[1 - \exp(-\lambda t_{B,s})]}{[1 - \exp(-\lambda t_{B,x})]} \frac{e^{-\lambda t_{D,s}}}{e^{-\lambda t_{D,x}}} \qquad (2)$$

For eqn. (2), the beam currents, I_s and I_x, were measured directly. The ranges R_s and R_x were taken from the literature [20, 21]; a_s and a_x are the peak areas divided by the counting time (live time) used for the measurement of the standard and the sample; $t_{B,s}$ and $t_{B,x}$ are the irradiation periods; and $t_{D,s}$ and $t_{D,x}$ are the waiting periods between the end of irradiation and the midpoint of the measuring time for the standard and sample.

RESULTS AND DISCUSSION

The γ-ray spectrum of an irradiated tungsten sample is shown in Fig. 1. Besides the γ-lines of the impurities, the spectrum shows the radionuclides ^{183}Os, ^{184}Re and ^{187}W, which are obviously formed by reactions on the matrix itself under the present irradiation conditions. The nuclear reactions giving rise to these nuclides are listed in Table 1.

The Coulomb barrier for reactions between ^{3}He and tungsten nuclei is about 21 MeV. Thus, with particle energies of 14 MeV, the reactions observed on the matrix are due to tunnelling. Moreover, neutrons are created by (^{3}He,n), (^{3}He,2n) etc. reactions on the matrix and also the impurities in the matrix. The possibility of these neutrons giving rise to (n,γ) reactions on the matrix cannot be fully excluded. However, the contribution by these neutron-induced reactions is assumed to be negligible since the total number of neutrons is very small and they must be moderated before they can undergo a reaction like ^{186}W (n,γ) ^{187}W. Some comparative tests with 14-MeV and 25-MeV ^{3}He particles indicated that the above assumption was correct.

The main nuclear reactions used for the identification and determination of the impurity elements are listed in Table 2. The primary interfering reactions are listed in Table 3. All the Q-values, half-lives and γ-ray intensities are taken from the literature [22, 23]. Table 4 shows the mean values, including the standard deviation from the mean, of the experimentally determined concentration of the trace elements.

Besides nuclear interferences, γ-ray interferences must be considered if different nuclides emit γ-rays of nearly the same energy. In many cases, they can be avoided or minimized by the choice of irradiation and decay periods. The nuclear and γ-ray interferences encountered in the measurement of different trace elements and their method of elimination are discussed below.

It may be noted that chromium, a common impurity in tungsten, could not be determined, as the useful nuclide ^{53g}Fe [from the ^{52}Cr(^{3}He,2n) ^{53g}Fe reaction] has a half-life of only 8.5 min, which is too short for the sample transport facilities used here at present.

Titanium

Titanium as an impurity was detected through the reaction ^{48}Ti(^{3}He,2n)^{49}Cr but because of its low concentration and the high background in the spectrum, an accurate measurement of the 0.153-MeV γ-line of ^{49}Cr could not be made.

Vanadium

Vanadium can be determined by the isomeric nuclides ^{52m}Mn and ^{52g}Mn. With short irradiation times, ^{52m}Mn allows a more sensitive determination. The γ-ray interference caused by the 1.434-MeV line of ^{52g}Mn on ^{52m}Mn

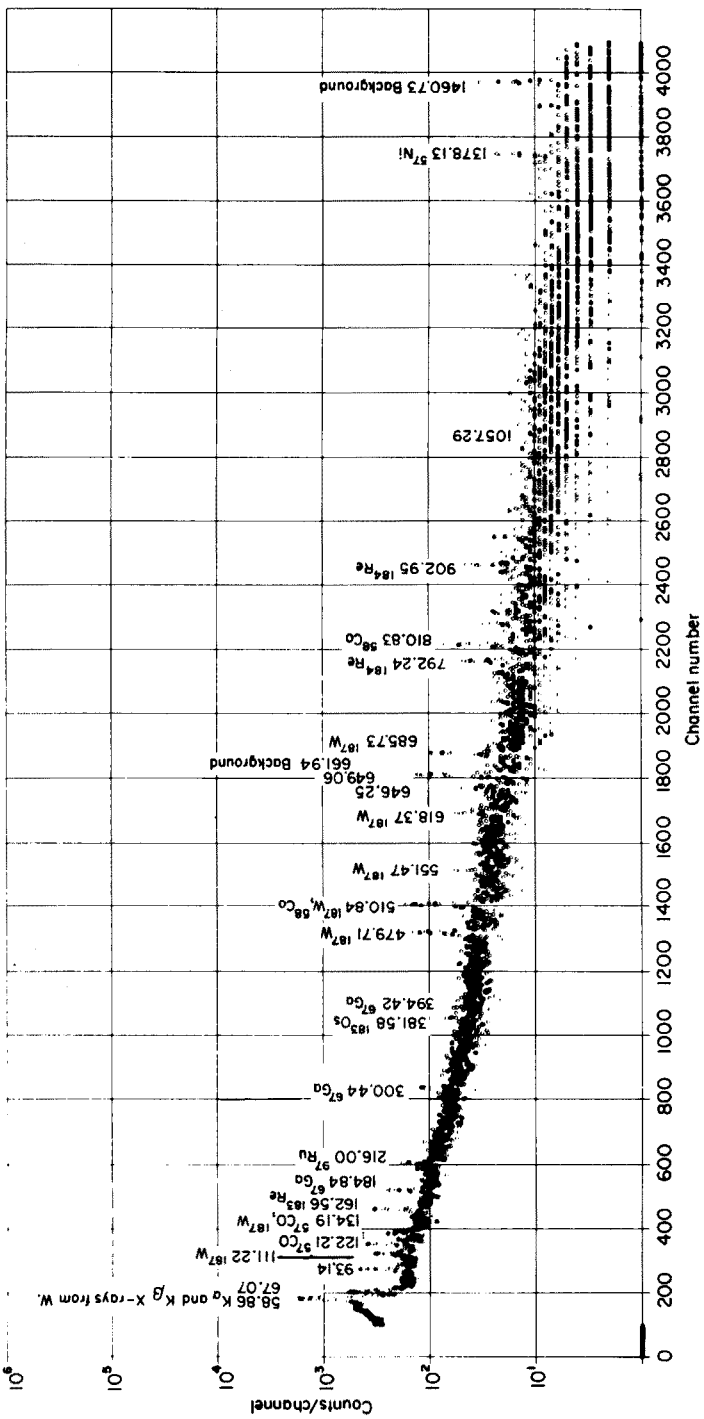

Fig. 1. γ-Ray spectrum of a tungsten sample irradiated with ^{3}He ions at 14-MeV. Irradiation conditions: current, 5 μA; time, 3 h. Start of measurement, 94 h after the end of irradiation. Time of measurement, 15 h.

TABLE 1

Production of radionuclides on tungsten matrix by irradiation with 14-MeV ^{3}He particles

Isotope	Percentage abundance	Nuclear reaction	Q-value (MeV)	Half-life	Main γ-energies (MeV (absolute intensities given in percentage within brackets)
^{182}W	26.3	^{182}W(^{3}He,p)^{184g}Re	+2.3	38.0 d	0.111(17), 0.792(36) 0.894(16), 0.903(36)
		^{182}W(^{3}He,2n)^{183m,g}Os	−6.5	10.0 h 14.0 h	1.102(34), 1.108(15) 0.114(24), 0.168(10) 0.382(87)
^{183}W	14.3	^{183}W(^{3}He,3n)^{183m,g}Os	−3.4	10.0 h 14.0 h	1.102(34), 1.108(15) 0.114(24), 0.168(10) 0.382(87)
^{184}W	30.7	^{184}W(^{3}He,p2n)^{184g}Re	−11.3	38.0 d	0.111(17), 0.792(36) 0.894(16), 0.903(36)
^{186}W	28.6	^{186}W(^{3}He,2p)^{187}W	−2.3	24.0 h	0.134(10), 0.479(26) 0.685(32)

TABLE 2

Identification of trace elements of interest

Element	Principal nuclear reactions useful for identification	Isotope abundance (%)	Q-value (MeV)	Half-life	Major γ-rays (MeV) (absolute intensities indicated within bracket
V	^{51}V(^{3}He,2n)^{52m}Mn	99.75	−2.7	21.3 m	0.511(19.3), 1.434(100)
	^{51}V(^{3}He,2n)^{52g}Mn	99.75	−2.7	5.6 d	0.511(56), 0.744(85) 0.935(93), 1.434(100)
Fe	^{56}Fe(^{3}He,pn)^{57}Co	91.7	−1.7	270.0 d	0.122(85), 0.136(10)
	^{56}Fe(^{3}He,p)^{58}Co	91.7	+6.9	71.3 d	0.511(30), 0.810(99)
Ni	^{60}Ni(^{3}He,pn)^{61}Cu	26.42	−2.9	3.3 h	0.283(13), 0.511(120)
Zn	^{66}Zn(^{3}He,pn)^{67}Ga	27.8	−2.4	78.1 h	0.093(37), 0.184(20) 0.300(15)
Mo	^{95}Mo(^{3}He,n)^{97}Ru	15.9	+5.1	2.88 d	0.215(91), 0.324(11)

depends on the irradiation and decay times. It was estimated from the intensity of the 0.935-MeV and 0.744-MeV γ-lines of ^{52g}Mn, and found to be less than 1% for short irradiation periods. Nuclear interference is observed from chromium. The level of interference is $<2\%$ for ^{52m}Mn and $<0.1\%$ for ^{52g}Mn when equal concentrations of Cr and V are present.

TABLE 3

Primary interference reactions

Element sought	Principal nuclear reaction	Interfering reaction	For interfering reaction	
			Q-value (MeV)	Isotope abundance (%)
V	$^{51}V(^{3}He,2n)^{52m,g}Mn$	$^{52}Cr(^{3}He,p2n)^{52m,g}Mn$	−13.2	83.79
Fe	$^{56}Fe(^{3}He,pn)^{57}Co$	$^{55}Mn(^{3}He,n)^{57}Co$	+8.5	100
		$^{59}Co(^{3}He,\alpha n)^{57}Co$	+1.5	100
	$^{56}Fe(^{3}He,p)^{58}Co$	$^{59}Co(^{3}He,\alpha)^{58}Co$	+10.1	100
Ni	$^{60}Ni(^{3}He,pn)^{61}Cu$	$^{63}Cu(^{3}He,\alpha n)^{61}Cu$	+1.5	69.1
		$^{59}Co(^{3}He,n)^{61}Cu$	+6.6	100
Zn	$^{66}Zn(^{3}He,pn)^{67}Ga$	$^{65}Cu(^{3}He,n)^{67}Ga$	+6.5	30.9
		$^{69}Ga(^{3}He,\alpha n)^{67}Ga$	+2.0	60
Mo	$^{95}Mo(^{3}He,n)^{97}Ru$	$^{98}Ru(^{3}He,\alpha)^{97}Ru$	+10.3	1.9

TABLE 4

Determination of impurities in tungsten

Element	No. of detns.	Average value (p.p.m.)
V	2	$<0.26 \pm 0.16$
Fe	3	1.3 ± 0.1
Ni	3	1.3 ± 0.2
Zn	2	0.92 ± 0.13
Mo	3	4.1 ± 0.26

Iron

For the determination of iron, either the 0.122-MeV γ-line of ^{57}Co or the 0.811-MeV γ-line of ^{58}Co can be used, but the former nuclide provides better sensitivity. Moreover, when ^{58}Co is used for the identification, the nuclear interference caused by cobalt is 20% for equal concentrations of Fe and Co. Because of the long half-life of ^{57}Co ($t_{1/2}$ = 270 d) the measurement can be started conveniently after the Compton continuum caused by many short-lived 0.511-MeV emitters has reduced to a negligible level. The nuclear interferences caused by Mn and Co on ^{57}Co were found experimentally to be <1% and 8%, respectively, when all three elements were present at equal concentration levels. The γ-ray interference caused by the 0.121-MeV γ-line (16.5%) of ^{75}Se can be checked by looking for its strong 0.264-MeV (58%) and 0.279-MeV (25%) lines.

Nickel

Nickel is identified by the ^{61}Cu line. There are nuclear interferences from Cu and Co, and the interference levels are 12% and 10%, respectively, for equal concentrations of Ni, Cu and Co. The γ-ray interference possible

from the 0.281-MeV γ-line of ^{182}Re from the matrix can be checked by looking for its other intense lines; their absence indicated the absence of this interference in the present work.

Another nuclear reaction possible for the identification of nickel is ^{58}Ni(^{3}He,p)^{60}Cu. There is a nuclear interference of <1% from copper but nearly 100% from cobalt for equal concentrations of Ni, Cu and Co. For this reason, the nuclide ^{60}Cu is not used.

Zinc

For the determination of zinc, the 0.300-MeV γ-line of ^{67}Ga is used. This nuclide has nuclear interferences from Cu and Ga. For copper the interference level was determined experimentally, and for gallium it was computed theoretically; the levels were found to be <5% and 8%, respectively, for equal concentrations of Zn, Cu and Ga, so that their influence can be neglected. There is a possible γ-ray interference caused by ^{77}Br through the reaction ^{75}As(^{3}He,n)^{77}Br, which has a γ-line intensity of 4.2%, but the absence of its strong 0.521-MeV line (23%) shows the absence of this interference. There is also a possible interference from the matrix itself from the 0.299-MeV (3.1%) γ-line of ^{182}Re but the absence of any of its strong lines 0.178 MeV (18%), 0.229 MeV (25%), 0.256 MeV (13%) etc., indicated the absence of this nuclide.

Molybdenum

In the determination of molybdenum, the 0.215-MeV γ-line (91%) of ^{97}Ru is used. ^{98}Ru with a natural abundance of 1.9% can cause nuclear interference, but the theoretically calculated level of interference is less than 1% when both Mo and Ru are present at the same concentration levels. The matrix can interfere by the formation of ^{184m}Re which emits 0.216-MeV γ-rays with 100% relative intensity, but the absence of its other intense lines, e.g. 0.317 MeV (71%), 0.384 MeV (36%), 0.536 MeV (43%) and 0.920 MeV (88%), indicated the absence of this nuclide.

The authors thank the operating staff of the JULIC cyclotron for kind cooperation.

REFERENCES

1 K. C. Li and C. Y. Wang, Tungsten, Reinhold, New York, 1955.
2 C. J. Smithells, Tungsten, its Metallurgy, Properties and Applications, Chemical Publishing Co., New York, 1953.
3 N. B. Hannay, in G. H. Morrison (Ed.), Trace Analysis, Physical Methods, Interscience-Wiley, New York, 1965, p. 43.
4 G. Ehrlich, H. G. Döge, A. Drescher, K. Friedrich, and R. Gerbatsch, Spurenanalyse in hochschmelzenden Metallen, VEB Deutscher Verlag für Grundstoffindustrie, Leipzig, 1970.
5 J. F. Cosgrove and G. H. Morrison, Anal. Chem., 29 (1957) 1017.
6 A. A. Samadi, P. Ailloud and M. Fedoroff, Anal. Chem., 47 (1975) 1847.

7 G. Pinte, Rapport CEA-R-3267, Saclay, 1967.
8 A. Z. Nagy, A. Csöke, L. Pocs, E. Szabo, B. Vorsatz, S. Cseh and S. Saly, J. Radioanal. Chem., 11 (1972) 231.
9 C. Vandecasteele and J. Hoste, J. Radioanal. Chem., 27 (1975) 465.
10 D. L. Swindle, L. R. Novak and E. A. Schweikert, Anal. Chem., 46 (1974) 655.
11 H. Petri and C. S. Sastri, Z. Anal. Chem., 277 (1975) 25.
12 J. N. Barrandon, J. L. Debrun, A. Kohn and R. H. Spear, Nucl. Instrum. Methods, 127 (1975) 269.
13 V. Krivan, J. Radioanal. Chem., 26 (1975) 151.
14 S. S. Markowitz and J. D. Mahony, Anal. Chem., 34 (1962) 329.
15 Ch. Engelmann, J. Radioanal. Chem., 7 (1971) 89.
16 H. Petri and C. S. Sastri, Radiochem. Radioanal. Letters, 21 (1975) 225.
17 B. Parsa and S. S. Markowitz, Anal. Chem., 46 (1974) 186.
18 E. Ricci and R. L. Hahn, Anal. Chem., 39 (1967) 794.
19 E. Ricci and R. L. Hahn, Anal. Chem., 37 (1965) 742.
20 C. F. Williamson, J. P. Boujot and J. Picard, Tables of range and stopping power of chemical elements for charged particles of energy 0.05 to 500 MeV. Rapport CEA-R-3042, Saclay, 1966
21 A. C. Demildt, UCRL-10647 (1963).
22 K. A. Keller, J. Lange and H. Münzel, *Q*-values for nuclear reactions, Landolt Börnstein, New Series, Vol. 5/a, Springer Verlag, Berlin 1973.
23 G. Erdtmann and W. Soyka, Die γ-Linien der Radionuklide, JÜL-1003-AC, Jülich, 1973.

Analytica Chimica Acta, 89 (1977) 151—156

THE DETERMINATION OF TRACES OF ARSENIC IN WATER BY ARSINE GENERATION AND RADIOMETRIC ANALYSIS

HENG-FATT GIAN and SOO-LOONG TONG

Department of Chemistry, University of Malaya, Kuala Lumpur (Malaysia)

(Received 19th July 1976)

SUMMARY

A tracer method based on the concentration-dependent distribution principle has been developed for trace arsenic determination. Standard and sample arsenic solutions labelled with a fixed amount of radioactive arsenic-74 are isolated by arsine generation with sodium borohydride followed by absorption in potassium iodide—iodine solution. The separated arsenic(III) is then extracted with equal but limited amounts of zinc diethyldithiocarbamate in chloroform and determined radiometrically by the concentration-dependent distribution principle. The method is practically free from interferences, and arsenic in aqueous solution as low as 0.5 ng ml^{-1} can be determined. Results for natural and environmental water samples are compared with results obtained by the arsine generation-atomic absorption technique.

Most analytical methods for the determination of traces of arsenic are based on classical colorimetric methods, neutron activation analysis, and atomic absorption spectrophotometry. Colorimetry, though sensitive, is tedious and subject to serious interferences [1]. Neutron activation analysis [2, 3] gives very much higher sensitivity but access to nuclear reactors is limited and the cost of equipment is high. In recent years, these methods have given way to atomic absorption spectrophotometry (a.a.s.). Although flame a.a.s. is inadequate in detection capability and suffers from matrix and flame interferences, utilization of the arsine generation technique in conjunction with flame a.a.s. [4, 5] has eliminated the interference problems and improved the detection limit. Nonetheless, the reproducibility of the latter technique depends largely on the analyst's manipulative skill. The precision is poor for arsenic in the lower p.p.b. range as a result of the relatively high flame background absorptions [6].

The tracer method based on the concentration-dependent distribution principle [7—9] was developed as an extension of substoichiometric isotope dilution analysis (s.i.d.a.) for trace element determinations; it offers detection sensitivities comparable with the neutron activation method and uses simple radiocounting equipment and low-level radioactive tracers. However, no detailed investigation on the application of this technique to trace arsenic analysis has been reported. Application of the related s.i.d.a.

method to trace arsenic determination was limited by the fact that no substoichiometric separation system which would give satisfactory sensitivity and specificity has been found suitable for arsenic. The solvent extraction method with a substoichiometric amount of zinc diethyldithiocarbamate ($Zn(DDC)_2$) [10] was unable to fulfil the two requirements. Attempts to remove the interfering elements by a pre-separation extraction with sodium diethyldithiocarbamate while keeping the arsenic as As(V), originally proposed for neutron activation analysis of trace arsenic [2], is too complicated and time-consuming. This paper describes a very sensitive and interference-free approach for the determination of arsenic by the radiometric concentration-dependent distribution principle. A simple and rapid procedure for the pre-separation and concentration of the ^{74}As-labelled arsenic from aqueous samples by arsine generation is employed prior to the radiometric determination by solvent extraction with $Zn(DDC)_2$.

EXPERIMENTAL

Apparatus

Scintillation counter. A 50 × 50-mm NaI(Tl) well-type detector, in conjunction with an ORTEC NIM series single-channel analyzer, was used. Counting was carried out over the range 50—700 keV; at least 10^4 counts were accumulated in each case.

A Varian model-1200 atomic absorption spectrophotometer, equipped with an arsine generation kit, was used for the comparative study.

Reagents

Radioactive arsenic-74 of specific activity >1 mCi μg^{-1} was purchased (Amersham Radiochemical Centre, U.K.) as arsenic acid in 0.04 M HCl. All reagents were of analytical reagent grade. Deionized-distilled water was used throughout.

Stock arsenic(III) solution. (0.100 mg As ml^{-1}). Dissolve 132 mg of arsenic trioxide in 2 ml of 1 M sodium hydroxide solution; dilute to 1 l with water after neutralization with 1 M HCl. Working solutions with and without ^{74}As tracer were prepared by appropriate dilution of stock solution and addition of the ^{74}As isotope of very high specific activity.

Sodium borohydride solution. Dissolve 5 g of $NaBH_4$ in 100 ml of water containing 0.1% NaOH. The solution for the absorption of arsine contained 0.2 g of I_2, 0.3 g of KI and 1 g of $NaHCO_3$ in 100 ml of water.

Stock zinc diethyldithiocarbamate ($2.88 \cdot 10^{-3}$ M $Zn(DDC)_2$). Mix two 50-ml portions of solutions containing 0.130 g of sodium diethyldithiocarbamate and 0.260 g of $ZnSO_4 \cdot 7\,H_2O$ each and extract the resulting precipitate of $Zn(DDC)_2$ into 100 ml of chloroform. The solution is stable for at least 14 d when kept in a dark bottle in a refrigerator. Prepare working $Zn(DDC)_2$ solutions before use by appropriate dilution of the stock solution.

Procedure

Arsine generation. Calibration standards and sample solutions in the range of 25—500 ml in 2 M HCl are used. Tracer solutions of ^{74}As, containing equal amounts of arsenic (1 or 2 μg) and a suitable level of radioactivity, are added to the reaction flask (a conical flask with sidearm) with a 0.1-ml precision micropipette before the addition of hydride generation reagent. A cold-trap (a coil of 0.4-mm i.d. glass tubing of 4 turns immersed in small chips of dry ice in a Dewar) serves to remove volatile interfering elements such as mercury, antimony and bismuth formed in the process of arsine generation. A scrubber (essentially an ion-exchange column tube with a glass sinter) containing 8 ml of KI—I_2 solution is used to absorb the arsine generated. The sodium borohydride solution is added through the stopper of the conical flask by a long-needle syringe with its tip immersed in the solution. The solution is kept stirred and the injection rate is controlled so that gas generation does not become too excessive. Approximately 10 ml of the sodium borohydroxide solution are required. When the reaction is complete, 2 ml of the absorber solution are removed by pipette and counted.

Radiometric analysis. The KI—I_2 absorber solution containing pure arsenic is transferred to a 25-ml stoppered test tube and made up to 3.5 M in H_2SO_4, final volume 12 ml. The solution is treated with 1 ml of 7% ascorbic acid and placed in a water bath at 60—70°C for 30 min with occasional swirling to ensure complete reduction to the As(III) state. After cooling, 5 ml of $4 \cdot 10^{-6}$ M $Zn(DDC)_2$ in chloroform are used if 1 μg of ^{74}As has been added to the calibration standard and sample solutions initially; $8 \cdot 10^{-6}$ M $Zn(DDC)_2$ should be employed for 2 μg of ^{74}As tracer. Extraction is completed in 15 min with an electric shaker. Exactly 4 ml of the organic extract are pipetted into a small vial suitable for counting. Samples are normally counted for 3 min. A calibration curve is obtained by plotting the ratios of the extracted activities to the total activity added against the amount of stable arsenic used in the calibration standards.

Analysis of water samples

Water samples were taken in 2-l bottles. After addition of sufficient HCl to render the solution ca. 2 M in HCl, the samples were filtered through Whatman No. 1 filter paper to remove suspended matter.

Exactly 200 ml of the sample were measured into the arsine generation flask and ^{74}As-labelled solutions, each containing 1 μg of arsenic, were added and mixed thoroughly. Calibration standards were prepared from equal volumes of distilled-deionized water containing the same amounts of ^{74}As tracer (1 μg) but with concentrations of stable arsenic ranging from 0.1 to 10 μg. Arsine generation and radiometric analysis were carried out as described above.

A number of water samples were also analyzed by the arsine generation-atomic absorption technique with a Varian model-1200 atomic absorption spectrometer. The samples were treated with potassium iodide—ascorbic acid in a water-bath (60—70°C) prior to the determination.

RESULTS AND DISCUSSION

Arsine generation from the reaction flask with $NaBH_4$—HCl showed no significant losses on passing through the cold-trap at about −60°C. The arsine scrubber contained only an optimum amount of KI—I_2 solution to avoid iodide interference from an excess of iodide during the solvent extraction at a later stage. The percentage recoveries of arsenic from the scrubber ranged from 96.7% to 99.6% for total arsenic contents of 1—20 μg and total volumes of sample solutions of 25—250 ml with 5—12 ml of borohydride.

Volatilization of the analyte by the present method eliminates interferences from the sample matrix constituents except for a few volatile elements such as mercury, antimony and bismuth, which may be evolved simultaneously under the experimental conditions. Radiometric analysis of arsenic by solvent extraction with $Zn(DDC)_2$ following the separation would not be specific if these elements were present [11]. The cold-trap was introduced to overcome this problem; up to 20 μg of each of these elements could be removed effectively.

The sensitivity of radiometric determination of arsenic by the s.i.d.a. method with a substoichiometric amount of $Zn(DDC)_2$ in chloroform to extract arsenic(III) is restricted by the stability constant of the $As(DDC)_3$ complex. The method reported by Arnold et al. [10] was applicable only to the determination of arsenic at levels above 20 μg. The extraction at a lower concentration range for a series of solutions containing 0.2 to 20 μg of arsenic with equal amounts of $Zn(DDC)_2$ corresponding to the total extraction of 2 μg of arsenic as $As(DDC)_3$, has been studied. The experimental results (Curve 1, Fig. 1) show marked deviations from the theoretical extraction of stoichiometric equivalents of arsenic as $As(DDC)_3$ (Curve 2) which forms the basis of the s.i.d.a. principle. When the arsenic present was deficient or just slightly in excess, less than the stoichiometric equivalents of arsenic were extracted. This is to be expected since the stability constant of the complex is not favorable at very low concentrations. However, for arsenic in more than two-fold excess, the amounts extracted exceeded the stoichiometric equivalents anticipated. Evidently, the mixed-ligand complexes of arsenic (e.g. $As(DDC)_2I$ and $As(DDC)I_2$) were also being extracted.

Under such circumstances, the present extraction scheme may still be employed in accordance with the concentration-dependent distribution principle [7—9] provided that the distribution of the element between the two phases is reproducible. This requirement is satisfied under the present experimental conditions. Results from repetitive extractions of a series of solutions containing 2 μg of ^{74}As tracer each and additional stable arsenic (0.2—20 μg) with 5 ml of $8 \cdot 10^{-6}$ M $Zn(DDC)_2$ showed excellent reproducibility. A linear calibration curve is obtained by plotting the ratio of the total activity added to the extracted activity versus the amount of stable

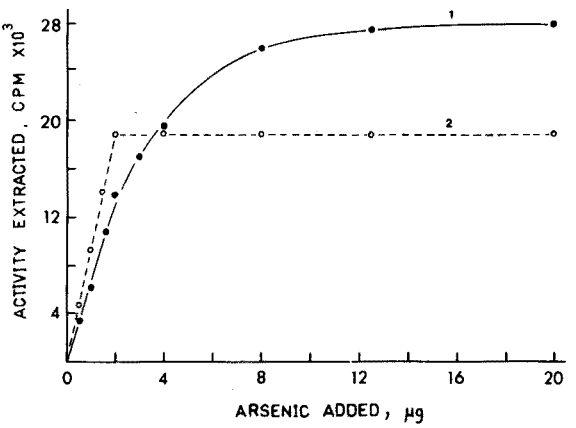

Fig. 1. Extraction of arsenic(III) in 12 ml of 3.5 M H_2SO_4 with 5 ml of $8 \cdot 10^{-6}$ M $Zn(DDC)_2$ in chloroform. Specific activity of arsenic added: 9500 c.p.m./μg As. 1. Experimental curve. 2. Theoretical curve assuming stoichiometric extraction.

arsenic used (Fig. 2). The precisions around 0.2 μg and 20 μg were about 8% in terms of the standard deviations from a series of repetitive determinations. Better precision was obtained (3—5%) in the optimum concentration range (0.4—16 μg As). It should be noted that the present method offers a much wider range of working concentrations than other radiometric tracer methods.

Extraction of less than 1 μg of arsenic under the present conditions with $Zn(DDC)_2$ shows poor reproducibility. The limit of the present extraction system for arsenic determination with 1 μg of ^{74}As tracer is about 0.1 μg, with

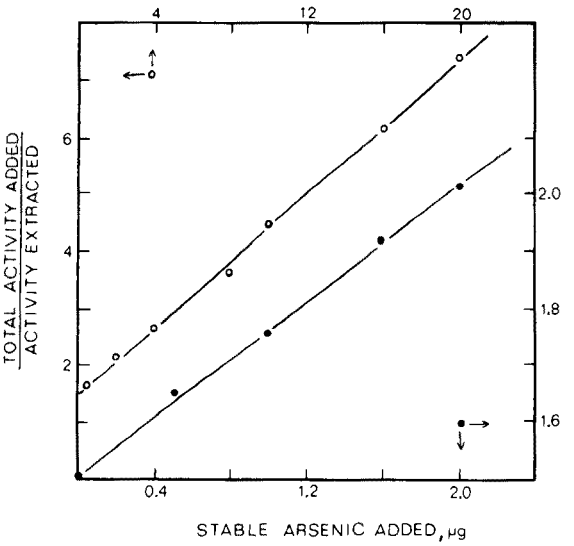

Fig. 2. Typical calibration graphs for radiometric determination of arsenic with 2 μg of ^{74}As tracer and 5 ml of $8 \cdot 10^{-6}$ M $Zn(DDC)_2$ in chloroform.

standard deviation of less than 10%. The overall sensitivity of detection by the method combining arsine generation and radiometric determination is ca. 0.5 ng ml^{-1} of arsenic in aqueous solution.

Results from the application of the present method to some natural and environmental water samples are presented in Table 1. High levels of arsenic were found in places, possibly from uncontrolled effluent discharges and the extensive use of sodium arsenite as a weed-killer before a ban was introduced recently. The standard deviation for triplicate determinations of arsenic in the lower p.p.b. region was about 5% (about 2% for higher ranges). A number of samples was also analyzed by the arsine-generation-atomic absorption technique with a nitrogen-entrained air—hydrogen flame. The two sets of results (Table 1) show excellent agreement. Special precautions to ensure the complete conversion of all arsenic to the As(III) state were necessary: recorder tracings showed that the oxidation state of the arsenic critically affects the absorption peak-height response.

TABLE 1

Amounts of arsenic in water samples

Sample	Arsenic $\mu g\ l^{-1}$	
	Present method	Atomic absorption method
Tap water	5.2 ± 0.2	4.5 ± 1.0
Creek A	14.4 ± 0.8	17.1 ± 1.6
Creek B	152 ± 5	140 ± 6
Creek C	49.4 ± 1.0	47.3 ± 4
River K at point 1	55.2 ± 2.2	60.2 ± 2.0
at point 2	69.7 ± 2.2	71.3 ± 3.1
at point 3	74.7 ± 1.0	80.8 ± 3.9
at point 4	120 ± 3	117 ± 8.5

The authors gratefully acknowledge the support of the University of Malaya.

REFERENCES

1 E. B. Snell, Colorimetric Determination of Trace Metals, 3rd edn., Interscience, New York, 1959.
2 A. Zeman, J. Růžička, J. Stary and E. Kleckova, Talanta, 11 (1964) 1143.
3 A. P. Grimanis and A. G. Souliotis, Analyst (London), 92 (1967) 549.
4 W. Holak, Anal. Chem., 41 (1969) 1712.
5 F. J. Fernandez, At. Absorpt. Newsl., 12 (1973) 93.
6 F. J. Schmidt, J. L. Royer, and S. M. Miur, Anal. Lett., 8 (1975) 173.
7 M. Kyrs, Anal. Chim. Acta, 33 (1965) 245.
8 J. Růžička and J. Stary, Substoichiometry in Radiochemical Analysis, Pergamon Pres Oxford, 1968, p. 50.
9 J. Růžička and C. G. Lamm, Talanta, 15 (1968) 689.
10 A. Arnold, S. Davis and A. L. Jordan, Analyst (London), 94 (1969) 664.
11 J. Stary, Solvent Extraction of Metal Chelates, Pergamon Press, Oxford, 1964.

Analytica Chimica Acta, 89 (1977) 157—166

SPECTROPHOTOMETRIC DETERMINATION OF CATECHOL, EPINEPHRINE, DOPA, DOPAMINE AND OTHER AROMATIC VIC-DIOLS

DENNIS W. BARNUM

Department of Chemistry, Portland State University, Portland, Oregon, 97207 (U.S.A.)

(Received 19th July 1976)

SUMMARY

Aromatic vic-diols such as catechols, epinephrine, norepinephrine, dopa, and dopamine can be determined spectrophotometrically by nitration with sodium nitrite in slightly acidic solution. The method is selective for aromatic vic-diols in which either the 3- or 4-position is unsubstituted and these positions are not sterically blocked. Tungstate or molybdate ions increase the color intensity, probably by stabilizing the nitrated phenol by complex formation. Molybdate is more effective than tungstate. For most diphenols the optimum pH is around 5.0—5.5 (acetate buffer) but this depends on the diphenol as well as on the particular buffer system. The optimum time for nitration (2—30 min) also depends on the diphenol. After nitration for the optimum duration, the solution is made basic; an absorption band appears at about 500 nm with a molar absorptivity of ca. 10^4 l mol^{-1} cm^{-1}. The system follows Beer's law provided that molybdate ion is present and both the pH and reaction time are optimized. The minimum detectable amount of diphenol is about 5 nmol, for an absorbance of 0.01 in a 1.00-cm cell. Phenol, hydroquinone, resorcinol, pyrogallol, phloroglucinol, guaiacol, and veratrole, do not interfere.

During studies of reactions between natural organic matter and minerals, a spectrophotometric method of analysis for aromatic vic-diols was sought. A method first used by Arnow [1] for the spectrophotometric estimation of 3,4-dihydroxyphenylalanine seemed promising: the unknown solution is treated with sodium nitrite and either sodium molybdate or sodium tungstate; when the solution is made basic, an intense red color is produced. Evans [2] used the method for the determination of catechol. Nair and Vaidyanathan [3] investigated the method further and showed that epinephrine, norepinephrine, and dopa also give the same red color. Recently, Spiegel and Christian [4] developed a semi-automated analysis for 3,4-dihydroxyphenylacetic acid in urine, using this method. Bhatia et al. [5] investigated the reaction for the detection of aromatic vic-diols on paper chromatograms and showed that many different diphenols give a red color.

In spite of these reports, common parameters in a spectrophotometric analysis such as optimum pH, time required for complete color development, optimum reagent concentrations, adherence to Beer's law, and stability of the color have not been established. Furthermore, the extent to which the method is selective for aromatic vic-diols, and whether other substances interfere, must also be known. The results of such a study are reported here.

EXPERIMENTAL

Chemicals

Sodium nitrite, sodium molybdate, sodium tungstate, and the components of buffer solutions were reagent grade, used without further purification.

Epinephrine and DL-dopa were sufficiently pure for use as received. Norepinephrine and dopamine were dried to constant weight in vacuum over P_2O_5. All other diphenols were purified by recrystallization or sublimation. The recrystallization of 3,4-dihydroxybenzaldehyde was done under a nitrogen atmosphere.

General procedure

After several preliminary experiments the following method was devised.

Reactions were carried out in an open 50-ml beaker (see below). A sample containing up to 2.0 μmol of aromatic vic-diol in 2.00 ml or aqueous solution was taken. Buffer solution (1.00 ml) was added, followed by 1.00 ml of a solution that was 2.0 M in sodium nitrite and 0.10 M in sodium molybdate the solution turned yellow within a few seconds. After the solution had stood for the prescribed length of time (usually 15—20 min), 1.00 ml of 6 M NaOH was added; a red color was produced.

For 500 nmol or less of diphenol the absorbance was measured directly. If more than 500 nmol of diphenol was present, the solution was transferred quantitatively to a 25-ml volumetric flask and diluted to the mark before measuring the absorbance.

Because 2.0 M sodium nitrite solution is slightly basic, the buffer solutions must be fairly concentrated to offset the influence of the nitrite. The buffers were prepared from 3.0 M sodium acetate by adding glacial acetic acid until the desired pH was obtained. Even so, the pH during nitration was always greater than the pH of the buffer. To achieve the desired pH, preliminary trials were required to find the correct buffer. All pH values in Figs. 1 and 2 and Table 1 were measured with a glass electrode after the diphenol, sodium nitrite, sodium molybdate and buffer, had been mixed, i.e. the pH of the actual reactant solution is recorded. The pH remains constant throughout the nitration reaction. The optimum pH and reaction time depends on the diphenol; the values are summarized in Table 1.

Reaction with 2,3-dihydroxypyridine

With 2,3-dihydroxypyridine the above method gives an undesired absorption band around 415 nm. The intensity of the band is erratic but, fortunately, it has only a very slight effect on the intensity of the 488-nm band. Thus, the above method can be used with only a slight decrease in accuracy.

However, the 415-nm band can be avoided by doing the nitration reaction in a more dilute solution of the diphenol. Thus, the total volume during

TABLE 1

Optimum reaction conditions for aromatic vic-diols

Aromatic vic-diol	pH	Reaction time (min)	λ_{max} (nm)	ϵ_{max} ($l\ mol^{-1}\ cm^{-1}$)
Catechol	5.2	30	503	$1.39 \cdot 10^4$
l-Epinephrine	4.2	1—40	502	$8.9 \cdot 10^3$
Norepinephrine	5.1	2—30	500	$1.07 \cdot 10^4$
DL-dopa; 3-(3,4-dihydroxyphenyl)-DL-alanine	5.1	2	498	$1.00 \cdot 10^4$
Dopamine; α-(3,4-dihydroxyphenyl)-β-aminoethane)	5.3	8—40	500	$1.11 \cdot 10^4$
3,4-Dihydroxyphenylacetic acid	5.2	20	493	$1.16 \cdot 10^4$
3,4-Dihydroxybenzoic acid	5.2	24	497	$1.25 \cdot 10^4$
3,4-Dihydroxybenzaldehyde	4.0	12—40	500[c]	$3.06 \cdot 10^3$
3,4-Dihydroxypropiophenone	4.7	18	505	$4.13 \cdot 10^3$
3,4-Dihydroxycinnamic acid	5.8	12	495	$3.87 \cdot 10^3$
Quercetin	6.1	32	500	$7.0 \cdot 10^3$
4-Nitrocatechol	—[a]	—[a]	512	$1.26 \cdot 10^4$
2,3-Dihydroxypyridine	5.35	20	488	ca. $6 \cdot 10^3$
Tiron; 4,5-Dihydroxy-*m*-benzenedisulfonic acid disodium salt	2.65	50[b]	496	$3.0 \cdot 10^3$
3,5-Di-tert-butylcatechol	6.6[d]	8	473	$1.7 \cdot 10^3$[d]

[a] 4-Nitrocatechol gives the red color simply by making the solution basic; reaction with sodium nitrite is unnecessary.
[b] There is no optimum reaction time up to 100 min but the rate of increase in absorbance at 496 nm is very slow after 50 min.
[c] A shoulder, not a maximum.
[d] Beer's law is obeyed only up to a concentration of $1.2 \cdot 10^{-4}$ M. Rapid deviation occurs at higher concentrations.

nitration was increased from 4.00 to 8.00 ml and the concentration of the nitrite—molybdate nitration reagent was increased to 4.0 M sodium nitrite and 0.05 M sodium molybdate.

RESULTS AND DISCUSSION

Evidence for nitration of the aromatic ring

The red color results from nitration of the aromatic ring, as illustrated below for catechol. Evidence for this reaction sequence is as follows. (1) The absorption spectrum of the red solution produced from catechol is the same as that of a basic solution of authentic 4-nitrocatechol. The wavelengths for catechol and 4-nitrocatechol in Table 1 do not agree because, as the reaction time increases from 2 min to its optimum at 30 min, λ_{max} shifts from 512 to 503 nm. This indicates that reactions other than the one shown above are taking place. (2) After reaction of catechol with sodium nitrite, 4-nitrocatechol was extracted with diethyl ether and identified by its i.r. absorption spectrum, its R_F value on paper, and a mixed melting

point with authentic 4-nitrocatechol. (3) Several other workers have reported rather easy nitration of aromatic rings by aqueous sodium nitrite at room temperature or at 0°C [6—14]. Nitroso derivatives are often isolated if the reaction is run under sufficiently mild conditions but the nitroso group is easily oxidized to a nitro group. (4) The red color is also produced in the absence of molybdate or tungstate. This eliminates any notion that the color is given by a coordination complex. (5) The isolation of 4-nitrocatechol and a small amount of 3-nitrocatechol from the reaction of catechol with potassium nitrate in sulfuric acid at room temperature has been reported [11, 12]. Frejka et al. [8], however, treated sodium nitrite with catechol in aqueous acetic acid at 0°C and obtained the sodium salt of tetranitrosocatechol. Under similar conditions, Frejka and Zika [7] obtained a mono- and a di-nitroso derivative from 3,4-dihydroxybenzenesulfonic acid: these studies were done in strong acid solution, whereas the present work was done at pH 3—6.

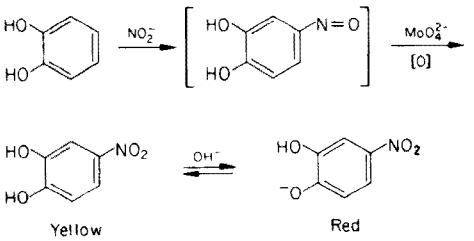

The reaction of salicyclic acid with aqueous sodium nitrite at 0°C gives *o*-nitrophenol and carbon dioxide [9, 10]. A similar decarboxylation was observed in the present work with 3,4-dihydroxybenzoic acid; the product was 4-nitrocatechol, which was extracted from the reaction mixture with diethyl ether and identified by two-dimensional chromatography on silica gel. Two other unidentified spots were obtained.

In view of these results for catechol and 3,4-dihydroxybenzoic acid, there are two possible color-forming reactions in the case of other diphenols. One possibility is that the substituent in the 4-position of the aromatic vic-diol is displaced by a nitro group, as occurs with 3,4-dihydroxybenzoic acid. If this were the case then epinephrine, norepinephrine dopa, dopamine, and 3,4-dihydroxyphenylacetic acid would all give 4-nitrocatechol, but this was not isolated from their reaction products. Thus, 3,4-dihydroxybenzoic acid is a unique case. In fact the nitro group simply adds to the ring by displacing a hydrogen atom, probably at the 5-position. This conclusion is supported by the observation that aromatic vic-diols in which the 4- and 5-positions are blocked, such as 2,3-dihydroxynaphthalene and tetrachlorocatechol, do not give an absorption band near 500 nm by this procedure. Also, diphenols such as tiron and 3,5-di-tert-butylcatechol, in which steric hindrance of nitration is expected, either do not give a color or the reaction is slow and the intensity is low.

Effect of pH on the nitration reaction

The rate of the nitration reaction, and the intensity of the red color produced when the solution is made basic, depends on pH. Figures 1 and 2 show the results for catechol, epinephrine, and 2,3-dihydroxypyridine. All the diphenols studied showed the same kind of double maximum pH dependence. Erratic results were sometimes obtained in the valley between the two maxima, as seen for catechol in Fig. 1.

The buffer also affects the pH-dependence. With quercetin, for example, the optimum pH is 6.1 for an acetate buffer but 5.5 for a pyridine buffer. For 2,3-dihydroxypyridine the difference between acetate and phosphate buffers can be seen in Fig. 1.

The pH-dependence shown for l-epinephrine in Fig. 2 suggests that the determination might also be done at pH 2.7. Indeed, Beer's law is followed when the nitration is done at this pH. In most cases however, a more intense color is developed at the higher pH maximum and the intensity is more reproducible.

The unusual affect of pH suggests either that two different reactions occur or that two different mechanisms operate. Hughes et al. [15] have studied the nitrosation of aromatic amines in detail and their results seem to be applicable here. They concluded that in acidic solutions the electrophile is the $HONOH^+$ ion, whereas in nearly neutral solutions it is the N_2O_3 species. They also observed catalysis by chloride, bromide, iodide, and acetate, which they attributed to general base catalysis. Thus, the double pH maxima observed here may be due to the two different electrophiles; the fact that the buffer influences the color development may be due to catalysis by one or more components of the buffer.

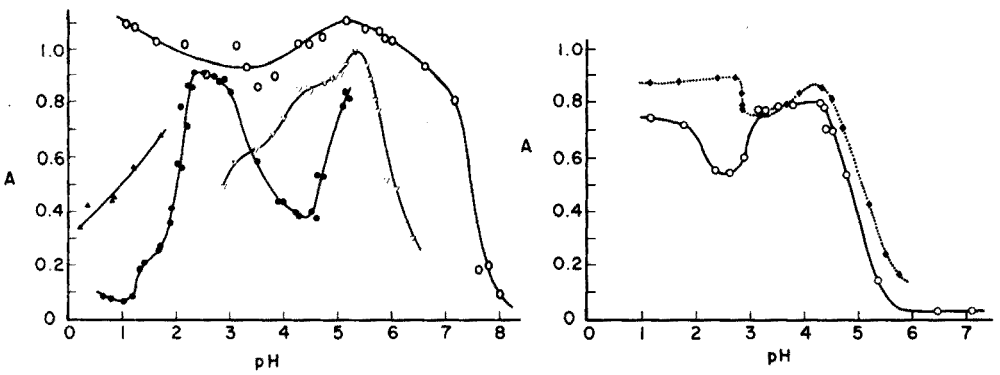

Fig. 1. Effect of pH and buffer on the nitration of aromatic vic-diols with sodium nitrite. All reactions were run for 20 min at room temperature (ca. 22 °C). ○, Catechol in acetate buffer. ▽, 2,3-Dihydroxypyridine in acetate buffer. ●, 2,3-Dihydroxypyridine in phosphate buffer. ▲, 2,3-Dihydroxypyridine in HCl—acetic acid.

Fig. 2. Effect of pH, molybdate, and tungstate on the nitration of epinephrine. All reactions were run for 15 min at room temperature. ♦, Sodium molybdate. ○, Sodium tungstate.

Reaction time

Figures 3—5 show how the intensity of the red color depends on the duration of the nitration reaction. Each data point was determined by allowing the nitration to proceed for a certain duration at its optimum pH and then adding 6 M NaOH to stop the reaction. Table 1 shows that the optimum reaction time depends on the diphenol. For norepinephrine, dopamine, and epinephrine (Fig. 4) the intensity is nearly independent of reaction time between 2 and 40 min in the presence of molybdate. The wavelength of maximum absorption also depends slightly on the reaction time. The wavelengths in Table 1 correspond to the optimum pH and reaction time for each diphenol.

Of particular interest is the effect of molybdate and tungstate ions shown in Figs. 4 and 5. The exact rôle of the metal is not clear from the data obtained, but it is probably not due to catalysis. The data for 2,3-dihydroxy-

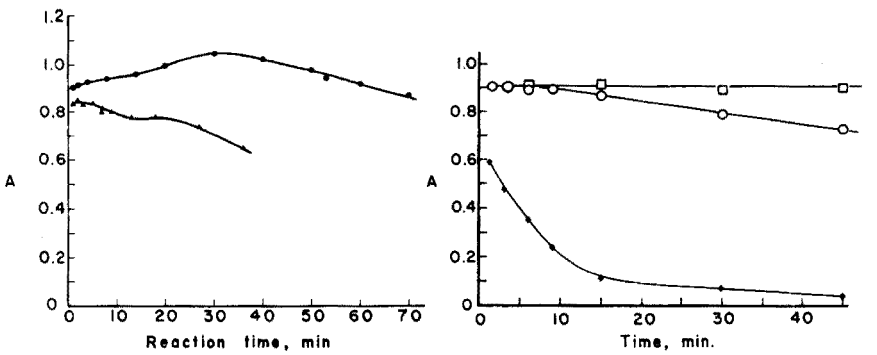

Fig. 3. Effect of reaction time on color intensity. •, Catechol. ▲, 3,4-Dihydroxyphenylalanine.

Fig. 4. Influence of molybdate and tungstate on the rate of reaction of epinephrine with sodium nitrite. □, Sodium molybdate. ○, Sodium tungstate. ♦, No added metal.

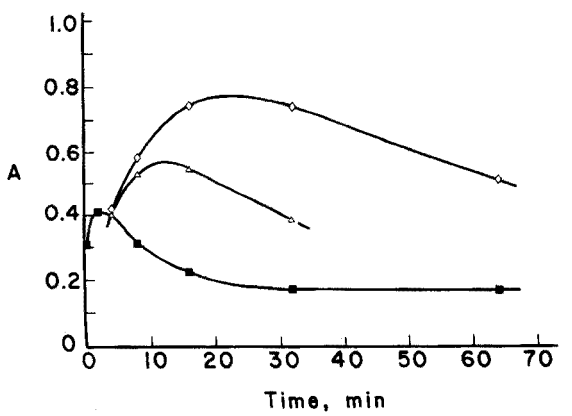

Fig. 5. Effect of molybdate and tungstate on the nitration of 2,3-dihydroxypyridine. ◇, Sodium molybdate. △, Sodium tungstate. ▪, No added metal.

pyridine in Fig. 5, for example, show that the intensity is actually greater in the absence of molybdate or tungstate if the nitration is stopped after only 1—2 min. A similar result was obtained with other diphenols. It appears that the metal ion may stabilize the colored product, perhaps through formation of a coordination complex; the color fades less rapidly in the presence of molybdate or tungstate, molybdate being more effective.

Several workers have investigated coordination complexes of aromatic vic-diols with tungstate and molybdate [16—20]. Complexes are formed in slightly acidic, neutral, and slightly basic solutions, i.e. the pH range for the nitration reaction. In strongly basic solution the complexes break up because the equilibrium involves the hydroxide ion

$$MoO_4^{2-} + 2\ C_6H_4O_2^{2-} + 2\ H_2O = MoO_2(C_6H_4O_2)_2^{2-} + 4\ OH^-$$

This is consistent with the conclusion that the red color does not involve a complex. It is proposed that during the nitration reaction at pH 5—6 the product is stabilized by complex formation, but when the solution is made basic the complex dissociates.

Reaction in open beakers

With epinephrine, consistently higher absorbance values were obtained if nitration was carried out in open beakers instead of a 25-ml volumetric flask. If the reaction is run in a volumetric flask with a slow stream of nitrogen playing on the surface of the solution, there is no diminution of absorbance. However, in a static nitrogen atmosphere in a volumetric flask the result is about 15% low. This suggests that the gases formed, probably NO and NO_2, hinder the reaction and must escape for the optimum color intensity to form. If the reaction is carried out with a slow stream of oxygen playing on the surface, the final absorbance is about 25—30% low. It is known that oxidizing agents such as hexacyanoferrate(III) and peroxide interfere with color development. However, it was not found necessary to run reactions under an inert atmosphere. Apparently the lower concentration of oxygen in air, the absence of agitation, and the evolution of nitrogen oxides combine to make the effect of atmospheric oxygen negligible.

In view of these results the nitration reaction with other diphenols was run in open beakers.

Optimum concentrations of nitrite and molybdate

The effects of changing the concentration of sodium nitrite and sodium molybdate on the color intensity were studied for epinephrine. The nitration reaction was run at pH 4.2 for 20 min; the ion concentrations mentioned below are those present in the reacting solution, before adding sodium hydroxide. The effect of molybdate is maximal and essentially constant over the range 0.01—0.02 M, and decreases slightly up to 0.025 M, when the concentration of sodium nitrite is held constant at 0.50 M. Similarly, the effect of nitrite is essentially constant over the range 0.2—0.4 and then decreases gradually up

to 1 M when the concentration of sodium molybdate was held constant at 0.025 M. These results suggested that the optimum concentrations should be 0.35 M sodium nitrite and 0.015 M sodium molybdate. However, this combination gave a slight decrease in color intensity compared to the concentrations adopted earlier by trial and error. The optimum combination therefore is 0.05 M nitrite and 0.025 M molybdate.

Beer's law

In preliminary experiments, the color intensity deviated from Beer's law if the molybdate was omitted or if the optimum reaction conditions were not used. With the conditions recommended in Table 1 all of the diphenols except 3,5-di-tert-butylcatechol adhere to Beer's law up to an absorbance of 1.8 in a 1.00-cm cell. The relative standard deviation (coefficient of variation) is ±2.4% for solutions having no interferences.

Color stability

With catechol, epinephrine, and 2,3-dihydroxypyridine, the intensity of the red color decreased by about 1—2% in 1 h; all absorbance measurements were made within 20 min after adding the excess of sodium hydroxide.

Selectivity for aromatic vic-diols

To investigate the selectivity of the method the behavior of other phenolic compounds was investigated. A red color was not produced by phenol, resorcinol, hydroquinone, phloroglucinol, or pyrogallol.

No color is expected from 1,2-dimethoxybenzene. Even if it is nitrated, there is no acidic proton that can be removed to produce the red anion. When this reaction was attempted only a faint yellow color was produced ($\epsilon_{500} = 64\ l\ mol^{-1}\ cm^{-1}$). In the case of 2-methoxyphenol there is a phenolic proton but reaction with sodium nitrite followed by addition of excess of sodium hydroxide did not give the usual red color. The molar absorptivity at 500 nm was, however, rather high ($1.4 \cdot 10^3\ l\ mol^{-1}\ cm^{-1}$).

Additional aromatic vic-diols that do not give a red color are listed in Table 2. Other compounds that were tested for possible interference are listed in Tables 3 and 4.

Tiron

The behavior of tiron is somewhat different from that of the other diphenols. The optimum pH is much lower than for any other compound and the reaction is quite slow. In a graph of absorbance vs. reaction time the absorbance still increases after 100 min, although the curve becomes nearly flat after 50 min. Nevertheless, the system follows Beer's law if the optimum conditions given in Table 1 are used.

TABLE 2

Aromatic vic-diols that do not produce an absorption band near 500 nm by the present method. (In each case the nitration reaction was run for 15 min at pH 5.5.)

Aromatic vic-diol	ϵ_{500} ($l\ mol^{-1}\ cm^{-1}$)	Aromatic vic-diol	ϵ_{500} ($l\ mol^{-1}\ cm^{-1}$)
2,3-Naphthalenediol	$2.0 \cdot 10^2$	Digallic acid	$4.8 \cdot 10^2$
Tetrachlorocatechol	$2.1 \cdot 10^2$	Ellagic acid	—[a]
3,4,5-Trihydroxybenzoic acid	$1.2 \cdot 10^2$	1,2,3-Trihydroxybenzene	$2.7 \cdot 10^2$

[a]Insoluble in water and ethanol.

TABLE 3

Possible organic interferences[a]. (In each case the nitration reaction was run for 15 min at pH 5.5.)

Compound	ϵ_{500} ($l\ mol^{-1}\ cm^{-1}$)	Compound	ϵ_{500} ($l\ mol^{-1}\ cm^{-1}$)
Phenol	$7.0 \cdot 10$	Salicyclic acid	<10
1,3-Dihydroxybenzene	$1.2 \cdot 10^2$	4-Aminosalicyclic acid	$3.1 \cdot 10^2$
1,3,5-Trihydroxybenzene	$1.2 \cdot 10^2$	*p*-Aminobenzoic acid	10
2-Methoxyphenol	$1.4 \cdot 10^3$	2-Methoxyaniline	$2.8 \cdot 10^2$
1,2-Dimethyoxybenzene	$6.4 \cdot 10$	*o*-Aminophenol	$9.3 \cdot 10^2$
1,4-Dihydroxybenzene	$6.5 \cdot 10^2$	3,4-Dihydroxycyclobutene-dione	10

TABLE 4

Compounds tested for interference in the determination of epinephrine at pH 4.2

Substance	Molarity[a]	% Decrease in absorbance	Substance	Molarity[a]	% Decrease in absorbance
Iodide	0.02	100	Hexacyanoferrate(III)	0.04	100
Bromide	0.08	0	Hexacyanoferrate(II)	0.04	100
Chloride	0.08	0	Cyanide	0.04	6
Oxalate	0.04	15		0.08	11
	0.08	28	Dihydrogen phosphate	0.02	3
Hydrogen sulfite	0.04	26		0.04	7
				0.06	10
Hydrogen tartrate	0.04	2		0.08	10
	0.08	8	Ammonium	0.40	0
Citrate	0.04	22		0.90	0
	0.08	18			
Hydrogen peroxide	0.002	0	Hydroxyl-ammonium	0.04	5
	0.18	47		0.08	3
			Tetramethyl-ammonium	1.2	0
Nitrate	0.08	0			

[a]These values are the molar concentrations present during the nitration reaction; i.e., before the addition of excess of sodium hydroxide.

The author is indebted to John Kane and Jack Mason for many of the experimental measurements.

REFERENCES

1 L. E. Arnow, J. Biol. Chem., 118 (1937) 531.
2 W. C. Evans, Biochem. J., 41 (1947) 373.
3 P. M. Nair and C. S. Vaidyanathan, Anal. Biochem., 7 (1964) 315.
4 H. E. Spiegel and R. P. Christian, Anal. Letters, 6 (1973) 877.
5 I. S. Bhatia, J. Singh, and K. L. Bajaj, J. Chromatogr., 79 (1973) 350.
6 H. Feuer (Ed.), The Chemistry of Nitro and Nitroso Groups, Chapter 5, Interscience, New York, 1969.
7 H. Frejka and J. Zika, Collect. Czech. Chem. Commun., 5 (1933) 253.
8 J. Frejka, J. Zika,and H. Hamersky, Collect. Czech. Chem. Commun., 3 (1931) 550.
9 R. A. Henry, J. Org. Chem., 23 (1958) 648.
10 K. M. Ibne-Rasa, J. Am. Chem. Soc., 84 (1962) 4962.
11 R. Benedikt, Chem. Ber., 11 (1878) 362.
12 P. Weselsky and R. Benedikt, Monatsh. Chem., 3 (1882) 386.
13 J. Willenz, J. Chem. Soc., (1955) 1677.
14 N. V. Sidgwick, The Organic Chemistry of Nitrogen, Clarendon Press, Oxford (1966).
15 E. D. Hughes, C. K. Ingold, and J. H. Ridd, J. Chem. Soc., (1958) 88.
16 D. H. Brown, J. Inorg. Nucl. Chem., 17 (1961) 146.
17 D. H. Brown and J. D. McCallum, J. Inorg. Nucl. Chem., 25 (1963) 1483.
18 H. Buchwald and E. Richardson, J. Inorg. Nucl. Chem., 15 (1960) 133; Talanta, 9 (1962) 631.
19 G. P. Haight and V. Paragamian, Anal. Chem., 32 (1960) 642.
20 J. Halmekoski, Ann. Acad. Sci. Fennicae, Ser. A, II, No. 96 (1959) 64 pp; Chem. Abst., 54, 1151g.

Analytica Chimica Acta, 89 (1977) 167—175

A NEW METHOD OF REMOVING EXCESS OF REAGENT FROM ORGANIC PHASES IN THE SOLVENT EXTRACTION OF METAL COMPLEX ANIONS WITH QUATERNARY AMMONIUM SALTS. SPECTROPHOTOMETRIC DETERMINATION OF MICRO AMOUNTS OF COBALT WITH 2-NITROSO-1-NAPHTHOL-4-SULFONIC ACID

SHOJI MOTOMIZU and KYOJI TÔEI

Department of Chemistry, Faculty of Science, Okayama University, Tsushima, Okayama-shi (Japan)

(Received 18th August 1976)

SUMMARY

The removal of excess reagent extracted into an organic phase in the solvent extraction of a metal complex anion with a quaternary ammonium ion is discussed. With a given chelating ligand (HO—R—SO_3H), the order of extractability is HO—R—SO_3^- > $M(OR—SO_3)_n^{n-}$ > X^- > $^-O—R—SO_3^-$ when an anion such as nitrate or halide is added. If suitable amounts of the anion are added, only the excess of reagent can be removed. The principle is applied to the extraction with zephiramine of the cobalt complex anion formed with 2-nitroso-1-naphthol-4-sulfonic acid. Micro amounts of cobalt in pure nickel salts were determined spectrophotometrically.

The solvent extraction of metal—complex anions with large or long-chain cations, such as dyes, quaternary ammonium salts and diphenylguanidinium, has frequently been studied. In such extraction systems, chelating reagents with a sulfonic acid group are often used because of their ability to form ion pairs with suitable cations; these ion pairs are extracted more easily than those of reagents possessing hydroxyl or carboxyl groups. In such cases, however, the excess of reagent is extracted into the organic phase along with the complex. Accordingly, the absorbance of the reagent itself is large, and worse, the reagent blank will be affected severely by co-existing anions such as nitrate and halide. These features are undesirable in an extraction—spectrophotometric method when the absorbance is measured in the organic phase for the determination of micro amounts of a metal.

Many studies of extraction with long-chain amine or quaternary ammonium salts have been made, but none has been concerned with a method for removing excess reagent extracted into the organic phase. In spectrophotometric determinations, the smaller the absorbance of the reagent, the better will be the sensitivity and accuracy. Accordingly, this aspect has been examined in the work described here. The principle is as follows. The order of extractability of an anion with a quaternary ammonium ion is R—SO_3^- > R—O

where R is an organic radical. With a given chelating reagent ($HO—R—SO_3H$) which possesses both a hydroxyl group bonding with a metal ion (M^{n+}) and a sulfonic acid group, the order of extractability is expected to be $HO—R—SO_3^-$ $>[M(O—R—SO_3)_n]^{n-} > {}^-O—R—SO_3^-$. The ion-pair formed between a quaternary ammonium ion and a monovalent anion which does not absorb at the wavelength of measurement, e.g. nitrate or halide, can also be extracted into the organic phase. Thus, at a defined concentration of the monovalent anion, the order of extractability is expected to be $[M(O—R—SO_3)_n]^{n-}$ > anion (NO_3^- or halide) > $^-O—R—SO_3^-$. It should therefore be possible, by adding nitrate or halide to an extraction system, to remove the excess of reagent from the organic phase to the aqueous phase.

In this work, several extraction equilibrium constants were determined, and the general principle of removing the excess of reagent was established for the cobalt—2-nitroso-1-naphthol-4-sulfonic acid system with tetradecyldimethylbenzylammonium salt as the reagent forming the ion-pair. The method was applied to the determination of micro amounts of cobalt in several kinds of pure nickel salts which are commercially available.

EXPERIMENTAL

Apparatus

A Shimadzu Model QV-50 spectrophotometer and a Hitachi Model EPS-3T recording spectrophotometer were used with 10-mm quartz cells. An Iwaki Model KM shaker was used.

Reagents

2-Nitroso-1-naphthol-4-sulfonic acid. The reagent (NNS) was obtained by nitrosation of the parent compound in aqueous solution with sodium nitrite [1]. The crude nitroso compound was recrystallized twice from water. Aqueous solutions were used.

Cobalt(II) solution. Solutions of cobalt chloride hexahydrate were standardized by EDTA titration.

Tetradecyldimethylbenzylammonium chloride solutions. Dotite zephiramine chloride (ZCl; Dojindo Co. Ltd., Research Laboratory) was used. The reagent was dried at reduced pressure (about 5 mm Hg) and 50—60 °C to constant weight, and dissolved in distilled water [2].

Aqueous solutions of sodium chloride, bromide, iodide and nitrate were used as the monovalent anion solution. Chloroform was used as the extractant. Phosphate buffer solution (0.1 M), trisodium citrate solution (1.5 M) and ammonia (4 M)—ammonium chloride (4 M) buffer solutions were prepared.

Determination of the equilibrium constants

The exchange equilibrium constant, $K_{A^{n-}}^{nX^-}$, refers to the following reaction

$$A^{n-}_{(a)} + n\,ZX_{(o)} \rightleftharpoons n\,X^-_{(a)} + Z_n A_{(o)}; \quad K_{A^{n-}}^{nX^-} = \frac{[X^-]_a^n\,[Z_nA]_o}{[A^{n-}]_a\,[ZX]_o^n} \qquad (1)$$

where A^{n-}, Z^+ and X^- are the n-valent anion, the zephiramine cation and the monovalent anion (nitrate or halide) respectively, and the subscripts o and a refer to the organic and aqueous phases respectively.

The exchange equilibrium constants for A^{n-} and X^- were determined by extracting A^{n-} with ZX into chloroform from aqueous solutions containing various amounts of X^- and measuring the absorbances of Z_nA in chloroform.

The plots of log $([Z_nA]_o/[A^{n-}]_a)$ against log $([X^-]_a/[ZX]_o)$ for R^{2-} (R^{2-} = divalent anion of NNS) are shown in Fig. 1. These plots are all linear and their slopes are almost −2. The constants determined are listed in Table 1.

For the extraction equilibrium state, the absorbances of the cobalt complex, MR_3^{3-}, in the organic phase plotted against the concentration of chloride in the aqueous phase are shown in Fig. 2. The absorbance of the cobalt complex extracted into organic phase with $1 \cdot 10^{-3}$ M zephiramine

TABLE 1

The exchange equilibrium constants calculated (25 °C)

	Cl^-	NO_3^-	Br^-	I^-
log $K_{HR^-}^{X^-}$	2.49	1.46	1.28	0.01
log $K_{R^{2-}}^{2X^-}$	3.37 ± 0.05	1.30 ± 0.02	0.95 ± 0.05	−1.58 ± 0.10
log $K_{MR_3^{3-}}^{3X^-}$	11.87 ± 0.04	8.79	8.24	4.44

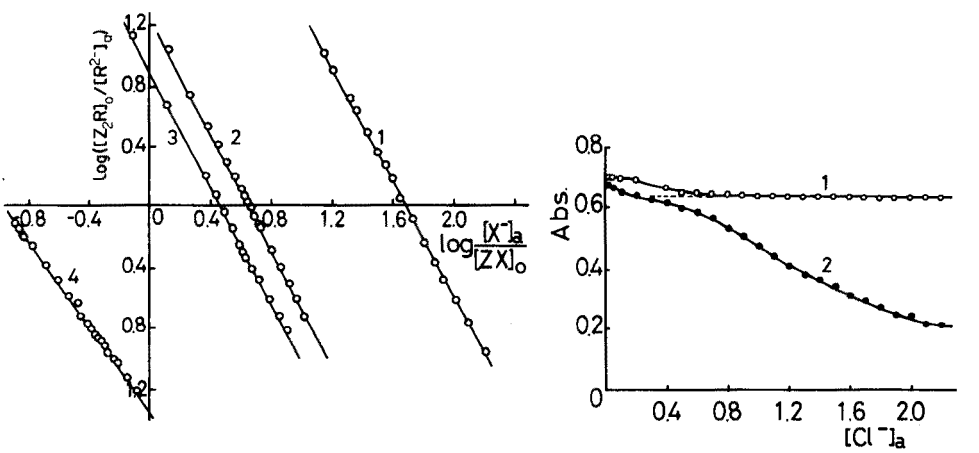

Fig. 1. The plot of log $([Z_2R]_o/[R^{2-}]_a)$ against log $([X^-]_a/[ZX]_o)$. Curve 1, chloride. Curve 2, nitrate. Curve 3, bromide. Curve 4, iodide. $[NNS]_{total} = 8 \cdot 10^{-5}$ M, $[Zephiramine]_{total} = 1 \cdot 10^{-3}$ M, pH 8.6.

Fig. 2. Absorbance of the cobalt complex in the organic phase against the concentration of chloride ion in the aqueous phase. Curve 1, $[Zephiramine]_{total} = 1 \cdot 10^{-3}$ M. Curve 2, $[Zephiramine]_{total} = 2 \cdot 10^{-4}$ M. $[Cobalt]_{total} = 1.6 \cdot 10^{-5}$ M, $[NNS]_{total} = 8 \cdot 10^{-5}$ M, at 368 nm.

chloride is almost constant from 0.8 to 2.2 M of chloride ion. Figure 3 shows the plot for the cobalt complex. From these results, the exchange equilibrium constant for the cobalt complex was calculated to be 11.87 ± 0.04.

From the constants for HR^- and R^{2-} and the acid dissociation constant of HR^-, eqn. (2) is obtained.

$$Y = \log \frac{[ZHR]_o}{[Z_2R]_o} + \log \frac{[ZCl]_o}{[Cl^-]_a} = \log \frac{K_{HR^-}^{Cl^-}}{K_{R^{2-}}^{2Cl^-}} + pK_a - pH \qquad (2)$$

NNS was extracted at constant chloride concentration and various pH values; after the extraction had reached equilibrium, the absorbances of NNS in the organic phase were measured. The results obtained are shown in Fig. 4, where the plot of Y against pH is also given. The plot is linear and its slope is about −1. From these results, $\log (K_{HR^-}^{Cl^-}/K_{R^{2-}}^{2Cl^-})$ was calculated to be −0.88 ± 0.04; 6.16(± 0.03) was used for the pK_a value, which was determined spectrophotometrically at ionic strength μ = 0.1, and agrees well with literature data [3, 4]. From the value of $\log (K_{HR^-}^{Cl^-}/K_{R^{2-}}^{2Cl^-})$ and $\log K_{R^{2-}}^{2Cl^-}$, $\log K_{HR^-}^{Cl^-}$ was calculated to be 2.49. Other constants of $\log K_{HR^-}^{X^-}$ were calculated from eqn. (3):

$$\log K_{HR^-}^{X^-} = \log K_{HR^-}^{Cl^-} + \frac{1}{2}(\log K_{R^{2-}}^{2X^-} - \log K_{R^{2-}}^{2Cl^-}) \qquad (3)$$

The constants calculated are listed in Table 1.

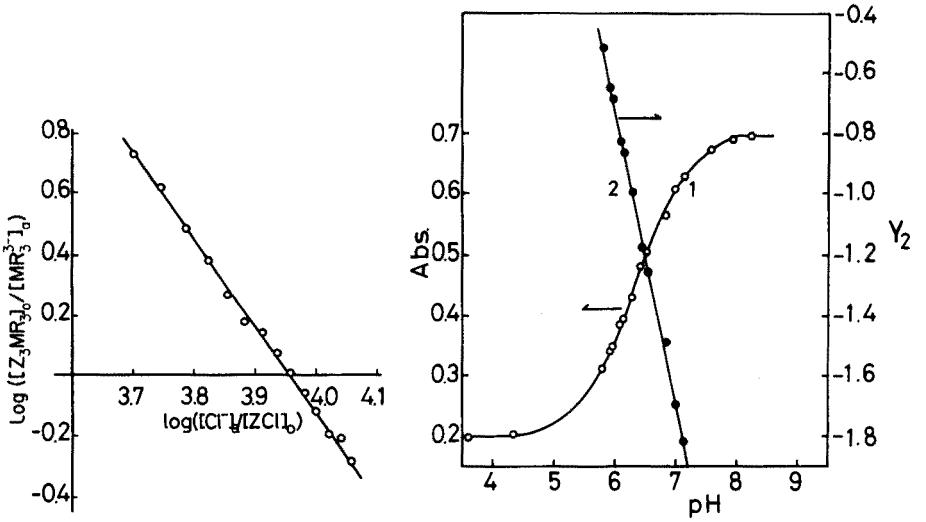

Fig. 3. The plot of $\log ([Z_3MR_3]_o/[MR_3^{3-}]_a)$ against $\log ([Cl^-]_a/[ZCl]_o)$ [Zephiramine]$_{tot}$ = $2 \cdot 10^{-4}$ M.

Fig. 4. Absorbance of NNS in the organic phase against pH and the plot of Y against pH. Curve 1, absorbance against pH. Curve 2, Y against pH. $[NNS]_{total} = 8 \cdot 10^{-5}$ M, $[Zephiramine]_{total} = 1 \cdot 10^{-3}$ M, $[Cl^-]_a = 1 \cdot 10^{-2}$ M, at 440 nm.

Equation (4) was obtained similarly to eqn. (3)

$$\log K^{3X^-}_{MR_3^{3-}} = \log K^{3Cl^-}_{MR_3^{3-}} + \frac{3}{2}(\log K^{2X^-}_{R^{2-}} - \log K^{2Cl^-}_{R^{2-}}) \quad (4)$$

From eqn. (4), the other constants for the cobalt complex were calculated (see Table 1).

Establishment of optimal conditions

The distribution ratios of HR^-, R^{2-} and MR_3^{3-}, can be defined as follows

$$\log D_{HR^-} = \log([ZHR]_o/HR^-]_a) = (\log K^{X^-}_{HR^-} + \log[ZX]_o) - \log[X^-]_a \quad (5)$$

$$\log D_{R^{2-}} = \log([Z_2R]_o/[R^{2-}]_a) = (\log K^{2X^-}_{R^{2-}} + 2\log[ZX]_o) - 2\log[X^-]_a \quad (6)$$

$$\log D_{MR_3^{3-}} = \log([Z_3MR_3]_o/[MR_3^{3-}]_a)$$

$$= (\log K^{3X^-}_{MR_3^{3-}} + 3\log[ZX]_o) - 3\log[X^-]_a \quad (7)$$

In the general procedures, the concentrations of reactants were about 10^{-3} M zephiramine, below $2 \cdot 10^{-5}$ M cobalt and about $1 \cdot 10^{-4}$ M reagent. For such concentrations, the optimal concentration of X^- can be estimated from eqns. (5)—(7). When more than 99% of the reagent is present in the aqueous solution, i.e., $\log D_{HR^-}$ or $\log D_{R^{2-}} < -2$, the concentration of X^- can be calculated from eqns. (5) and (6). The calculated values are listed in Table 2. When above 99% of the cobalt complex is present in the organic phase, i.e. $\log D_{MR_3^{3-}} > 2$, the concentration of X^- can be calculated from eqn. (7) (see Table 2). In these calculations, $[ZX]_o$ is nearly equal to 10^{-3} M. Table 2 shows that the reagent present in the form HR^- is very difficult to remove from the organic phase, whereas the reagent present as R^{2-} is very easily removed from the organic phase. From these results, chloride gives the widest range of the four anions, and is the most useful for the removal of the excess of reagent in the form of R^{2-} in the determination of cobalt. The optimal concentration of chloride ion was found to be about 1 M. In Fig. 5,

TABLE 2

The optimal anion concentration

	$\log[Cl^-]$	$[Cl^-]$ (M)	$\log[NO_3^-]$	$[NO_3^-]$ (M)	$\log[Br^-]$	$[Br^-]$ (M)	$\log[I^-]$	$[I^-]$ (M)
MR_3^{3-}[a]	0.29	2.0	−0.73	0.19	−0.92	0.12	−2.15	0.0071
HR^-[b]	1.49	31	0.46	2.9	0.28	1.9	−0.99	0.10
R^{2-}[c]	−0.31	0.49	−1.34	0.046	−1.52	0.030	−2.79	0.0016

[a]The region where $\log D_{MR_3^{3-}} > 2$. Below these values.
[b]The region where $\log D_{HR^-} < -2$. Above these values.
[c]The region where $\log D_{R^{2-}} < -2$. Above these values.

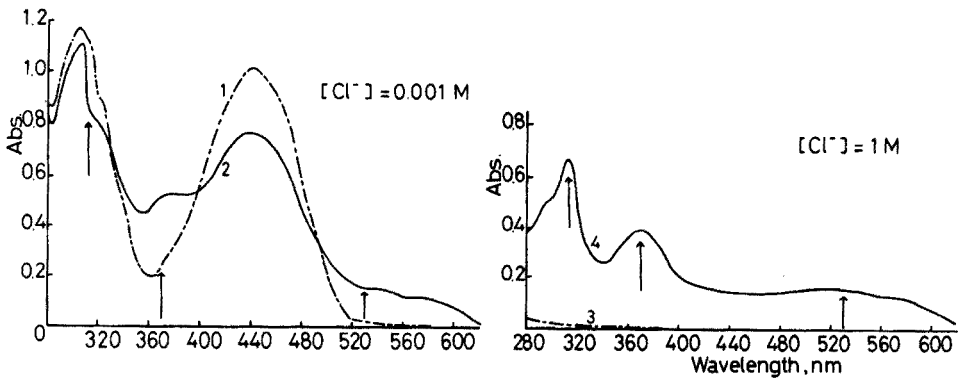

Fig. 5. Absorption spectra in chloroform. Curve 1, reagent blank. Curve 2, [Co] = $1 \cdot 10^{-5}$ M. For curves 1 and 2, [Cl^-] = $1 \cdot 10^{-3}$ M, pH = 8.6. Curve 3, reagent blank. Curve 4, [Co] = $1 \cdot 10^{-5}$ M. For curves 3 and 4, [Cl^-] = 1 M, pH = 9.3. In all cases, $[NNS]_{total} = 1 \cdot 10^{-4}$ M; $[Zephiramine]_{total} = 1 \cdot 10^{-3}$ M.

the absorbance spectra of the cobalt complex and the reagent blank are shown. When the excess of reagent in the organic phase is removed, the best sensitivity is obtained at 312 nm, at which the molar absorptivity is $6.6 \cdot 10^4$ l mol^{-1} cm^{-1}. The molar absorptivities at 368 and 530 nm are $3.8 \cdot 10^4$ and $1.3 \cdot 10^4$, respectively.

Determination of cobalt

General procedure. Pipette up to 5 ml of sample solution into a stoppered test tube, and dilute to 5 ml with distilled water. Add 1 ml of citrate solution and allow to stand for 10 min. Then add 1 ml of reagent solution ($2 \cdot 10^{-2}$ M) and allow to stand for 10 min. Add 0.5 ml of zephiramine solution and 2.5 ml of ammonia buffer solution, and shake with 5 ml of chloroform for 20 min. After the phases have separated, measure the absorbance of the organic phase at 312 nm or 368 nm.

Effect of co-existing ions. The effect of co-existing ions was examined (see Table 3). In the general procedure, iron(II), iron(III) and nickel(II) cause positive errors. The general method was therefore modified.

Improved method. Pipette up to 5 ml of sample solution into a stoppered test tube, dilute to 5 ml with distilled water, add 1 ml of citrate solution and allow to stand for 10 min. Add 1 ml of reagent solution and allow to stand for 30 min. Add 1 ml of hydrochloric acid (1 + 1) and 0.5 ml of zephiramine solution. Shake with 5 ml of chloroform for 20 min. Discard the aqueous phase. Shake the organic phase thrice with 5 ml of 0.05 M hydrochloric acid solution containing 0.1 M potassium chloride for 30 s by hand; then shake the organic phase with 5 ml of ammonia buffer solution (1 M NH_3-1 M NH_4Cl) containing 0.1 M sodium citrate for 10 min. After the phases have separated, measure the absorbance of the organic phase at 312 or 368 nm.

TABLE 3

Effect of diverse ions (at 312 nm)

Ion	Maximum tolerable concn. (M)
Na^+, K^+, Cl^-	1[a]
Citrate ion	0.4[a]
SO_4^{2-}, PO_4^{3-}	0.1[a]
NO_3^-, Br^-, Cu^{2+}	0.01
I^-	0.001
Mn^{2+}, Cr^{3+}, Al^{3+}, Cd^{2+}, Pb^{2+}, Zn^{2+}	10^{-4}[a]
Fe^{2+}, Fe^{3+}, Ni^{2+}	10^{-5}
Improved procedure	
Ni^{2+}	10^{-2}[a]
Fe^{3+}	10^{-4}[a]

[a]Maximum tested.

In the improved procedure, nickel(II) at concentrations of 10^{-2} M and iron(III) at concentrations of 10^{-4} M did not interfere.

Determination of cobalt in pure nickel salts. Micro amounts of cobalt in commercially available nickel salts were determined by the improved method. Two calibration curves were prepared, one for the above general procedure, and one for the improved procedure. Both plots were straight lines in the cobalt concentration ranges up to $1.5 \cdot 10^{-5}$ M (312 nm) and $2.5 \cdot 10^{-5}$ M (368 nm) of cobalt, and the slopes of the plots were almost equal. The results obtained for various nickel salts are shown in Table 4.

DISCUSSION

The new, useful and simple method for the removal of an excess of reagent in the solvent extraction of a metal chelate anion with a quaternary ammonium cation proved satisfactory for the determination of cobalt with 2-nitroso-1-naphthol-4-sulfonic acid and zephiramine. The method was applied to the determination of micro amounts of cobalt in pure nickel salts. The molar absorptivity of the cobalt complex in chloroform is $6.6 \cdot 10^4$ at 312 nm, which is 5 times larger than that at 530 nm. Numerous methods for the determination of cobalt with nitrosonaphthol derivatives have been reported [5, 6]. Recently, extraction—spectrophotometric studies of cobalt with nitroso R salt [7, 8], 2-nitroso-1-naphthol-4-sulfonic acid [9] and long-chain amine or quaternary ammonium salt have been reported. In these methods, the reagent blank is very large, and the measurement of the absorbance of the cobalt complex is strongly affected by co-existing anions; thus the measurements must be made at wavelengths above 500 nm. The principle of the removal of excess of reagent was applied to

TABLE 4

Determination of cobalt in nickel salts

Sample	Supplier	Grade[a]	Sample solution (mg/50 ml)	Absorbance[b]	Co found[c] (%)
$NiSO_4 \cdot 6H_2O$	A	GR (<0.1%)	77.6	0.929[d] 0.546[e]	0.053 0.053
	B	GR (<0.1%)	72.8	0.453[d] 0.267[e]	0.028 0.028
	C	E (<0.3%)	13.0	0.782[d] 0.458[e]	0.27 0.26
$Ni(NO_3)_2 \cdot 6H_2O$	A	GR (<0.1%)	69.7	0.944[d] 0.551[e]	0.060 0.060
	B	GR (<0.1%)	70.6	0.579[d] 0.341[e]	0.0365 0.036
	D	E (<0.3%)	10.5	0.581[d] 0.341[e]	0.245 0.245
$NiCl_2 \cdot 6H_2O$	B	GR (<0.1%)	78.1	0.040[d] 0.026[e]	0.002_2 0.002_4

[a]GR, guaranteed reagent; E, extra-pure reagent. The value in parentheses is the cobalt content indicated in the guarantee certificate. [b]Reference, reagent blank. Average of 3 determinations; in no case did the reading differ more than 0.005 units from the average. A 5-ml aliquot of sample solution was taken in all cases. [c]Mean value. [d]Measured at 312 nm. [e]Measured at 368 nm.

other nitrosonaphthol derivatives. The molar absorptivities of the cobalt complexes in chloroform are listed in Table 5. From Table 5, the sensitivity with the 2-nitroso-1-naphthol derivatives is better than that with the 1-nitroso-2-naphthol derivatives; the sensitivity with 2-nitroso-1-naphthol-4-sulfonic acid was the best of all reagents examined.

The principle proposed can be applied to many other solvent extraction systems involving chelating reagents which possess a chelate-forming hydroxyl group and a sulfonic acid group, such as 8-hydroxyquinoline-5-sulfonic acid and naphthoquinonedioxime-6-sulfonic acid. Removal of the excess of reagent in the organic phase should lead to improved sensitivity in a given solvent extraction system, as well as providing better selectivity. Moreover, the addition of relatively large amounts of salts causes very effective salting-out, so that phase separation becomes faster.

TABLE 5

Molar absorptivities of cobalt complex extracted into chloroform with zephiramine

Reagents	λ (nm)	ε ($\cdot 10^4$ l mol^{-1} cm^{-1})
2-Nitroso-1-naphthol-4-sulfonic acid	312	6.6
	368	3.8
	530	1.3
2-Nitroso-1-naphthol-5-sulfonic acid	316	6.5
	369	3.9
	530	1.2
1-Nitroso-2-naphthol-6-sulfonic acid	315	4.2
	420	3.3
	500	1.2
1-Nitroso-2-naphthol-7-sulfonic acid	321	3.6
	424	3.4
	500	1.1
1-Nitroso-2-naphthol-3,6-disulfonic acid	323	4.2
	420	3.5
	500	1.4
1-Nitroso-2,7-dihydroxynaphthalene-	328	6.0
3,6-disulfonic acid	456	2.8
	500	1.4

REFERENCES

1 K. Tôei and S. Motomizu, Nippon Kagaku Zasshi, 92 (1971) 92.
2 K. Tôei and K. Kawada, Japan Analyst, 21 (1972) 1510.
3 O. Mäkitie, Maatalouden Tutkimuskeskus Maantutkimuslaitos, 79 (1961) 61. Chem. Abs., 56 (1962) 2635b.
4 V. N. Tolmachev, G. N. Podol'naya and L. N. Serpukhova, Zh. Neorg. Khim., 2 (1957) 2073. Chem. Abs., 52 (1958) 13510c.
5 F. D. Snell and C. T. Snell, Colorimetric Methods of Analysis, Van Nostrand, New Jersey, 1958, p. 352.
6 E. B. Sandell, Colorimetric Determination of Traces of Metals, 3rd edn., Interscience, New York, 1959, p. 409.
7 J. Adam and R. Pribil, Talanta, 18 (1971) 733.
8 K. Hasebe, T. Kambara and Y. Satoh, Nippon Kagaku Kaishi, (1975) 455.
9 N. Ishibashi and H. Kohara, Japan Analyst, 15 (1966) 1137.

Analytica Chimica Acta, 89 (1977) 177—187

AN IMPROVED TECHNIQUE FOR THE SPECTROPHOTOMETRIC DETERMINATION OF NITRATE WITH 2,4-XYLENOL

GEORGE NORWITZ* and HERMAN GORDON
Frankford Arsenal, Philadelphia, PA 19137 (U.S.A.)
(Received 28th June 1976)

SUMMARY

An improved method is proposed for the spectrophotometric determination of nitrate with 2,4-xylenol. The sample in aqueous (1.7 + 1) sulfuric acid is treated with 2,4-xylenol to produce 6-nitro-2,4-xylenol which is distilled into an ammoniacal water—isopropanol mixture. The intense yellow color of the ammonium salt of 6-nitro-2,4-xylenol is measured at 455 nm. The distillation is done in a Parnas—Wagner Kjeldahl semimicro distillation apparatus. The isopropanol keeps the excess of 2,4-xylenol in solution. Two procedures are described. In the first (applicable to samples containing alkali nitrates but no chloride, alkaline earth, or ammonium salts), the solution is evaporated to dryness, and (1.7 + 1) sulfuric acid and 2,4-xylenol in acetone are added. In the second (applicable to samples containing chloride, alkaline earth, or ammonium salts), concentrated sulfuric acid is added dropwise to a cooled aliquot and the 2,4-xylenol reagent is then added; if chloride is present, it must be removed by prior precipitation with silver sulfate. Nitrite shows a slight interference which depends on the amount of nitrate and nitrite present.

An improved spectrophotometric method for the determination of nitrate is needed because the present methods have many disadvantages. In this regard, the American Public Health Association [1] recommends several spectrophotometric methods for the determination of nitrate in water, and suggests that the analyst select the method most suitable.

Much effort has been devoted to the use of 2,4-xylenol (2,4-dimethylphenol) for the spectrophotometric determination of nitrate. Customarily, the 6-nitro-2,4-xylenol produced in the nitration is converted to the sodium salt (which gives an intensely colored yellow solution), either by distillation into sodium hydroxide solution, or by extraction with toluene followed by back-extraction into sodium hydroxide solution. The markedly varied conditions used by investigators of the distillation [2—13] and extraction methods [14—16] are summarized in Table 1. The methods described are subject to a greater or lesser extent to the following errors: susceptibility to interference (this is particularly true for the extraction procedures); failure to obtain stoichiometric and reproducible nitration because of unsatisfactory reaction conditions (some investigators [2—4] have indicated that the degree of nitration is only about 75 %); turbidity of the solution because of unreacted

*Present address: 2123 Hoffnagle Street, Philadelphia, PA 19152.

TABLE 1

Conditions used by previous investigators of the 2,4-xylenol method for nitrate

Investigators	Nitration technique	Temp.	Time (min)	H_2O added after nitration (ml)
Blom, Treschow [2]	2 ml treated with 50 ml of 50—70 % H_2SO_4 (vol) and 0.1 ml of 2,4-xylenol	30 °C	60—120	150
Treschow, Gabrielsen [3]	Plant material treated with 25 ml of 66 % H_2SO_4 (vol) and 0.1 ml of 2,4-xylenol	ambient	15—30	diluted to 100
Alten, Weiland [4]	Dried salts treated with 0.2 ml of 2,4-xylenol and 50 ml of (5 + 3) H_2SO_4	ambient (or 50 °C)	overnight (4 h)	diluted to 400
Alten et al. [5]	Plant material treated with 25 ml of 66 % H_2SO_4 (vol) and 0.1 ml of 2,4-xylenol	ambient	20	60
Hamy [6]	Dried salts treated with 25 ml of 66 % H_2SO_4 (vol) and 0.1 ml of 2,4-xylenol reagent (in acetic acid)	ambient	30	100
Yagoda [7]	Dried salts treated with 1 ml of 2,4-xylenol reagent (in acetone) and 15 ml of 62.5 % H_2SO_4 (vol)	ambient	30	100
Werr [8]	1 ml treated with 75 ml of 75 % H_2SO_4 (wt) and 1 drop of 2,4-xylenol	ambient	10—15	20
Yagoda, Goldman [9]	10 ml treated with 0.1 ml of 2,4-xylenol reagent (in triethylene or propylene glycol) and 17 ml of conc. H_2SO_4 (while cooling)	ambient	10	150
McVey [10]	1—5 ml treated with three times its volume of 85 % H_2SO_4 (wt) and 1 ml of 2,4-xylenol reagent (in acetic acid)	35 °C	30	100
Davidek et al. [11]	5 ml treated with 20 ml of 85 % H_2SO_4 (wt) and 1 ml of 2,4-xylenol reagent (in acetone)	ambient	20	100

TABLE 1 (continued)

Investigators	Nitration technique	Temp.	Time (min)	H_2O added after nitration (ml)
Vasak [12]	4 ml (cooled) treated with 7 ml of conc. H_2SO_4 and 3 drops of 2,4-xylenol reagent (in acetic acid)	ambient	25	diluted to 25
Rosene [13]	10 ml added to cooled mixture of 40 ml of 4 to 1 H_2SO_4 (vol) and 2 ml of 2,4-xylenol reagent (in NaOH)	ambient	30—45	100
Barnes [14][a]	5 ml treated with 15 ml of 85 % H_2SO_4 (wt) and 1 ml of 2,4-xylenol reagent (in acetic acid)	35 °C	30	80
Buckett et al. [15][a]	same as for ref. 14	34 °C	30	80
Public Health Service [16][a]	same as for ref. 14	60 °C	30	diluted to 80

[a] With an extraction technique.

2,4-xylenol (to overcome this error, some of the methods call for filtration [5], centrifuging [6], or the use of the minimum amount of reagent [7]); loss of nitro compound in the distillation because of adherence to the condenser [4].

In this paper, an improved method is proposed for the determination of nitrate by 2,4-xylenol under conditions that give excellent reproducibility. The nitration is conducted in (1.7 + 1) sulfuric acid medium and the nitroxylenol is distilled into a mixture of ammonia, water, and isopropanol; the latter reagent holds the excess of 2,4-xylenol in solution and prevents turbidity. The distillation is conducted very efficiently with a Parnas—Wagner Kjeldahl distillation apparatus.

EXPERIMENTAL

Apparatus and reagents

Beckman Model DU and Cary Model 15 spectrophotometers were used. The conventional Parnas—Wagner Kjeldahl distillation apparatus was modified by using a steam generator flask with a ground-glass joint, and by extending the condenser exit tube to reach the bottom of a 100-ml volumetric flask.

Potassium nitrate (dried at 150 °C for 1 h), isopropanol, acetone, ammonia liquor, and sulfuric acid (approximately 96 % H_2SO_4) were all of reagent grade. A dilute sulfuric acid solution (1.7 + 1) was prepared from 1 l of water and 1.71 o

sulfuric acid in the usual way, cooled and stored in a stoppered flask.

Standard nitrate solution (1 ml = 0.05 mg NO_3^--N). Dissolve 0.3610 g of KNO_3 in water and dilute to 1 l in a volumetric flask.

2,4-Xylenol solution (2.5 %). Dilute 5 ml of 2,4-xylenol (Eastman-Kodak) to 200 ml with acetone.

Procedures

Procedure 1 (for samples containing alkali nitrates but no chloride, alkaline earth, or ammonium salts). Prepare a calibration curve as follows. Transfer 1.0, 2.0, 3.0, and 4.0 ml of standard nitrate solution, measured with a semimicro buret, to 100-ml beakers and evaporate to dryness by heating gently on a hot plate. Cool to room temperature. Add 15 ml of sulfuric acid (1.7 + 1) from a graduated cylinder and leave for 5—10 min with occasional swirling to ensure complete dissolution of the salts. Carry along a reagent blank. Add 1.0 ml of 2,4-xylenol solution (2.5%) and swirl. Cover with watch glasses and allow the solutions to stand for 10—60 min.

Add 20 ml of water, 35 ml of isopropanol, and 5 ml of ammonia liquor to five 100-ml volumetric flasks. Place one of the flasks under the condenser extension tube of the Parnas—Wagner distillation apparatus so that the extension tube reaches to the bottom of the flask. Place an asbestos board or piece of cardboard between the burner and the distillation flask. With the steam generator sealed off, introduce the sample through the entry funnel into the distillation flask and wash in with 5—10 ml of water. Open the clamp from the steam generator and close the clamps on the entry funnel and the bottom of the steam trap. Steam-distill until the volume of liquid in the volumetric flask is about 95 ml. Remove the volumetric flask, shut off the burner, close the clamp between the steam generator and trap, and place a 150-ml beaker containing about 125 ml of distilled water under the condenser extension tube so that the tube reaches to the bottom of the beaker. After the solution in the distillation flask and the water from the beaker have been sucked back into the steam trap, open the clamp on the steam trap, so as to drain the water from the trap. Then close this clamp, open the clamps on the generator and entry funnel, and proceed with the next sample.

Dilute the solutions in the volumetric flasks to the mark and mix. Measure the absorbances at 455 nm against a reagent blank. Plot absorbance against mg of nitrate N (per 100 ml). (Note: Rinse the optical cells with concentrated sulfuric acid daily.)

For the analysis of a sample, proceed as follows. The solution should be neutral or slightly alkaline; if it is acid, add 0.1 M NaOH until alkaline to litmus paper. Pipet an aliquot containing up to 0.20 mg of nitrate-N into a 100-ml beaker and evaporate to dryness by heating gently on the hot plate. Cool to room temperature and proceed as described in the preparation of the calibration curve.

Procedure 2 (for samples containing chloride, alkaline earth or ammonium salts). Prepare a calibration curve as follows. Transfer 1.0, 2.0, 3.0, and 4.0 ml of standard nitrate solution measured with a semimicro buret, to 100-ml

beakers and evaporate to dryness by heating gently on the hot plate. Cool to room temperature, add 10.0 ml of water, and swirl to dissolve the salts. Cover the beakers and cool them in cracked ice for 10 min or more, to lower the temperature to 5 °C or below (an iced water bath is not satisfactory). While keeping the beakers in the ice, add 17.0 ml of concentrated sulfuric acid dropwise from a buret while swirling. Adjust the solutions to room temperature, add 1.0 ml of 2,4-xylenol reagent (2.5 %), swirl, and allow to stand for 10—60 min. Proceed with the distillation and color measurement as described in the preparation of the calibration curve in Procedure 1.

For the analysis of a sample not containing chloride, proceed as described in the subsequent paragraph. If chloride is present, proceed as follows. Transfer a 50- or 100-ml portion of the sample to a 250-ml beaker and add 0.5 ml of concentrated sulfuric acid. Heat to 70—80 °C and add aqueous silver sulfate solution (0.44 %) from a graduate while stirring. Use 1 ml more of the silver sulfate solution (0.44 %) than is required for complete precipitation, considering that 1 ml of this silver sulfate solution is equivalent to 1 mg of Cl (e.g., for 10 mg of chloride use 11 ml of silver sulfate solution). Boil for 1 min. Remove from the hot plate, and test for complete precipitation by adding a drop or two of silver sulfate solution down the sides of the beaker. Allow to stand for 15 min or more. Filter through a Whatman No. 42 filter paper into a 100- or 200-ml volumetric flask (depending on the size of the original aliquot and the amount of silver sulfate solution used) and wash with water. Dilute to the mark in the volumetric flask.

Pipet a 10-ml aliquot into a 100-ml beaker, cool the solution in cracked ice, and proceed as described in the preparation of the calibration curve for Procedure 2.

DISCUSSION AND RESULTS

The Parnas—Wagner distillation apparatus is classically used for the distillation of ammonia in the semimicro Kjeldahl method. The use of this apparatus in the present method reduces the time for the distillation considerably, because of the vacuum-jacketed distillation flask. The apparatus [17, 18] used is similar to the classical Parnas—Wagner type except for small modifications (see Experimental). There are modifications of the Parnas—Wagner apparatus on the market in which the clamps are replaced by stopcocks [19]. The Parnas—Wagner apparatus ordinarily has a silver column in the condenser to prevent leaching of alkaline interferences from the glass; there is no reason why a regular semimicro borosilicate condenser could not be used in the present method, since ammonia is not being determined. Possibly, semimicro Kjeldahl apparatuses [20, 21] other than the Parnas—Wagner type might be used.

The exact time for the distillation depends on the initial volume of solution in the distillation flask. When this volume was about 25 ml, the time to attain the 95-ml volume in the volumetric flask was about 4—5 min. Most of the

nitroxylenol compound distilled in 1—2 min, as judged by the yellow color of the condensate. When an additional 10 ml of water was added to the distillation flask, the distillation time increased to 7 min and most of the nitroxylenol compound distilled in 2—3 min.

The isopropanol ensures a clear distillate by keeping excess of 2,4-xylenol in solution; 35 ml of isopropanol was satisfactory, but with 25 ml the solution was slightly turbid. Some experiments indicated that ethanol or acetone could be used in place of isopropanol.

The amount of ammonia liquor is not critical. The same result was obtained with 1—15 ml of ammonia liquor; 5 ml is recommended. Some experiments indicated that sodium or potassium hydroxide solution could be used in place of ammonia.

The color is stable overnight. Also, it is not temperature-dependent; the change in absorbance was less than 0.005 for low and high amounts of nitrate in the interval 18—23 °C. Previous investigators have stated that the color, developed in an aqueous solution, was temperature-dependent [4, 15].

The amount of 2,4-xylenol reagent is not critical. The same result was obtained with 0.5—3 ml of the reagent (0.2 ml gave low results). The use of 1 ml is recommended. The reagent is prepared on a volume basis (2.5 % in acetone). The 2,4-xylenol, as purchased, is ordinarily a liquid. The melting point is given in the handbooks as 25—26 °C and by Eastman-Kodak [22] as 22—24 °C, but the material did not crystallize even when cooled to 15 °C.

To ensure completion of the nitration reaction, the solution should stand for at least 10 min after the addition of the 2,4-xylenol reagent. Allowing the solution to stand for 24 h did not change the results. A standing period of 10—60 min is recommended. Heating the solution at 50 °C for 15 min did not change the results.

A critical aspect of the method is the acidity used in the nitration reaction. The effect of acidity was studied on three ranges of nitrate-nitrogen by evaporating nitrate solutions to dryness and adding 15 ml of sulfuric acid of different concentrations (volume ratio); 1 ml of 2,4-xylenol reagent was then added, the solutions were distilled, and the absorbances were measured. A plot was then made of sulfuric acid concentration against absorbance (Fig. 1). The absorbances obtained with concentrated sulfuric acid (not shown) differed little from those obtained for (5 + 1) sulfuric acid. It can be seen that there is a plateau of maximum absorbance over the range (1.5 + 1) to (2.0 + 1) sulfuric acid. Also, the acidity is most critical for larger amounts of nitrate. The use of a sulfuric acid concentration of (1.7 + 1) is recommended. This is equivalent to 75.0 % H_2SO_4 by weight.

In Procedure 1, the same intensity of color was obtained with 10—30 ml of (1.7 + 1) sulfuric acid. The use of 15 ml of (1.7 + 1) sulfuric acid is recommended.

The absorbance spectra obtained against (1.7 + 1) sulfuric acid are shown in Fig. 2. Maximum absorbance occurs at about 455 nm. Previous investigators have reported maximum absorbance at about 450 nm, so possibly the presence of the isopropanol and ammonia causes a slight shift.

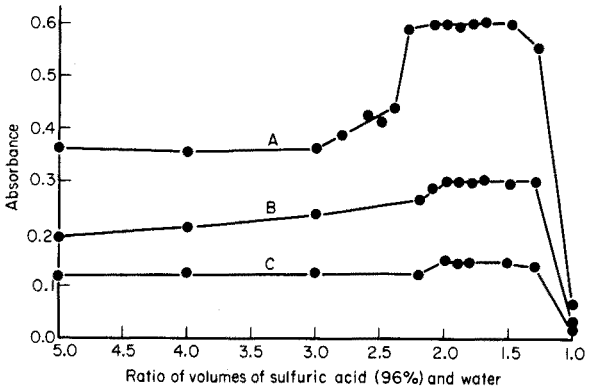

Fig. 1. Effect of concentration of sulfuric acid on the absorbance. (A) 0.20 mg NO_3^--N. (B) 0.10 mg NO_3^--N. (C) 0.05 mg NO_3^--N.

The calibration curves obtained for Procedures 1 and 2 differed slightly. It is, therefore, recommended that for greatest accuracy, two separate calibration curves should be prepared.

It is essential in Procedure 2 that the solution be cooled to 5 °C or below and that the sulfuric acid be added dropwise. If this is not done, some nitrate will be lost by volatilization from the hot concentrated sulfuric acid solution.

In dissolving the dried inorganic nitrate salts in Procedure 1, the solution must be allowed to stand for 5 min or more (with occasional swirling) after adding the (1.7 + 1) sulfuric acid. The 2,4-xylenol reagent must not be added first, since this causes the formation of a slurry and leads to erratic results.

Procedure 1 cannot be used for samples containing barium, strontium, or calcium, because the insoluble sulfates of these elements formed on addition of the sulfuric acid to the dried salts can occlude some nitrate. Also, Procedure 1

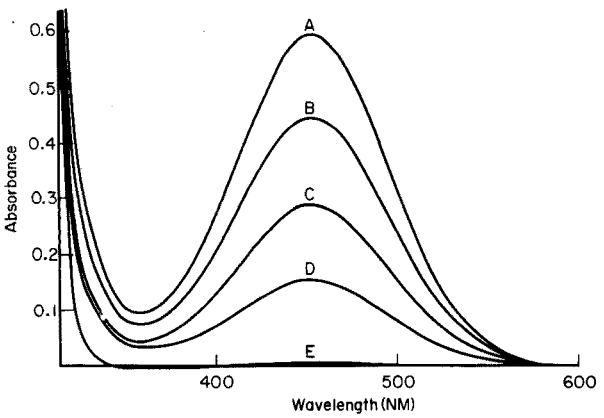

Fig. 2. Absorbance spectra. (A) 0.20 mg NO_3^--N. (B) 0.15 mg NO_3^--N. (C) 0.10 mg NO_3^--N. (D) 0.05 mg NO_3^--N. (E) Blank.

cannot be used for samples containing ammonium salts, because ammonium nitrate may be lost on evaporation to dryness. Procedure 1 should not be used for samples containing chloride. If the silver chloride precipitation is done and the solution evaporated to dryness (after adding alkali), the resultant mixture of silver and sodium salts cannot be readily dissolved.

The necessity of removing the chloride in the method is shown by the results obtained (Table 2) for nitrate in the presence of chloride on evaporating aliquots of potassium nitrate and sodium chloride solutions to dryness and proceeding as described in Procedure 1. The low results are probably due to the volatilization of NOCl. This volatilization apparently occurs for the most part during the initial stages of the distillation when the solution becomes hot.

In the precipitation of the silver chloride, the solution must be slightly acidic (with sulfuric acid). Precipitation of the silver chloride from a neutral solution can lead to occlusion of nitrate. The amount of sulfuric acid (0.5 ml) used for acidification does not cause difficulty in the spectrophotometric determination, since the amount of sulfuric acid in the aliquot (0.05 ml) is within the allowable error for the sulfuric acid concentration for the nitration. The solution should be boiled for 1 min to coagulate the silver chloride. This boiling causes no loss of nitrate from the essentially aqueous solution (no nitrate was lost even after boiling for 5 min).

The limited solubility of silver sulfate in water makes it necessary to use a rather large volume of silver sulfate solution in the precipitation of larger amounts of chloride. This is a minor inconvenience. The use of solid silver sulfate [24] for the precipitation is not recommended; most investigators have used silver sulfate solution [1, 11, 12].

Attempts were made to eliminate the interference of smaller amounts of chloride by merely adding the silver sulfate solution to an aliquot of the sample, diluting to 10.0 ml, and proceeding with the addition of the 17.0 ml of sulfuric acid and distillation without filtration. However, the results for nitrate were low because the silver chloride redissolved in the hot concentrated

TABLE 2

Interference of chloride with the 2,4-xylenol method for nitrate

NO_3^--N present (mg)	Cl^- present (mg)	NO_3^--N found (mg)	NO_3^--N present (mg)	Cl^- present (mg)	NO_3^--N found
0	50	0.00	0.20	0.1	0.166
0.10	0.0—0.1	0.102	0.20	0.2	0.146
0.10	0.2	0.096	0.20	0.5	0.140
0.10	1	0.084	0.20	1	0.050
0.10	5	0.078	0.20	5	0.011
0.10	10	0.076	0.20	10	0.004
0.10	25	0.036	0.20	25	0.002
0.10	50	0.028	0.20	50	0.001

sulfuric acid solution in the distillation flask. The use of mercury(II) sulfate (to complex the chloride) was also unsuccessful.

The interference from nitrite was studied by adding potassium nitrite solution (1 ml = 0.05 mg nitrite-N) to potassium nitrate solution, evaporating to dryness, and proceeding as in the method. The results (Table 3) show that nitrite can cause somewhat high results in a peculiar and erratic manner. For example, in the absence of nitrate N, 0.1—0.5 mg of nitrite-N gave an apparent nitrate-N result of about 0.02 mg, while in the presence of 0.10 mg of nitrate-N, 0.05—0.25 mg of nitrite-N did not interfere significantly. The interference from nitrite is apparently caused by formation of a nitroso compound (which seems to be formed initially quantitatively on adding the 2,4-xylenol reagent as judged by the colors in the absence of nitrate). This nitroso compound is only slightly volatile with steam, so the interference from nitrite is far less than might be expected. The interference could probably be entirely eliminated by adding urea or sulfamic acid to destroy the nitrite before the addition of the 2,4-xylenol reagent. This was not investigated.

The results obtained by Procedures 1 and 2 in the absence of chloride are shown in Table 4. The results obtained for Procedure 2 in the presence of chloride are shown in Table 5. All the results were satisfactory.

A few experiments indicated that a possible alternative procedure for the determination of nitrate might be to treat the sample with the sulfuric acid and 2,4-xylenol reagent, add water and isopropanol and make the absorbance measurements at 350 nm without a distillation. Another alternative might be to add water and isopropanol as above, neutralize with ammonia solution, and measure the absorbance at 455 nm. However, neither of these techniques is recommended, since they offer no advantage over the common phenoldisulfonic acid spectrophotometric method for nitrate [1]. The usefulness of the 2,4-xylenol distillation procedure is that it furnishes a means of isolating the nitro compound and measuring it accurately.

TABLE 3

Interference of nitrite with the 2,4-xylenol method for nitrate

NO_2^--N present (mg)	NO_3^--N found (mg)	NO_2^--N present (mg)	NO_3^--N found (mg)
No NO_3^--N present		*0.10 mg NO_3^--N present*	
0.05	0.012	0.0	0.102
0.10	0.022	0.05	0.100
0.15	0.018	0.10	0.104
0.20	0.022	0.15	0.096
0.25	0.028	0.20	0.098
0.5	0.018	0.25	0.104
1.25	0.050	0.5	0.114
2.5	0.050	1.25	0.118
3.75	0.064	2.5	0.132
5.0	0.162		

TABLE 4

Results for nitrate by Procedures 1 and 2 in absence of chloride

Salt	NO_3^--N present (mg)	NO_3^--N found (mg)	
		Procedure 1	Procedure 2
KNO_3	0.05	0.050	0.054
	0.10	0.102	0.098
	0.15	0.154	0.145
	0.20	0.208	0.212
$NaNO_3$	0.05	0.054	0.050
	0.10	0.092	0.102
	0.15	0.149	0.149
	0.20	0.202	0.198
NH_4NO_3	0.05	—	0.054
	0.10	—	0.102
	0.15	—	0.150
	0.20	—	0.194
$Ba(NO_3)_2$	0.05	—	0.054
	0.10	—	0.096
	0.15	—	0.156
	0.20	—	0.194

TABLE 5

Results for nitrate by Procedure 2 in the presence of chloride

Mixture[a]		Dilution after AgCl precipitation (ml)	NO_3^--N present (mg)[b]	NO_3^--N found (mg)
NO_3^--N (mg)	Cl^- (mg)			
0.5	5	100	0.05	0.054
0.5	25	100	0.05	0.050
1.0	5	100	0.10	0.102
1.0	25	100	0.10	0.098
1.5	5	100	0.15	0.154
1.5	25	100	0.15	0.156
2.0	5	100	0.20	0.197
2.0	25	100	0.20	0.206
1.0	35	200	0.05	0.054
2.0	50	200	0.10	0.098
2.0	50	200	0.10	0.102
0.5	100	200	0.025	0.030
1.0	100	200	0.05	0.056
2.0	100	200	0.10	0.104
4.0	100	200	0.20	0.202

[a] Prepared by adding nitrate-N solution (1 ml = 0.5 mg nitrate-N) and chloride solution (1 ml = 10 mg Cl^-) to water and diluting to about 50 ml with water.
[b] In 10-ml aliquot.

Probably 3,4-xylenol could be substituted for 2,4-xylenol, since the nitro derivative of 3,4-xylenol is volatile with steam and behaves much like the 2,4-xylenol derivative [23]. However, 2,6-xylenol cannot be used since the nitro derivative of that compound is not volatile with steam [24].

This work was conducted under an Army Materials Technology Program (AMS Code 53970M6350).

REFERENCES

1 Am. Public Health Assoc., Standard Methods for the Examination of Water and Waste Water, 13th edn., Washington, DC, 1971, pp. 233, 454.
2 J. Blom and C. Treschow, Z. Pflanzenernaehr., Duengung Bodenkd., 13A (1929) 159.
3 C. Treschow and E. K. Gabrielsen, Z.Pflanzenernaehr., Duengung Bodenkd., 32A (1933) 357.
4 F. Alten and H. Weiland, Z. Pflanzenernaehr., Duengung Bodenkd., 32A (1933) 337.
5 F. Alten, B. Wandrowsky, and E. Hille, Bodenkd. Pflanzenernaehr., 1 (1936) 340.
6 A. Hamy, Ann. Agron., 15 (1945) 126.
7 H. Yagoda, Ind. Eng. Chem., Anal. Ed., 15 (1943) 27.
8 F. Werr, Z. Anal. Chem., 109 (1937) 81.
9 H. Yagoda and F. H. Goldman, J. Ind. Hyg. Toxicol., 25 (1943) 440.
10 W. C. McVey, J. Ass. Offic. Agr. Chem., 18 (1935) 459.
11 J. Davidek, S. Klein, and A. Zackova, Z. Lebensm. Unters. Forsch., 119 (1963) 342.
12 V. Vasak, Prac. Lek., 17 (1965) 47.
13 C. J. Rosene, J. Ass. Offic. Anal. Chem., 52 (1969) 756.
14 H. Barnes, Analyst (London), 75 (1950) 388.
15 J. Buckett, W. D. Duffield, and R. F. Milton, Analyst (London), 80 (1955) 141.
16 U.S. Dept. of Health, Education and Welfare, Public Health Service, Robert A. Taft Sanitary Engineering Center, Selected Methods for the Measurement of Air Pollutants, Method J-1, Cincinnati, OH, 1965.
17 Arthur H. Thomas Co., Catalogue No. 7051-G10, Philadelphia, PA.
18 J. K. Parnas and R. Wagner, Biochem. Zeit., 125 (1921) 253.
19 Fisher Scientific Co., Catalogue No. 21-150, Pittsburgh, PA.
20 Arthur H. Thomas Co., Catalogue Nos. 7051-N10, 7052-D10, and 7052-J10, Philadelphia, PA.
21 Fisher Scientific Co., Catalogue No. 21-150, Pittsburgh, PA.
22 Eastman Kodak Co., Eastman Organic Chemicals, Rochester, NY, May 31, 1974, p. 96.
23 A. C. Holler and R. V. Huch, Anal. Chem., 21 (1949) 1385.
24 A. M. Hartley and R. I. Asai, Anal. Chem., 35 (1963) 1207.

Analytica Chimica Acta, 89 (1977) 189—197

ÉTUDE STATISTIQUE DES TITRAGES ACIDOBASIQUES EN SOLUTIONS AQUEUSES DILUEÉS
I. MÉTHODE ET ÉTALONNAGE

CLAUDE ROSSI et SERGE COMBET

Université de Provence, Laboratoire de Physico Chimie Ionique et Macromoléculaire, 3, place Victor Hugo, 13331, Marseille, Cedex 3 (France)

(Reçu le 12 juillet 1976)

RÉSUMÉ

La méthode de titrage présentée permet l'étude expérimentale précise des acides faibles dans un domaine de dissociation très étendu. Elle trouve sa double originalité dans la méthode d'étalonnage de la pile de mesure potentiométrique et dans le mode d'obtention du degré de dissociation de l'acide faible. La technique expérimentale conduit à des mesures de pH stables même en milieu très peu tamponné.

SUMMARY

A titrimetric method is presented for the precise experimental study of weak acids over a very wide dissociation range. Both the method of standardization in the potentiometric cell and the determination of the dissociation ratio of the weak acid are novel. With this experimental technique, steady potentiometric pH measurements are recorded even in very poorly buffered media.

L'étude en milieu aqueux des interactions entre les groupements fonctionnels d'un polyacide en fonction du degré de dissociation peut être abordée par potentiométrie à condition de pouvoir exploiter avec précision tout le domaine de pH [1, 2] expérimental. Lorsque l'acide étudié n'est pas très faible, l'addition d'un monoacide fort au milieu réactionnel permet de minimiser le phénomène d'autodissociation. Notre technique initiale [3] consiste pour toute valeur pH_i du pH à comparer graphiquement (Fig. 1) la courbe expérimentale (II) relative au mélange acide fort-acide faible à celle obtenue (I) dans des conditions d'analyse semblables mais en l'absence d'acide faible. Dans ces conditions tout point d'indice i du titrage II conduit à

$$[C_{H^+}]_i = \frac{v_{eII} - v_{iII}}{V + v_{iII}} m + \frac{h_i G 10^3}{V + v_{iII}} + \frac{K_w}{(C_{H^+} \gamma_{H^+}{}^2)_i} \quad (1)$$

où m est le titre molaire de la base forte non carbonatée [4], h_i le nombre de groupements dissociés par unité de masse de l'acide faible [1, 3], $[C_{H^+}]_i$ la concentration molaire en protons, $(\gamma_{H^+})_i$ le coefficient d'activité correspondant,

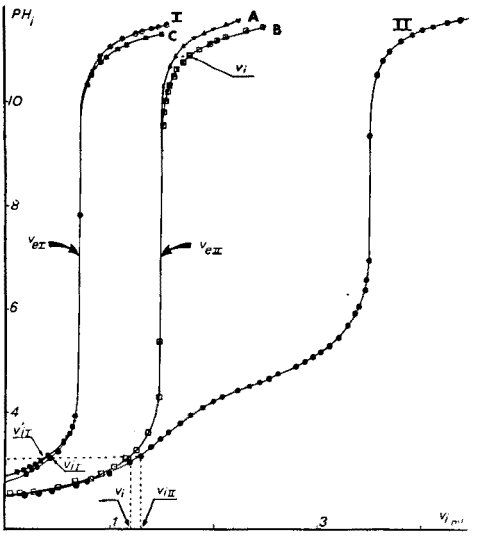

Fig. 1. Les courbes experimentales.

G la masse d'acide faible dans la prise d'essai exprimée en grammes, K_w le produit ionique apparent de l'eau défini comme suit: $pK_w = -\log (C_{H^+} C_{OH^-} \gamma_{H^+}{}^2)$, et V est le volume initial de solution à doser.

A tout point de la courbe II il correspond un point de la courbe I de même pH obéissant à la relation

$$[C_{H^+}]_i = \frac{v_{eI} - v_{iI}}{V + v_{iI}} m + \frac{K_w}{(C_{H^+} \gamma_{H^+}{}^2)_i} \tag{2}$$

Dans les mêmes conditions de dilution pour le titrage I que pour le titrage II, la courbe observée aurait été C telle qu'à pH_i l'on ait:

$$\frac{v_{eI} - v_{iI}}{V + v_{iI}} = \frac{v_{eI} - v'_{iI}}{V + v_{iII}} \tag{3}$$

et donc, à partir des éqns. (1), (2) et (3) on tire

$$h_i = (v_{iII} - v'_{iI}) \frac{m\ 10^{-3}}{G} - (v_{eII} - v_{eI}) \frac{m\ 10^{-3}}{G} \tag{4}$$

où v_{eII} et v_{eI} sont les volumes de réactifs théoriquement nécessaire pour neutraliser l'acide fort contenu respectivement dans II et I.

Ces volumes sont différents expérimentalement dans la plupart des cas et les courbes homologues de I et C pour la quantité d'acide fort utilisée dans le titrage II seraient respectivement A et B.

Dans ces conditions l'interpolation graphique nécessaire au calcul du terme variable du deuxième membre de l'éqn. (4) peut être remplacée avantageusement par une méthode numérique [5] consistant à calculer les

valeurs v'_{iI} de l'éqn. (4) à partir de la lecture directe des couples de valeurs expérimentales (pH_{lu}, v_{iII}) et des paramètres de titrage de l'acide fort. Ces paramètres résultent de l'exploitation statistique [5—7] de la courbe I. Tout revient à chercher la loi $pH_{lu} = f(v)$ applicable au titrage de l'acide fort I. Les paramètres qui en découlent rendent compte [2, 4, 5, 8] des caractéristiques de la pile électrochimique et de la solution à doser. Cette opération constitue pour nous le véritable étalonnage de la pile protométrique que nous allons développer.

ETALONNAGE DE LA PILE DE MESURE

Comme nous l'avons montré [4, 5, 8] la pente expérimentale de la courbe de réponse $pH_{lu} = f(pH_{réel})$ est un paramètre noté α^* ajustable dans la loi $pH_{lu} = f(v)$. La loi générale du titrage en milieu aqueux d'un acide fort par une base forte de titre molaire m s'exprime par la relation

$$10^{-(pH_{lu}/\alpha^*) - pH_E(1-(1/\alpha^*))} = \frac{v_e - v}{V+v} m\gamma_{H^+} + 10^{(pH_{lu}/\alpha^*) + pH_E(1-(1/\alpha^*)) - pK_w} \quad (5)$$

L'exploitation de cette expression peut être conduite de deux façons différentes faisant l'objet des développements ci-après.

(1) Nous avons montré [8, 9] que l'on peut en général considérer l'existence de deux domaines différents pour la détermination de α^*. L'un est constitué par le milieu acide l'autre par le milieu alcalin. Les valeurs α^* sont respectivement α_a^* et α_b^*, les droites correspondantes $pH_{lu} = f(pH_{réel})$ coupent la droite de pente unité en des points noté pH_E et pH'_E. La valeur pH_E est relative à l'opération préliminaire unique de standardisation [4]. L'expression [5] conduit aux relations [6] et [7] pour les milieux précités.

$$pH_{lu} = \alpha_a^* \log \frac{V+v}{v_e - v} + D'_a \quad \text{si} \quad \frac{C_{OH^-}}{m} << \frac{v_e - v}{V+v} \quad (6)$$

avec $D'_a = -\alpha_a^* \log m\,\gamma_{H^+} - pH_E\,(\alpha_a^* - 1)$

$$pH_{lu} = \alpha_b^* \log \frac{v - v_e}{V+v} + D'_b \quad \text{si} \quad \frac{C_{H^+}}{m} << \frac{v - v_e}{V+v} \quad (7)$$

avec $D'_b = \alpha_b^*\, pK_w + \alpha_b^* \log m\,\gamma_{H^+} - pH'_E\,(\alpha_b^* - 1)$

Les graphes correspondants [8] se coupent en un point repéré par un astérisque tel que l'on ait l'égalité

$$pH^* = \frac{pH^*_{lu}}{\alpha_a^*} + pH_E\left(1 - \frac{1}{\alpha_a^*}\right) = \frac{pH^*_{lu}}{\alpha_b^*} + pH'_E\left(1 - \frac{1}{\alpha_b^*}\right) \quad (8)$$

d'où l'on déduit l'expression (9) en tenant compte des relations précédentes:

$$pK_w = \frac{2}{\alpha_a^* + \alpha_b^*}\left(D'_a \frac{\alpha_b^*}{\alpha_a^*} + D'_b\right) + 2\,pH_E\left(1 - \frac{1}{\alpha_a^*}\right) \quad (9)$$

Les paramètres α_a* et α_b* englobent les effets produits par de faibles perturbations des mesures dues: à l'erreur d'alcalinité de l'électrode de verre, aux variations de son potentiel d'assymétrie, à celle du potentiel de jonction liquide, ou encore à une faible carbonation du réactif titrant.

Nos résultats sont en accord avec la littérature [10,11]. Liberti et Light [12] admettent une variation linéaire des potentiels de jonction liquide à force ionique 0,5 M en fonction des concentrations, soit en protons, soit en hydroxyles comprises entre $5 \cdot 10^{-3}$ et $8 \cdot 10^{-2}$ mol l^{-1}. De même notre point de vue revient à écrire en partant de la relation de Nernst avec
$pH = -\log (C_H \gamma_{H^+})$

l'expression (10) où E_j est le potentiel de jonction

$$E = E^0 - k\mathrm{pH} - E_j \tag{10}$$

soit pour l'opération préliminaire de standardisation repérée par l'indice E et pour toute autre mesure

$$(E_E - E^0 + E_{jE})/k = -\mathrm{pH}_E \tag{11}$$

$$(E - E^0 + E_{jE})/k = -\mathrm{pH}_{lu} \tag{12}$$

L'ensemble des relations précédentes permet d'écrire l'éqn. (13) pour le milieu acide et une expression semblable en milieu alcalin ($E_{j\mathrm{b}}$).

$$E_{j\mathrm{a}} = E_{jE} + (\mathrm{pH}_{lu} - \mathrm{pH}_E)(\alpha_a* - 1)\, k/\alpha_a* \tag{13}$$

On peut admettre aux extrémités de l'intervalle de variation de pH_{lu} une variation quasi linéaire de $E_{j\mathrm{a}}$ et $E_{j\mathrm{b}}$ en fonction des concentrations en protons.

En conclusion de ce mode d'exploitation nous notons que les éqns. (6) et (7) considérées dans les domaines où elles sont applicables permettent une détermination des grandeurs paramétriques utilisables par la suite en tout point du titrage.

(2) Cependant le développement de l'éqn. (5) donnant le volume v de réactif en fonction des autres grandeurs de cette expression conduit à la fonction monotone continue (relation 14) applicable dans chacun des deux domaines précédemment définis sans hypothèse restrictive contrairement aux expressions simplifiées (6) et (7).

$$v = \frac{v_e - V(10^{-(\mathrm{pH}_{lu}/\alpha*) + D_1} - 10^{(\mathrm{pH}_{lu}/\alpha*) - D_2})}{1 + 10^{-(\mathrm{pH}_{lu}/\alpha*) + D_1} - 10^{(\mathrm{pH}_{lu}/\alpha*) - D_2}} \tag{14}$$

où

$$D_1 = -\log m\, \gamma_{H^+} - \mathrm{pH}_E\,(1 - (1/\alpha*)) \tag{15}$$

$$D_2 = \log m\, \gamma_{H^+} - \mathrm{pH}_E\,(1 - (1/\alpha*)) + \mathrm{p}K_w \tag{16}$$

Dans ces conditions il est théoriquement possible d'ajuster $v = f(\mathrm{pH}_{lu})$ sur l'ensemble des points expérimentaux. Toutefois l'examen des résultats obtenus initialement à l'aide des éqns. (6) et (7) appliquées à des titrages d'acides forts pris à des concentrations comprises entre $1{,}76 \cdot 10^{-4}$ mol l^{-1}

et $3{,}21 \cdot 10^{-2}$ mol l^{-1} montre (Tableau 1) que dans chaque essai la différence entre les valeurs α_a* et α_b* est faible quoique le plus souvent significative. A partir de ces constations trois hypothèses sont envisagées par la suite.

La première suppose pour α* une valeur unique ajustable sur l'ensemble du titrage. La deuxième admet une variation linéaire de ce paramètre en fonction du pH en tout point du titrage alors que la troisième ne considère de variation linéaire de α* qu'à partir du point d'équivalence. Une étude comparée de ces différentes hypothèses est présentée dans le Tableau 2 et porte sur le dernier exemple du Tableau 1 ($C_{acide} = 3{,}2 \cdot 10^{-2}$ mol l^{-1}).

D'une façon générale les trois cas donnent une valeur unique pour le paramètre d'équivalence v_e, compatible avec celle observable graphiquement. Bien que les trois types d'exploitation comparés à celui du Tableau 1 ne conduisent pas à des résultats très différents, mise à part la remarque concernant v_e, nous avons choisi pour la suite de nos investigations de retenir le troisième cas qui traduit généralement le mieux le comportement connu de la pile à électrode en verre [13] en milieu alcalin. L'utilisation d'une équation unique applicable sans approximation à l'ensemble du titrage réalise un progrès au niveau de la théorie et de l'exploitation qui s'en trouve simplifiée.

PARTIE EXPERIMENTALES

Produits, réactifs et appareillage

Les produits utilisés sont des produits très purs (Merck) ou purifiés au laboratoire suivant les procédés classiques [14]. La solution de soude servant de réactif a la même force ionique que le milieu à doser et s'obtient à partir d'une lessive R.P. Prolabo.

La pile de mesure se compose d'une électrode de travail en verre à haute impédance (Metrohm, type EA 109 U ou équivalent) et d'une électrode de référence au calomel à double jonction (Tacussel, type RDJ/C10). D'autres électrodes ont fait l'objet de travaux antérieurs [2]. L'appareil de mesure est un pH-mètre au millième d'unité de pH (Beckman, type "Research"). La burette de précision (Metrohm 298) a été préalablement étalonnée [5]. Les mesures sont faites dans une cellule thermorégulée au centième de degré.

Méthode

L'eau servant à la préparation aussi bien des solutions titrées que de celles à doser ne doit pas contenir de CO_2 dissous [15, 16]. Le montage (Fig. 2) permet de satisfaire cette exigence en réalisant la purification du solvant et la préparation du réactif et des solutions acides dans une enceinte étanche purgée par un courant d'hélium ou d'hydrogène. Il comprend un appareil à distiller muni d'un ballon A des récupération du filtrat. Le tube de dérivation B permet soit de renvoyer l'eau distillée dans le bouilleur soit d'alimenter le réservoir D de préparation et de stockage de la solution de soude, ou encore de prélever par S_1 la quantité d'eau nécessaire à l'élaboration

TABLEAU 1

Resultats des titrages d'acides forts
(Ajustement des éqns. (7) et (8) respectivement sur les zones acides et basiques délimitées dans le tableau par des parenthèses. Température de la cellule 25 ± 0,01°C; σ_v = 0,0011; $\sigma_{pH_{lu}}$ = 0,001; pH_E = 1,098 (standardisation avec HCl 0,1 M); I = force ionique fixée par $NaNO_3$; t = paramètre du test de Student.)

C acide mol l^{-1}	I mol l^{-1}	V ml	Domaine de pH_{lu} exploité	$\alpha^*_{a\text{ ou }b} \pm t\,\sigma_{\alpha^*_{a/b}}$	$D_{a\text{ ou }b} \pm t\,\sigma_{D_{a/b}}$	$v_{ea\text{ ou }b} \pm t\,\sigma\,v_e$ ml	σ ext	Nombre de points	pK_w
$1.76 \cdot 10^{-4}$	0,20	50,00	(3,879—5,753)	$1{,}025 \pm 1 \cdot 10^{-2}$	$1{,}72 \pm 2 \cdot 10^{-2}$	$0{,}400 \pm 1 \cdot 10^{-3}$	$8{,}5 \cdot 10^{-4}$	18	13,24 ± 0,20
			(8,632—10,163)	$1{,}133 \pm 2 \cdot 10^{-2}$	$12{,}33 \pm 4 \cdot 10^{-2}$	$0{,}420 \pm 3 \cdot 10^{-3}$	$1{,}7 \cdot 10^{-3}$ 1	20	
$1{,}95 \cdot 10^{-2}$	0,71	40,00	(1,644—4,423)	$0{,}997 \pm 2 \cdot 10^{-3}$	$0{,}089 \pm 4 \cdot 10^{-3}$	$1{,}0994 \pm 4 \cdot 10^{-4}$	$5 \cdot 10^{-4}$	31	13,77 ± 0,05
			(9,526—11,634)	$0{,}970 \pm 1 \cdot 10^{-2}$	$13{,}47 \pm 2 \cdot 10^{-2}$	$1{,}109 \pm 1 \cdot 10^{-3}$	$1{,}1 \cdot 10^{-3}$	20	
$3{,}20 \cdot 10^{-2}$	0,64	40,00	(1,572—4,452)	$1{,}014 \pm 3 \cdot 10^{-3}$	$0{,}202 \pm 4 \cdot 10^{-3}$	$2{,}0028 \pm 7 \cdot 10^{-4}$	$9 \cdot 10^{-4}$	32	13,88 ± 0,05
			(9,916—12,144)	$0{,}982 \pm 4 \cdot 10^{-3}$	$13{,}643 \pm 6 \cdot 10^{-3}$	$2{,}0102 \pm 8 \cdot 10^{-4}$	$8{,}6 \cdot 10^{-4}$	25	

TABLEAU 2

Comparaison des résultats de trois hypothèses différentes
(Ajustement de l'éqn. (16) sur le titrage (C acide = $3{,}2 \cdot 10^{-2}$ mol l^{-1}) pour les domaines expérimentaux indiqués entre crochets.
Force ionique = 0,64 mol l^{-1}; V = 40,00 ml; σ_v = 0,0011 ml; $\sigma_{pH_{lu}}$ = 0,001; θ = 25 ± 0,01°C. (1) α^* unique; (2) $\alpha^* = \alpha_0 + \alpha_1\, pH_{lu}$;
(3) $\begin{cases} \alpha^* = \alpha'^*_a + \alpha'^*_b\ (pH_{lu} - pK_w/2) \\ \alpha^* = \alpha'^*_a \text{ si } (pH_{lu} < pK_w/2) \end{cases}$ t = paramètre du test de Student.)

Type d'exploitation	Domaine de pH_{lu} exploité	α^* ± $t\,\sigma_{\alpha^*}$	α_0 ou α'^*_a ± $t\,\sigma_{\alpha_0/\alpha'^*_a}$	α_1 ou α'^*_b ± $t\,\sigma_{\alpha_1/\alpha'^*_b}$	D_1 ± $t\,\sigma_{D_1}$	D_2 ± $t\,\sigma_{D_2}$	v_e ± $t\,\sigma_{v_e}$	σ ext	Nombre de points	pK_w
(1)	(1,572—4,452)	1,014 ± $3 \cdot 10^{-3}$	—		0,200 ± $4 \cdot 10^{-3}$	13,894 Fixe	2,0028 ± $7 \cdot 10^{-4}$	$8 \cdot 10^{-4}$	32	13,90 ± 0,05
	(9,916—12,144)	0,982 ± $4 \cdot 10^{-3}$	—		0,200 Fixe	13,894 ± 0,04	2,0102 ± $8 \cdot 10^{-4}$	$8 \cdot 10^{-4}$	25	
	(1,572—12,144)	1,013 ± $4 \cdot 10^{-3}$	—		0,202 ± $8 \cdot 10^{-3}$	13,52 ± $4 \cdot 10^{-2}$	2,0037 ± $1 \cdot 10^{-3}$	$2.18 \cdot 10^{-3}$	57	13,75 ± 0,05
(2)	(1,572—12,144)		1,027 ± $7 \cdot 10^{-3}$	−0,0012 ± $5 \cdot 10^{-4}$	0,182 ± $1 \cdot 10^{-2}$	13,52 ± $4 \cdot 10^{-2}$	2,0056 ± $1 \cdot 10^{-3}$	$1{,}82 \cdot 10^{-3}$	57	13,76 ± 0,05
(3)	(1,572—12,144)		1,022 ± $4 \cdot 10^{-3}$	−0,0014 ± $5 \cdot 10^{-4}$	0,186 ± $1 \cdot 10^{-2}$	13,50 ± $4 \cdot 10^{-2}$	2,0057 ± $1 \cdot 10^{-3}$	$1{,}77 \cdot 10^{-3}$	57	13,73 ± 0,05

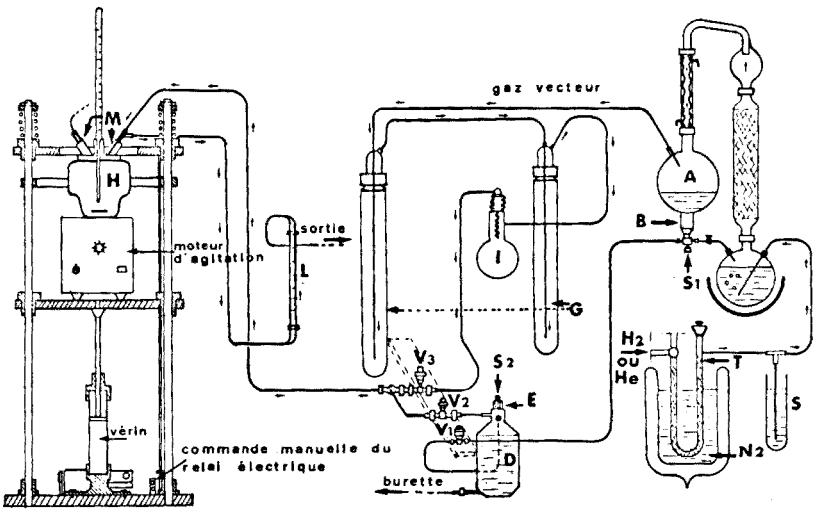

Fig. 2. Montage experimentale.

de la solution à analyser. Ce prélèvement se fait avec une seringue ou une burette à piston reliée à S_1.

Le réservoir D est fermé dans sa partie supérieure par un tube E permettant l'introduction du sel de fond, puis, après dégazage celle de la lessive de soude concentrée qui est alors injectée à l'aide d'une seringue à travers le bouchon étanche S_2. L'ensemble du dispositif est balayé par le courant gazeux traversant au préalable un tube en U rempli de tamis moléculaire T et immergé dans de l'azote liquide. Ce gaz barbote dans le bouilleur rempli de soude puis après une détente dans deux vases d'expansion G montés en série il est canalisé vers la cellule H en passant par une soupape antiretour. La cellule H et le flacon D peuvent être isolés grâce à un ensemble de vannes en acier inoxydable. La dilution de la solution concentrée de soude est commandée par une vanne V_1 tandis que V_2 permet une entrée de gaz au moment de l'aspiration du réactif par le piston de la burette. La vanne V_3 isole éventuellement la cellule H.

CONCLUSION

La détermination des 5 paramètres de l'étalonnage pour divers exemples donne les résultats des Tableaux 1 et 2. La méthode s'applique même aux milieux très dilués pour lesquels nous avons exploité des mesures parfaitement stables y compris au voisinage de la neutralité. Les écarts entre valeurs ajustées et expérimentales sont au maximum de l'ordre de grandeur de l'incertitude sur les mesures et présentent une répartition aléatoire.

Un titrage par cette méthode de l'acide polyméthacrylique permet de connaître rigoureusement la courbe de dissociation pH = f(α) dans

l'intervalle $\log(\alpha/(1-\alpha)) = \pm 3$ et d'aborder le calcul numérique de l'enthalpie libre de transition faisant l'objet d'un développement dans un prochain mémoire.

BIBLIOGRAPHIE

1 R. G. Bates, Determination of pH Theory and Practice, J. Wiley, New York, 1964.
2 S. Combet et C. Rossi, C.R. Acad. Sci., Sér. C, 271 (1971) 188.
3 S. Combet, Thèse Doctorat Sciences physiques, Montpellier, 1962.
4 C. Rossi et S. Combet, C.R. Acad. Sci., Sér. C, 274 (1972) 120.
5 C. Rossi, Thèse de Spécialité, Marseille 1972.
6 W. E. Wentworth, J. Chem. Educ., 42 (1965) 96.
7 W. E. Deming, Statistical adjustment of data, Dover Publ., New York, 1964.
8 C. Rossi et S. Combet, C.R. Acad. Sci. Sér. C. 280 (1975) 1195.
9 C. Rossi et S. Combet, J. Chim. Phys., 72 (1975) 3.
10 E. Ekedahll et L. G. Sillén, Ark, Kemi, 22A (1946) 7.
11 G. Biedermann et L. G. Sillén, Ark. Kemi, 5 (1953) 425.
12 A. Liberti et T. S. Light, J. Chem. Educ., 39 (1962) 236.
13 M. Dole, L'Électrode en Verre, Dunod, Paris, 1952.
14 D. D. Perrin et W. L. F. Armarego, Purification of Laboratory Chemicals, Pergamon Press, Oxford, 1966.
15 M. J. Welch, J. F. Lifton et A. Seck, J. Phys. Chem., 73 (1969) 3355.
16 J. T. Edsall et X. Wyman, Biophysical Chemistry, Academic Press, New York, 1958.

Analytica Chimica Acta, 89 (1977) 199—202

Short Communication

THE SPECTROPHOTOMETRIC DETERMINATION OF TITANIUM(IV) WITH SODIUM 2-BROMO-4,5-DIHYDROXYAZOBENZENE-4'-SULFONATE IN THE PRESENCE OF CETYLTRIMETHYLAMMONIUM CHLORIDE

YOSHINOBU WAKAMATSU

Department of Industrial Chemistry, Hachinohe Technical College, Hachinohe 031 (Japan)

(Received 19th April 1976)

The formation of ternary complexes often improves the sensitivity and selectivity of an analytical method. During studies on the sensitizing effects of cationic surfactants on the reaction of sodium 2-bromo-4,5-dihydroxyazobenzene-4'-sulfonate (abbreviated as BDAS) with various metal ions [1, 2], the addition of cetyltrimethylammonium chloride (CTMAC) to the titanium(IV)—BDAS complex was found to produce a large bathochromic shift in the wavelength of maximum absorption, and a marked increase in the molar absorptivity. This communication describes a sensitive method for the spectrophotometric determination of titanium(IV) by means of this ternary complex. The sensitivity is comparable to, or greater than that of methods based on hydrogen peroxide and xylenol orange [3], 4-(2-pyridylazo)-resorcinol [4] or chromazurol S [5]; 1,3-diphenylguanidine and indoferron [6] or tiron [7]; hexamethylenetetramine and stilbazo [8]; or diantipyrylmethane and pyrogallolsulfonic acid [9].

Experimental

Reagents. The BDAS used was synthesized from 4-bromopyrocatechol and sodium sulfanilate as described previously [1].

A standard titanium(IV) solution was prepared by dissolving the hydrolysis product of pure titanium(IV) chloride in 3 M sulfuric acid and diluting with water. It was standardized complexiметrically and diluted with water as required.

The CTMAC solution was prepared in aqueous 20 % (v/v) methanol.

All the other chemicals used were of analytical grade.

Apparatus. A Hitachi model 124 spectrophotometer with 10-mm quartz cells and a Toa Dempa model HM-5A pH meter were used.

Procedure. Transfer an aliquot of titanium(IV) solution to a 25-ml volumetric flask. Add 4 ml of 10^{-3} M BDAS, 10 ml of buffer solution (0.25 M monochloroacetic acid and 0.25 M sodium acetate adjusted to pH 2.8—3.0), and 3.5 ml of 10^{-2} M CTMAC. Dilute to the mark with water. Measure the absorbance at 515 nm against a reagent blank.

Results and discussion

Absorption spectra. The absorption spectra of the reagent and its titanium(IV) chelate at pH 2.9 in the presence of an excess of CTMAC are shown in Fig. 1. Included for comparison is the spectrum of the binary titanium(IV)—BDAS chelate formed at pH 5.0. The ternary complex has an absorption maximum at 515 nm and is stable for at least several hours. The binary complex with its absorption maximum at 490 nm is stable at pH 5 for several hours, but is completely dissociated below pH 3. For the determination of titanium, the ternary complex is superior to the binary one in regard to sensitivity and selectivity.

Effects of experimental conditions. Standard amounts of titanium(IV), BDAS and CTMAC solutions were buffered at varying pH values. A plot of absorbance against pH showed that maximal and constant absorbance was obtained at pH 2.6—4.6. Subsequent determinations were carried out at pH 2.9, because the absorbance of the reagent blank increased markedly above pH 3.5.

The effect of the CTMAC concentration on the complex formation was investigated for solutions containing 9.4 μg of titanium ($7.8 \cdot 10^{-6}$ M). Maximum color formation was found when the CTMAC concentration exceeded $8.0 \cdot 10^{-4}$ M. It was also found that both the titanium(IV) complex and the reagent are precipitated when less than about $3 \cdot 10^{-4}$ M CTMAC is added. This suggests that the uncharged titanium(IV)—BDAS—CTMAC and BDAS—CTMAC species are present as finely dispersed particles protected within the CTMAC micelles in solution.

The effect of the BDAS concentration on the color formation was then investigated by varying the BDAS concentration. A constant absorbance was obtained when the BDAS concentration exceeded $1.0 \cdot 10^{-4}$ M.

Calibration curve. With the above optimal conditions, a linear calibration curve was obtained over the concentration range 0—14 μg of titanium. The

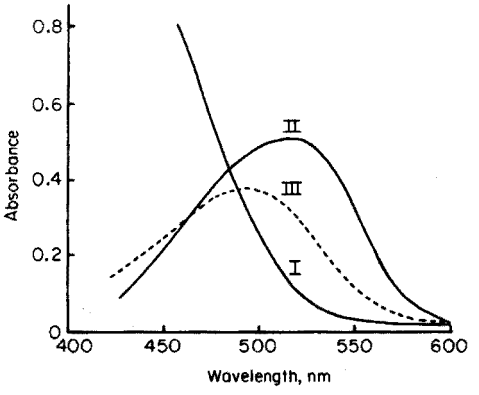

Fig. 1. Absorption spectra. (I) [BDAS] = $1.6 \cdot 10^{-4}$ M; [CTMAC] = $1.4 \cdot 10^{-3}$ M; pH 2.9; reference, water. (II) [Ti] = 9.4 μg ($7.8 \cdot 10^{-6}$ M); [BDAS] = $1.6 \cdot 10^{-4}$ M; [CTMAC] = $1.4 \cdot 10^{-3}$ M; pH 2.9; reference, reagent blank. (III) [Ti] = 9.4 μg; [BDAS] = $1.6 \cdot 10^{-4}$ M; pH 5.0; reference, reagent blank.

apparent molar absorptivity was calculated to be $6.2 \cdot 10^4$ l mol^{-1} cm^{-1} at 515 nm, and the sensitivity of the reaction was $7.3 \cdot 10^{-4}$ μg cm^{-2}.

Nature of complex. The titanium : BDAS ratio in the ternary complex formed at pH 2.9 was determined by the continuous variations method to be 1 : 3. The mole ratio method confirmed this conclusion.

Effect of foreign ions. The effect of foreign ions on the determination of 9.6 μg of titanium was studied. Of the anions examined, chloride, nitrate and sulfate ions showed no interference at all concentrations; fluoride, thiosulfate, citrate and nitrilotriacetate ions did not interfere in 100-fold molar amounts, or tartrate and phosphate ions in 10-fold amounts. Perchlorate ion, however, must be absent.

About 100-fold concentrations of divalent metal ions, such as nickel, cobalt, cadmium, zinc, lead, calcium and magnesium, did not interfere. The results for the other ions examined are presented in Table 1. Some of the interfering ions could be masked by EDTA, although too large excess of EDTA gave negative errors.

The color development of the ternary complex was retarded by addition of EDTA. The reaction time was measured in the absence of EDTA and in the presence of $8.0 \cdot 10^{-4}$ M EDTA (100 times that of the titanium), the EDTA being added before the BDAS. About 100 min was required to obtain maximal absorbance of the ternary complex in the presence of EDTA, only a few min being sufficient when it was absent. If EDTA is used as a masking agent for interfering ions, therefore, the absorbance should be measured 2 h after preparation of the final solution.

Analysis of standard steel sample. The proposed method was applied to the determination of titanium in a standard steel sample NBS 6f. The procedure was as follows: decompose the sample with equal volumes of hydrochloric and nitric acids, and after removal of insoluble materials, separate the iron(III) by ether extraction from a 6 M hydrochloric acid solution; add EDTA as a

TABLE 1

Effect of foreign ions for the determination of 9.6 μg of titanium(IV)

Ion	Added ([Ion]/[Ti])	Ti found (μg)	Ion	Added ([Ion]/[Ti])	Ti found (μg)
Cu(II)	50	9.7	Th(IV)	50	10.2
Ga(III)	1	11.8	Zr(IV)	1	11.5
	10	9.6[a]		1	9.9[a]
Al(III)	50	9.8	U(VI)	1	10.1
In(III)	5	9.8	W(VI)	1	11.1
	50	10.2		10	10.0[b]
Fe(III)	1	12.0	Mo(VI)	1	17.3
	50	9.6[a]		1	13.4[c]

[a] 2 ml of 10^{-2} M EDTA added. [b] 1 ml of 0.1 M sodium citrate added. [c] 2 ml of 10^{-2} M sodium tartrate added.

masking agent for minute amounts of iron and other interfering ions, and determine the titanium content as described above.

An average value of 0.061 % was obtained (certificate value, 0.063 %).

The author is grateful to Dr. M. Otomo of Nagoya Institute of Technology for his critical reading of the preliminary manuscript and valuable suggestions.

REFERENCES

1 Y. Wakamatsu and M. Otomo, Anal. Chim. Acta, 79 (1975) 322.
2 Y. Wakamatsu and M. Otomo, unpublished.
3 M. Otomo, Bull. Chem. Soc. Jpn., 36 (1963) 1341.
4 T. Ozawa, Bunseki Kagaku, 16 (1967) 435.
5 H. Nishida, Bunseki Kagaku, 19 (1970) 30.
6 Y. Wakamatsu and M. Otomo, Bunseki Kagaku, 20 (1971) 862.
7 Y. Wakamatsu and M. Otomo, Bull. Chem. Soc. Jpn., 45 (1972) 2764.
8 T. Ozawa, Nippon Kagaku Zasshi, 92 (1971) 522.
9 A. I. Busev and N. G. Solovieva, Zh. Anal. Khim., 27 (1972) 1283.

Analytica Chimica Acta, 89 (1977) 203—207

Short Communication

PREVENTION OF ^{15}N CROSS-CONTAMINATION DURING DISTILLATION AND POTENTIOMETRIC TITRATION OF ^{15}N-LABELLED SAMPLES

P. G. SAFFIGNA* and S. A. WARING

Department of Agriculture, University of Queensland, St. Lucia, Queensland 4067 (Australia)

(Received 3rd May 1976)

Nitrogen-15 is widely used to study the fate of nitrogen in soil, plant and aquatic systems [1]. However, many errors may occur during sample preparation and analysis [2, 3]. During steam distillation of ammonia, cross-contamination may occur between samples unless special precautions are taken [4, 5]. The use of metal components in the distillation unit, and proper steaming of the condenser between distillations virtually eliminates memory effects [6, 7]. Photometric [8] and potentiometric [9] methods have been used; cross-contamination has not been reported with the glass electrode [6, 10].

During preliminary evaluations of a stainless-steel modification of the distillation apparatus and of an automatic potentiometric titration unit, memory effects were found when ^{15}N-labelled ammonium sulphate was distilled and titrated before unlabelled ammonium sulphate. Further results showed that ^{15}N cross-contamination occurred by retention of ^{15}N-labelled ammonia/ammonium on the glass electrode, and on the stainless-steel condenser. Methods are described here for preventing isotopic cross-contamination during routine distillation and titration of samples from ^{15}N tracer studies.

Experimental

Apparatus. A stainless-steel modification of an earlier glass assembly [5] was used. The major modification was the stainless-steel dismountable spray trap (Fig. 1); the condenser was a stainless-steel tube surrounded by a water jacket. The spray trap is easy to make and clean, and differential thermal expansion between the thin metal cone and the ground-glass socket of the distillation flask caused no problems. The water jacket is rapidly emptied for condenser steaming by opening the tap of the filter pump on the cooling water supply.

Titrations were done automatically with a Metrohm Herisau automatic titration assembly.

---

*Present address: Department of Soil Science, Lincoln College, Canterbury, New Zealand.

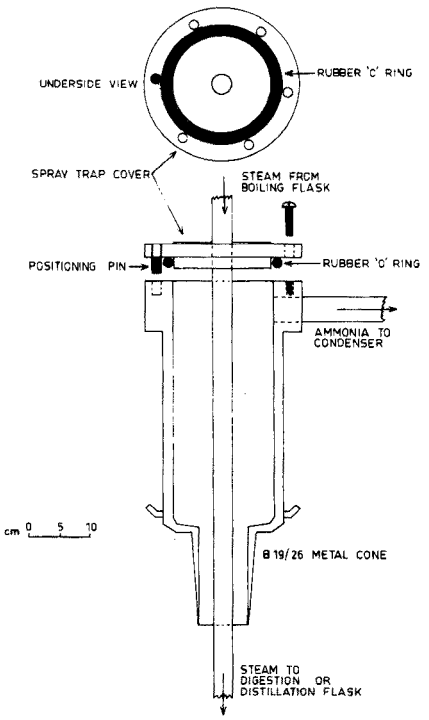

Fig. 1. Stainless-steel spray trap.

Reagents. For the ammonium borate wash solution (ca. 2 M, pH 7.6), steam-distil 150 ml of reagent-grade ammonium sulphate into 150 ml of 2 % boric acid and make up to 1 l with deionized water. Magnesium oxide, Devarda alloy, standardized sulphuric acid (0.005 M, 0.03 M) and 10 M sodium hydroxide were as described previously [8, 11], as were boric acid (2 %), hydrofluoric acid (1 %) and sulphuric acid (0.05 M) [12].

Procedure. Steam-distil samples with sodium hydroxide (or magnesium oxide, then Devarda alloy) into boric acid [8, 11]. Between samples steam out the metal condenser for 2 min by emptying the water jacket and distilling a 15-ml aliquot of deionized water without added reagents. Rinse all distillation and digestion flasks with hydrofluoric acid to prevent memory effects [12]. Potentiometrically titrate the distillates (pH 7.5—8.5) to pH 5.0 with dilute sulphuric acid. Remove the beaker from the electrode and rinse the electrode with deionized water. Place a beaker containing 35 ml of ammonium borate wash solution (pH 7.5—8.5) under the electrode and stir for 30 s. Remove the beaker and rinse the electrode with deionized water before the next titration. Rinse sample beakers with hydrofluoric acid to prevent memory effects. Acidify the titrated distillates to pH ca. 3.0 with 1 ml of 0.05 M sulphuric acid before conversion to nitrogen gas as described previously [12]. Mass spectrometric analysis of the nitrogen gas was done with an AEI MS-20 double collector mass spectrometer [13].

The 2-min steaming of the metal condenser removes any residual ^{15}N (and ^{14}N), and the ammonium borate wash replaces any ^{15}N-labelled ammonium on the glass electrode with unlabelled ammonium, so preventing any cross-contamination.

Results

Condenser memory. A small proportion (0.11 %) of ^{15}N-labelled ammonia/ammonium was retained by the stainless-steel condenser after steam distillation of ^{15}N-labelled ammonium sulphate. Newman [7] reported a similar memory (0.09 %) with a silver condenser. The ammonium retained by the stainless-steel condenser increased the enrichment of the following unlabelled sample from 0.000 to 0.010 atom % excess ^{15}N. There was no carry-over of ^{15}N into the next unlabelled sample distilled after this contaminated distillate. When ^{15}N-labelled ammonium sulphate was distilled after an unlabelled sample, there was no significant memory effect (Table 1). This was expected if the memory was still 0.11 % as the contaminating 1.1 μg of ^{14}N (0.11 % of 1000 μg ^{14}N) would not appreciably contribute to the 885 μg ^{14}N present in the labelled solution. Washing the condenser for 2 min after distillation of the labelled ammonium sulphate halved the cross-contamination of the unlabelled

TABLE 1

Effect of condenser and electrode pre-treatments on ^{15}N-cross-contamination during distillation and titration of unlabelled and ^{15}N-labelled ammonium
(All values are means of 3 replicates.)

Approach for preventing cross-contamination	Enrichment of contaminated sample[a] (atom % excess ^{15}N)	Cross-contamination[b] (%)
No treatment		
Unlabelled ammonium after ^{15}N-labelled ammonium	0.013	0.14 (0.012)[c]
^{15}N-labelled ammonium after unlabelled ammonium	11.451	not detectable
2-min condenser wash only	0.007	0.08 (0.017)
2-min condenser steaming only	0.003	0.03 (0.010)
2-min condenser steaming and 30-s alkaline ammonium borate wash	0.000	0.00 (0.010)

[a] Values are for unlabelled ammonium after ^{15}N-labelled ammonium unless shown otherwise.
[b] Percentage of ^{15}N from the ^{15}N-labelled (11.457 atom % excess ^{15}N) solution measured in the unlabelled (0.000 atom % excess ^{15}N) ammonium. For ^{15}N-labelled ammonium distilled and titrated after unlabelled ammonium, the cross-contamination is calculated on a ^{14}N basis. The samples contained 1 mg of nitrogen.
[c] Figures in parentheses are standard deviations.

sample. Steaming the condenser for 2 min completely eliminated memory effects. Longer (4—5 min) steaming [6, 7] is unnecessary with the stainless-steel condenser used.

Electrode memory. A small proportion (0.03 %) of ^{15}N-labelled ammonia was retained by the glass electrode during titration of a ^{15}N-labelled distillate. This "sorbed" ammonium caused an enrichment of the following unlabelled distillate from 0.000 to 0.003 atom % excess ^{15}N. There was no carry-over of ^{15}N into another unlabelled distillate titrated subsequently. When a ^{15}N-labelled distillate was titrated after an unlabelled sample, the enrichment of the labelled sample was not affected significantly, as would be expected if the memory was 0.03 %. Washing the electrode with water between titrations did not reduce cross-contamination from labelled samples, but a 2-min wash with acidic (pH 5.0) ammonium borate solution reduced the memory from 0.03 % to 0.01 %. Washing for 30 s with alkaline (pH 8.0) ammonium borate solution completely eliminated cross-contamination. The retention (and release) of ammonia/ammonium by the glass electrode probably occurs in the first 30 s of titration when the distillate is still alkaline. During automatic titration, the initial rapid addition of acid neutralizes the alkaline distillate (ammonium borate) in 30 s and reduces the pH to 5.0 after a further 90 s. Only a small proportion is present as ammonia below pH 8.0 [14].

Memory during distillation and titration. When no precautions were taken during the entire distillation and titration stage, the cross-contamination from a ^{15}N-labelled to an unlabelled sample of ammonium sulphate was 0.14 % (Table 1). No memory effects were detected when a ^{15}N-labelled sample was distilled and titrated after an unlabelled sample. In agreement with the results obtained for the separate stages, cross-contamination during the entire procedure was eliminated when a 30-s alkaline ammonium borate wash of the electrode accompanied the 2-min steaming of the stainless-steel condenser (Table 1). This confirmed that the condenser and the electrode were the only cross-contamination sites.

Discussion

The efficacy of the above procedure under routine conditions was tested by distilling and titrating an unlabelled ammonium sulphate standard after an ^{15}N-labelled standard (11.457 atom % excess ^{15}N) with every batch of soil and plant samples analysed during one year. No ^{15}N contamination of the unlabelled standard was detected.

Although washing glass condensers with hot ethanol [5], hydrochloric acid [5], and hydrofluoric acid [4], have each proved successful in eliminating ^{15}N cross-contamination with glass condensers, they were not evaluated for routine use with the glass electrode. Hot ethanol washing would require prolonged reconditioning of the electrode, and hydrofluoric acid cannot be used on glass electrodes. Washing the electrode with hydrochloric acid between titrations is not recommended as very careful cleaning is necessary to remove residual acid.

When the electrode washing procedure is used with samples containing only a few μg of nitrogen (e.g. emission spectroscopy [10]) the concentration of the unlabelled ammonium borate wash solution should be reduced to avoid any carry-over of unlabelled ammonium.

The authors thank Dr. A. E. Martin for conducting a substantial number of the ^{15}N determinations, and Dr. D. R. Keeney for advice and constructive criticism of the manuscript.

REFERENCES

1 R. D. Hauck, J. Environ. Qual., 2 (1973) 317.
2 A. E. Martin, E. F. Henzell, P. J. Ross and K. P. Haydock, Aust. J. Soil Res., 1 (1963) 169.
3 J. M. Bremner, H. H. Cheng and A. P. Edwards in The Use of Isotopes in Soil Organic Matter Studies, Report of FAO/IAEA Tech. Meeting, Pergamon Press, Oxford, 1966, pp. 429—442.
4 R. Huser, Z. Anal. Chem., 197 (1963) 16.
5 J. M. Bremner and A. P. Edwards, Proc. Soil Sci. Soc. Amer., 29 (1965) 504.
6 A. E. Martin and P. J. Ross, Trans. 9th Int. Cong. Soil Sci., Int. Soc. of Soil Sci., Angus and Robinson, Sydney, 1968, pp. 521—529.
7 A. C. D. Newman, Chem. Ind., 3 (1966) 115.
8 J. M. Bremner and D. R. Keeney, Anal. Chim. Acta, 32 (1965) 485.
9 A. E. Martin and P. J. Ross, Pl. Soil, 28 (1968) 182.
10 R. Fiedler and G. Proksch, Anal. Chim. Acta, 78 (1975) 1.
11 J. M. Bremner, in C. A. Black et al. (Eds.), Methods of Soil Analysis, Part 2, Amer. Soc. Agron., Madison, Wis., 1965, pp. 1149—1178.
12 P. J. Ross and A. E. Martin, Analyst (London), 95 (1970) 817.
13 G. L. Kerven and P. G. Saffigna, 1st Aust. Conf. Mass Spectrometry, Macquarie Univ., N.S.W., 1971.
14 J. N. Butler, Ionic Equilibrium: A Mathematical Approach, Addison-Wesley, London, p. 132.

Analytica Chimica Acta, 89 (1977) 209—211

Short Communication

COPPER-SELECTIVE AND CADMIUM-SELECTIVE ELECTRODES AS INDICATOR ELECTRODES IN THE TITRATION OF VANADYL IONS WITH EDTA

ALDO NAPOLI and MARCO MASCINI

Istituto di Chimica Analitica, Città Universitaria, 00185 Roma (Italy)

(Received 2nd June 1976)

Ion-selective electrodes are used mainly for direct potentiometric determinations but they can also be applied in potentiometric titrations of some metal ions, e.g. Ni, Zn, Co, for which selective electrodes are not available. In such titrations, copper- and cadmium-electrodes have been used with a wide variety of chelating agents [1—5]; the ion to which the electrode is selective is added to the sample before titration and the change in its activity at the end-point is measured.

Precise, reliable and accurate determinations of vanadium are important for technological processes where classical titrations with permanganate or with colour indicators cannot be used. This communication reports a study of potentiometric titrations of vanadyl ions with EDTA, in which copper- and cadmium-selective membrane electrodes are used in different buffer systems.

Experimental

An AMEL (Milan) expanded-scale pH meter model 331 was used with AMEL copper- and cadmium-selective electrodes. A Beckman glass electrode was used for pH measurements. A double-junction saturated calomel electrode was employed as reference with KNO_3 in the outer compartment.

All chemicals were analytical reagent grade. Solutions utilized for the Reilley plots were 0.1 M in KNO_3. Copper- and cadmium-indicator stock solutions were prepared by titrating 0.1 M $Cu(NO_3)_2$ and $Cd(NO_3)_2$ with EDTA and stopping just before the end-point.

Results and discussion

Preliminary titrations of vanadyl ion in acetate buffer (pH 4.5) showed that better results were obtained with the cadmium electrode than with the copper electrode. This was somewhat surprising as higher potential jumps were expected from the copper electrode. Comparison of the formation constants of metal—EDTA complexes indicates the following order: $K_{Cd} < K_V < K_{Cu}$ ($K_{Cd} = 10^{16.46}$; $K_V = 10^{18.77}$; $K_{Cu} = 10^{18.80}$ [6]). If the complexing

effect of the buffer is neglected, the variation of pM (M being the free metal indicator ion) can be calculated for points between 50 % and 200 % of the equivalence point of the titration of vanadyl ion with EDTA, and it can be shown that the potential jump with the copper electrode should be higher than that with the cadmium electrode. However, the situation is different when the effects of the buffers are considered. Figures 1 and 2 show the pH—potential curves for the copper and cadmium electrodes, respectively; these are presented similarly by the method of Reilley and Schmid [7]. For each electrode three sets of curves are plotted, without buffer and with

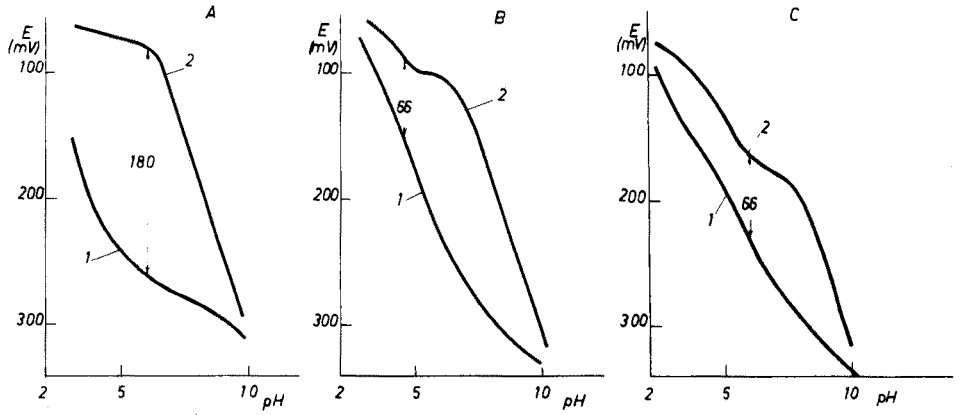

Fig. 1. Potential pH—diagrams for the copper electrode. A, no buffer. B, acetate buffer. C, maleate buffer. Curve 1: [CuEDTA] = 10^{-3} M; [VO^{2+}] = [VOEDTA] = 10^{-3} M. Curve 2: [EDTA] = [CuEDTA] = 10^{-3} M. The arrows indicate the maximum jump obtained in plot A, and in plots B and C the jumps at pH = pK of the buffers.

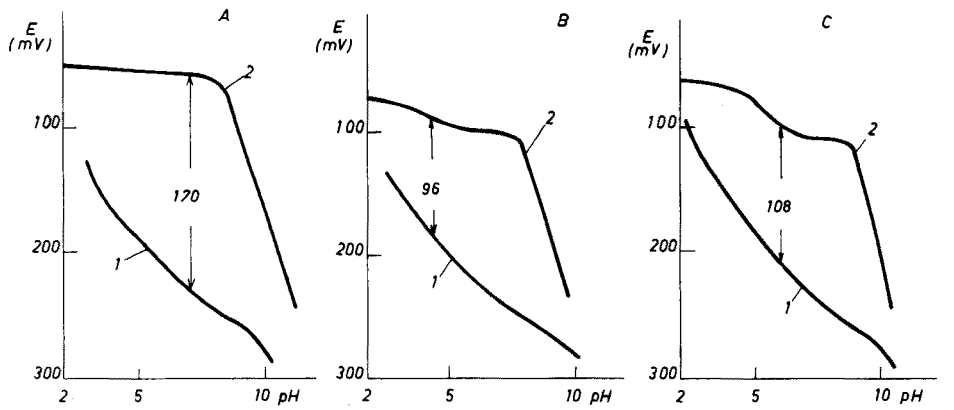

Fig. 2. Potential—pH diagrams for the cadmium electrode. A, no buffer. B, acetate buffer. C, maleate buffer. Curve 1: [CdEDTA] = 10^{-3} M; [VO^{2+}] = [VOEDTA] = 10^{-3} M. Curve 2: [EDTA] = [CdEDTA] = 10^{-3} M. The arrows indicate the maximum jump obtained in plot A, and in plots B and C the jumps at pH = pK of the buffers.

acetate and maleate buffers. These curves clarify why the potential jumps decrease when buffer systems are present. In unbuffered solutions, the potential jump with the copper electrode is greater than that with the cadmium one, in agreement with theoretical considerations, but in buffered solutions (acetate or maleate), the potential jump with the copper electrode is lower than that with the cadmium electrode. This effect is due to the complexing effect of the buffers on the metal ions. In Figs. 1 and 2 the potential jumps at pH 4.5 for the acetate buffer and at pH 6 for the maleate buffer are marked (pH = pK).

Figure 3 shows the titration curves obtained with different buffer systems with the copper- and cadmium-selective electrodes. The potential jump with the cadmium-selective electrode is much higher than that with the copper electrode with both buffers utilized, and it is obvious that reliable and precise end-points can be obtained only with the cadmium-selective electrode. With this system, useful titration curves could be achieved even for 10^{-4} M vanadyl solutions, the relative standard deviation being about 1 %.

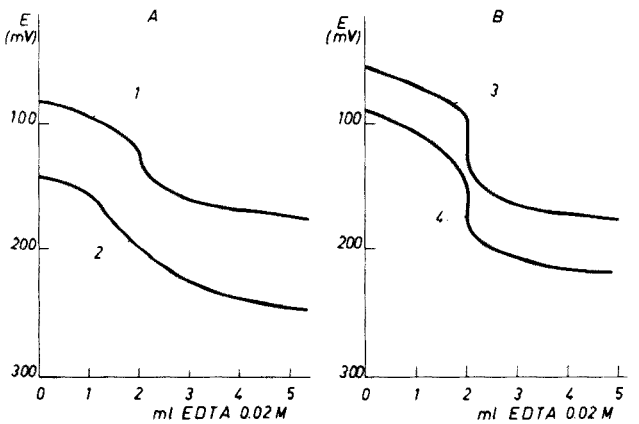

Fig. 3. Titration curves. A: 20 ml of solution ([Cu^{2+}] = [VO^{2+}] = 10^{-3} M) titrated with EDTA in the presence of acetate buffer (pH 4.5, curve 1) or maleate buffer (pH 6, curve 2). B: 20 ml of solution ([Cd^{2+}] = [VO^{2+}] = 10^{-3} M) titrated with EDTA in the presence of acetate buffer (pH 4.5, curve 3) and of maleate buffer (pH 6, curve 4).

REFERENCES

1 J. W. Ross Jr. and M. S. Frant, Anal. Chem., 41 (1969) 1900.
2 M. Mascini, Anal. Chim. Acta, 56 (1971) 316.
3 J. M. van der Meer, G. den Boef and W. E. van den Linden, Anal. Chim. Acta, 76 (1975) 261.
4 E. W. Bauman and R. M. Wallace, Anal. Chem., 41 (1969) 2072.
5 E. A. Moya and K. L. Cheng, Anal. Chem., 42 (1970) 1669.
6 G. Schwarzenbach, R. Gut and G. Anderegg, Helv. Chim. Acta, 37 (1954) 937.
7 C. N. Reilley and R. W. Schmid, Anal. Chem., 30 (1958) 947.

Analytica Chimica Acta, 89 (1977) 213—216

Short Communication

THE ATOMIC ABSORPTION SPECTROMETRIC DETERMINATION OF MANGANESE IN PYROLUSITE AFTER TREATMENT WITH HYDROXYLAMMONIUM CHLORIDE

S. MUKHOPADHYAY and B. P. CHATTERJEE

Chemical Laboratory, Geological Survey Department, Dodoma (Tanzania)

(Received 20th April 1976)

The rapid determination of manganese in pyrolusite is a longstanding problem. The conventional methods for the analysis of the oxide ores are tedious [1]. Spectrophotometry has been applied [2]. Atomic absorption spectrometry has been applied to the determination of manganese in rocks [3], cement [4], soil [5, 6] and plant materials [7], but not to ores.

This communication describes a relatively rapid and simple method for the determination of total manganese in pyrolusite. Hydroxylammonium chloride was found to be a very good substitute for acid in the dissolution of the ores; it reacts vigorously with pyrolusite even at room temperature, bringing all the manganese(IV) into solution as manganese(II) chloride. Only traces of the iron, aluminium, calcium, magnesium, barium, etc. present in the ore are dissolved, and there is no interference in the subsequent determination of manganese by atomic absorption spectrometry.

Treatment of the pyrolusite with an aqueous solution of hydroxylammonium chloride at ordinary temperature dissolves most of the manganese, leaving a small amount in the residue which can be recovered after fusion with sodium carbonate.

The accuracy and the precision of the proposed method were established by analysing standard manganese ores, and by comparing results for some unknown pyrolusites with those obtained by a classical method.

Experimental

Apparatus. A Pye-Unicam SP90 B atomic absorption spectrometer was used with a 10-cm slot burner head and a Pye-Unicam manganese hollow-cathode lamp. The instrumental parameters were: wavelength, 279.5 nm; slit width, 0.15 mm; lamp current, 4 mA; burner height, 0.8 cm; acetylene pressure, 0.7 kg cm^{-2} (10 p.s.i.); air pressure, 2.1 kg cm^{-2} (30 p.s.i.).

Manganese standard solution. Dissolve electrolytic manganese (99.00 % Mn) in aqueous 10 % hydroxylammonium chloride solution at room temperature. Dilute to give a stock solution containing 500 μg Mn ml^{-1}. Prepare working standards freshly by diluting with distilled water.

All the reagents were of analytical grade.

Recommended procedure. Transfer 0.2 g of powdered ore (100 mesh, dried at 100 °C) to a 200-ml beaker covered with a lid. Add 25 ml of aqueous 10 % hydroxylammonium chloride solution carefully, as there is a vigorous reaction even at room temperature. After subsidence of the reaction (10—15 min), rinse the lid and wall of the beaker with distilled water. Filter through a Whatman paper no. 42 into a 500-ml volumetric flask. Wash the residue with 5 ml of 1 % hydroxylammonium chloride solution 3—4 times and then with distilled water. Transfer the filter paper containing the residue to a platinum crucible, dry carefully and ignite. Fuse the residue with 1 g of anhydrous sodium carbonate in the crucible in the usual way, heating carefully until fusion is complete (10—15 min). After cooling, dissolve the melt in 10 ml of 5 % hydroxylammonium chloride solution at room temperature, and filter through a Whatman paper no. 42 into the 500-ml volumetric flask containing the original solution. Wash the residue with 5 ml of 1 % hydroxylammonium chloride 2—3 times and then with distilled water. Dilute the solution to the mark with distilled water and mix well. Dilute a suitable aliquot (5—10 ml, depending on the manganese content of the ores, as indicated approximately from the residue left after dissolution) to 100 ml with distilled water in a volumetric flask. Use this for the determination of manganese by atomic absorption spectrometry. Measure a blank of distilled water containing the same quantities of hydroxylammonium chloride and sodium carbonate.

Results and discussion

The accuracy and reproducibility of the proposed method were obtained by analysing three standards and five typical pyrolusite ores selected for their variety of manganese content (Pyr. 1—5). The results are shown in Table 1.

Some separate analyses for the hydroxylammonium chloride-soluble manganese (solution A) and that of the fused melt of the residue extracted with hydroxylammonium chloride (solution B) were carried out. The results (Table 2) show that the manganese content in the residue (solution B) was in the range 0.2—0.5 %, which proves clearly the effectiveness of hydroxylammonium chloride in bringing most of the manganese in the ore into solution.

The results in Table 2 show that the MnO_2 values obtained by conversion from the Mn value found in "solution A" are higher than the MnO_2 contents determined by the usual oxalate method. This indicates that the manganese present in forms other than MnO_2, probably bivalent, is also brought into solution by hydroxylammonium chloride. The manganese remaining in the residue is probably present as silicates.

In the recommended procedure, the final concentration of hydroxylammonium chloride ranges from 30 mg to 60 mg/100 ml. Tests showed that there was essentially no variation in the absorption signal of manganese (10 and 15 μg Mn ml^{-1}) when the solution contained 10—100 mg of hydroxylammonium chloride per 100 ml. Precise measurement of this reagent is therefore unnecessary.

TABLE 1

A comparison of results obtained by the atomic absorption and titrimetric methods on manganese ores

Sample	% Mn		
	A.a.s.[a]	Bismuthate method[b]	Certified mean value
B.C.S. A176[c]	51.24	51.44	51.3
B.A.S. 18[d]	51.16	51.32	51.2
B.A.S. 18aG[d]	58.33	58.50	58.3
Pyr. 1	36.64	36.56	—
Pyr. 2	23.69	23.75	—
Pyr. 3	42.58	42.65	—
Pyr. 4	31.53	31.47	—
Pyr. 5	55.13	55.28	—

[a]Each value is the mean of 5 determinations. [b]Each value is the mean of 3 determinations. [c]British Chemical Standard manganese ore. [d]Bureau of Analysed Samples, Ltd.

The main impurities in pyrolusite ores are SiO_2, Fe, Ca, Mg, Ba, Al and P along with traces of Cu, Ni, Pb, Ti, As, etc. In the proposed method, hydroxylammonium chloride extracts small quantities of Fe, Ca, Mg, Al and Ba along with traces of Cu, Ni, Pb, etc. It does not extract Si or P. The main extractable interfering elements were determined in the main solutions prepared by the recommended procedure. The results (Table 3) show that the main solutions (0.2 g of sample diluted to 500 ml) contain at the maximum

TABLE 2

Results of separate analyses of main solution and residue

Sample	Total Mn in soln. A[a] (%)	Total Mn in residue (soln. B) (%)	MnO_2 calcd.[b] (%)	Certified MnO_2 value (%)	MnO_2 (oxalate method[c] (%)
B.C.S. 176	50.94	0.35	80.60	77.90	77.96
B.A.S. 18	50.78	0.47	80.35	77.19	77.22
B.A.S. 18aG	58.00	0.47	91.77	89.75	89.63
Pyr. 1	36.15	0.42	57.20	—	55.33
Pyr. 2	23.32	0.43	36.89	—	33.50
Pyr. 3	42.43	0.25	67.13	—	66.11
Pyr. 4	31.16	0.45	49.30	—	46.02
Pyr. 5	55.14	0.28	87.24	—	82.90

[a]Each result is the mean of 5 a.a.s. analyses. [b]Results calculated as MnO_2 from the Mn contents of Solution A (column 2). [c]Each result is the mean of 3 analyses.

TABLE 3

Major extractable interfering elements found in the main solutions (All results in p.p.m.)

Sample		Ca	Mg	Fe	Al	Ba
B.C.S.	176	1.84	0.92	1.09	3.04	0.56
B.A.S.	18	1.87	1.42	2.07	0.87	0.79
B.A.S.	18aG	1.95	1.48	1.22	4.18	0.67
Pyr.	1	0.62	0.24	2.01	2.04	0.92
Pyr.	2	0.59	0.25	2.64	3.20	0.32
Pyr.	3	1.17	0.52	2.73	1.47	0.54
Pyr.	4	0.78	0.36	3.22	2.11	0.62
Pyr.	5	1.32	0.62	0.73	1.11	0.46

3.22 p.p.m. Fe, 1.95 p.p.m. Ca, 1.48 p.p.m. Mg, and 4.18 p.p.m. Al; these levels come much below the range of interference found by Allan [8] and Belcher and Kinson [9]. After the final dilution of solutions for the determination of manganese, the possible interfering elements become far more diluted than they were in the original solutions.

In the recommended procedure, 1 g of anhydrous sodium carbonate was used for the fusion of the residue left after the preliminary dissolution. The sodium content of the final diluted solution thus lies in the range 43—87 p.p.m., which is much below the range of interference reported by Allan.

The proposed method has several advantages over the classical one. Tedious acid digestions and other time-consuming steps are eliminated. The method can be successfully used for routine analyses for total manganese in pyrolusite.

REFERENCES

1 See e.g. A.S.T.M. Method of Chemical Analysis of Metals, 1960.
2 R. W. Bane, Analyst (London), 90 (1965) 756.
3 F. J. Langmyhr and P. E. Paus, Anal. Chim. Acta, 43 (1968) 397, 508.
4 J. T. H. Roos and W. J. Price, Analyst (London), 94 (1969) 89.
5 M. Nadorshaw and A. H. Confield, Analyst (London), 93 (1968) 475.
6 L. R. Hossner and L. W. Ferrara, At. Absorpt. Newsl., 6(3) (1967) 71.
7 F. Hoffman, Albrecht-Thear Arch., 11(6) (1967) 503.
8 J. E. Allan, Spectrochim. Acta, 10 (1959) 800.
9 C. B. Belcher and K. Kinson, Anal. Chim. Acta, 30 (1964) 483.

Analytica Chimica Acta, 89 (1977) 217—219

Short Communication

THE ATOMIZATION PROCESSES OF CALCIUM, ALUMINUM AND MANGANESE OXIDES ON A MOLYBDENUM FILAMENT

TSUNEO HASEGAWA, MASAAKI YANAGISAWA and TSUGIO TAKEUCHI

Department of Synthetic Chemistry, Faculty of Engineering, Nagoya University, Chikusa-ku, Nagoya (Japan)

(Received 10th October 1975)

The graphite furnace atomizer of L'Vov [1] is now widely employed in non-flame atomic absorption spectrometry, and it is well known that the reductive ability of carbon plays an important rôle in the atom formation processes. Thermodynamic and kinetic investigations have been made [2—4]. However, atomization processes on metal evaporation filaments have scarcely been studied.

The present communication shows that in atom formation processes on a molybdenum filament, the reductive ability of molybdenum also plays an important rôle.

Experimental

The atomization device with the molybdenum filament (Fig. 1) was used in combination with a Techtron atomic absorption spectrometer Model AA-4 and a Hitachi recorder Model QPD-54.

To obtain reproducible atomization curves, the form of the filament is very important; if temperature gradients exist where the sample solutions are applied, the atomization peaks broaden. Filament temperatures were measured with an optical pyrometer and corrected for spectral emissivity. Preheating to eliminate the solvent (water), which was followed by the atomization step, was done rapidly at a temperature above 100°C. Power to the filament was supplied through a Variac and transformer. All atomic absorption

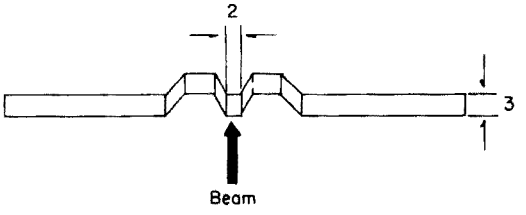

Fig. 1. The molybdenum filament atomizer, (50 mm long, 2 mm wide and 0.05 mm thick). The light beam is 1 mm in diameter.

measurements were made with Hitachi hollow-cathode lamps; the lamp beam was condensed to a very narrow beam (about 0.8 mm diameter) by a slit and lens placed just before the atomizer. Argon was used as the inert gas at a flow rate of 1.7 l min^{-1}. The reducing gas was a mixture of 5 % hydrogen in argon at a flow rate of 1.7 l min^{-1}.

Standard solutions were prepared by dissolving the pure metals (aluminum and manganese) or carbonate (calcium) in the minimum quantity of nitric acid and then diluting appropriately with deionized water.

Solutions were placed on the filament with microliter syringes.

Results and discussion

Metal nitrates are readily converted to metal oxides by thermal decomposition, so that the atomization peaks observed should correspond to atomization processes from metal oxides. Two mechanisms of atom formation are possible: thermal decomposition and reduction by molybdenum

$$M_m O_{2n} \rightarrow mM + nO_2 \quad (1)$$

$$M_m O_{2n} + kMo \rightarrow mM + Mo_k O_{2n} \quad (2)$$

Thermodynamically, reaction (2) is favored, because the standard free energies of formation of molybdenum oxides are negative. The atomization rate in a reducing atmosphere is greater than in an argon atmosphere (Fig. 2), which shows that the evaporation step does not control the rate of atomization. Therefore, the atomization curves show directly either reaction (1) or (2). If reaction (1) occurs, the atomization curves should be exponential, indicating a first-order reaction, and this is not so (Fig. 2). If reduction by molybdenum occurs, the atomization peaks should be controlled by the contact area between the metal oxides and the filament; thus the form of the sample crystals, which depends on the temperature used to eliminate solvent (water), and the amount of sample, contribute to the atomization

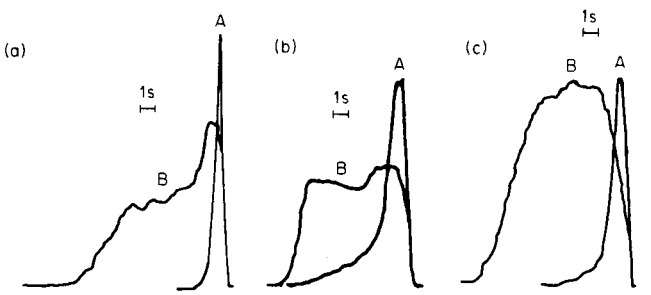

Fig. 2. Atomization curves. (a) Calcium oxide. A: 10 mm above filament at 1780 °C in hydrogen. B: 2 mm above filament at 1760 °C in argon. (b) Manganese oxide. A: 12 mm above filament at 1440 °C in hydrogen. B: 2.5 mm above filament at 1400 °C in argon. (c) Aluminum oxide. A: 7 mm above filament at 1840 °C in hydrogen. B: 1 mm above filament at 1870 °C in argon. In all cases, the filament temperature was reached within 2 s.

of metal oxides. In this work the solvent was eliminated rapidly above 100 °C, the sample density being about 1 μg mm^{-2}. This amount visibly covered almost all the sampling area. The contact area remained almost constant over a time range while the amount of sample was reduced. Figure 2 shows that the model described can be applied.

REFERENCES

1 B. V. L'Vov, Spectrochim. Acta, 17 (1961) 17.
2 W. C. Campbell and J. M. Ottaway, Talanta, 21 (1974) 837.
3 J. Aggett and A. J. Sprott, Anal. Chim. Acta, 72 (1974) 49.
4 C. W. Fuller, Analyst (London), 99 (1974) 739.

Analytica Chimica Acta, 89 (1977) 221—223

Short Communication

THE DETERMINATION OF METALS IN PETROLEUM SAMPLES BY ATOMIC ABSORPTION SPECTROMETRY
PART IV. THE EFFECT OF HALOGEN ON THE DETERMINATION OF VANADIUM AND NICKEL IN XYLENE SOLUTIONS

G. ŠEBOR and I. LANG

Department of Petroleum Technology and Petrochemistry, Institute of Chemical Technology, 166 28 Prague (Czechoslovakia)

(Received 12th July 1976)

The dependence of the atomic absorption signals of vanadium and nickel on the type of organometallic compound in xylene solutions has already been discussed [1, 2]. The determination of these metals, which are very important in petroleum analysis, is to a high degree dependent on the type of compound used for calibration. To solve this important problem, it is necessary to seek a method of eliminating this dependence in the simplest possible way.

Kashiki et al. [3, 4] studied this problem in the determination of metals in petroleum samples diluted with methyl isobutyl ketone (MIBK) and removed the dependence of the absorption signals of vanadium and nickel on the type of compound used by adding halogen (preferably iodide). Sugihara et al. [5] found that vanadium is released both from synthesized vanadyl porphyrins and from porphyrins present in petroleum samples by the effect of chlorine and sulphuryl chloride at low temperatures. They also studied the addition of halogen in the determination of vanadium by a.a.s. after diluting samples of various crude oils containing known amounts of vanadium with 1-methylnaphthalene; however, halogen had no effect [6].

In this communication, the effects of halogen on the absorption signals of organometallic compounds of vanadium and nickel in xylene are discussed. The effects of halogen on the values of absorption signals for these metals in real petroleum samples diluted with xylene are also described.

Experimental

A Varian-Techtron Model AA6 instrument was used with the conditions described earlier [2, 7].

Xylene solutions of vanadyl tetraphenylporphyrin (VOTPP), vanadyl benzoylacetonate (VOBA), vanadyl acetylacetonate (VOAA), Conostan vanadium standard (VCON), nickel tetraphenylporphyrin (NiTPP), nickel acetylacetonate (NiAA), nickel cyclohexanebutyrate (NiCHB), Conostan nickel

standard (NiCON) and real petroleum samples containing 12 μg V ml^{-1} and 5 μg Ni ml^{-1} were examined. The amounts of iodine, bromine and chlorine added were 50, 100, 200 and 400 μg ml^{-1}.

Xylene solutions of the above organometallic compounds were prepared by diluting the stock standard solutions, the preparation of which has already been described [1, 2, 7]. Xylene solutions of the halogens (1000 μg ml^{-1}) were prepared by dissolving 1.0 g of iodine or bromine in 1000 ml of xylene. For chlorine, the initial compound was CCl_4 (1.085 g of CCl_4 in 1000 ml of xylene). The real petroleum samples were asphaltenes from Romashkino crude oil (USSR) and their acetonitrile and acetone extracts dissolved in xylene.

For comparison, the dependence of the absorbances of MIBK solutions of vanadyl acetylacetonate, nickel acetylacetonate and nickel naphthenate (NiNAPH) (containing 10 μg V or Ni ml^{-1}) on the addition of iodine and chlorine (250, 400, 600 and 750 μg ml^{-1}), as described by Kashiki et al. [3, 4], was studied. MIBK solutions of the organometallic compounds were prepared by diluting stock standard solutions analogously to xylene solutions. The stock standard solution of nickel naphthenate (100 μg ml^{-1}) was prepared by dissolving a weighed amount of the standard [2] in 30 ml of MIBK and 7 ml of 2-ethylhexanoic acid; after temperature stabilization, the solution was diluted to 100 ml with MIBK. MIBK solutions of the halogens (1000 μg ml^{-1}) were prepared in the same way as the xylene solutions.

Results

Within experimental error (± 5 %), the addition of iodine, bromine or chlorine in concentrations up to 400 μg ml^{-1} had no effect on the absorption signals of vanadium and nickel in xylene solutions either for the individual standard solutions or for the real petroleum samples. As an example, Table 1 shows the effect of iodine on the absorption signals of vanadium and nickel for standard solutions of the organometallic compounds.

TABLE 1

The effect of iodine on the absorbance of xylene solutions of organometallic compounds of vanadium and nickel
(The values given are the absorbances of the corresponding solutions.)

Compound	Iodine added (μg ml^{-1})				
	0	50	100	200	400
VOTPP	0.335	0.329	0.331	0.326	0.325
VOBA	0.260	0.254	0.259	0.264	0.268
VOAA	0.265	0.265	0.275	0.275	0.276
VCON	0.147	0.148	0.141	0.148	0.148
NiTPP	0.428	0.431	0.432	0.429	0.415
NiAA	0.412	0.412	0.405	0.406	0.403
NiCHB	0.348	0.336	0.346	0.346	0.348
NiCON	0.356	0.368	0.370	0.370	0.350

Under the present experimental conditions it was also not possible to demonstrate any effect of iodine and chlorine in MIBK solutions, as can be seen from the values for iodine given in Table 2. Aromatic hydrocarbons are, however, more suitable as solvents for high molecular weight petroleum fractions than MIBK in which asphaltenes are precipitated [8, 9].

The above results show that the simple method based on the addition of halogen to various organometallic compounds of vanadium and nickel, which are relevant to the determination of these metals in petroleum samples, cannot be utilized in the system chosen here.

TABLE 2

The effect of iodine on the absorbance of MIBK solutions of organometallic compounds of vanadium and nickel
(The values given are the absorbances of the corresponding solutions.)

Compound	Iodine added (μg ml^{-1})				
	0	250	400	600	750
VOAA	0.120	0.116	0.119	0.119	0.118
NiAA	0.238	0.241	0.242	0.244	0.241
NiNAPH	0.231	0.229	0.229	0.231	0.225

REFERENCES

1 G. Šebor, I. Lang, P. Vavrečka, V. Sychra and O. Weisser, Anal. Chim. Acta, 78 (1975) 99.
2 I. Lang, G. Šebor, V. Sychra, D. Kolihová and O. Weisser, Anal. Chim. Acta, 84 (1976) 297.
3 M. Kashiki, S. Yamazoe and S. Oshima, Anal. Chim. Acta, 54 (1971) 533.
4 M. Kashiki and S. Oshima, Bunseki Kagaku, 20 (1971) 1398.
5 J. M. Sugihara, J. F. Branthaver and K. W. Willcox, Am. Chem. Soc., Div. Petrol. Chem., Prepr., 18 (1973) 645.
6 J. M. Sugihara et al., Am. Petrol. Inst., Res. Project, 60 (1972) 35.
7 I. Lang, G. Šebor, O. Weisser and V. Sychra, Anal. Chim. Acta, 88 (1977) 00.
8 R. M. Yutkewich and V. M. Minut, Khim. Tekhnol. Topl. Masel, 17 (1972) 54.
9 D. A. Keyworth, in J. A. Dean and T. C. Rains (Eds.), Flame Emission and Atomic Absorption Spectrometry Vol. 3, M. Dekker, New York, 1975, p. 437.

Analytica Chimica Acta, 89 (1977) 225—229

Short Communication

DETERMINATION OF NORETISTERONE IN TABLETS BY DIFFERENTIAL PULSE POLAROGRAPHY

LISE-NETTE OPHEIM

Department of Chemistry, University of Oslo, Oslo 3 (Norway)

(Received 28th June 1976)

Noretisterone(17α-etinyl-17β-hydroxy-4-estren-3-on) is used in oral contraceptives, either alone (low-dosage or mini pills) or in combination with an estrogen (combination pills). A procedure for the determination of the drug in tablets by t.l.c. spectrodensimetry has been outlined by Shroff and Shaw [1]. The polarographic behaviour of steroids related to noretisterone has been investigated by several workers [2—4]. The present communication describes a rapid differential pulse polarographic method for the determination of the drug in tablets.

Experimental

Apparatus and solutions. Polarograms were recorded with a PAR Model 174 Polarographic Analyzer. A Metrohm EA 427 Ag/AgCl(satKCl) reference electrode, and a platinum wire counter electrode were used. The pH values were measured with a Metrohm EA 120 glass electrode and a Beckman H5 pH meter. As the solutions contained 40 % methanol, the pH values are relative values only.

Pharmaceutical grade noretisterone and mestranol, Conlumin tablets, and tablet material for placebo Conlumin tablets were obtained from Astra AB, Sweden. All other reagents were of p.a. grade.

Stock solutions (1 mg ml^{-1}) were prepared by dissolving the appropriate amount of noretisterone in ethanol or methanol. These solutions could be stored for several weeks without deterioration. Buffer mixtures of phosphoric, acetic, and boric acid and sodium hydroxide (Britton—Robinson [5]) were used for the pH investigations.

Dissolved air was removed from the solutions by bubbling oxygen-free nitrogen through the cell for 20 min and passing it over the solution during the experiments, all of which were done at 25.0 ± 0.2 °C.

Recommended procedure. For the analysis of tablets, transfer one tablet (containing 1 mg of noretisterone) to a 100-ml volumetric flask and add a few drops of distilled water. When the tablet has completely disintegrated, add 40 ml of methanol and shake the flask vigorously. Add 20 ml of 0.2 M tetramethylammonium bromide solution, and dilute to the mark with

distilled water. Transfer 25 ml of the solution to a polarographic cell, remove dissolved air, and record the differential pulse polarographic peak.

For the standard sample method, prepare a 10 p.p.m. standard solution by treating a mixture of the stock solution and excipients corresponding to one tablet in exactly the same manner as the tablet, and a blank solution by treating excipients the same way. The amount of noretisterone in the tablets is then calculated as the ratio of the peak currents of the tablet solution and the standard solution, measured against the blank.

Results and discussion

Choice of solvent and supporting electrolyte. Hrdý [3] studied several Δ^4-3-keto-steroids in 1:1 solutions of ethanol and Britton—Robinson buffers. Preliminary differential pulse polarograms of noretisterone in this medium (pH 8.0 in the ethanolic solution) showed that ethanol produced a peak which interfered strongly with the reduction peak of the steroid. The same result was obtained with a phosphate buffer (pH 7.8 in the ethanolic solution). Spahr and Knevel [4] reported that ethanol produced a tensammetric peak on a.c. polarograms from methyltestosterone and progesterone in 50 % ethanolic solutions with a 0.5 M KCl or KNO_3 supporting electrolyte. Tensammetric waves of ethanol have been described in detail by Breyer and Hacobian [6]. Organic quaternary ammonium compounds were also tested as supporting electrolytes for noretisterone in 50 % ethanolic solutions. While the use of tetraethylammonium perchlorate or hydroxide gave differential pulse polarograms similar to those described earlier, the use of tetraethylammonium iodide or tetramethylammonium bromide gave rise to a small peak at a potential slightly less negative than the noretisterone peak. Although the electrocapillary curves (Fig. 1) showed that ethanol is adsorbed on the mercury drops in tetramethylammonium bromide, the small peak was most probably due to the reduction of an impurity, as it had a corresponding d.c. wave, and there was no depression of the differential pulse baseline. Spahr and Knevel [4] reported that commercial ethanol contained reducible impurities, and that the ethanol, after purification, caused no tensammetric wave when tetrabutylammonium iodide was used as supporting electrolyte for methyltestosterone and progesterone.

To avoid a time-consuming purification step, other solvents for noretisterone were tested; methanol was well suited. From the electrocapillary curves (Fig. 1), it is evident that methanol is not so strongly adsorbed on the mercury drop as ethanol. Furthermore, the commercial p.a. quality methanol was polarographically inert in the potential region of interest.

The solubility of oxygen in mixtures of water and organic solvents is much greater than in water [7]. Experiments with mixtures of water and ethanol or methanol showed that dissolved oxygen could be removed satisfactorily from a 50 % alcoholic mixture by bubbling nitrogen for 30—40 min, whereas a 20 % or less alcoholic solution was deaerated in 10—15 min.

Effect of pH. The effect of pH on the peak current and the peak potential

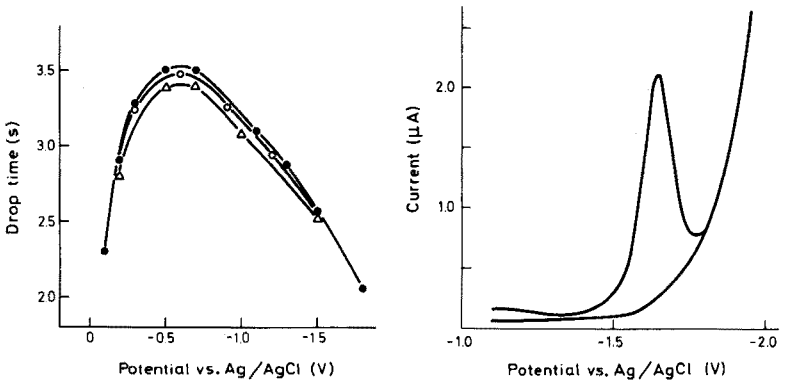

Fig. 1. Electrocapillary curves for solutions of 0.04 M tetraethylammonium hydroxide. •, no alcohol; ○, 50 p.p.m. methanol; △, 50 p.p.m. ethanol.

Fig. 2. Differential pulse polarograms of a 40 % methanolic solution of 20 p.p.m. noretisterone in 0.04 M tetramethylammonium bromide.

TABLE 1

Effect of pH on peak potential and peak current of noretisterone in 40 % methanolic solution

pH	E_p (V vs. Ag/AgCl)		i_p (μA)	
	Peak 1	Peak 2	Peak 1	Peak 2
2.9	−1.17		4.12	
3.9	−1.23		2.84	
5.0	−1.33		2.16	
6.1	−1.42		1.96	
7.1	−1.47	−1.65	1.32	—
7.6	−1.47	−1.65	0.72	1.68
8.1	−1.50	−1.63	—	1.68
9.0		−1.63		1.84
9.8		−1.65		1.96
11.0		−1.68		2.20
11.6		−1.71		2.64

was investigated by recording differential pulse polarograms of 20 p.p.m. solutions of noretisterone in Britton—Robinson buffers. The results (Table 1) are in accordance with the pH-dependence of the d.c. halfwave potential of several testosterones and progesterones [2, 3]. As the electrolyte decomposition wave is shifted towards less negative potentials as the pH decreases, at about the same rate as the noretisterone peak, the separation of the latter from the final rise is approximately the same within the pH range 3—11.

Concentration range and precision. The d.c. polarographic wave of noretisterone is not well defined, and is unsuitable for analytical purposes, as the

halfwave potential is close to the electrolyte decomposition potential. Similar ill-defined waves are common for the reduction of many steroids [4]. The best method of calculating the diffusion current was to measure the wave height against the polarographic curve of a blank solution, at a fixed potential on the plateau, as suggested by Meites [8]. Although the reduction peak of the differential pulse polarogram of noretisterone is better defined than the d.c. wave, the peak current should be measured against a blank, as indicated in Fig. 2.

D.c. and d.p. polarograms were recorded from 40 % methanolic solutions with various amounts of noretisterone present. For d.p. polarography, the peak current increases linearly with concentration over the range 2—200 p.p.m. i.e. $7 \cdot 10^{-6}$ M—$7 \cdot 10^{-4}$ M. The d.c. diffusion current increases linearly with concentration in the range 4—40 p.p.m., but at higher concentrations the slope decreases.

The standard deviation of the peak current was determined by analyzing 5 different preparations of a 10 p.p.m. solution. Better reproducibility was obtained from unbuffered solutions (s_r = 1.5 %) than from solutions buffered with 0.01 M Britton—Robinson buffer (s_r = 2.5 %).

Analysis of tablets

As most of the estrogens used in combination pills are not reducible at the DME, separation of the steroids should not be necessary for the determinatior of noretisterone in such pills. When d.p. polarograms were recorded from solutions containing 10 p.p.m. noretisterone, 0.5 p.p.m. mestranol was found to have no effect.

Although tablet excipients are not usually electroactive, interference may occur if ingredients are adsorbed on the DME. To investigate such effects, d.p. polarograms were recorded from several solutions of noretisterone, with various amounts of the Conlumin excipients added. The background current (i.e. the current of a blank solution measured at the peak potential of noretisterone) increased when tablet material was added; this agrees with a study of the effect of excipients in tablets containing clopoxide and diazepam [9]. Furthermore, the slope of the standard curve of noretisterone decreased with increasing concentration of tablet excipients.

When Conlumin tablets were analyzed by the recommended procedure, different values were obtained for noretisterone, when the standard addition method and the standard sample method [8] were used. Comparison of these results with those of a spectrophotometric method showed that the values given by the standard sample method were in better agreement.

The author thanks Dr. Walter Lund, Department of Chemistry, for valuable discussions, and Dr. Leif Uppstrøm, AB Astra, Södertälje, for the supply of the drugs and tablets used and for the spectrophotometric data.

REFERENCES

1 A. P. Shroff and C. J. Shaw, J. Chromatogr. Sci., 10 (1972) 509.
2 P. Zuman, J. Tenygl and M. Březina, Collect. Czech. Chem. Commun., 19 (1954) 46.
3 O. Hrdý, Collect. Czech. Chem. Commun., 27 (1962) 2447.
4 J. L. Spahr and A. M. Knevel, J. Pharm. Sci., 55 (1966) 1020.
5 H. T. S. Britton, Hydrogen Ions, Vol. I, Chapman & Hall, London, 1955, p. 365.
6 B. Breyer and S. Hacobian, Aust. J. Chem., 9 (1956) 7.
7 I. M. Kolthoff and J. J. Lingane, Polarography, Vol. II, Interscience, New York, 1952, p. 625.
8 L. Meites, Polarographic Techniques, Interscience, New York, 1967, pp. 150 and 394.
9 W. Lund and L. N. Opheim, 88 (1977) 275.

Analytica Chimica Acta, 89 (1977) 230

ERRATUM

A. R. Rodriguez et C. Poitrenaud, Étude d'Équilibres en Solution à l'aide des Échangeurs d'Ions. I. Dissociation du Perchlorate d'Argent et de l'Acide Nitrique dans les Mélanges Eau—Acide Acétique—Acide Perchlorique ou Acide Nitrique, *Anal. Chim. Acta*, 87 (1976) 125—140.

Pages 134, 135 et 137, Figures 3, 4 et 7, lire sur l'axe des abscisses 1/Co au lieu de H_2O (%).

Corrected
V. Ph.
22 June
1977

(continued from page 4 of cover)

Short Communications

PRINTED IN THE NETHERLANDS

VOL. 89 No. 1 ANALYTICA CHIMICA ACTA MARCH 1977

CONTENTS

(continued on inside page of the cover.